Subsurface Andesite Geology and Hydrothermal Alteration at an Exploration Prospect North of Waihi

A thesis submitted in partial fulfilment

of the requirements for the degree

of

Master of Science (Research)

in Earth Sciences

at

The University of Waikato

by

William Starzynski

THE UNIVERSITY OF
WAIKATO
Te Whare Wānanga o Waikato

2022

Abstract

The Coromandel Volcanic Zone hosts the Hauraki Goldfield in the North Island of New Zealand. The goldfield consists of approximately 50 low sulphidation Au-Ag deposits. Situated in Coromandel Group rocks, which host 95% of the gold production in the region, the area of focus of this study is a prospect located 4 km north of the world class Martha Hill Mine. Such epithermal deposits are characterised by zones of altered rock called halos. Seven angled exploratory drill holes from the area were examined in this study. These cores were logged using high resolution photographs from a geological perspective for the first time. Samples were taken for petrographic and mineralogical analysis including X-ray diffraction analysis and for X-ray fluorescence spectroscopy. Leapfrog was used to display the spatial relationship of these results. The aim of this study was to determine the volcanic geology and alteration origins of this project. This was achieved by identifying facies as well as their spatial distribution, determining the mineralogical properties of the facies and their variations down-hole, as well as identifying the style and spatial extent of alteration.

Eight new facies were identified which are hosted in andesitic rock. Three of the facies were based on visible crystal concentration which ranged from, 3% – 65% and occurred throughout the core. Fresh samples were dominated by plagioclase, with relatively minor amounts of quartz and pyroxenes and altered samples comprised of calcite+quartz assemblages with various suits of sulfides and oxides, predominantly pyrite and magnetite. The mineral assemblages and their abundances are comparable to the Waipupu Formation andesite with vast similarities to active andesite volcanoes and Late Archean examples. The rocks exhibit seriate porphyritic textures and glomeroporphyritic clots that are consistent with polybaric fractionation. The textures resulted in the host rocks innate high porosity and permeability which increases with each propagation of hydrothermal fluid. While the common resorption of quartz indicates magma mingling occurring in the magma chamber, these same resorption features as well as observed swallowtail plagioclase microlites also reflect degassing processes within the magma during ascent. Four breccia facies were described based on the concentration and orientation of breccia clasts. These facies occurred dominantly around the edge of alteration zones, which can be attributed to their relatively higher porosity. While some breccia display properties of auto breccia, hydrothermal breccia's are dominant with all breccia likely altered to some degree. Finally, an irregular facies was described and relates to hydrothermal alteration processes exclusive to moderate and high alteration zones. Using the mineralogy data, in conjunction with stratigraphic logs, zones of alteration could be

identified and designated based on intensity, describing two zones of high intensity alteration separated by a zone of moderate alteration and low alteration occurring closer to the surface. These zones give an insight into the flow of paleo fluid during alteration and can hint at the location of Au bearing veins.

Acknowledgements

I would like to extend my thanks to the follow people for assisting me with their, expertise time and support, this study would not have been possible without your contribution:

Firstly, I thank my supervisor Adrian Pittari for your knowledge and guidance with this project. Your insightful ideas and discussion paved the direction of this study, challenging my level of judgement and analysis, helping me expand my geological proficiency.

This project was supported in kind by OceanaGold through access to drill core and in house core data, and a training course on epithermal mineralisation. To the people at OceanaGold, especially Shannon Richards who helped with the sampling, providing the basis for the study and organising opportunities to develop a deeper knowledge of Gold I really appreciate your time. I would also like to give a special thank you to Stewart Simmons for delivering insightful seminars on epithermal deposits, providing information that would be very useful in this study.

I would also like to thank Kirsty Vincent from the technical staff from the University of Waikato for the exceptional laboratory training. As well as providing me with the guidance and tools needed to get through the preparation of samples, including organising some often last-minute sample processing. I would also like to thank Annette Rodgers for the training of the use of the ring mill.

For the constructive (and not so constructive) discussions, laughs, gym breaks and boosts in morale I would like to thank my friends and fellow MSc student Gian, as well as Caleb, Carlos, Wesley, Nick and Jason, also, the boys from Masterton Jack, Zac, Dylan, Mark, Cameron, Ihaia, Taine and Gareth. For the valuable proofreading and assisting my transition into full time work while still completing this thesis I thank my co-worker Anya for her time.

Of course, to my family who have encouraged me every step of the way, thank you, Mum and Dad for keeping me level-headed and on track with your (mostly), weekly catch ups and my brother, Mikael for the study break calls. Finally, to my girlfriend Carla for the incredible patience, support, proofreading and assistance and helping me successfully complete this project I really appreciate it and couldn't have done it without you.

Table of contents

List of figures

List of tables

Chapter 1
Introduction

1.1 Introduction

The Coromandel Volcanic Zone (CVZ) hosts the Hauraki goldfield, an intracontinental arc displaying dominant andesite-dacite-rhyolite volcanism (Brathwaite & Faure 2002), consisting of approximately 50 epithermal Au-Ag deposits and porphyry Cu deposits (Brathwaite, 1989). The Martha Hill deposit in the southern region of the Hauraki goldfield in Waihi, is the largest of these deposits. This deposit has produced 210,944 kg of gold and 1,299,893 kg of silver, accounting for approximately 66% of the total gold and 89% of the total silver produced from the Hauraki goldfield (Spörli & Cargill, 2011). Within 3 km of the Martha deposit are the Correnso, Favona, Union-Trio, and Moonlight deposits. Despite 127 years of prospecting and mining at Waihi, deposits such as Corenso and Favona were discovered relatively recently in the form of blind deposits. Such discoveries highlight the prospect of new deposits being discovered in the area. This study focuses on an area roughly 4 km to the north of the Martha Hill deposit (Fig 1.1.). There is little known about the prospect, with limited drill holes and limited knowledge about the host rock and how it relates to the surrounding lithologies as well as the alteration style of the deposit and and its relationship to other orebodies in the region.

1.2 Research aims and objectives

This project is a fundamental geological study to reconstruct the volcanic geology and alteration styles of the prospect. This can allow for a reconstruction of past volcanic processes acting on this geology, and a proposal of potential halo zones along with their mineral assemblages which can assist with exploration and prospecting purposes.

To achieve these aims, this study will address the following objectives:

- Classify facies types based on host rock and altered rock characteristics.
- Determine spatial variation in facies.
- Determine petrographic and geochemical characteristics of these facies.
- Determine the alteration styles and extents down-hole.

The general methods used to carry out these objectives are as followed:

- Logging of core from photos and hand samples.
- Creation of thin sections for transmitted and reflected light analysis
- Prepare low-sulfide content samples for x-ray fluorescence (XRF) spectrometry analysis.
- Correlate data down-hole and make associations based on texture, petrography, and geochemistry based on depth and extent.

1.3 Outline

Chapter two is a review of epithermal systems, and alteration styles, focusing on literature aiding in the pursuit of exploration. Chapter 3 reviews the local geology of the Coromandel Volcanic Zone with an emphasis on the local mineralisation, structure, and alteration of the Waihi Region. Chapter 4 presents the data collected from the extensive core logging, providing facies parameters, down-hole descriptions, and graphic logs. Chapter 5 outlines the petrographical and mineralogical findings, with reflected and transmitted light descriptions of thin sections from hand samples. Chapter 6 presents the results collected from geochemical analysis, including portable x-ray fluorescence (pXRF) and XRF analysis. X-ray diffraction (XRD) bulk rock analysis results will also be recorded in this chapter. The discussion of the results will be at the end of each corresponding chapter and the thesis is summarised and concluded in chapter 8.

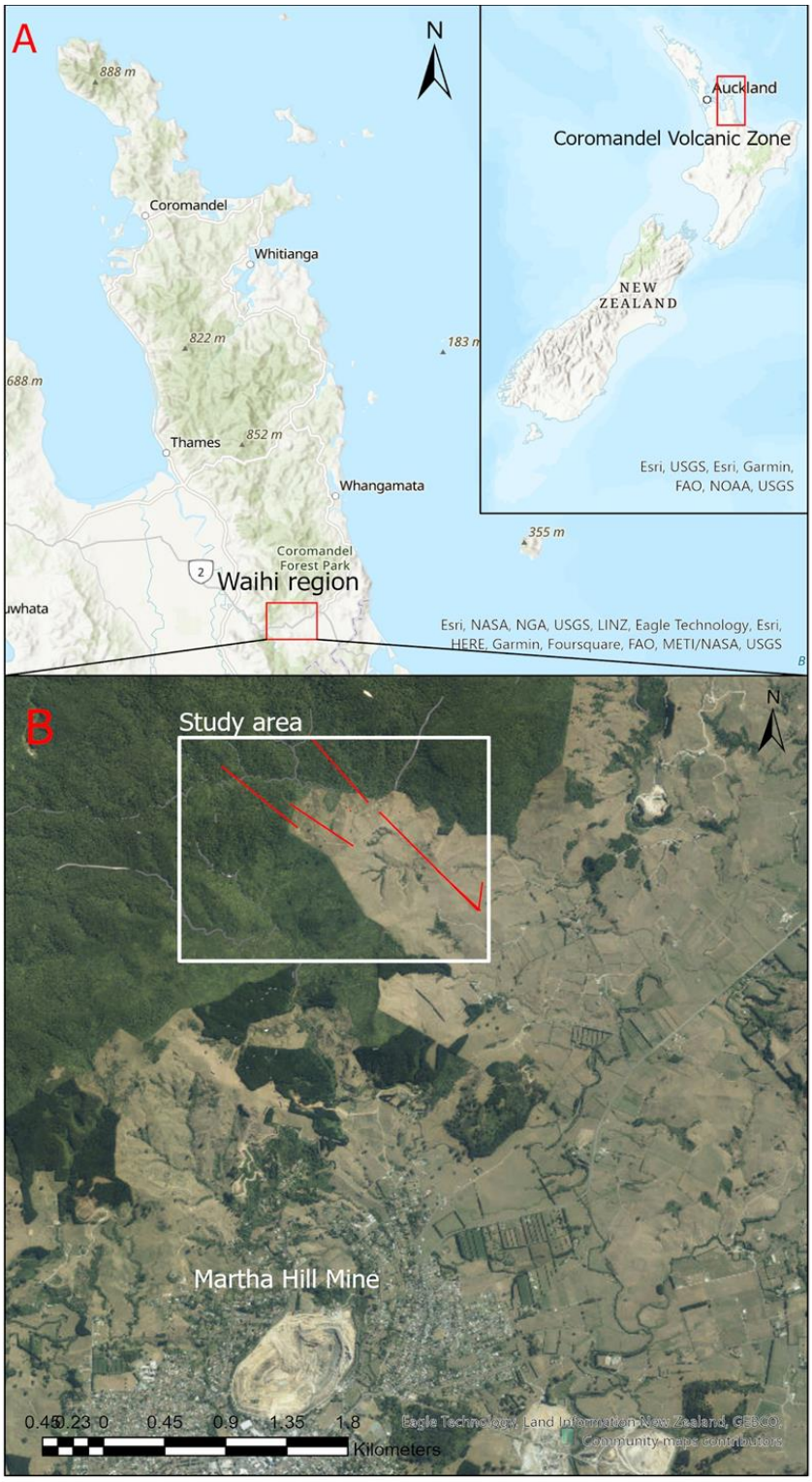

Fig. 3.1. (A) Regional map of the Coromandel Volcanic Zone with reference to New Zealand, and the Waihi area highlighted. (B) Local base map of the Waihi area including Martha Hill Mine and the area of study. Red lines in the area of study represent drill hole locations.

Chapter 2:
Epithermal systems

2.1 Introduction

This chapter reviews past literature in epithermal systems, specifically their characteristics, mineral assemblages, and geological setting. The focus will be on low sulphidation systems, mineralisation conditions in epithermal systems as well as their controls and limitations with emphasis on the accumulation of gold. This chapter also reviews hydrothermal alteration processes, characteristics and common styles of hydrothermal alteration including the common mineral assemblages associated with each.

2.2 Definition

The term 'epithermal' is derived from a combination of 'epi' meaning shallow and 'thermal' meaning heat. The term epithermal was first used by Lindgren, in 1922, as a form of hydrothermal deposit formed by ascending hot water near the surface in or near effusive rocks at relatively low pressure and temperature (Lindgren, 1922). Lindgren (1922) acknowledges criticism due to the lack of strict logical categories in his initial description and continues to describe epithermal deposits in his book on Mineral deposits (Lindgren, 1933). The development of epithermal deposits occur within large, predominantly subaerial, high-temperature hydrothermal systems from a range of temperature against pressure (depth) ore-forming conditions (Simmons et al., 2005).

Due to the dynamic nature of epithermal deposits, it can be difficult to describe them with a strict, yet well-represented definition of the term. However, the parameters of an epithermal deposit have changed little since they were described by Lindgren (1922, 1933). Epithermal systems were described as shallow systems with formation occurring above 1 kilometre depth at temperatures of 50 to 200 °C, with a pressure limit of 100 bars. The most notable update is recorded in terms of temperature, as fluid inclusions in mineral assemblages and textures distinctive of the epithermal environment recorded a maximum temperature of 300 °C. While this is much greater than originally thought, temperatures of most epithermal deposits typically reside in the range of 160-270 °C and seldom exceed 300 °C (Hedenquist et al., 2000; Henley

et al.1984). As these deposits occur in the shallow supergene, and are at equilibrium, maximum temperatures are controlled by depth as the vapour pressure of boiling liquids limits the maximum temperature at given depths due to the hydrostatic pressure. Temperatures of approximately 150-300 °C facilitate precipitation of ore minerals along steep temperature and pressure gradients controlled by the geological environment. Most epithermal deposits occur at depths of 50 to 700 m below the paleowater table where these temperatures and chemical changes predominantly occur. Deposits in the epithermal environment rarely form below 1000 m (Simmons, 2021; Hedenquist et al., 2000). Temperature and pressure are the primary physical controls on epithermal deposits with the other main control being the hydrothermal solution (Fig 2.1.). These solutions are necessary as they influence the transportation and deposition of metal. The range of origins and composition of these solutions result in variations of metal contents which can influence the quality or grade of the ore. Epithermal orebodies can range

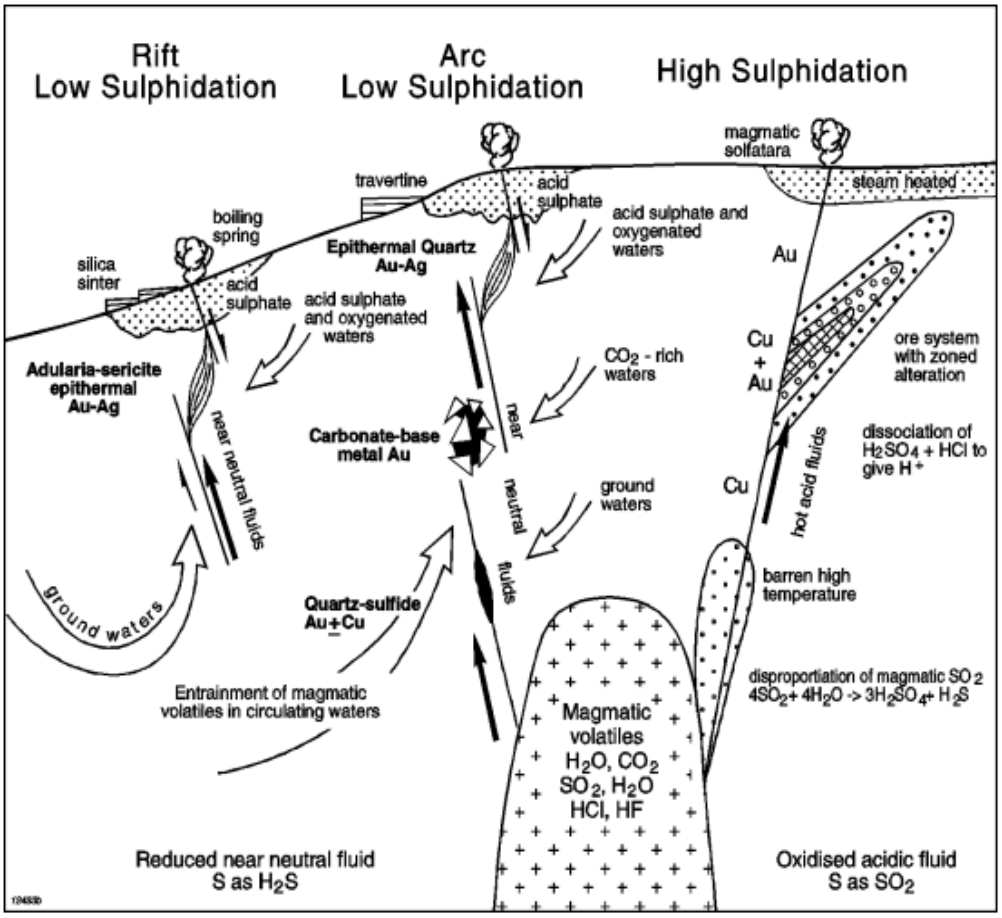

Fig. 4.1. Processes in high sulphidation, rift and arc low sulphidation epithermal systems, including their fluid and heat origin and pathways. Derived from Corbett (2002).

over areas from <10 to >100 km^2 and display a wide range of characteristic features, with many classification schemes having been proposed since the late 1970s (Simmons et al., 2005).

Epithermal systems are of significant relevance regarding the exploration of gold and silver bearing epigenetic ore. Nearly 6% of all mined gold and 16% of all mined silver have originated from epithermal deposits (Simmons et al., 2005). Epithermal deposits consist of gold-bearing orebodies which accumulate as gold is mobilised and transported by a hydrothermal fluid before being trapped and deposited. Such orebodies are anomalies in the Earth's crust, containing high concentrations, or a high grade, of gold that is economically viable to mine. The grade of the orebody describes the concentrations of the desired minerals present. Grades for gold in orebodies are often within the range of 2 to more than 100 grams of gold per tonne with the average minimum exploitable grade being 1 gram per tonne (Simmons, 2021; Evans, 2009). These concentrations are a significant amount relative to the natural accumulation of gold in the Earth's crust which on average is 0.001 to 0.006 grams per tonne (Jones, 1968).

2.3 Common features

Hosts of epithermal deposits typically consist of coveal and older volcanic rocks as well as underlying basement rocks. Less commonly, deposits can be hosted by sub-volcanic intrusions. Orebodies predominantly occur in steeply dipping veins, produced through dilation and extension (Simmons et al., 2005). Structures such as faults can act as a host with minor faults of <10 m displacement being more common than major faults. Rock rheology is important, as brittle failure allows for optimum structural development. The large variety of shapes displayed by orebodies represents the influence of structural and lithological controls on their genesis (Simmons et al., 2005). These orebodies also represent zones of paleopermability. Lithological characteristics including contrasting permeability and porosity are relevant as they permit the concentration and flow of fluid through permeable masses of brecciated rock or along formation contacts. Permeability and porosity may be primary features of the original rock or may form as a by-product of hydrothermal brecciation or hydrothermal alteration and chemical dissolution. Factors such as faults and fracture networks, coarse clastic rocks, breccia, and intensely leached rocks can affect the morphology of the orebody and account for the spectrum of veins related to disseminated ores. These spectrums can range hundreds to thousands of metres laterally and tens to hundreds of metres vertically. Most ores are typically hard and resistant to weathering, this is due to quartz being the dominant gangue mineral in epithermal deposits

with pyrite as the dominant sulfide. Sulfide quantities generally range from <1 to >20 percent volume (Simmons et al., 2005).

2.4 Classification of epithermal systems

There is a vast degree of variation within epithermal systems, making them difficult to classify. This has also led to many classification attempts of epithermal systems, including classifications based on mineralogy, deposit form, alteration, host rock, and genetic models. Such classifications have their pros and cons. However, a simple fluid chemistry classification derived from the form of the deposit in addition to the vein and alteration mineralogy and zoning is preferred (White & Hedenquist, 1990). This can effectively classify epithermal deposits of both vein and bulk tonnages into three general categories based on the oxidation state of sulfur present in the hypogene sulfide assemblages (Sillitoe & Hedenquist, 2005; Hedenquist et al., 2000). These are high sulphidation (HS) epithermal deposit (+4 or +6 oxidation state), an intermediate sulphation (IS) deposit (+2 oxidation state), or a low sulphidation (LS) deposit (0 or -2 oxidation state) (Sillitoe & Hedenquist, 2005). Variations in deposit locations in relation to the magma intrusion also differ between high and low sulfidation states. LS deposits typically occur several kilometres above the magma source while HS deposits are located relatively closer to the intrusion (Cooke & Simmons, 2000). Low sulfidation and high sulphidation (also referred to as adularia-sericite and acid-sulfate), represent the two end-member sulfidation states and are important to distinguish for exploration purposes.

The sulfide assemblage groups mark key differences in ore fluids such as origin and rock interaction. In HS systems, fluid origins are primarily magmatic and fluid-rock interaction is fluid-dominated. The fluids in HS environments have acidic and oxidised characteristics (Hedenquist et al., 2000) which are linked to relatively sulfide-rich assemblages of high sulphidation state such as pyrite-luzonite, pyrite-covellite, pyrite-enargite and pyrite-famatinite. These HS system fluids typically occur in host, leached silicic rock with a halo of advanced argillic minerals (Sillitoe & Hedenquist, 2003). In contrast, the LS system's fluid origins are primarily meteoric/evolved magma-dominated and rock-fluid interactions are rock-dominated (Sillitoe & Hedenquist, 2005) (Fig 2.1). Mineralising fluids in low-sulphidation environments are reduced with a near-neutral pH and are generally meteoric in origin, although some systems' reactive gasses and water are magmatic in origin. LS fluids are in equilibrium with host rocks as they ascend from depth, resulting in a low salinity and potentially, CO_2 and H_2S dominant, gas-rich liquid. gasses

(Hedenquist et al., 2000). LS deposits support the formation of the low-sulphidation pair, pyrite-arsenopyrite, with arsenopyrite usually occurring in relatively minor quantities, within banded quartz, chalcedony, and adularia veins or subordinate calcite (Sillitoe & Hedenquist, 2003). Cu may also occur in minor amounts in the form of chalcopyrite. These contrasts in fluids between the two styles are primarily due to the degree of which they have equilibrated with their host rocks below the level of ore deposition.

Differences in redox conditions hosted by the hydrothermal fluid in low and high sulphidation systems causes multiple distinct contrasts in ore mineralogy and gangue mineralogy. There is some overlap between the two styles with most differences seen in the sulfide mineralogy (White & Hedenquist, 1995). Specific minerals differentiate between HS and LS styles. Arsenopyrite and sphalerite typically occur in LS deposits but are usually rare in HS deposits, while Cu minerals, especially enargite-luzonite (high-sulphidation state sulfosalts) are exclusively common in HS deposits. The dominant sulfide in both HS and LS deposits is pyrite, therefore total sulfide abundance does not classify either style as it could either be concentrated or scarce (Table 2.2). Dominant gangue minerals also show a similar overlap, with quartz being dominant in both styles. The differences in these minerals are typically controlled by the pH or reactivity of the altering fluid. Calcite and adularia are representative of low pH levels and are the most common, after quartz, in LS deposits while being absent from HS deposits. HS deposits host acidic conditions, facilitating the formation of kaolinite and alunite among a suite of others in minor abundances. While it can be noted that kaolinite and alunite can occur in LS deposits, it is only as an overprint and not as a primary gangue mineral (White & Hedenquist, 1995; table 2.2).

LS and HS deposits show contrasts in texture, where LS deposits display a wide variety of textures in contrast to HS deposits. Textures displayed by LS deposits include banded, crustiform quartz and chalcedony veins, druse-lined cavities, and multiple-episode vein breccias. Bladed, lattice-textured calcite is also common in LS deposits as a product of boiling although the calcite may be replaced by quartz as the system cools. (Simmons & Christenson, 1994). Where there is little erosion, silica sinters can be deposited at the paleosurface as a result of discharge, on the surface from boiling neutral pH spring water (White & Hedenquist, 1995).

Table 2. 2. Different characteristics of low and high sulphidation deposits and examples. Modified from White and Hedenquist (1990).

	High Sulphidation	**Low Sulphidation**
Host rocks	Subaerial, acid to intermediate volcanics and underlying basement rock	Subaerial, acid to intermediate volcanics and underlying basement rock
Localizing controls	Sub volcanic intrusions and major regional faults	Any faults and fractures, especially those close to volcanic centers
Depth of formation	Approximately 500 to 2000 m	Mostly 0 to 1000 m
Character of fluid	Mostly low salinity, magmatic origin often mixed with meteoric waters, acidic, oxidised, typically high S content	Low salinity, meteoric origin magmatic fluid interaction possible, near neutral pH, reduced typically low total S content
Associated alteration	Propylitic alteration in low water:rock ratio areas. Deep deposits = pyrophyllite alteration. Pervasive clay alteration present in near-surface deposits.	Propylitic alteration in low water:rock ratio areas, clay alteration dominant in low temperatures, argillic and advanced argillic peripheral and overlapping.
Mineralisation features	Typically disseminated mineralisation, open space and cavity filling not common.	Mineralisation in open space cavities, layered vein fillings with multi-stage brecciation common stockwork or disseminated common in near -surface
Characteristic textures	Vuggy silica, massive silica	Crustiform banding, coliform banding, banded quartz-chalcedony, vugs, vein breccia, lattice texture.
Mineralogical features	Chalcedony mostly absent, adularia absent, alunite may be abundant, enargite-luzonite typically present	Chalcedony veins common, adularia present alunite minor, enargite-luzonite absent
Location examples	Temora- Australia, Mt Kasi- Fiji, Nansatsu district- Japan	Pajingo- Australia, Emperor- Fiji, Waihi- New Zealand.
Ubiquitous minerals in Au rich ores	Pyrite, enargite-luzonite,	Pyrite
common minerals in Au rich ores	Sphalerite, Galena Chalcopyrite, covellite, electrum, native gold.	Sphalerite, Galena, Chalcopyrite, arsenopyrite, native gold
rare minerals in Au rich ores	Arsenopyrite, Cinnabar	Enargite-luzonite, covellite, cinnabar

Alternatively, HS deposits show little textural variation, where massive bodies of vuggy quartz are the most characteristic texture. While typical of Nansatsu-type deposits (High sulphidation, disseminated gold deposits in massive, strongly silicified bodies), veins and breccia can also be significant ore hosts (Takeda et al., 2001). Vuggy quartz is the result of leaching by strong acid (pH <2) (Stoffregen, 1987), in which open spaces are created leaving residual silica that recrystallises to quartz with the addition of pyrite and quartz from solution. Massive quartz bodies may also be cut by sulfide veins made up of pyrite and enargite. HS deposits can't support the formation of sinters. In terms of texture, it is rarely difficult to distinguish sulphidation styles (White & Hedenquist, 1995) (Table 2.1)

2.5 Mineralisation and setting

For an epithermal system to form a gold-bearing ore deposit, a geological source, transport and trap must be present. Gold sources include magma and country rock, whereas fluids are often of magmatic and/or meteoric origin. The fluid mobilises and transports the metal to a trap where it will be deposited (fig2.2.). Processes that cause abrupt changes in chemical and physical conditions are often a precursor to the deposition of metal. Many of these factors differ between each epithermal deposit showing diversity in geological settings, local complexities, chemical variations, and in the products and mineral assemblages formed (White & Hedenquist, 1990). The igneous, tectonic, and structural settings of mineralisation can vary. Zones of igneous activity are relevant as they are temporally and spatially associated with subareal igneous rocks and their corresponding subvolcanic intrusions (Sillitoe & Bonham, 1984). These intrusions provide the heat required to generate a hydrothermal convection cell and contribute a component of the total gasses to the overlying hydrothermal system (White & Hedenquist, 1990). Volcanic-hosted deposits often occur with pyroclastic or effusive rocks (Sillitoe & Bonham, 1984), and typically display intermediate to acid volcanic settings. Calc-alkaline to alkaline suites have been the host of significant deposits whereas bimodal suites are also known to hold deposits (Mitchell & Garson, 1982). Some basic volcanics with shoshonitic or alkaline attributes have been known to act as epithermal deposit hosts, but this is a rare occurrence (e.g.Emperor, Fiji), (White & Hedenquist, 1990).

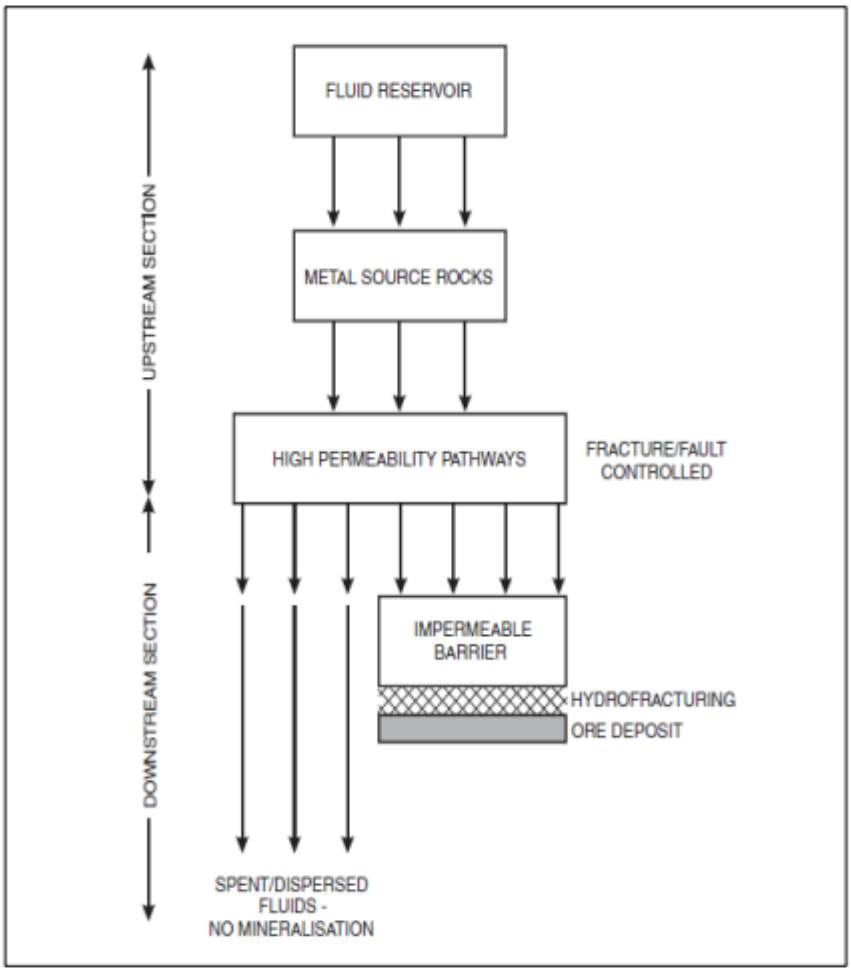

Fig. 2.2. Conceptual Fluid Flow Model showing fluid movement in hydrothermal systems. With upstream section depicting the fluid channeling through progressively smaller pathways before interacting with metal source rocks in the downstream section. The downstream section showing ore deposition if there is an impermeable barrier or dispersion from a lack of a barrier. Derived from Piranjo (2009).

In modern volcanic environments where hydrothermal activity is occurring settings can include grabens, calderas, andesitic stratovolcanoes, volcanic islands, and cordillera volcanism. Each setting is characterised by its own hydrothermal regime which dictates the discharge and recharge of the hydrothermal system as well as the distribution of conduits, the types and distribution of hydrothermal alteration products, and the possible areas of deposition of ore minerals (White & Hedenquist, 1990).

Tectonic settings may occur in conjunction with the igneous environments described above and can act as hosts for epithermal deposits. Such settings mainly occur as volcanic arcs in subduction zones between oceanic-oceanic or oceanic-continental plate margins. This setting can result in the development of back-arc rifting which can evolve into a marine back-arc basin. A back arc basin is no longer a prospect for epithermal deposits, due to the submarine characteristics of back-arcs basins which form massive sulfide deposits. Similarly, most ocean ridge settings are also non-prospective for the same reason. (White & Hedenquist, 1990). Other related settings that do not appear prospective for deposits include continental flood basalts, due to small and/or deep magma chambers and narrow conduits inhibiting the formation of a major shallow hydrothermal system. Primitive island-arc settings (e.g. Tonga-Kermadec chain), also appear to be unprospective, likely because large magma chambers are yet to develop, and cannot supply the necessary heat flow conditions to facilitate major hydrothermal activity (White & Hedenquist, 1990).

Structural settings are widely recognised for their relation to gold deposits due to the permeability enhancement caused by fractures in the near surface (White & Hedenquist, 1990). At a regional level, epithermal deposits are associated with volcanic-related structures, including felsic caldera-related structures and andesitic vent complexes, observed at Colorado (USA), Japan, and the southwest Pacific. Regional faults are also highly relevant as common controls of epithermal deposits, in guiding the emplacement of the magmatic heat source and influencing subsequent hydrothermal activity (White & Hedenquist, 1990). While major faults have regional control on deposit localisation, the major regional structure is seldom the location of mineralisation. In contrast, mineralisation commonly occurs on subsidiary faults or splay faults. Even minor structures in the prospect area such as bedding planes, joints, and joint intersections can potentially influence permeability and in turn the distribution of mineralisation (White & Hedenquist, 1990).

Economic gold deposits in epithermal systems are the product of a series of interacting processes and factors; and can vary depending on the fluids involved and the geological setting (Cooke & Simmons, 2000; Sillitoe & Hedenquist, 2003). For gold to be transported and deposited in epithermal systems, it is mobilized as gold is made soluble in an aqueous solution. Bisulphide (HS^-) and chloride (Cl^-) are essential sulfide ligands in gold-bearing solutions, promoting the solubilisation of gold (Zhu et al., 2011; Cooke & Simmons, 2000). In reduced, near-neutral pH environments, typical of LS systems $Au(HS)^-_2$ is the favoured gold transporting complex. In

contrast, at higher temperatures (>300 °C), Au is more likely to be transported by Cl^- (Zhu et al., 2011). $Au(Cl)^-_2$ is the preferred transporter of Au in fluids with higher saline and acidity contents, typical in HS systems. It is important to note the Arsenic-gold (As-Au) correlation. Experimental work has shown that the solubility of Au increases as the As concentration increases in an alkaline fluid. Gold and As-bearing minerals such as pyrite and arsenopyrite correlate positively so As is considered to play an important role in the concentration of Au in hydrothermal systems when S content is extremely low. Pressure and depth also play an important role in Au solubility. When Au depressurizes as it ascends faults as a fluid, becoming 90% less soluble, promoting deposition (Zhu et al., 2011).

Boiling a prevalent process that occurs in epithermal systems and contributes to many of the stages involved with ore deposition. Boiling produces vapour and liquid, to act as a medium for carrying and transporting ore-forming elements (Zhu et al., 2011). Boiling can also increase the pH of the liquid in the form of CO_2 loss. The increase in pH will initially increase the solubility of gold, allowing it to be absorbed in the solution but eventually, as H_2S drops from the solution, the solubility of gold will decrease leading to its precipitation and deposition (Henley et al., 1984).

2.6 Hydrothermal Alteration

Hydrothermal alteration can be described as a complex process resulting in mineralogical, textural, and chemical changes, resulting from the interaction of hot aqueous fluids and the rocks with which they circulate, under evolving physio-chemical conditions (Pirajno, 2009) Alteration halo zones are produced from hydrothermal alteration and extend well beyond the limits of mineralisation. Studying alteration can help narrow down the prospective mineralisation area, showing where to focus exploration efforts and therefore reduce costs. Hydrothermal alteration can be hosted in a suite of environments and controlled by a range of factors. Adularia-quartz epithermal systems such as those displayed at Waihi, show distinct geological settings related to crustal rifting in a back-arc rift zone (Corbett & Leach, 1998). The heat source in these environments is deep-seated (>5 km) and consists of melted continental crust, primarily granitic in composition (Henley, 1958). The water source is of meteoric origin and interacts with the heat source at depths where it becomes chemically active with the addition of gasses and other elements. This process results in the formation of chloride-rich fluids which propagate through the host rock via primary and secondary permeabilities, creating chemical disequilibrium

between the fluid and host rocks. As a result, chemical and mineralogical changes occur in the host rock, causing alteration of the original minerals to new mineral assemblages in order to restore equilibrium. Fluids may also undergo changes due to interacting with the wall rock (Browne, 1978).

2.6.1 Controls

There are multiple factors controlling hydrothermal fields that vary in importance from field to field and can be so closely related it is impossible to separate one factor from another (Browne, 1978). Browne (1978) outlined these factors as temperature, pressure, rock type, permeability, duration of rock-fluid interaction, and fluid composition. These factors are widely agreed on the literature with several studies (Muffler et al., 1968; Bird and Elders, 1976), demonstrating that permeability and fluid composition are usually at least as important as temperature. Understanding these factorss is important as many alteration minerals are stable at certain ranges of temperature and pH levels (fig 2.3.) Thus, the geochemical and thermal structure of the hydrothermal system can be reconstructed based on the alteration minerals present.

2.6.2 Mineral zoning

As mentioned above, the geochemical and thermal structures of hydrothermal systems can be reconstructed based on alteration minerals due to their stability over specific pH and temperature levels (fig 2.3.). As epithermal deposits form within a dynamic environment at shallow depths they are prone to significant modification during hydrothermal activity. It is important to distinguish alteration that overprints the system from alteration associated with ore (White & Hedenquist, 1995).

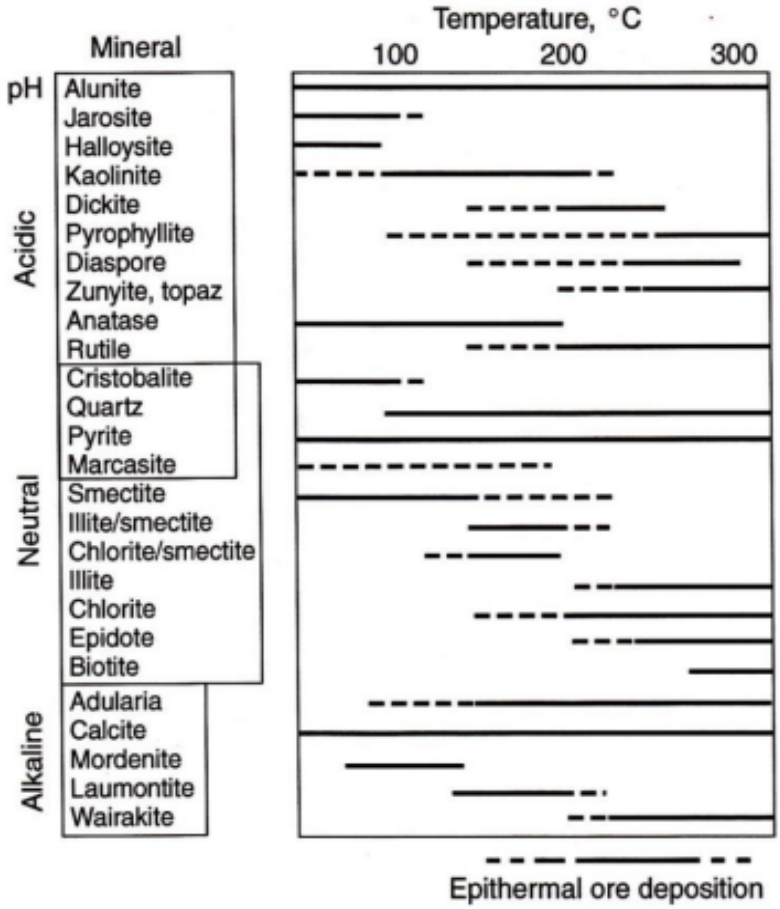

Fig. 2.3. Thermal stability and temperature range of deposition for various epithermal minerals occurring at different pH levels. Derived from Hedenquist (2000).

Near-neutral pH waters are the cause of ore-associated alteration in LS deposits. This water decreases in temperature with decreasing depth and increasing distance from the conduit fluid flow (White & Hedenquist, 1995). Temperature and alteration can be measured directly in active deposits, thus providing an indication of the range of thermal stability of temperature-dependent minerals (Henley & Ellis, 1983). This information can then be used to construct paleoisotherms to aid in locating conduits of paleoflow and infer the level of surface erosion since mineralisation. Data like this is significant as major ore accumulations occur in conduit zones. Erosion information is important as most epithermal-related ore is deposited in the

temperature range of 180 - 220 °C which is equivalent to a depth of approximately 100 m - 800-1500 m below the paleowater table. Low range paleotemperatures indicate a higher likelihood of an epithermal deposit in contrast to temperatures >280 °C which indicate the prime epithermal potential has been eroded (White & Hedenquist, 1995). Paleotemperatures can be inferred based on the variations of basal spacing of clay minerals which are common in the LS alteration environment. Smectite (stable at 160 °C), will alter to interstratified illite-smectite with increasing temperature, while illite on its own, is typically stable at 220 °C (Reyes, 1990). Such progression in thermal stability in LS environments will often result in a distinctly upward and outward zonation of minerals from orebodies. Adularia and calcite occur in the ore zone and are temperature insensitive, however, they indicate the highest pH due to boiling causing CO^2 loss in conduits, increasing pH. Temperature sensitive minerals include zeolites (stable at <220 °C except wairakite), and Ca silicates, including epidote which are stable at temperatures above 200-240 °C. Hydrothermal biotite and amphiboles are indicative of temperatures above approximately 280 °C and are found near the base of the hydrothermal deposit (White & Hedenquist, 1995).

Acidic conditions of HS systems support the stability of minerals such as kaolinite, dickite, pyrophyllite, diaspore and alunite (Reyes, 1990), with a variety of these minerals being temperature sensitive. With high silica concentration, pyrophyllite can form at temperatures <160 °C, however, if it co-exists with illite, dickite or diaspore, then temperatures of >200 °C can be inferred. Topaz, zunyite and andalusite indicate high temperatures (>260 °C) and acidic conditions as they are advanced argillic alteration assemblages. Illite and smectite can become stable further from the conduit as acidic water interacts with the host rock and progressively neutralises. It is important to note that kaolinite and alunite, while acid stable minerals at lower temperatures, can form in LS systems in close proximity to steam-heated water (White & Hedenquist, 1995). Acid-sulfate waters usually occur near 100 °C and can be heated further if they propagate downward along fractures (Reyes, 1990), resulting in hydrothermal alunite and kaolinite occurring in deposits which overprint/overlay ore and make up the top of a low sulphidation deposit. Weathered sulfides can also produce a similar alteration overprint (White & Hedenquist, 1995).

Distinguishing LS and HS mineralisation types is important for exploration as they have varying distribution of alteration zones and the greatest economic potential of each is related to different parts of the system. In HS deposits ore is typically associated with the most acid altered zone. Here, the ore will be surrounded with mineral assemblages indicating less acid conditions. In contrast, LS deposit ore is typically associated with the least acidic alteration with minerals such as adularia and illite or calcite. Acidic advanced argillic alteration in LS systems, containing kaolinite and alunite, represents a near surface overprint and is not directly related to ore mineralisation (White & Hedenquist, 1995).

2.6.3 Styles of alteration

Hydrothermal alteration can be divided into different alteration styles showing variable mineral assemblages forming from each and their respective conditions. This can provide important information about the alteration environment and expected minerals present at different locations of the alteration zone. Dominant mineralogy and chemical changes produced from fluid-host rock interaction are the basis on which the alteration styles are classified (Gifkins et al., 2005). The alteration intensity and mineral assemblages are a function of temperature as well as pressure and it is possible for these to change from one type to another as pressure and temperature conditions change (fig 2.4.).

Potassic alteration

Potassic alteration occurs in deeper, higher temperature areas of the epithermal system, and is characteristic of higher pressures and temperatures relative to other alteration types (Pirajno, 2009). Neutral and basic pH conditions are typical where potassic alteration occurs and common minerals include K-feldspar, adularia, quartz, and magnetite. Sulfide minerals include pyrite, chalcopyrite, galena, and iron sulfides. Minerals such as sericite, albite, apatite and anhydrite may also be present (Corbett & Leach, 1998).

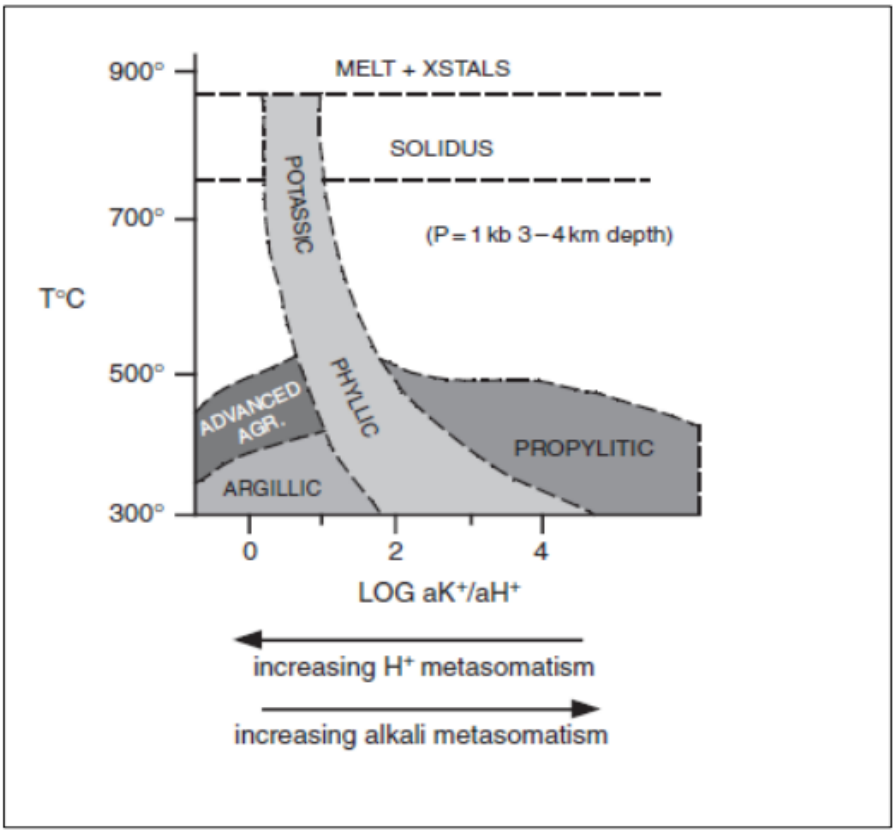

Fig. 2.4. Conceptual evolutionary model displaying alteration types as a function of temperature, K+ and H+. Derived from Piranjo (2009).

Propylitic alteration

Propylitic alteration occurs in temperature conditions of roughly <200 - 250 °C and in near neutral to alkaline conditions. This type of alteration is characterised by the addition of H_2O and CO_2 and locally S with no appreciable H+ metasomatism. Minerals commonly found in propylitic alteration zones include epidote, chlorite, albite, K-feldspar, carbonates, and pyrite. Also, sericite, Fe-oxides, montmorillonite, and zeolite may be common in some places. Zeolites are of significance due to their well-defined pressure and temperature stability at depth. This can aid in the indication of the proximity to the heat source as well as boiling zones where higher-grade gold mineralisation may occur (Pirajno, 2009).

Phyllic alteration

Phyllic (a.k.a. sericitic) alteration is one of the most common types of hydrothermal alterations. It typically occurs at temperatures ranging from >200 - 350 °C in hydrothermally altered sequences. Phyllic alteration commonly distinguishes the margins of epithermal deposits (Corbett & Leach, 1998). This style is typified by quartz-sericite-pyrite mineral assemblages, which is associated with mineral phases such as K-feldspar, calcite, rutile, biotite, kaolinite apatite, and anhydrite. Phyllic alteration grades into potassic alteration by increasing the amounts of K-feldspar and/or biotite. If the number of clay minerals increases then it will grade into argillic type alteration (Pirajno, 2009).

Argillic alteration

Argillic alteration occurs at temperatures between 100 - 300 °C and at a relatively low pH of 4 - 5. It is characterised by clay mineral formations as a result of intense H+ metasomatism and acid leaching (Pirajno, 2009). Argillic alteration will grade inwardly into phyllic zones and will outwardly merge into propylitic zones. Argillic alteration will become intermediate alteration as the presence of chlorite, montmorillonite, illite, kaolin group clays (kaolinite, dickite, halloysite, allophane) and minor sericite becomes present (Pirajno, 2009). In intermediate argillic alteration, K-feldspars may remain unaltered with Ca, K, Na, and Mg not completely leaching out. Zoning can also occur with sericite occurring closer to the phyllic zones and montmorillonite occurring near the outer areas (Pirajno, 2009). Advanced alteration can also occur due to intense acid attack, which causes most of the alkali cations to leach out and the complete destruction of feldspars and mafic silicate phases. Advanced argillic alteration typically occurs in high-sulfur epithermal deposits with the typical mineral assemblages including dickite, kaolinite, pyrophyllite, barite, alunite, and diaspore. At base leaching above 300 °C pyrophyllite, andalusite, quartz, topaz, and pyrite assemblages will be produced (Pirajno, 2009).

Chapter 3
Local geology and structures

3.1 Introduction

The following chapter describes the geological and tectonic context of the study area with an outline of the geological genesis and evolution of the Coromandel Volcanic Zone and its tectonic characteristics. These will be discussed in relation to the epithermal deposits of the region with a focus on the local geology in the study area. The local structure, stratigraphy, alteration, and vein systems also be briefly touched on.

The Coromandel Peninsula makes up the subaerial sector of the Coromandel Volcanic Zone (CVZ), forming a section of the Hauraki Volcanic Region (HVR) of New Zealand (fig 3.1.) originating from the late Cenozoic (Adams et al., 1994). The CVZ is composed of a continental volcanic arc formed under an extensional tectonic regime. This is related to subduction activity associated with the Australian-Pacific boundary. The CVZ was the locus of volcanism in the North Island from the late early Miocene to late Pliocene and is known as the precursor to the Quaternary volcanism and Taupo Volcanic Zone (Adams et al., 1994). The CVZ hosts approximately 50 epithermal Au-Ag bearing deposits situated on a north-south oriented belt extending from Great Barrier Island to Te Puke, 200 km in length and 40 km in width. Christie (2007) divided the goldfield into three provinces, the northern, eastern and southern, based on the host rock and geological setting of the deposit and other characteristics. The HVR has a variety of lithologies, ranging from basalt to rhyolite (Clarke & Govett, 1990), although, andesite and dacite represent 61% of exposed rocks in the goldfield. Miocene-aged Coromandel Group andesite and dacite host 97% of total past gold production, (fig 3.2) with Waihi's Martha Hill deposit as the most productive deposit in the goldfield to date.

3.2 Geological history

The geological history of the Coromandel region began 163 - 145 Ma with the basement sequences of the Manaia Hill Group deposited in the late Jurassic. These metagreywacke rocks accreted onto the Gondwana's margin and are now exposed in the northern and northwest areas of the Coromandel Peninsula. From 105 to 82 Ma extension resulted in the opening of

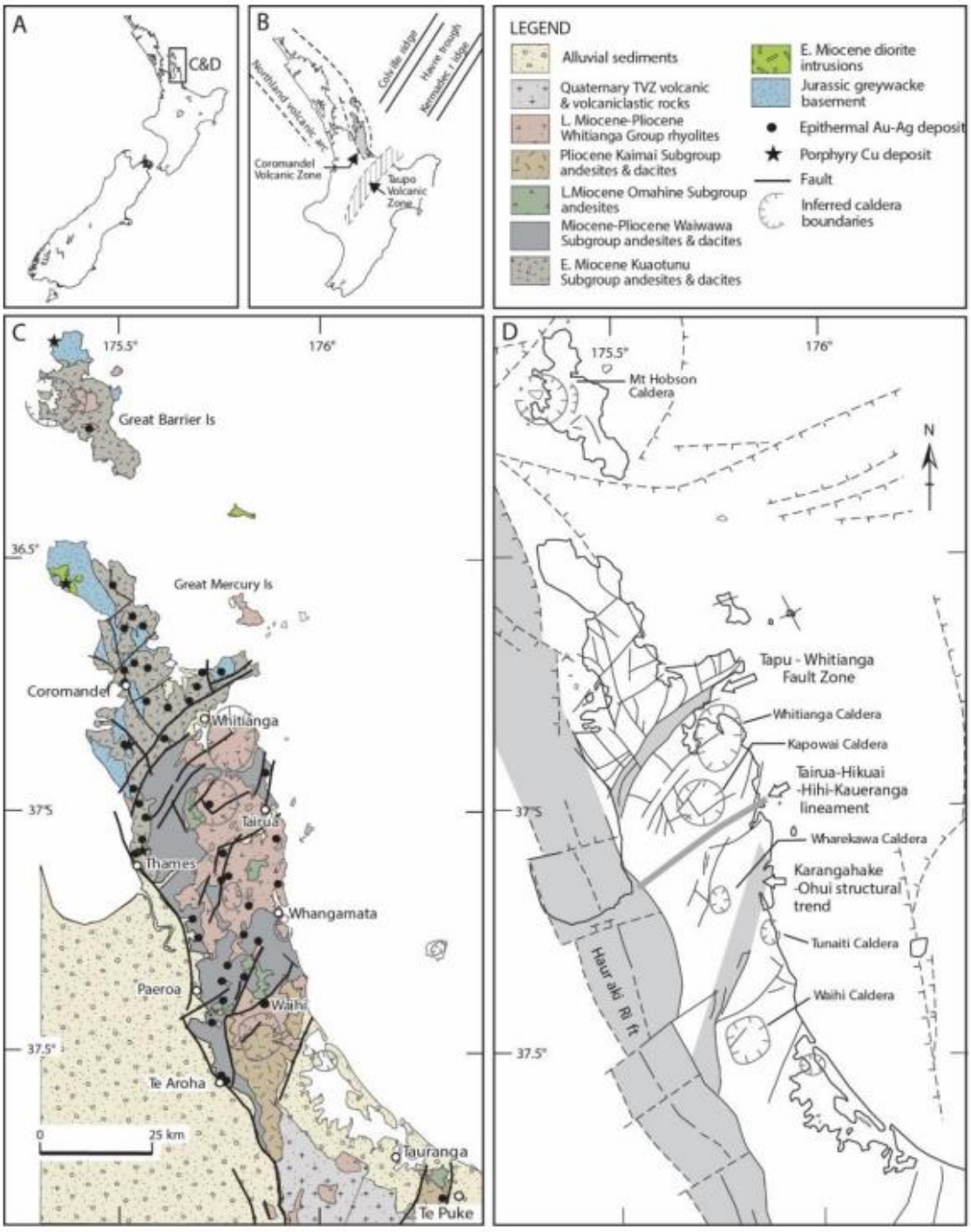

Fig. 3.1. (A) and (B) show the location of the Coromandel Volcanic Zone (CVZ) and the Hauraki goldfield. The regional mineral deposits and geology are shown in (C), while (D) shows the structural features of the Hauraki goldfield and CVZ. Derived from Christie (2007).

the Tasman Sea as New Zealand separated from Gondwana, causing extended periods of marine sedimentation and extensional faulting (Christie et al., 2007). This rifting caused deformation in basement greywacke, resulting in block-faults, some being rejuvenated in the overlying Tertiary rocks (Christie et al., 2007). The folded basement rocks are overlain by Oligocene and early Miocene sedimentary rock in this region, with the Colville Formation of the Waitemata Group acting as the first evidence of volcanism in the form of a volcaniclastic mass flow deposit.

Interpretations of the Cenozoic history of the CVZ vary from paper to paper. However, it is generally agreed that a profound change in tectonism arising from the propagation of the Australian-Pacific plate boundary in the late Oligocene, following the long dormancy of tectonic and volcanic activity, developed a convergent margin representative of today's environment. Subduction of the Pacific Plate was the catalyst to a series of volcanic arcs in the northern North Island; the first one being the Northland Volcanic Arc, primarily composed of basalt and basaltic andesite which was active from 25 Ma until 15 Ma. The CVZ hosted an andesite and dacite belt with volcanism beginning in the early Miocene resulting in predominantly magmas of andesitic and lesser dacitic composition. The continued changing nature and alignment of the Australian-Pacific plate boundary resulted in a propagation of volcanism from Northland to the CVZ. (Christie et al., 2007). Volcanism began in the CVZ approximately 18 Ma with dominant andesite and dacite volcanism. An onset of extension was followed by major bimodal rhyolitic and minor basaltic volcanism. This was followed by a transition to basaltic eruptions occurring from 6 to 4 Ma (King, 2000). Volcanism transitioned across to the current volcanic arc, the Taupo Volcanic Zone, during the period 2.9 - 1.9 Ma; manifested as the Tauranga Volcanic Center (Briggs et al., 2005; Pittari et al., 2021). The mode of volcanism here is represented by voluminous eruptions of rhyolite plus lesser andesite and dacite (Christie et al., 2007).

The dominant lithology of the CVZ is calc-alkaline, medium K rocks, with 61% of exposed rocks in the CVZ being andesite and dacite of the Coromandel Group (Christie et al., 2007). The subdominant lithology is dacite, rhyolite, and rhyodacite rocks of the Whitianga group which make up 30% of exposed CVZ lithology. Kerikeri Group basalts make up <0.1% and Manaia Hill Group greywacke contributes the final 9%. Two key features seen from the volcanism include the younging of volcanic units southward and eastward across the region, and the contrast of predominant andesitic volcanism in western areas and predominant rhyolitic volcanism in the eastern areas (Christie et al., 2007).

3.3 Geology

The geological groups are split into subgroups (table 3.1.) based on differences in age, and erosion due to periods of volcanic and tectonic quiescence. Andesites and dacites of the Coromandel Group comprised the Kuaotunu (early to middle-Miocene), Waiwawa (middle to late -Miocene), Omahine (late-Miocene to Pliocene), and Kaimai (late-Miocene to Pliocene) Subgroups (fig 3.1.; table 3.1.; Christie et al., 2007). The Kuaotunu Subgroup is most abundant in eastern regions of the peninsula, consisting of 17 formations including Cuvier and Paritu Plutonics of the late to early Miocene (Skinner, 1986). The andesitic Beesons Island Volcanic Formation is another formation to the west of the peninsula, made up of subaerial and subaqueous pyroclastic, epiclastic breccias and conglomerates, and intensively hydrothermally altered propylitic, argillic, and siliceous assemblages (Skinner, 1986). The Waiwawa subgroup is divided into Tapuaetahi and Taurahuhue Andesite formations. These formations outcrop north of the Waihi region in the eastern and southern parts of the peninsula (Adams et al., 1994). The Taurahuehue formation is characterised by pyroclastics, sheet-like flows, and minor intrusives of phyric to glassy andesite rocks. and marks the outer northern, and western rim of the Kapowai Caldera. In contrast, the Tapuaetahi Andesite formation consists mainly of coarsely phyric andesite flows, pyroclastics, and intrusives that define the eastern rim of the Kapowai Caldera (Adams et al., 1994). Kaimai and Omahine Subgroups are similar in both composition and age with both subgroups originating from the late Miocene/Pliocene. The Omahine Subgroup comprised the Tauraukiau Andesiteand are characterised by glassy, silicic andesite-dacite flows. These minor intrusives have formed a high plateau between the Waiwawa, upper Rangihau, and Kauaeranga Valleys (Adams et al., 1994). The Kaimai Subgroup formations include the Pukepanga, Uretara, and Waipupu Formations. The Waipupu Formation is the dominant host of epithermal deposits in the Waihi Region and is associated with extensive alteration dating back to the late Miocene (Adams et al., 1994).

In the northern and central Coromandel Peninsula, geological features including subvolcanic dikes, stocks, and plugs of porphyritic dacite and andesite as well as local plutons of quartz diorite to granodiorite intrude the basement and volcanic rocks of the Coromandel Group. However, the mineralogy between the subgroups varies. Alternating pyroxene andesite and hornblende-pyroxene andesite to dacite sequences characterize the Kuaotunu Subgroup while

pyroxene andesite is the predominant mineralogy of the Waiwawa and Omahine subgroups (Christie et al., 2007).

The Whitianga Group consists of the Minden, Coroglen, and Ohinemuri, rhyolitic subgroups (table 3.1.), of the late Miocene to Pliocene (Christie et al., 2007). The Whitianga Group is preceded by the Kuaotunu and Waiwawa Subgroups of the Coromandel Group and are typically overlain by the Omahine Subgroup. The Minden Group is comprises flow-dome and caldera

Table 3.1. Stratigraphy and ages of CVZ lithologies. Modified from Skinner

Group	Sub Group	Formations	Mid Pleistocene
Whakamarama		Waitearíki Ignimbrite Aongatete Ignimbrite	Mid-Pleistocene
	"Waitawheta Dacite"	Informal	Pliocene - Pleistocene
Kerikeri Volcanic	Mercury Basalts	Mercury Islands Woody Hill Colville Ridge	Late-Pleistocene and/or younger
Whitianga	Minden Rhyolite	Ahu Ahu Rhyolite Whenuakite Rhyolite Ohena Rhyolite Purangi Rhyolite Ruahine Rhyolite Rangihau Rhyolite	Late-Miocene to Pliocene
	Coroglen (Ignimbrite)	Ahu Ahu Ash Pumpkin Rock Ignimbrite Wharepapa Ignimbrite Carina Rock Ignimbrite	Late-Miocene to early-Pliocene
Coromandel	Omahine	Taurauikau Andesite	Late-Miocene to Pliocene
	Kaimai	Pukepanga Uretara Waipupu	Late-Miocene to Pliocene
	Kiwitahi	Several centres	Mid to late-Miocene
	Waiwawa	Tapuawtahi Andesite Taurahuehue Andesite Maumaupaki Whiritoa Andesite	Late-Miocene
	Kuaotunu	Cook Intrusives Huruhi Andesite Maunganui Basaltic Andesite Mahinapua Andesite Waitaia Sinter Rauporoa Basaltic Andesite Te Tutu Andesite Parakete Materangi Andesite Whangapoua Andesite Beesons Island Volcanics Tuateawa Andesite Te Karaka Andesite Kai-iti Porphyrites Kokumata Dacite Omoho Formation Port Charles Andesite Paritu Plutonics Cuvier Plutonics	Early to mid-Miocene Early-Miocene
Waitemata	Kawau and Warksworth	Colville	Early-Miocene
Te Kuiti		Torehina	Mid to late-Oligocene
Manaia Hill		Several formal units	Late-Jurassic

complexes, originating from felsic calc-alkaline to alkaline lavas that are predominant in the east and west of the Waihi region. The Ruahine Rhyolite from the Minden Formation Subgroup can be found across the Whitianga and Kapowai areas, characterised as phyric, glassy, and perlitic crystal-rich rhyolite intrusive domes (Adams et al., 1994). The Coroglen Subgroup varies from the Minden Subgroup in that it consists of rhyolitic pyroclastic and volcaniclastic sedimentary rocks. The main formations of this subgroup are Carina Rock Ignimbrite, Pumpkin Rock Ignimbrite, and Wharepapa Ignimbrite. The Minden and Coroglen Subgroups are most abundant in the southern and central regions of the Coromandel Peninsula (Christie et al., 2007). Finally, the youngest phases of the Whitianga Group are represented by the Ohinemuri Subgroup. This subgroup is composed of Pleistocene ignimbrites and occurs in the south of the CVZ.

Another group in the CVZ is the Kerikeri Volcanic Group (table 3.1.). This group exclusively occurs in the north-eastern part of the peninsula and offshore islands. This volumetrically minor group consists of the Mercury Basalts, ranging in composition from olivine and olivine-augite basalt to pyroxene basalt and basaltic andesite. The group's estimated age is of the late Miocene and /or younger. The Mercury Basalts form a bi-modal rhyolite-basalt assemblage with the rhyolites of the Whitianga Group (Skinner, 1986; Christie et al., 2007).

3.4 Coromandel Volcanic Zone Structure

During the Cretaceous Period, multiple block faults formed in the Manaia Hill Group basement greywacke. These faults were inferred to have reactivated in the volcanic rocks of the CVZ, representing many of the faults across the Coromandel Peninsula (Christie et al., 2007). These range from major faults which cut across the whole peninsula to individual faults a few hundred to a few thousand metres in length, including those filled with epithermal quartz veins. Some veins are also related to the active Hauraki Rift in the west, and the Colville Ridge to the east (fig 3.1.; Christie et al., 2007). The veins and faults have strikes of NNW and NNE to ENE, with the NNW striking faults equally downthrown to the east and west. However, most of the NE and ENE striking faults are downthrown to the south (Skinner, 1986). The Jurassic Basement has been lowered to the south due to this fault displacement, causing the volcanic sequences to thicken toward the TVZ with stratigraphy gently tilting eastward (Christie et al., 2007).

Other structures include a NNW-aligned belt of calderas, including the Waihi, Whitianga, Kapowai, Wharekawa, and Tunaiti calderas, which are present across the eastern Coromandel Peninsula (fig 3.1.), and are associated with Whitianga Group rhyolites. Another major structure is the currently active Hauraki Rift which bounds the peninsula to the west and extends from Little Barrier Island to more than 300 km south to the TVZ, where it is buried beneath ignimbrites from the late Pleistocene (Briggs et al., 2005). The Hauraki rift structure has downthrown volcanic rocks of the Miocene to Pliocene by one to three kilometres (Hochstein & Ballance, 1993). The initiation of the rift structure is estimated to have occurred in the late Miocene while the main subsidence took place later on, roughly between one and two million years ago (Briggs et al., 2005; Hochstein & Ballance, 1993).

3.5 Hauraki Goldfield

The Hauraki Goldfield stretches the length of the Coromandel Peninsula, and is a major gold-producing region, hosting approximately 50 adularia-sericite low sulphidation Au-Ag deposits. Having produced 320,000 kg of Au and 1.5 million kg of Ag since 1862, the economically significant deposits include Broken Hills, Ohui, Onemana, Favona, Golden Cross, Karangahake, and the world-class Martha Hill. The majority of these deposits are hosted in pyroclastics and andesite, with few rhyolite hosts. Massive andesites host the widest veins as opposed to well as silicified breccia zones and rhyolite which hosts thin quartz veinlets due to its weaker structure. Such quartz veins occur as open-space fissure fillings in epithermal systems with frequent crustiform banding textures. Apart from quartz, vein minerals include adularia, barite, siderite, calcite, manganiferous carbonate, and anhydrite. Sulfides can also occur in veins with pyrite being the most common. Electrum and native gold make up the predominant economic ore minerals (Christie et al., 2006). Christie et al (2007) split the goldfield into provinces based on age, host rocks, Au/Ag ratios, variability of vein strike, grain size of quartz, differences in vein texture, and relative abundance of key minerals such as adularia, calcite, and arsenopyrite. These provinces were named the northern, eastern, and southern (fig 3.3.).

The Southern Province is of most relevance to this study with the south of the Eastern Province along the province margin also being of interest. Gold deposits occur in a range of lithologies (fig. 3.2.), and in the Eastern Province they are primarily hosted in the rhyolite of the Whitianga group, but may also be hosted by, or extend downward into the Waiwawa Subgroup andesite

and dacite in local instances (Broken Hills, Neavesville; Christie et al., 2007). Mineralisation in this province generally dates from 7.1 to 6.3 Ma with deposits typically occurring in the shallow epithermal environment and eroded to shallow levels, indicated by hydrothermal eruption breccias and the presence of sinters. Relative to the underlying andesites of the Coromandel Group, the Whitianga Group rhyolites host thinner veins, often tightly clustered, with less extension by vein opening. This is due to the higher porosity and weaker structural integrity of the rhyolite which can facilitate disseminated Au-Ag mineralisation resulting in the disseminated Au present at Broken Hills and Neavesville. Other common features of this province include host rock being replaced by adularia in veins and veins having a wide range of strike directions (fig 3.3.; Christie et al., 2007).

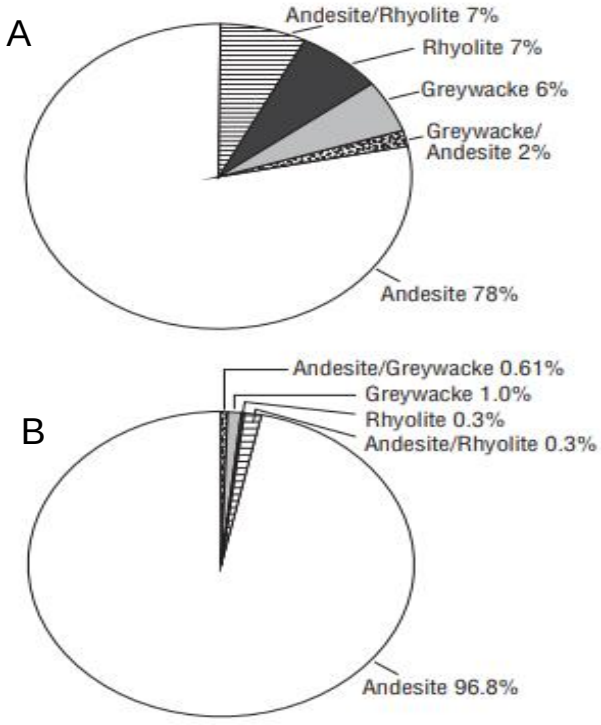

Fig. 3.2. Proportion of major lithologies in relation to numbers of Au-Ag deposits (A), and Au production (B). This shows that while deposits were found in all lithologies (A) the majority of production was in andesite/dacite (B). Andesite = andesite and/or dacite.

The Southern Province has produced more than 80% of the recovered Au from the Haruaki goldfield. Such deposits occur in the Waiwawa Subgroup andesites and dacites, (fig 3.2) rarely extending upward into the overlying Whitianga Group rhyolites (Karangahake) (Christie et al., 2007). Host rocks typically formed 8 Ma with inferred (radiometric dating) simultaneous mineralisation with host rock formation approximately 7 and 6 Ma. Deposits are typically eroded to intermediate levels with the exception of Martha Hill and Karangahake which exhibit large vertical intervals of erosion. Southern Province deposits have a relatively low range of vein strike directions, most commonly NE. Crustiform and colloform textures are common in veins which are filled with cryptocrystalline or finely crystalline quartz and accompanied by accessory minerals including adularia and calcite. The host rocks surrounding the vein are often replaced with adularia. These deposits often have relatively low Au/Ag ratios.

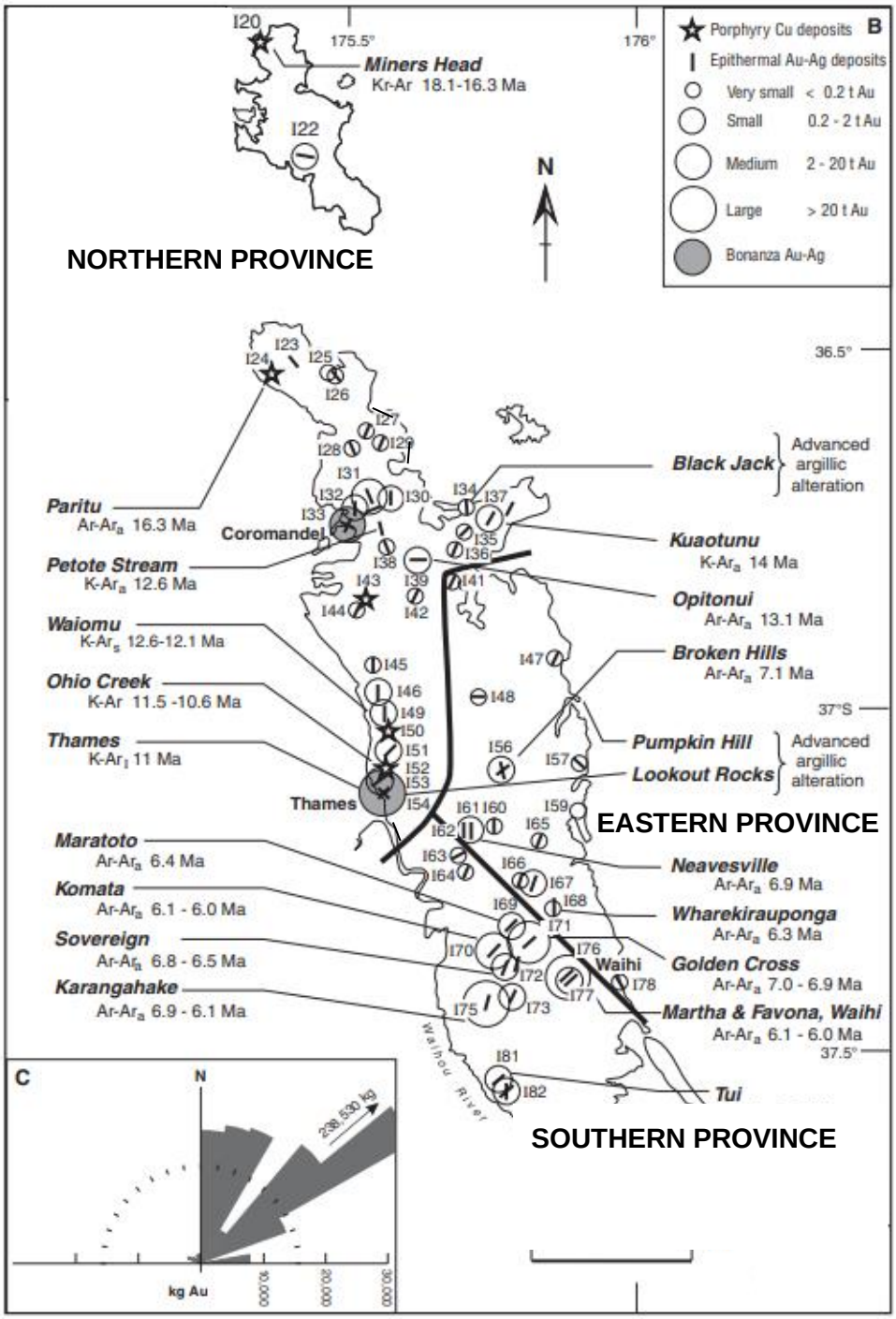

Fig. 3.3. Division of Hauraki Goldfield into Northern eastern and southern provinces. Location of mineral deposits in the Hauraki goldfield, past Au production, and ages of deposits with bar direction indicating main strike of veins at each deposit and Subscripts show the type of mineral dated: a = adularia, i = illite, mo = molybdenite, s = sericite(B). Vein strike directions scaled to gold production. Where there are different vein trends within the same deposit (e.g., Hauraki and Thames), they are shown separately where possible. The plot shows the lack of production from veins with strikes between 270° and 360° and between 070° and 090° (C). Derived from Christie (2007).

3.6 The mineralisation and alteration at Martha Mine

Although this study is not focused on Martha Mine, an understanding of the epithermal processes occurring here could help in making inferences on the prospect in this study, located approximately 4 km NNE. The epithermal deposits of the Hauraki goldfield are quartz ± calcite ± adularia ± illite types. Propylitic alteration (quartz + calcite + chlorite + illite + pyrite), potassic alteration (quartz + adularia + illite + pyrite ± chlorite ± albite) and argillic alteration (illite + smectite + chlorite + pyrite) are the three main alteration styles identified at Martha Mine with deposits hosted in hydrothermally altered andesite of the Waipupu Formation (Brathwaite et al., 2006). The majority of argillic alteration is restricted to the uppermost part of the vein system, specifically in the eastern region on the Martha lode hanging wall where the argillic alteration locally overprints the other alteration styles. Propylitic and potassic alteration is largely controlled by the proximity to quartz veins, with the quartz veins immediately surrounded by a zone of pervasive potassic alteration which is, in turn, surrounded by a zone of propylitic alteration.

Microcrystalline to medium-grained quartz and quartz vein breccias are the fill of the major lodes at Martha Hill, accompanied by pyrite, sphalerite, galena, chalcopyrite, and acanthite occurring as sulfide-bearing bands. A complete paragenesis of the veins is intricate and complex. However, there have been numerous phases that have been identified, deducing that the early stages of mineralisation of the major lodes consist of platy calcite + quartz, followed by the main stage of quartz + sulfides and a late stage of amethyst (Brathwaite & Faure, 2002; Brathwaite et al. 2006). Multiple vein-forming phases occurring over an extended length of time make up the main quartz stage, while amethyst, although only representing a minor phase, distinctly marks the final event of the vein deposition sequence (Fig 3.4.) (Brathwaite & Faure 2002; Brathwaite et al. 2006). Vein paragenesis can be altered due to depth and this can be seen in the texture of the veins. Above approximately 70 m above sea level (asl) or 1070 m relative level (RL), quartz forms as colloform and crustiform veins composed of mm-scale bands of microcrystalline and fine-grained crystalline quartz. The fine-grained crystalline quartz often occurs as fine comb quartz, enclosing small cavities. The colloform quartz locally hosts minor pyrite, chalcopyrite, electrum, sphalerite, acanthite, and tetrahedrite. It can be inferred that adularia was deposited early in the vein-filling sequence from the minor adularia bands in contact with the wall rock. Contrarily, below approximately 70 m asl or 1070 m RL, interbanded

crustiform veins of fine to medium-grained quartz and sulfides, including pyrite, chalcopyrite, galena, and sphalerite, make up 3 - 80% of some bands. Hydrothermal breccia consisting of angular vein quartz or fragments of wall rock in a fine-grained quartz matrix are common in veins. Cockade overgrowths of quartz and sulfide often form around the wall rock fragments.

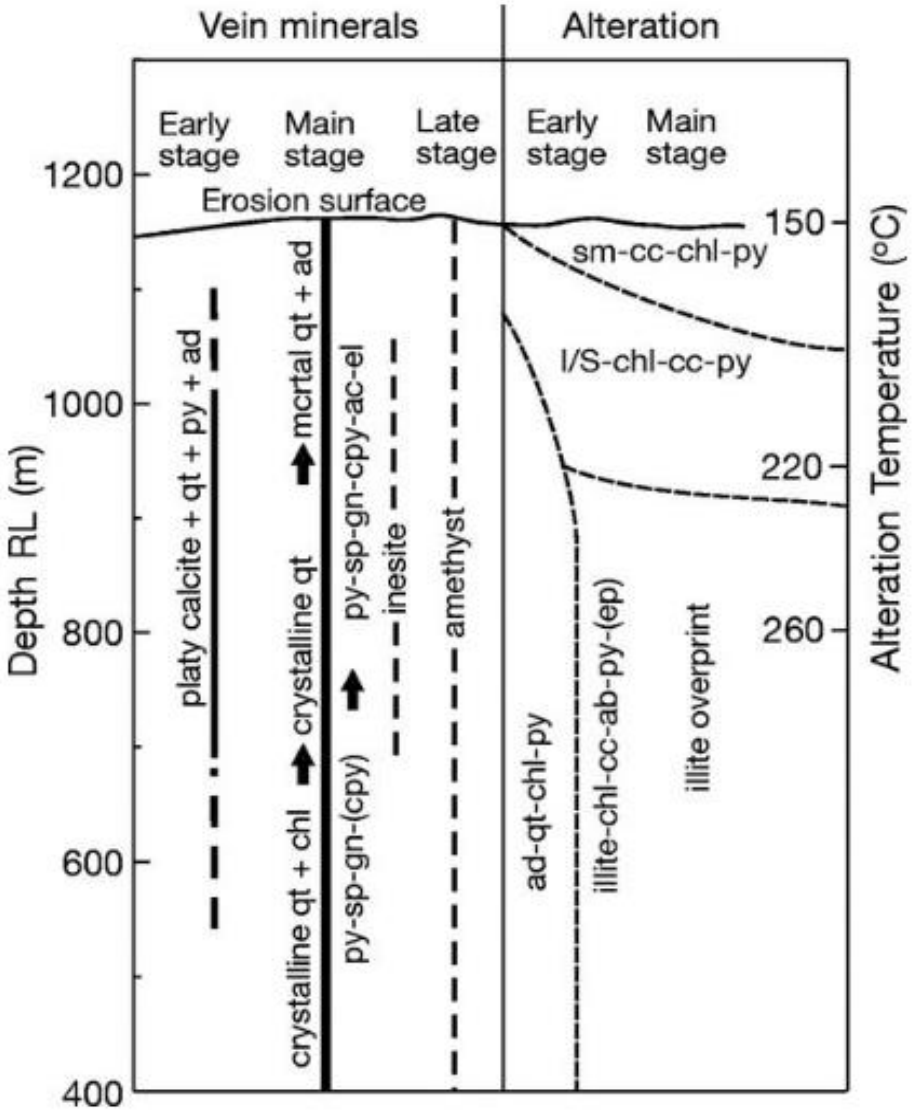

Fig. 3.4. Variation in hydrothermal alteration of the Waihi epithermal system with depth and time. Abbreviations: ab = albite, ad = adularia, cc = calcite, chl = chlorite, cpy = chalcopyrite, el = electrum, ep = epidote, gn = galena, I/S = interlayered illite/smectite, mcrtal = microcrystalline, py = pyrite, qt = quartz, sm = smectite, sp = sphalerite. Derived from Brathwaite and Faure (2002).

3.7 Study area Geology

The study area is located in an area approximately 4 km NNE of the Martha Hill mine, covering approximately 1.5 x 2 km over both farmland and conservation land. The geology specific to the area was mapped by Brathwaite & Christie (1996), which includes the surface geology of the Whiritoa andesite, a phyric, plagioclase and two pyroxene andesite including dacite flows and domes with tuff breccias and lithic crystal tuff, in the southeast of the study area, and the Waipupu Formation, a phyric, plagioclase and two pyroxene andesite and dacite with local quartz phenocrysts, minor tuff breccia, crystal tuff, and lacustrine sediments, in the northwest. The Waipupu Formation displays extensive hydrothermal alteration. The boundary between these formations bears a propylitic and argillic hydrothermal alteration zone with quartz-adularia-sericite adjacent to the quartz loades. This alteration assemblage occurs on the Waipupu Formation side of the boundary, before cutting westward across the Whiritoa Formation. The Whiritoa andesite occurs in the southern section of the study area, continuing down to approximately 750 m below sea level where it overlays the Manaia Hill Group. The contact between the Whiritoa and Waipupu Formations extends to the Manaia Hill group where the Whiritoa overlays the Waipupu at an angle of roughly 22°. For the rest of the study area, the Waipupu Formation is the dominant lithology (Brathwaite & Christie, 1996).

Chapter 4
Volcanic facies and core log descriptions

4.1 Introduction

Chapter 4 defines and identifies the facies and variations on macroscopic scales from the drill core. The methods used to log the core, including detailing the parameters used to make descriptions and the process of digitisation are outlined first. Facies are then defined and described with examples from the core photos. The geological facies characteristics down each hole will be described and accompanied by a digitised graphic log. Categorising these facies is useful for determining the volcanic origin of the core as well as making comparisons to other units with similar characteristics, which can also give an idea as to some of the processes responsible for the genesis of the facies identified.

4.2 Core logging methods

Primary core sampling was conducted at the Oceana Gold core shed in Waihi. Samples of core from seven holes were collected with their primary use to be made into thin sections, observed for XRD analysis and XRF analysis. Core was selected primarily based on where visible changes in the core's texture and colour were observed. A sample, approximately 15 - 110 cm, was taken from the core for each new texture. At each location where the core was taken, the depth of the core, (e.g 85.25 m - 85.67 m) and the destination of the sample (University of Waikato) was recorded for Oceana Gold's records. A project record was also made to easily manage the samples in the future. There was limited availability to physical core early in this project, so analysis was restricted to on-site sampling and desktop logging from photographs, supported by the samples collected.

Five holes are investigated in this study: WNDD005, WNDD006, WNDD007, WNDD009 and WNDD011. A complete photographic record of the core was acquired from these holes totaling 2,888.5 m of core. Some of the holes had been logged for geotechnical purposed but for several of these cores, this study was the first time they are described from a geological perspective. Logging from the photos was conducted on the holes using a logging template that focused on the geology of the core with each page logging 100 m with 2.5 m intervals (Fig. 4.1.).

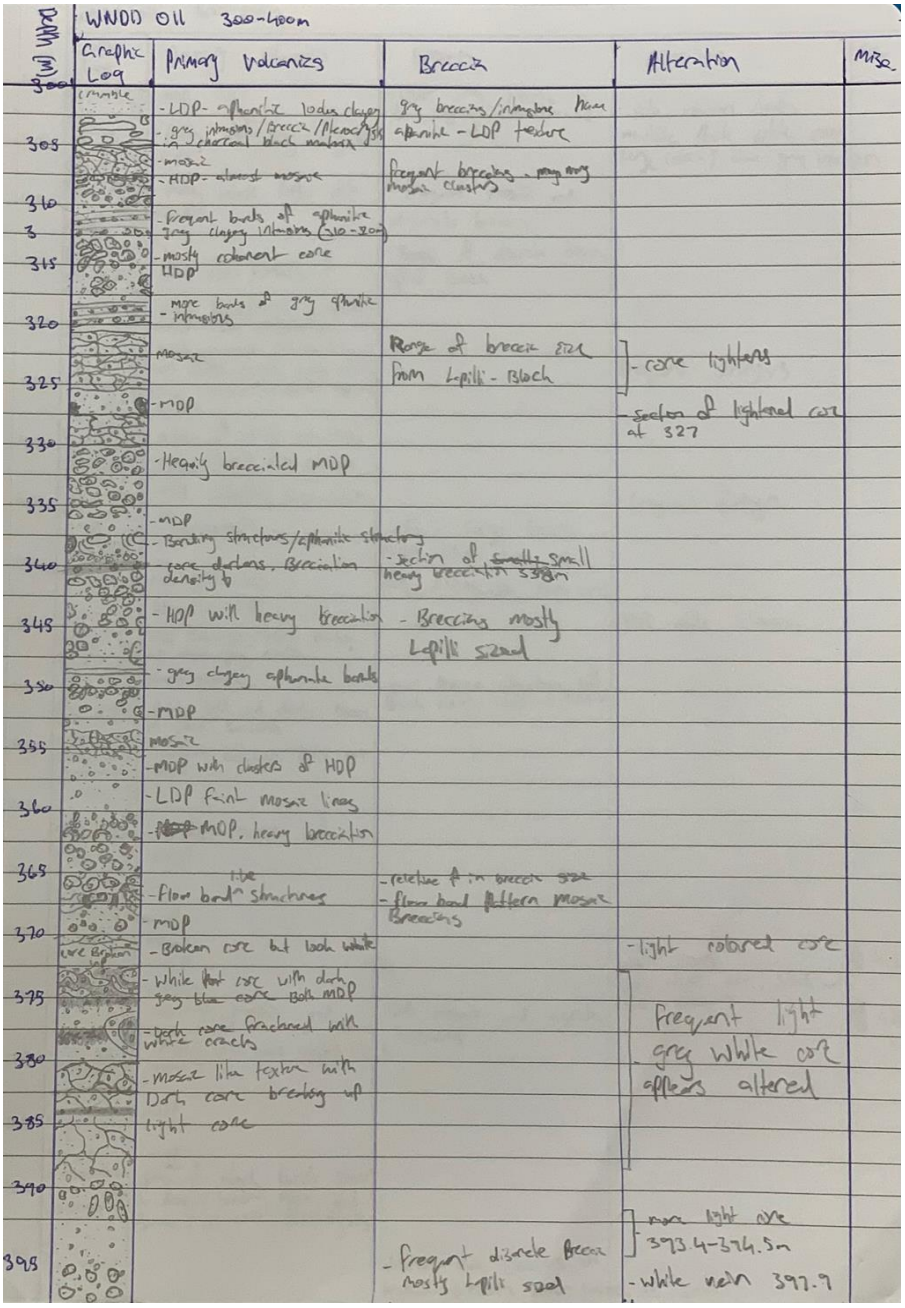

Fig. 4.1. Template used for the initial hand logging of core photos.

The logs were drawn by hand and summary logs were digitised. The core descriptions were broken up into three categories: primary volcanics, breccia and alteration along with a miscellaneous column for any notable features and labeling where each sample was collected.

Observations for logging the core had to be made primarily based on the physical appearance as seen in the photographs.

The primary volcanics column described the texture of the core based on the coherency of the fabric (i.e., coherent versus brecciated), as well as the visual concentration of phenocrysts (i.e., low to high concentration). This was based on eye estimations, using a phenocryst to groundmass percentage template shown in figure 4.2., (Cas et al., 2009). It was recorded whenever the texture changed. The colour and banding were also described in this section with colour being taken, in some places using the Munsell colour chart when needed to define discrete colour changes. Grain colour was also noted as mafic if they were dark or felsic if they were light. Features such as irregular banding patterns in the core and intermittent bands of varying colour were noted and described.

In the breccia section, the breccias were described based on their clast size, colour, and the phenocrysts. Size could be measured based on the relative length against the known length of the core box. It was also noted whether the breccia occurred in a mosaic pattern or if the clasts were separated in a random orientation and if so, the concentration was noted. The extent of brecciated textures was also recorded in some sections of the core. In some sections increases and decreases in brecciation intensity are noted based on the concentration of breccias.

In The alteration section, veins were noted and their colour was described. It was also noted if the veins occurred as a stringer vein or larger vein. The vein orientation was recorded, along with their shape, where relevant, and any internal textures, if present. This section was also used to assess if the rock appeared altered or not, primarily based on colour, along with the extent of the inferred alteration. Notable features such as sharp boundaries, thick veins or unusual textures were also noted with their depth recorded.

A graphic log was also recorded to provide a generalized visual overview of the textures in the core and how they changed. This log only applied sharp boundaries when observed in the core. Graduations in facies were blended graphically.

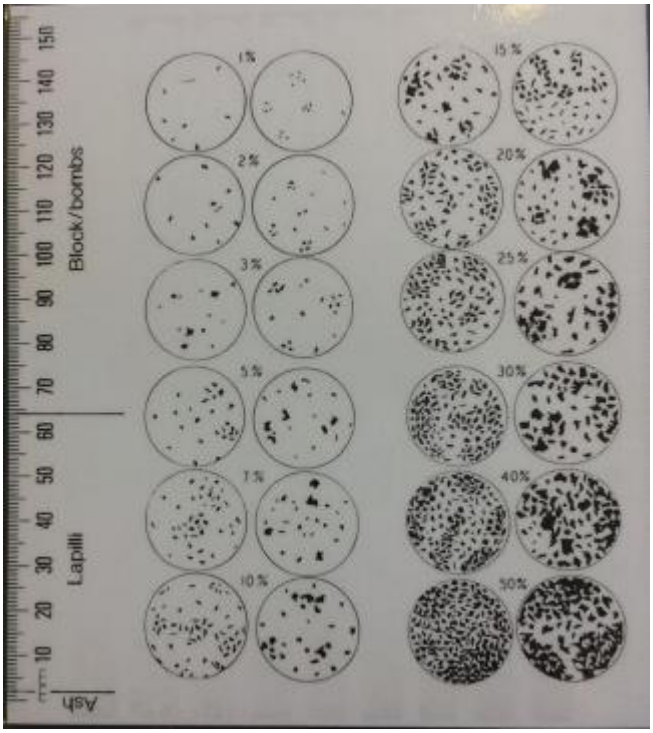

Fig. 4.2. Template from Cas et al (2009) used to visually estimate phenocrysts to groundmass percentage.

This logging process resulted in 35 pages of hand drawn core log; each hole was simplified to one - two pages and digitised using Adobe Illustrator. The template was recreated in the software using a standardised scale with 12.5 m intervals to allow for comparisons. Templates were then created to represent different textures and features in the log such as mosaic breccia and banding. This was done in order to digitize the core in a reasonable time, with distinct features being manually drawn when they occurred. Parts of templates could also be mixed with others to represent the flow of textures in the core as opposed to a graphic log showing sharp inaccurate boundaries at every change in texture. Colours were used to represent the main facies type with graphics depicting the variations of facies. Finally, opaque white rectangles were used to represent the sections that had undergone alteration. The samples were also recorded where they occurred in the core with their corresponding slide number.

4.3 Facies descriptions

Facies were primarily based on the visible coherency of the rock fabric, before being characterised by their estimated phenocryst concentration, brecciation and concentration of breccia clasts. The presence of irregular banding structures was also included in the classification of facies as it is representative of the rock fabric. As there was almost 3 km of core logged, generalised facies were required. Sub-facies were then described (e.g., lapilli-sized medium-concentration porphyritic), based on single factor characteristics such as grain size, intensity of brecciation, breccia size and phenocryst content. Often, facies can also be combined (e.g. brecciated, low-concentration porphyritic).

4.3.1 Porphyritic facies

The porphyritic facies represent coherent sections of the core and are subdivided into Low crystal concentration porphyritic (LCCP), medium crystal concentration porphyritic (MCCP), and high crystal concentration porphyritic (HCCP) (Fig. 4.3.). Crystal concentration was the primary characterising agent of these facies, using visual estimation based on the crystal concentration chart from Cas et al, (2009). LCCP facies are porphyritic in texture, verging on aphanitic with a crystal concentration of 1 - 5% and can consist of mafic and felsic crystals typically 0.2 mm to 64 mm in size. MCCP facies have a porphyritic texture with a crystal concentration of 6 - 24% consisting of mafic and felsic crystals from less than 0.2 mm to 6 mm in size and often occur concurrently with other facies. HCCP facies have a porphyritic texture, sometimes verging on phaneritic with a concentration of >25%. Consists of mafic and felsic crystals ranging in size from 0.2 mm to 6 mm. All the facies above can occur across a range of core colours.

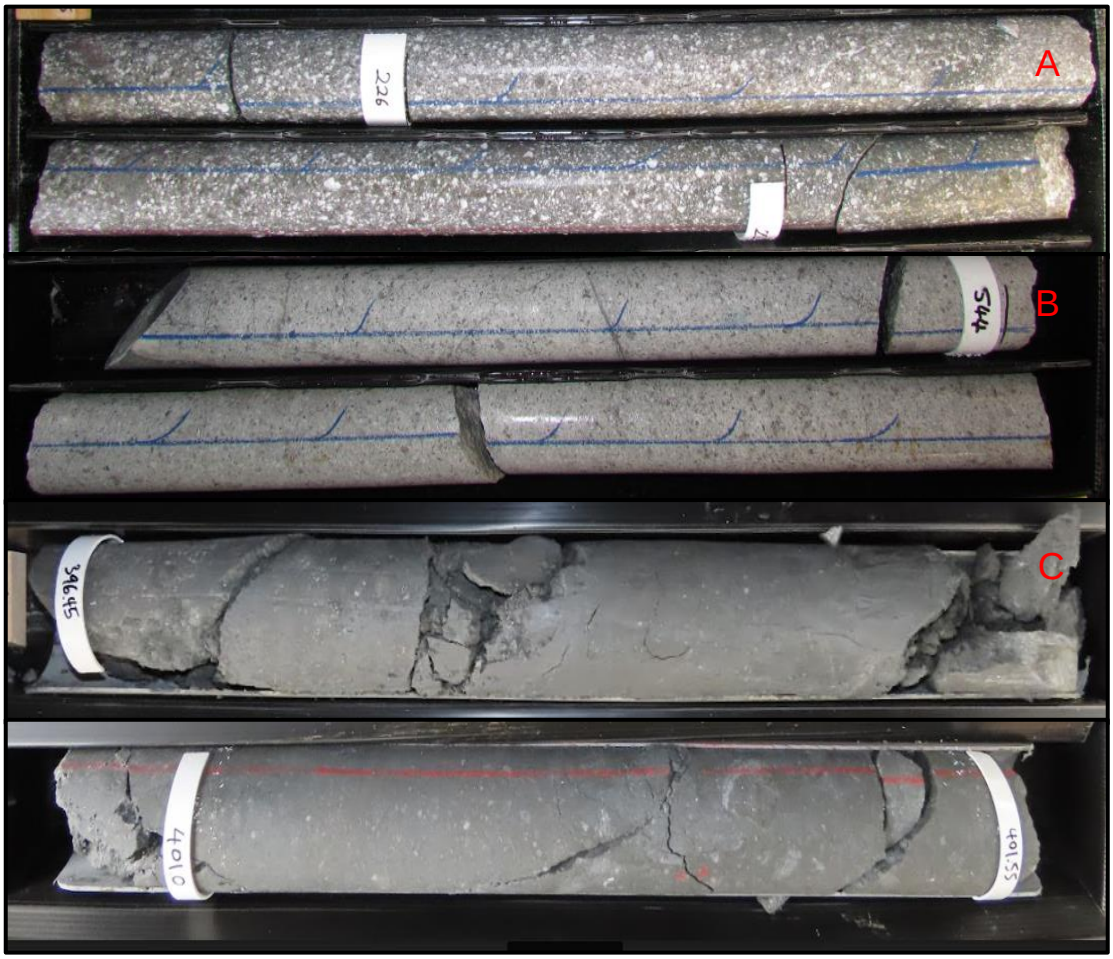

Fig. 4.3. Porphyritic facies: (A) High density porphyritic, (B) medium density porphyritic, (C) Low density porphyritic.

4.3.2 Intermittent pattern facies (IP)

The Intermittent Pattern (IP) facies describes the area of the core where the fabric alternates between different colours in an irregular banding pattern (Fig. 4.4.). This facies is commonly used in conjunction with other facies but represents a break of coherency in the core that is not represented by any of the breccia facies described below. Such patterns often occur on the scale of thickness from 2 mm to >64 mm and can take the form of irregular flow-like shapes. However, these most commonly occur as crescents bearing 0.2 mm to 6 mm sized crystals. Colours can vary in shades from charcoal grey to cream white, sometimes occurring together in the same pattern.

Fig. 4.4. Intermittent pattern facies.

4.3.3 Brecciated facies

The brecciated facies includes **sparse discrete breccia**, (SDB), **discrete breccia** (DB), **weak mosaic breccia**, (WMB), and **mosaic breccia** (MB) (Fig 4.5.). These four facies are characterised by the concentration of breccia clasts and their spatial distribution in relation to neighboring breccia clasts. The SDB facies consists of individual breccia clasts which do not frequently occur within close proximity to other breccia clasts and show a clast concentration of less than 10%. The DB facies follows the same characteristics as the SDB facies, but clasts occur more closely to each other while still maintaining their individual separation. The WMB facies occurs as breccia clasts that are situated within close proximity to each other and begin to align with the breccia clasts surrounding it but have poorly distinctive clast margins making them appear to blend in with the groundmass; they also occur in low concentrations. MB facies display tightly clustered breccia clasts which are orientated with each other resulting in a "jigsaw" like fit. All these facies can host breccia clasts of sizes ranging from lapilli to blocks/ bombs as well as a variation of crystal concentrations within the clasts. As a result, they are often paired with other facies or have these factors described to form sub-facies.

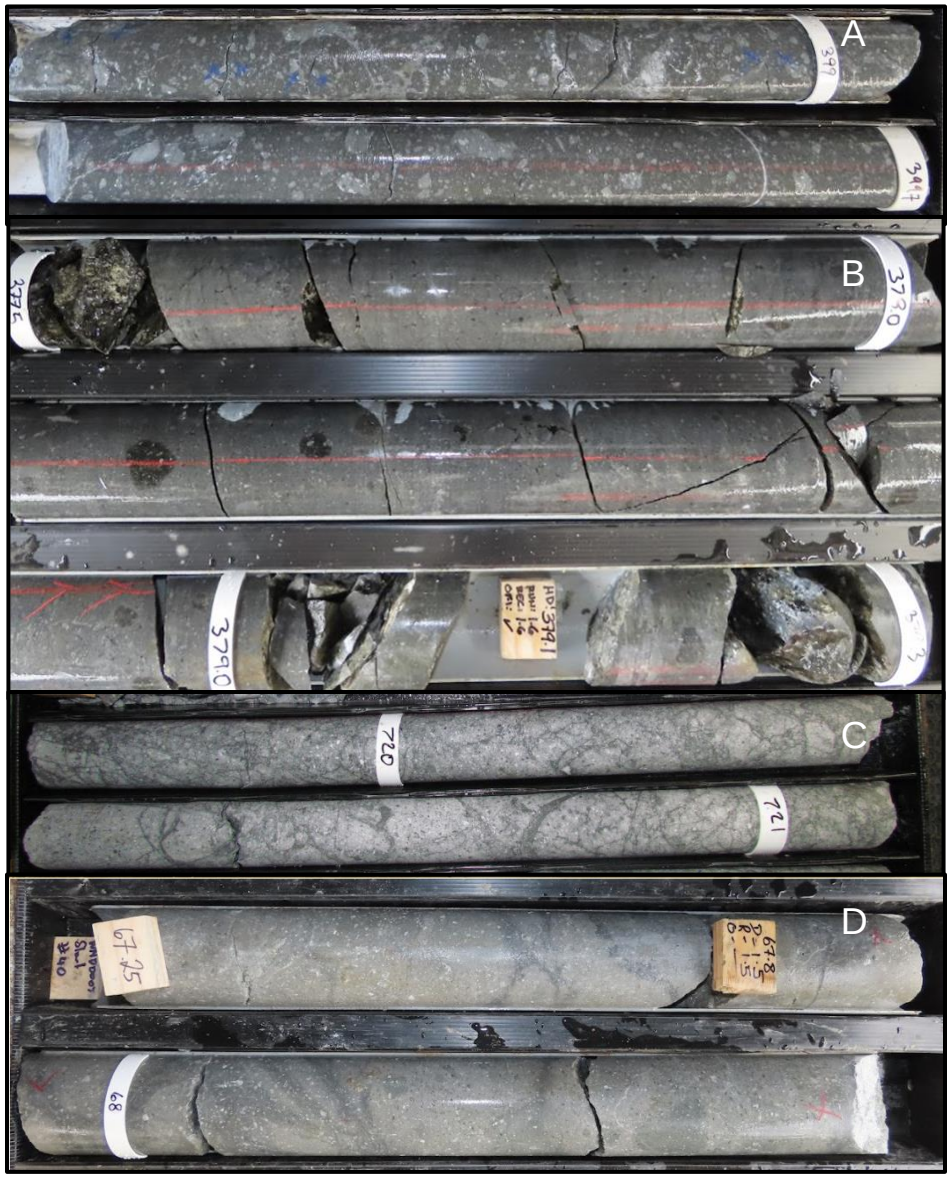

Fig. 4.5. Brecciated facies: (A) discrete brecciation, (B) sparse discrete brecciation, (C) mosaic brecciation, (D) weak mosaic brecciation.

4.4 Down-hole descriptions

The figures below (4.6. - 4.10.), illustrate the facies distribution and inferred zones of alteration down each drill hole. As mentioned above, the logging provided a very general overview where changes in facies of <3 metres have typically been ignored unless it is the dominant facies in each 12.5 m segment. A more detailed description can be found in appendix A.

4.4.1 WNDD005

Hole WNDD005 is the western most drill hole (Fig. 1.1.). It is an angled drill hole in the northwest direction (bearing 309) with a dip of roughly 60°. The hole starts at 276 m above sea level and is 838.8 m long, finishing at a depth of 143.5 m below sea level. The first 17 m of the core is made up of brown/orange soil and clay, before a section of light grey crumbled core, too broken to determine any textures or facies, continues to 50 m deep. The consolidated core begins at around 50 m with the SDB facies merging into the DB facies and finally into MB at 75 m. Breccias display a light grey to orange colour, hosting mafic phenocrysts grading into light grey mosaic breccia clasts approximately 10 m to >50 mm in size. The next consolidated core begins at 82 m with a light grey to chalk white coloured LCCP texture, hosting a high concentration of white veins including many stringer veins, continuing until 112 m. At 112 m the light grey MB facies grades in, then grades out into the DB facies. At 136 m the core sharply changes to the HCCP facies with 2 mm to 6 mm, predominantly felsic phenocrysts. This continues until 160 m where breccia-like clasts, lapilli to block/bomb in size begin to occur leading to a HCCP-SDB facies continuing until 175 m. The next 125 m displays a variety of porphyritic facies with some IP facies. Predominantly HCCP - MCCP facies occurs with segments of porphyritic IP facies. The first of which, occurring from 176 m to 185.5 m displays grey and charcoal grey band-like structures, mostly in crescent-like shapes facing downhole but other orientations are also present. This banding also occurs in a minor section at 200.5 m to 206 m. Aphanitic sections of fine-grain clay material <2 m in length occur between 192.5 m and 208.2 m. MCCP facies precedes this with a very slight brown-green tint which grades into a segment of light grey HCCP core with mafic and felsic phenocrysts. Light core colour in some areas appear altered but they are very minor. IP facies occur in the middle of the HCCP segment and again at the end at 253 m. A small section of MCCP core follows this before a long section of the porphyritic WMB core with varying grades of brecciation are observed. IP facies occur here in minor

quantities. This section continues to 329 m hosting IP facies with white and black irregular banding structures, thick white veins, and chalky white coloured core. At 329 m the veins continue, primarily as white stringers in a MCCP facies with lapilli-sized phenocrysts and a slight green tinge to the core. The next 70 m consists of the MCCP facies just described amongst segments of frequent IP facies and WMB facies with continuous white veins of various orientations and thicknesses, some bearing phenocrysts or fragments of groundmass. These facies appear to be in weakly altered rock, due to the light green tinge as well as very light grey-chalk white rock. At 400 m facies become more consistent with a large section of large ash to small lapilli MCCP core, hosting a variety of white veins in multiple orientations with a range of thicknesses. Intense alteration appears to begin at 416.5 m as the rock becomes bleached white. This remains consistent with the abundant white veins subsiding at 450 m and minor IP facies and irregular structures occurring from 450 m onward until 595 m where a dominant porphyritic IP facies begins, this grades into a WMB facies briefly before continuing with the IP facies until 553 m where it is once again changes to a WMB facies. This facies is still overprinted by a MCCP texture and continues until 697.8 m (with brief intermissions of MCCP, MB and IP facies), where it grades into a MCCP facies. Throughout this segment of IP and WMB facies core, the intense bleached white colour is less consistent, grading back and forward with a darker grey colour. The bleached white core becomes consistent again at 698 m where a brief MCCP facies occurs with brief segments of IP and MB facies, showing a similar pattern as further up-hole. Some IP facies display thick black bands (744.5 m) bearing phenocrysts or groundmass fragments, there are also sediment flow-like bands present (745.2 m). At 745 m the dominant facies becomes MB of bleached white groundmass-coloured breccias, broken up by a charcoal grey section, overprinted with a MCCP texture. This continues until 763 m before it grades into WMB and then into MCCP facies. DB occurs at 777.5 m which grades through WMB to MB and back to WMB until 800.3 m where MCCP once again becomes the dominant facies until the end of the core log. The last 100 m of core host frequent band-like structures with the last 50 m showing thick charcoal grey breaks and patches in the white groundmass (Fig. 4.6.).

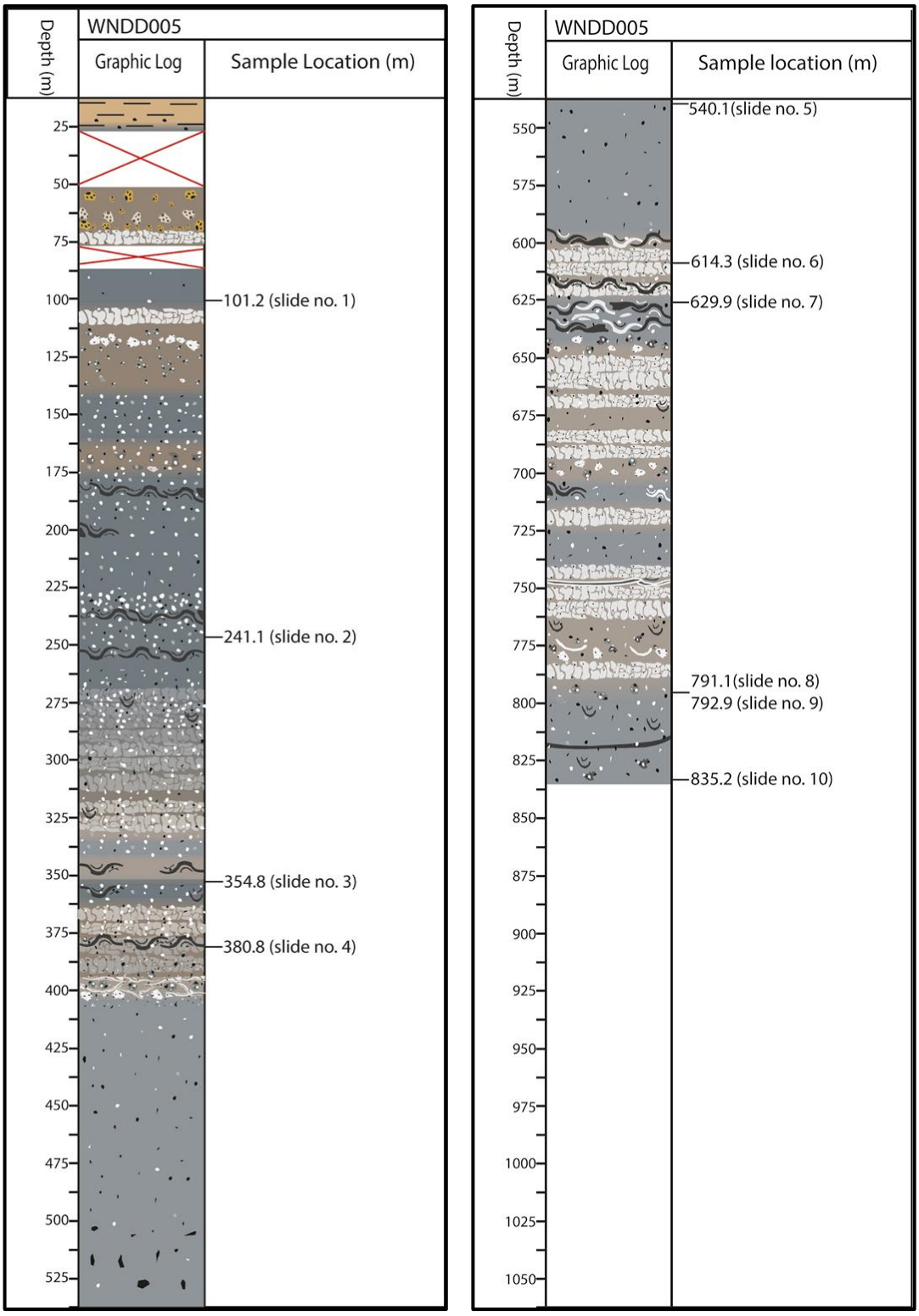

Fig. 4.6. Hole WNDD005 digital graphic log.

4.4.2 WNDD006

Hole WNDD006 is located approximately 434 m to the ESE of the beginning of WNDD005 (Fig 1.1) and is also an angled hole staring at 318 m above sea level, drilled at an angle or approximately 59°, 652.70 m in length, finishing at 16.52 m below sea level. The hole begins with 12 metres of orange-brown soil/clay which changes at 21 m of orange-brown coherent MCCP rock with 0.2 mm - 5.0 mm mafic and felsic phenocrysts. At 33.5 m the MCCP facies grades to a grey colour with minor orange staining and an apparent orange interior. This continues until 83.2 m where the whole core is a dark grey colour. The core appears to be dominant in 0.1 mm - 2.5 mm phenocrysts and remains consistent until 131 m where the core transitions to a HCCP texture. At 131 m there are only a few patches of MCCP and the average crystal size increased, dominated by 4 mm phenocrysts. The core also develops a slight green tinge and some large black clusters can be observed where the core is broken as well as a few veins. Just 19 m later at 149.8 m the MCCP facies grade to host slightly larger (8 mm - 20 mm) phenocrysts which are predominantly felsic. Here, the green tinge subsides, until 155 m where it resumes. The white vein hosting MCCP texture does not change again, until 194.5 m where WMB grades in before phasing out to DB at 204.5 m. The WMB clasts are black in colour and host 0.2 mm - 7 mm mafic and felsic crystals. The breccia clasts range from lapilli to block/bomb sizes and some of the black bands may be large breccia. White veins become more frequent in various directions. From 235.3 m - 238.3 m a section of crumbled core displays white and turquoise green colours, followed directly by white and crimson red colours. This colour pattern reappears again at 240.6 m. By 247 m the presence of veins has mostly subsided along with the green tinge, only visible in the broken core. SDB and MCCP facies are interchangeably dominant until 307 m where DB is observed. DB clasts range in size from large lapilli to blocks/bombs and in colour from dark charcoal grey to light grey, hosting primarily felsic phenocrysts. In some cases, breccia clasts will host other breccia clasts. At 330 m the MB facies appears to merge into the WMB core briefly before returning to a breccia-dense DB facies. The majority of breccia here are light grey and are primarily lapilli sized with a few in the size range of blocks/bombs, and are felsic phenocryst dominant. From 340 m to 363 m the core is crumbly and, in some sections, appears clayey. This crumbly section is imediately followed by a 2 m section of extensive veining. The core brightens in colour, to a washed-out light grey with a porphyritic DB facies. Phenocrysts appear to commonly exceed 10 mm, primarily felsic with sparse mafic crystals. Some irregular banding structures begin to appear around 370 m and by

393 m IP has become the dominant facies. The core colour also lightens to a bleached white, appearing altered in some places. This facies continues until 435 m with thick black bands in various orientations breaking up the white core fabric. Bands range from LCCP to almost aphanitic. Breccia clasts are also present in this section. By 435 m DB is the dominant facies, displaying a porphyritic pattern with frequent lapilli-sized white breccia clasts. Some areas appear to have a faint WMB overprint. Brecciation is interrupted from 451.2 m - 453.2 m with a section of LCCP core that grades into a felsic dominant LPD facies. Brecciation resumes at 465 m in the form of DB after some band-like structures cut across the core. At 467 m MCCP-HCCP facies continue with few breccia clasts occurring and frequent thick bands, possibly representing large breccia. Thinner band and irregular banding structures are present in minor quantities. The interchanging MCCP and HCCP facies grades into an IP facies, potentially hosting large breccia, at 505.3 m and continues until 530 m. A MCCP facies follow the IP faccies, dominated by felsic phenocrysts 4 mm - 8 mm in size. At 551.2 m the facies revert back to a porphyritic IP facies showing irregular patterns in the core fabric and hosting block/bomb-sized breccia clasts as well as frequent veins. Veins commonly occur as crescent shapes in the core, with the vertex of some veins oriented up-hole and other oriented down hole. The vein hosting IP faccies continues with patches of MCCP core hosting frequent veins of varying thicknesses. Throughout this segment of core patches of bleached white, likely altered, core occur up to 598 m. At 598 m the core grades into a WMB facies followed by a DB facies bearing light grey to charcoal grey breccia clasts, typically large-scale lapilli in size. The core from 612 m - 621 m shows a bleached white colour. At 616.3 m there is a charcoal grey intrusion running down the core hosting bleached white groundmass chunks. At 629 m the core grades back into a WMB facies for roughly 5 m before grading into the MCCP facies until the end of the hole, showing few irregular band structures (Fig. 4.7.).

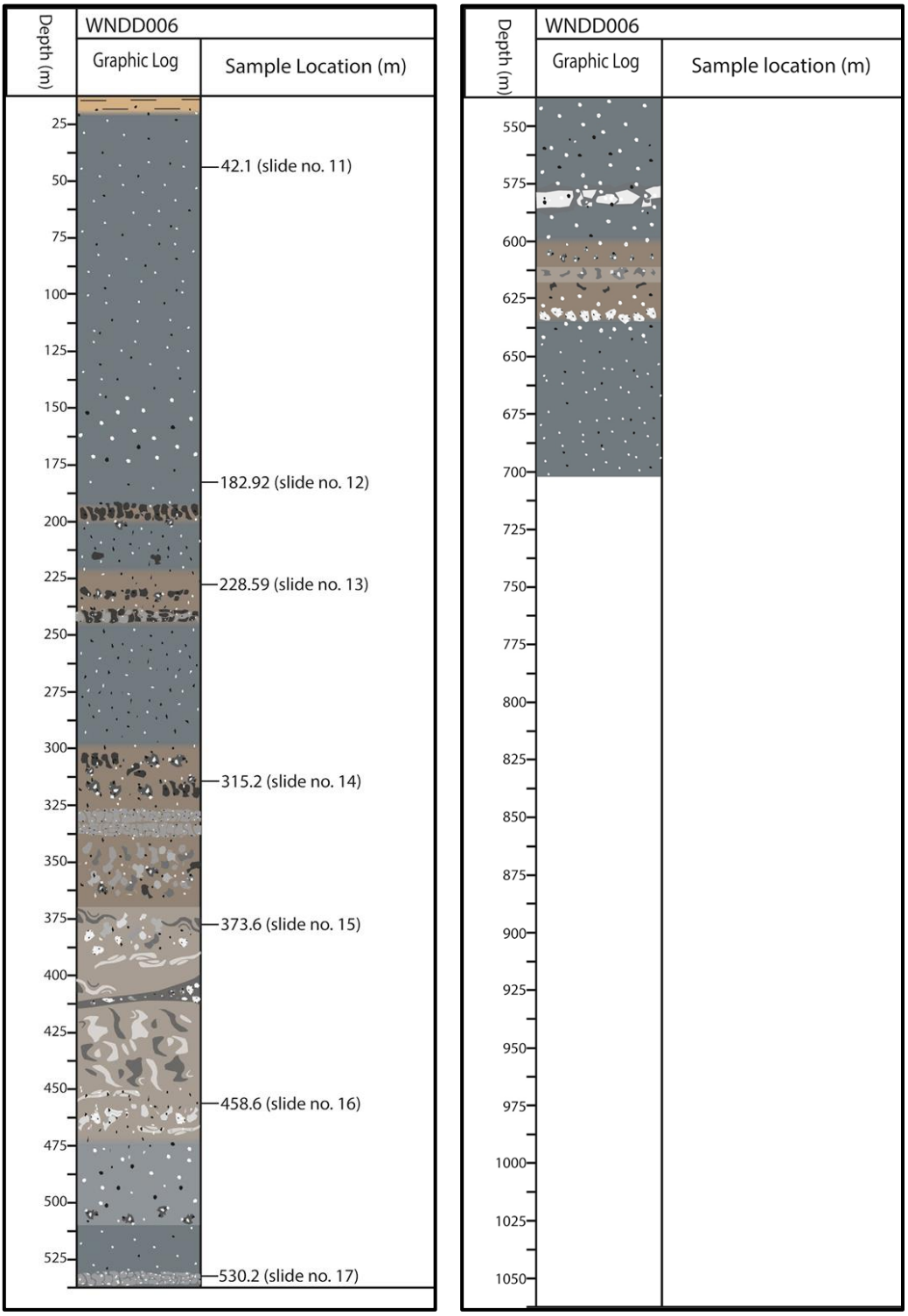

Fig. 4.7. Hole WNDD006 digital graphic log.

4.4.3 WNDD007

Hole WNDD007 is a vertical hole located centrally in the study area (Fig. 1.1), roughly 415 m ENE of the beginning of WNDD005. The hole begins at 327 m above sea level and is 231 m long, ending at 5.62 m below sea level. It begins with orange-yellow clay for the first 4 m followed by grey clay until the core becomes consolidated rock at around 26.3 m showing a grey porphyritic DB facies with minor patches of consistent MCCP and LCCP facies. Breccia clasts are typically grey and light grey in colour, similar to the matrix of the breccia and are predominantly lapilli sized with few block/bomb sizes. The core has a mix of mafic and felsic phenocrysts, becoming felsic dominant at 39 m, where the core also displays a brown/green tinge. From 32 m veins become frequent, mostly stringer veins in various orientations. At 53.2 m veins align lengthwise with the core briefly, before dominant brecciation ceases and patches of MCCP and LCCP facies take over. The segments of LCCP are almost aphanitic and display a clay texture. This occurs from 54.5 m - 63.3 m where dominant brecciation resumes as the WMB facies. Breccia clasts in the block/bomb range are often larger than the core diameter making them difficult at times to distinguish from thick bands. This grades into DB at 87.4 m with various sized (lapilli to block/bomb), and coloured, (light grey to charcoal grey) breccia clasts. A faint green-blue tinge can be observed again from 75 m, grading into a green-brown tinge after 94 m. The DB facies continues, with breccia clasts increasing in concentration and often showing zoning textures within the clasts in the form of lighter-coloured breccia clasts having darker interiors and vice versa with Breccia clasts dominantly hosting felsic phenocrysts. At 123 m banded-like zone of LCCP with sharp boundaries can be observed at 115 m. At 123 m the core transitions through a brief DB faccies into a porphyritic WMB facies with patches of phenocrysts in high concentrations. Frequent stringers and irregular banding structures are also present. Breccia clasts are predominantly block/bomb in size and continue until 146.4 m with some breccia matrix fragments appearing to be held in a white vein at 144.5 m. After a brief LCCP facies interval from 146.4 m - 150.2 m brecciation continues as a DB facies with a few intervals of MB. From 158 m - 160.2 m the breccia matrix colour darkens from light to dark grey. Breccia clasts in this section vary and are lapilli to block/bomb sized and host a mix of mafic and felsic phenocrysts. They appear to fold in some sections and have a medium to high-concentration porphyritic texture occurring in a range of shades of grey, often similar to the breccia matrix colour. The concentration of breccia clasts varies across the core with some sections grading briefly into the WMB and MB facies. From 197.3 m breccias begin to show interior zonation

patterns again, and display a bleached white colour. This Bleached zonation continues as the breccia grades into a MB facies at 200.9 m with a charcoal black breccia matrix. The facies then grade to a brief MCCP facies where it transitions into a MB facies at 204.2 m, but this time the breccia matrix is bleached white and the breccia clasts are a charcoal grey colour. There are also a few band-like structures and thick veins in this segment of the core. By 206.5 m the core has resumed to a DB facies with light grey breccia clasts in a dark matrix and continues for the remainder of the core with a few white veins of varying thickness and charcoal grey banding structures also present (Fig. 4.8.).

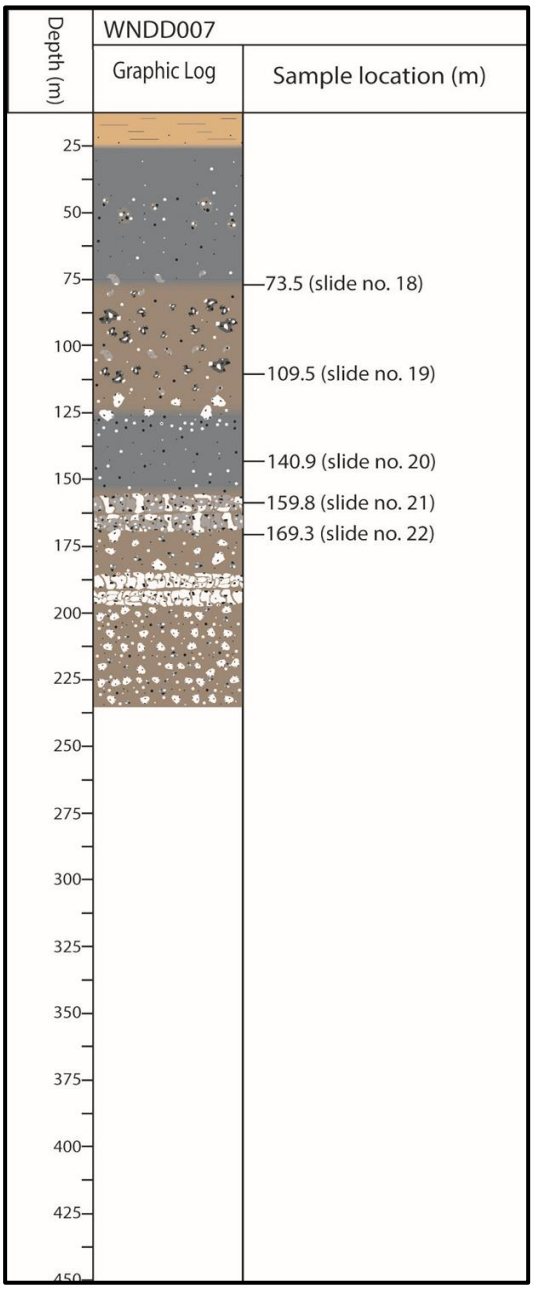

Fig. 4.8. Hole WNDD007 digital graphic log.

4.4.4 WNDD009

Hole WNDD009 is located to the southeast of the study area (Fig 1.1) and is roughly 1490 m ESE of the beginning of 005. It is an angled hole, drilled at an angle of roughly 73° in the NW direction. The hole starts at 321.7 m above sea level and is 460.0 m long, ending at 95.8 m above sea level. The hole begins with brown to red clay with streaks of red and beige. The consolidated core begins at 29 m with a MCCP facies as well as minor intervals of HCCP. The crystals are 8 mm - 20 mm in size and range in colours, including white, black, red and shades of brown. The core ranges in colour from a light grey (hue 7.5, yr 8/2) to a dull yellow-orange (hue 10, yr 7/3), with areas of red (hue 7.5, yr 4/4-4/8). Some brief IP looking structures occur from 40.9-42.2 m, alternating between red, orange and yellow patterns, resulting in a flame-like resemblance in the core fabric due to the colours and banding feat. There are a few bands of different shades of orange with sharp boundaries in the core as well as some lapilli to block/bomb-sized breccia clasts that are red (hue 7.5, yr 4/8), in colour. There are also very sparsely occuring red vein structures. The MCCP facies continues until 53.5 m where a 4.7 m section of beige to orange LCCP facies occurs with a clayey look to it, hosting predominantly mafic phenocrysts. The MCCP facies is followed by a SDB facies which grades into a DB facies at 63.75 m. This section alternates with darker orange zones with sharp boundaries and in these darker-coloured sections, the breccia clast concentration is increased. Breccia clasts are typically large lapilli sized with a few being block/bomb sized. The breccia clasts here have the largest diversity in colour, including black, cream, orange, red and various shades of brown. They typically host felsic, lighter-coloured phenocrysts. At 72.1 m sandy-looking, fine-grained, aphanitic crescent bands appear in the core and continue as crescents and straight bands until 81.9 m. In this section, the facies also changes to a beige MCCP until 87 m where it becomes a porphyritic SDB facies, hosting lapilli to block/bomb-sized breccia. Some sections such as at 99.4 m appear to host large breccia clasts, but apparent clasts are too large to identify from the core. By 107 m the core grades into a DB facies hosting a variation of breccia clast colours as mentioned earlier at 63.75 m. The core colour also changes to a slightly lighter greyer colour hosting a mix of mafic and felsic phenocrysts. This remains consistent until 126.4 m where the core grades to a lighter grey and develops a greenish-yellow tint, and displays some ‘fiamme-like’ patterns. In some sections, a MB facies is present with the space between the breccia matrix displaying an orange/red colour. The core from 126.4 m - 152.9 m displays various

colours/facies and patterns over a small distance. At 152.9 m the core grades from a MCCP facies to a DB facies with frequent irregular banding structures before a sharp boundary occurs to a grey DB facies that is more similar in colour to the rock in the other holes. The breccia clasts are lapilli in size and black in colour with felsic phenocrysts as the most dominant. Some sections show faint WMB textures. At 168.2 m there is a small (15 cm) section of the core with a strong green tinge that is then followed by a heavily crumbled core until 186.6 m where DB resumes. Breccia clasts begin to show internal zoning-like patterns at 209.4 m, with some core hosting breccia clast-like structures with a HCCP fill. At 217.3 m the core shows a green tinge, this intensifies, at 231.3 m where the green colour becomes more prominent and vivid, with the green colour most dominant at 232.7 m. By 242.0 m the green tinge has subsided and the grey DB facies resumes. The DB facies continues until 287 m where the core fabric is broken up by a pale grey claying-looking material, resulting in a WMB facies, continuing until 293 m where it begins to grade back into a DB facies. At 203.6 m the facies changes to a MCCP facies, hosting predominantly white phenocrysts and a few white veins. This texture remains until 339.0 m where a section of clay-like aphanitic core occurs until 340.5 m, where a section of LCCP core begins with a very slight green tinge (hue 10, yr 6/2). By 346.0 m a crumbled MCCP facies becomes dominant and lasts until 355.5 m, with the core changing to a dusky red (hue 10, yr 4/6). The core then shifts to a SDB facies with patches of DB and resumes to the standard grey colour after a bright red band at 364.3 m. The porphyritic SDB facies here has a mix of mafic and felsic phenocrysts, and the breccia clasts are lapilli sized, rounded, black and host felsic phenocrysts. This facies ends at 392.2 m where a clay-like LCCP facies takes over, with sections of the core displaying irregular shaped white veining. A DB facies then begins at 402 m and continues until 434.2 m with two minor breaks. One between 410 m and 413.6 m where the core shows a clay-like LCCP texture, and the other from 420 m - 421 m where the core is crumbly. Towards the end of this facies, breccia clasts begin to increase in size, with a higher a frequency of block sized clasts present. From 434.2 m to the end of the hole a MCCP facies is dominant with patches of LPD and SDB (Fig. 4.9.).

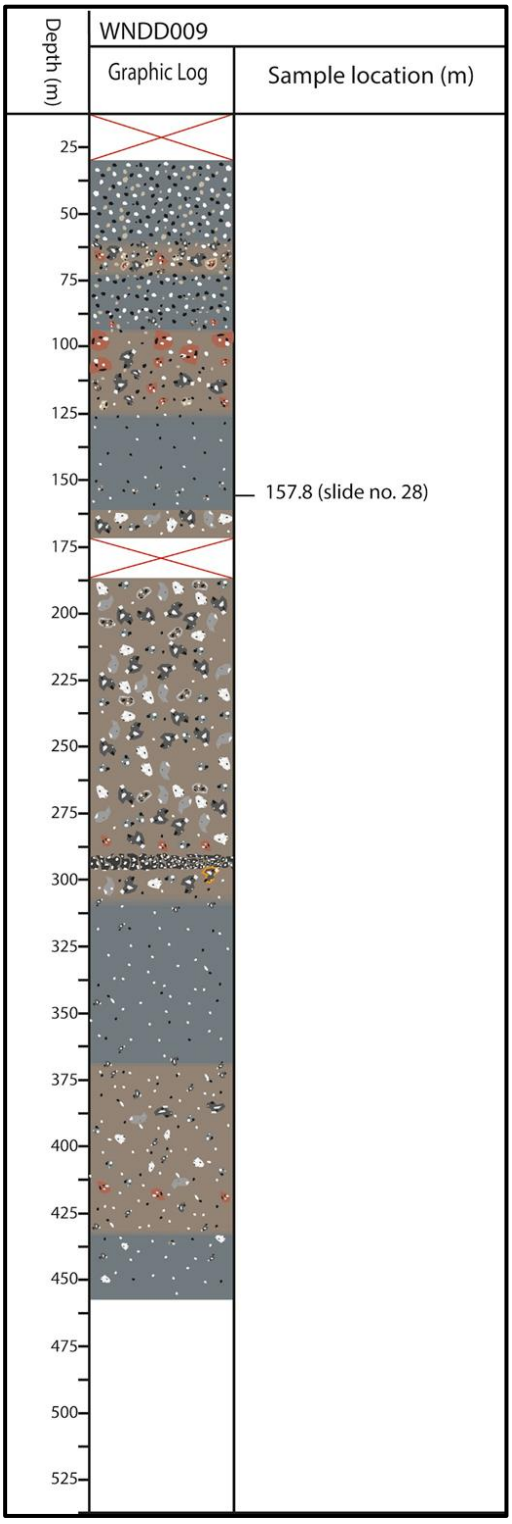

Fig. 4.9. Hole WNDD009 digital graphic log.

4.4.5 WNDD011

Hole WNDD011 is an angled hole that has been drilled down at an angle of roughly 69.5°. It begins at 205 m above sea level and extends 706.8 m to 43.16 m below sea level. It is in the northeast of the study area (Fig. 1.1), roughly 554 m ENE of WNDD005. The core begins at 20.2 m with yellow-brown clay and crumbly core before becoming consolidated at 27.0 m in the form of a LCCP grey facies. The core develops a slight green tinge with orange patches at 28.5 m, transitioning to a DB facies before grading to a SDB facies at 32.4 m. Breccia clasts are lapilli in size and range from various shades of brown and grey, displaying a green tint. Breccia clasts host 0.2 mm - 4 mm sized phenocrysts, dominantly felsic. Veining begins at 37.9 m in the form of white stringer veins commonly in crescent shapes with their vertex in the up-hole direction. Breccia clasts become block sized at 39.5 m. At 46 m the green tinge in the core subsides and the core colour changes to a light grey. The core at 46 m still has a LCCP-DB texture and veining appears to intensify, showing stockwork structures. The core also becomes crumbly and appears slightly clayey. The core reconsolidates at 52.3 m with veins still common, now showing a MCCP-WMB texture. This continues until 69.3 m where the brecciation shifts to DB in the porphyritic core. It should be noted that some breccia clasts here are red in colour and the phenocrysts throughout the core are felsic dominated. The DB facies continues as the dominant facies, with intervals of MB, and MCCP facies, as well as segments of bleached white core at 69 m, 81.2 m and 99.3 m, becoming more frequent after 100 m. Veining remains fairly consistent at varying intensities and some dark grey-black bands and veins also begin to occur after 100 m, up to 50 mm in thickness. By 144 m the core consistently changes facies to a MB facies with bleached white clasts and a charcoal grey coloured matrix, lasting until 151.6 m where the core resumes to a MCCP facies. At 169.1 m a brief IP facies occurs, followed by a minor MCCP facies interval before intervals of MB facies grade into a WMB facies, succeeded by a DB facies. This pattern continues until 205 m where there is a section of the IP facies lasting through to 213.5 m before brecciation occurs in the form of DB with intervals of MCCP core. Thick white veins extend the length of the core from 224 m to 225.3 m. The DB facies continues until 232.0 m where a MB facies begins. This grades to WMB and then back to MB lasting until 246 m where it changes to a MCCP facies and grades into SDB at 259.5, followed by intense white veining, leading to the core having a MB-like texture. WMB with frequent IP intervals succeeds this, displaying a low crystal concentration to aphanitic texture at 287.8 m and grading into DB amongst a LCCP clayey matrix at 291 m.

At 300.5 m a 60 cm section of aphanitic clay-like sediment occurs and is followed by a DB facies with a clay-like aphanitic texture and Frequent aphanitic bands. This grades into a MB facies with patches of HCCP facies. By 319 m the extensive clay has subsided and the predominantly MB facies continues, as light grey breccia clasts in a dark grey matrix with limited veining. This continues with a few minor intervals of IP and HCCP facies until 375 m where a bleached white and dark grey porphyritic IP facies occurs which grades into a MB facies with bleached white, block sized breccia clasts being held in a dark grey matrix. By 394.5 m the bleached white has subsided and a high-concentration DB facies occurs with light grey breccia clasts in a dark grey matrix, typically lapilli in size with few blocks. White veins become more extensive again here. Blue breccia clasts or inclusions are observed At 406.1 m and 412 m. At 226 m a short segment of HCCP core occurs which grades into a LCCP section at 442.9 m. This grades into a WMB facies at 444.2 m, followed by MB at 463.3 m. Alternating WMB and MB facies continue until 522.3 m with the segments alternating between high and low crystal concentrations. Crescent veins and fractures are common, Crescent vertexes are most commonly oriented in the downhole direction. Next at 522.3 m, the DB becomes the dominant facies with breccia clasts ranging in size from lapilli to blocks and varying in colour from light grey to charcoal grey. At 534 m there is a thick break in the core with sharp boundaries showing an aphanitic texture rock. The DB brecciation continues after this, with some black bands bearing felsic minerals also present. At 556.7 m an IP facies becomes dominant with frequent black vein and band-like structures in multiple orientations. This extends to 654.1 m with a brief interval of MCCP facies from 611 m to 624.5 m. It can also be noted that around 604 m, dark grey clay-like aphanitic bands similar to those at 300.5 m occur, as well as red staining and red phenocrysts from 595.8 m - 604.8 m. At 649 m thick white crescent veins become common and the separations between the creamy white core and the charcoal grey core in the IP facies become thicker than usual. This IP facies grades into a brief felsic vein-rich DB facies, followed by a MCCP facies, extending to 690.3 m. from 663.4 m to the end of the hole the core remains consistently bleached white. Some red stained segments on the core also occur around 664.8 m - 668 m. Finally, a DB facies with irregular lapilli breccia clasts, charcoal grey in colour in a bleached white matrix extends from 690.3 m to the end of the hole at 706.8 m (Fig. 4.10.).

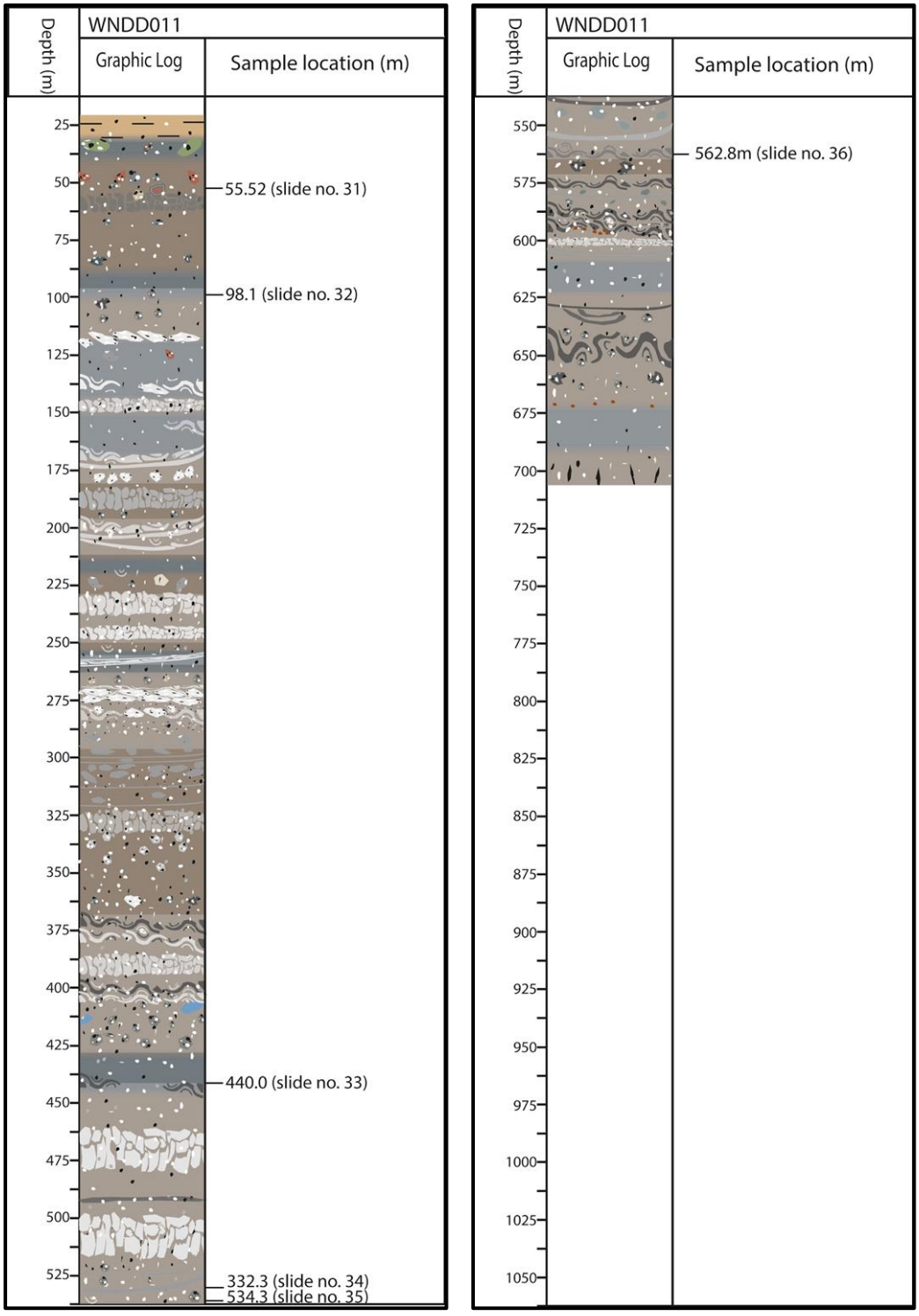

Fig. 4.10. Hole WNDD011 digital graphic log.

4.5 Facies Distribution across holes

Porphyritic and brecciated facies occur relatively evenly throughout the holes, with holes WNDD005 and WNDD006 being dominated by porphyritic facies, hole WNDD009 showing an even distribution, and holes WNDD007 and WNDD011 being breccia dominated. This is especially true in WNDD011 with less than 150 m of the 706.8 m hole being free of breccia facies. The majority of the facies occur throughout all depths. Figure 4.11. displays the facies distribution of all holes while figure 4.12. displays the facies distribution of the holes WNDD005, WNDD006, WNDD007 and WNDD011 which are of interest as they are within a relatively closer spatial proximity of each other and the data from these holes is the most consistent, allowing for more accurate results which facilitates improved comparisons and interpretation. The most common facies was the MCCP facies, occurring prominently in all holes, which also displays the thickest continuous intervals, occurring in thickness of up to 160 m as observed in hole WNDD006 (Fig. 4.11. and 4.12.). This is followed in abundance by the DB facies which is observed in each hole and can occur in continuous intervals of up to 101 m. Hole WNDD009 which begins further south east of the others (Fig. 1.1.), has a relative lack of mosaic breccia facies relative to the other cores and is also free from any significant IP facies intervals. The IP facies also only occurs at depth, with its shallowest appearance at 71 m depth or 196 m ASL. This facies only occurs significantly in core from WNDD005, WNDD006 and WNDD011. The IP facies usually has a low thickness, rarely exceeding 15 m and commonly occurs adjacent to breccia facies in areas of moderate to high alteration. The SDB facies occurs the most extensively in hole WNDD006 with a 28 m layer as well as in also in WNDD005 and WNDD009. The LCCP facies is rarely observed in thicknesses significant enough to be represented on most logs, more often occurring sporadically as intervals amongst the MCCP facies. The digitally logged LCCP, only occurs shallowly at 24.3 m deep in WNDD007 and at 508 m deep down WNDD006. The MB facies occurs abundantly and is observed in each hole, often between a DB facies and porphyritic facies as they grade between each other; however, they are not observed exclusively like this. The MB facies sparsely occurs shallowly and are more common at depth. WMB occurs in a similar “grading” location between facies as the MB does occurring, most extensively in WNDD011 and with interval thicknesses of up to of 45 m but is not thick enough to be logged in the digitised logs where it occurs in the other holes.

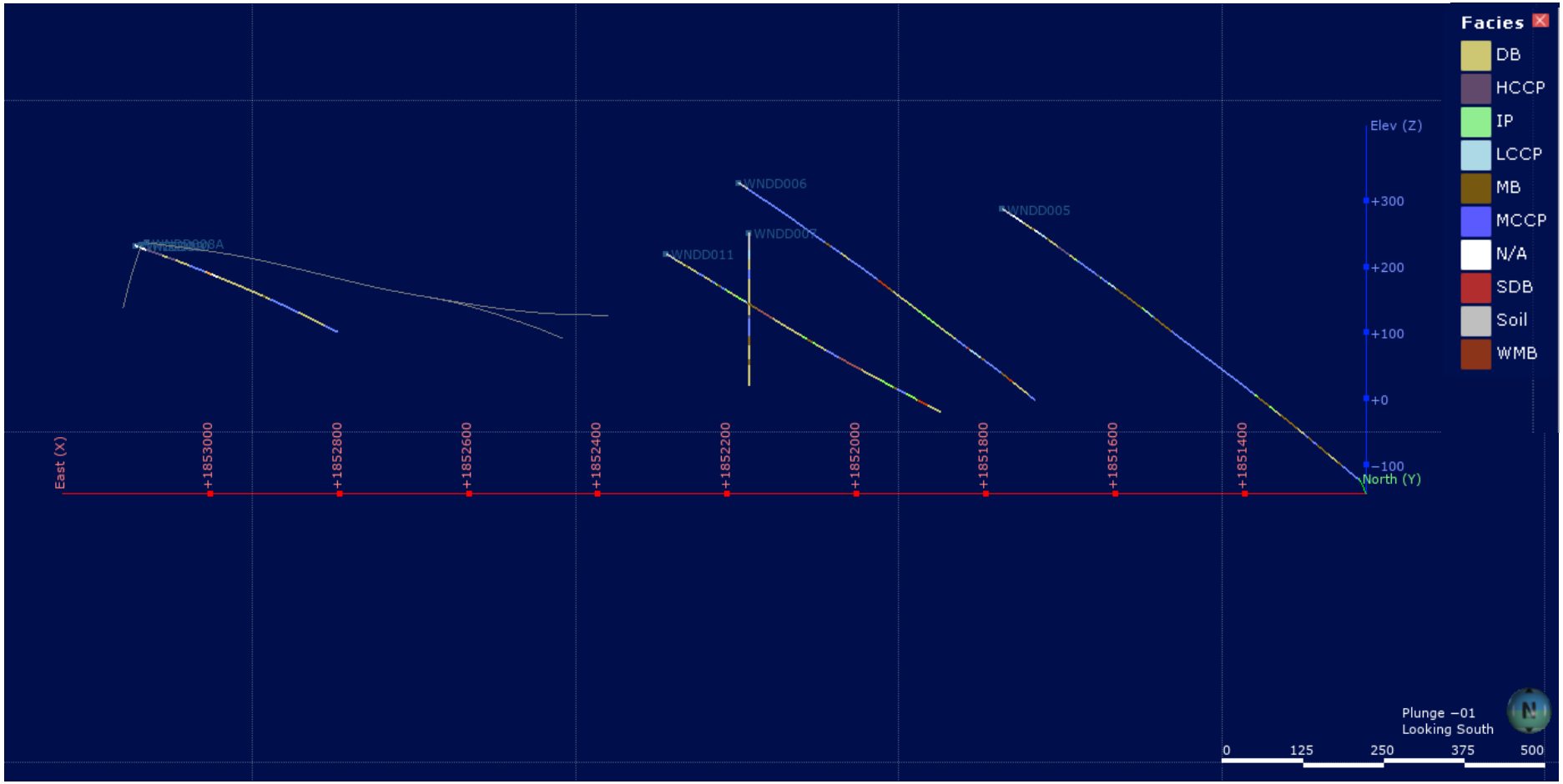

Fig. 4.11. Facies distribution across all drill holes, looking south DB= discrete breccia, SDM= sparse discrete breccia, MB= mosaic breccia, WMB= weak mosaic breccia, IP= irregular pattern, HCCP= high crystal concentration, MCCP= medium crystal concentration, LCCP= low crystal concentration.

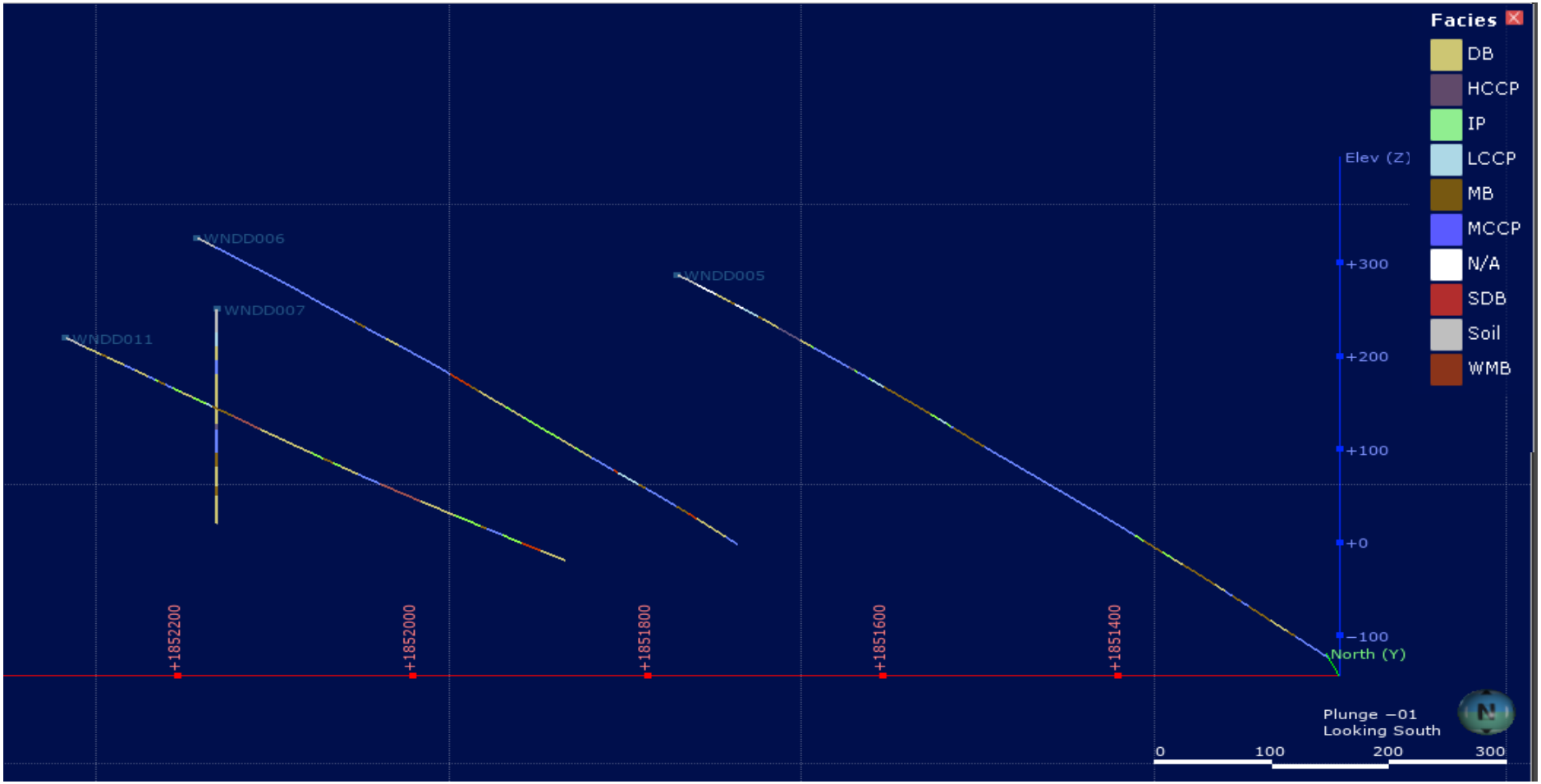

Fig. 4.12. Facies distribution across holes 005, 006, 007 and 011 looking south DB= discrete breccia, SDM= sparse discrete breccia, MB= mosaic breccia, WMB= weak mosaic breccia, IP= irregular pattern, HCCP= high crystal concentration, MCCP= medium crystal concentration, LCCP= low crystal concentration.

Chapter 5

Mineralogy and Petrography

5.1 Introduction

This chapter is about presenting the petrographic observations and mineralogical data from the XRD analysis. It includes the method of thin section preparation, petrographic analysis, sample preparation for XRD and XRD analysis. Mineralogical and petrographical analysis of the thin sections allows for a vastly more detailed view of small sections of the core providing information regarding the minerals present and their abundances. Alteration and secondary features can also be observed and give an insight into the origin of the core as well as some of the processes that have acted upon it. This can provide a better idea of the potential properties of the rock and its past environment, revealing information that can be useful in prospecting, regarding ideal host rocks as well as hinting as to where processes of interest have occurred. XRD analysis further supports the petrographic analysis by confirming major minerals which can sometimes be difficult to identify due to the impacts of alteration on mineral texture.

5.2 Methods

5.2.1 Thin section preparation

Thin sections were made with the purpose of carrying out reflected and transmitted light observation. Sections of the core that were chosen for the thin sections represented the texture, primary and secondary features of the core. The selected sections from the core were cut using the rock saw into roughly 4 cm length by 2 cm width by 1 cm depth blocks. Once cut to shape, the face to be represented in the thin section was ground smooth by rubbing the sample in a figure-of-eight movement against a flat glass base with water and silica powder between the sample and the glass for roughly five minutes or until the sample was flat. The sample was then air dried on a hot plate at 80°C in a fume hood for at least 12 hours. The glass for the slides had to be prepared by grinding them flat in the discoplane. These needed to dry on the 80°C hotplate for 45 minutes. To attach the glass to the rock a 7:3 resin-to-hardener combination was used. 2.3 g of resin and 1 g of hardener were combined on a scale in a plastic boat and mixed over the hotplate. A thin layer of the resin mixture was spread over the smooth face of the sample, then attached to the ground surface of the glass slide. When pushing the glass against

the sample it was slid across the sample to remove any air bubbles before being aligned to cover the face of the sample. Five to ten minutes after this was done the slides were checked to make sure the glass had stayed in place and was adjusted if it had moved. The samples and slides were then left to have the resin cure overnight.

Once cured most of the sample block was cut off using the saw on the discoplane. The remaining block was ground down, first to ~200 microns, then using the birefringence colours of quartz as a guide, to a final thickness of ~40 - 50 microns where the quartz became a straw yellow to white birefringence (Fig 5.1.).

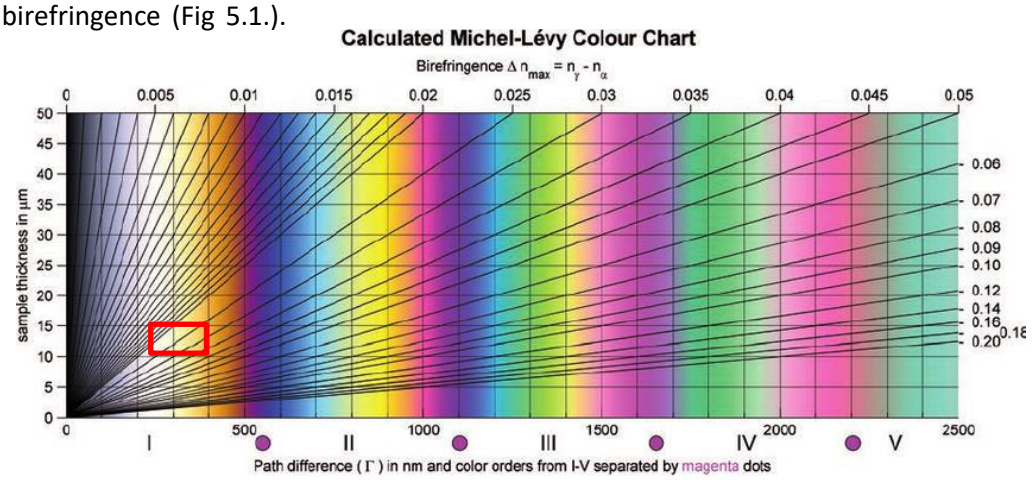

Fig. 5.1. Michel-Levy cross birefringence colour chart modified from Sørensen (2013).

The final step to complete the thin section was to polish it, this would allow for analysis under reflected light microscopy. The sample was first sanded using 500 grit sandpaper, checking it regularly under the microscope until most of the sample was at the desired thickness, (30 microns). This was followed by sanding the sample using 1200 grit sandpaper until the sample was at its final desired thickness. The sample was then polished on a suede polishing disk with 0.3 micron aluminium powder. During this step, there was no risk grinding off too much of the sample but after every few minutes of polishing checking the sample under the reflected light microscope was required to check for scratches, determining how much longer it needed to be polished. Samples were polished until the majority of the scratches in the reflective minerals were smoothed out. This usually took 15 to 20 minutes.

5.2.2 Microscope analysis

Once the slides were ready to be viewed, they were analysed using transmitted and reflected light microscopy. Analysis under transmitted light was divided into three categories, including a fresh or relict description, an alteration description and a description of main secondary features such as veins and breccia. The relict description focused on the original volcanic textures and

minerals of the slide, describing the fresh phenocrysts and inferring the original relict phenocrysts. This included their mineral name, crystal shape, average size and estimated quantity. The alteration description focused on aspects of the components that had changed or been altered since the original genesis of the rock. This included describing relict phenocrysts, including their composition where possible, texture, crystal shape, average size, estimated quantity and alteration effects on the groundmass. Groundmass observations were made on the bulk texture, and inferences such as average size and quantities, on the mineral composition. In the final transmitted light category, veins and other notable secondary structures were described. The composition of veins was described and the sizes of veins larger than stringers were measured. Orientations of veins were also given in some cases. Breccia were described where they were present with observations made on the size of components, texture, colour and composition. The slides were also described under reflected light microscopy in order to observe opaque minerals. Under reflected light the minerals were named, with crystal shape, average size and estimated quantity noted. The mineral distribution was also noted, distinguishing if the mineral occurred in the groundmass, veins or phenocrysts. Abundance percentages were acquired using visual estimations and sizes were deduced using the measuring crosshair in the microscope based on the corresponding magnification.

Detailed descriptions of all slides have been recorded and can be found in the appendix B.

5.3 Thin section descriptions

5.3.1 WNDD005

Transmitted light:

Relict description

There were 10 thin sections from hole WNDD005. All samples display a porphyritic texture with seriate porphyritic textures common. The majority of fresh phenocrysts in WNDD005 were quartz. Quartz levels were relatively consistent with a range of 7% (354.79 m) - 12% (791.12 m), across the WNDD005 samples with an average size ranging from 0.36 mm - 2.0 mm. Quartz phenocrysts were typically anhedral in shape with light to heavy fracture, and embayments became common at depth. Other fresh phenocrysts include orthopyroxene which was first observed at 629.93 m. Some orthopyroxene phenocrysts were partially altered, displaying a yellow-green colour and a texture riddled with opaque minerals. Fresh plagioclase was first observed in the deepest slide of 835.0 m at a concentration of 15%, with an average size of

2.5 mm (Table 5.1.). Plagioclase in this slide had an anhedral to euhedral shape and many phenocrysts were partly altered, however, polysynthetic twinning was still visible.

Alteration description of altered volcanic components

Samples from WNDD005 displayed a relatively consistent level of altered phenocrysts ranging from 20-30%. The most common identifiable alteration mineral was calcite, making up the abundant plagioclase pseudomorphs observed (Fig. 5.2.). There were also some dark yellow-green phenocryst pseudomorphs, presumably altered from pyroxenes; these were commonly riddled with opaque minerals. Opaque minerals were also often observed bordering relict phenocrysts. The other common alteration phenocryst pseudomorph was comprised of an amorphous 'sandy' material that was brown to grey in colour. Some altered phenocrysts displayed Glomeroporphyritic

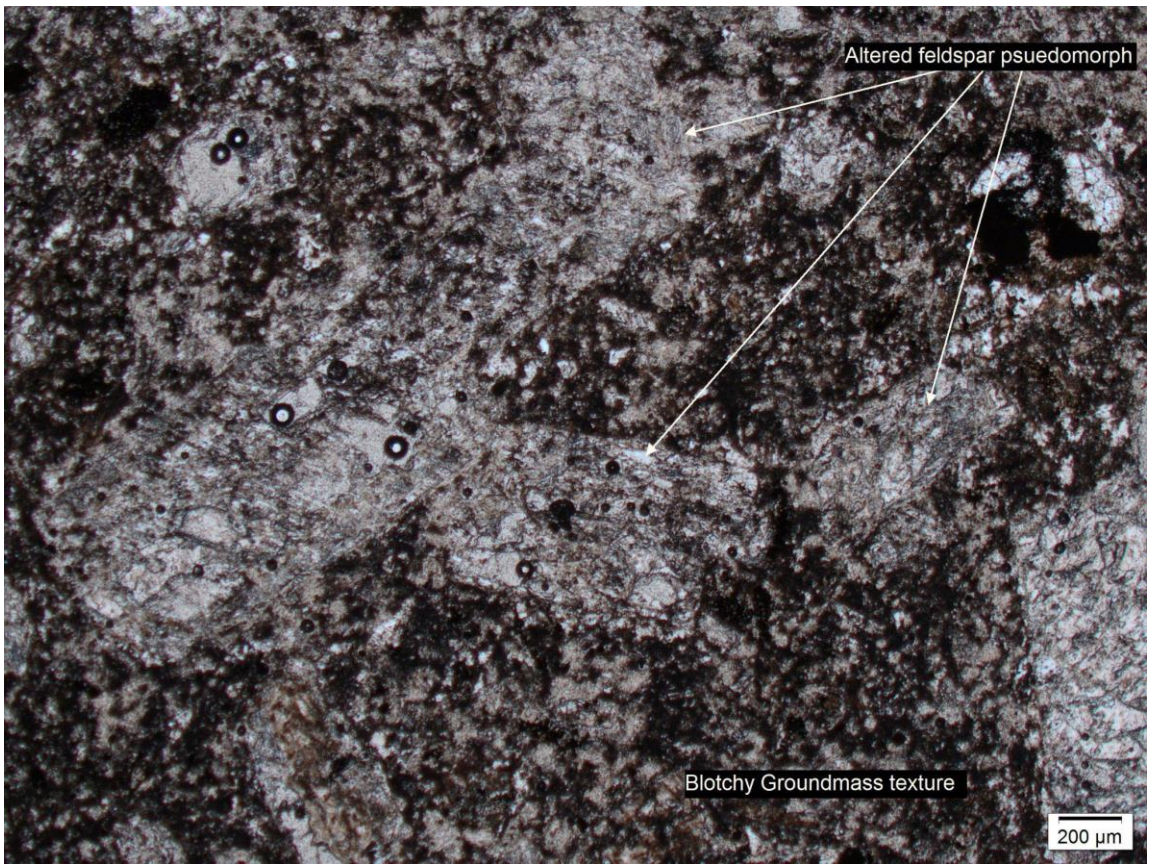

Fig. 5.2. photomicrograph of the sample at 641.25 m from hole WNDD005 under x2.5 plane polarised light (PPL) showing a blotchy textured groundmass as well as altered phenocrysts (glomeroporhyritic-like clot) in centre

clots making individual crystals hard to identify due to the cluster. Significant differences occur between the unaltered and altered grains in the groundmass. The percentage of altered grains in the groundmass appears to increase with depth, with a maximum altered grain percentage at 792.94 m with 90% of the groundmass appearing altered. Groundmass grain size was coarsest at

354.79 m at 0.25 mm. Groundmass grains were comprised of calcite, quartz, plagioclase and clays, displaying a variety of textures from patches of holocrystalline to a seriate grain distribution with blotchy textures being the most common (Fig 5.2.). This texture was consistent in areas of the core with a higher percentage of altered groundmass grains. It should also be noted that plagioclase microlites were observed at 791.12 m in a slide displaying a groundmass consisting of 70% brown/altered grains.

Secondary alteration structures

The slides of WNDD005 host a variety of veins, beginning with red-brown fibrous veins (0.8 mm thick), at 101.2 m, (Fig. 5.3.), while they were hard to identify they grade into identifiable calcite and were likely to consist of calcite themselves. Some opaque and felsic grain veins were observable by 241.14 m, within a larger calcite vein. Further down the hole, veins lessen in width and length with shorter stringer veins becoming more common. These were primarily calcite, but some were composed of opaque minerals or low birefringence felsic grains. By 540.07 m there were no observable secondary structures. At 614.25 m veins were observable again as thin, (0.035 mm), stringers that were mostly holocrystalline in texture, composed of felsic crystals, opaque minerals and calcite. With an increase in depth from 629.93 m, felsic and calcitic veins phase out

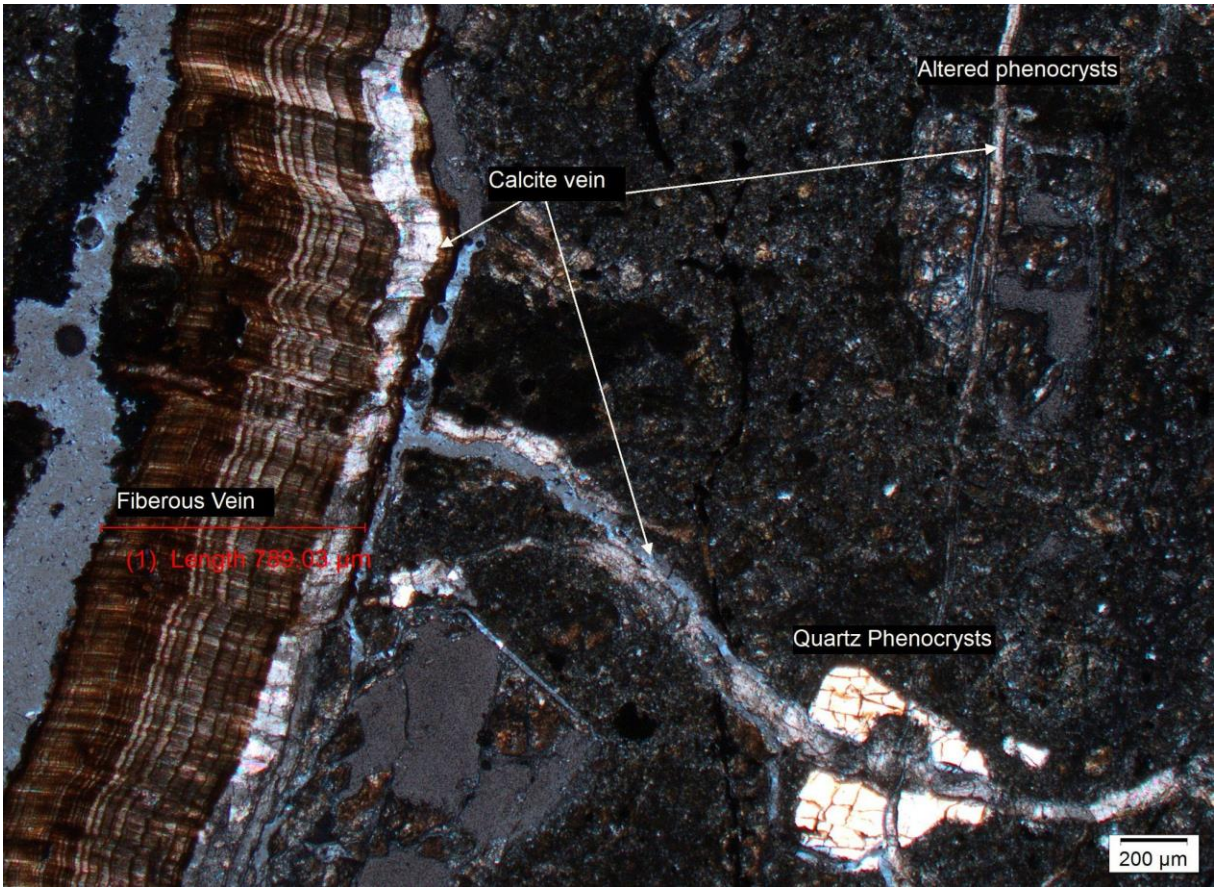

Fig. 5.3. Photomicrograph of the sample from 101.20 m down hole WNDD005 under x2.5 cross polarised light showing large fibrous vein as well as thinner calcite veins.

and veining predominantly comprises of opaque minerals with the slides at 791.12 m and 792.94 m hosting opaque veins that penetrate phenocrysts. By 835.19 m veining has ceased once again.

Reflected light:

From the reflected light analysis, pyrite dominated samples in WNDD005 occurring commonly in the groundmass, as well as in veins and phenocrysts. Galena, chalcopyrite and possible arsenopyrite and hematite were also observed in smaller quantities. Reflective minerals increased with depth, increasing from 2% at 101.2 m to 12% at 614.25 m where it had the highest concentration, before becoming consistent, averaging at 5% for the rest of the hole. In the lower percentages, pyrite and galena were the only observable reflective minerals. At 540.07 m and 614.25 m, a broader range of minerals were observed, including pyrite, galena arsenopyrite, chalcopyrite and hematite. The average size of pyrite crystals ranged from 0.01 mm at 614.25 m to 0.25 mm at 354.79 m where pyrite was also its coarsest at 5 mm. It should also be noted that some reflective grains at depths 629.93 m and 380.83 m appeared to resemble gold but as anisotropy and subtle colour changes were difficult to detect in grains that size (0.05 mm), they may also be chalcopyrite.

Table 5.1. Petrographic summary of WNDD005

Hole 5	Phenocrysts				Groundmass		Opaques	
Depth (m)	Fresh Pheno %	present phenos (qnty)	present phenos (size)	≈Relict pheno %	≈Brown/ altered GM%	Avg Grain size (mm)	Opaque %	opaque minerals
101.2	8	quartz (8%)	quartz (0.36mm)	20		0.025	2	pyrite, galena
241.1	8.5	quartz(8%), Orthopyroxene(<1%)	quartz(0.7mm) Orthopyroxene	25	50	0.05	3	pyrite, galena
354.79	7	quartz(7%)	quartz (2mm)	30	45	0.25	3	pyrite, arsenopyrite
380.83	10	quartz(10%)	quartz (1mm)	30	35	`	3	pyrite, galena, chalcopyrite
540.07	10	quartz, (10%)	quartz, (1.15mm)	27	45	0.015	8	pyrite, galena, arsenopyrite, chalcopyrite
614.25	8	quartz(8%)	quartz(8%)	20	55	0.035	12	pyrite, galena, arsenopyrite, hematite
629.93	12	quartz(12%), partly fresh orthopyroxene	quartz (1mm) partly fresh orthopyroxene	22	75	0.014	5	pyrite, galena, chalcopyrite
791.12	14	quartz(12%), partly fresh orthopyroxene (2%)	quartz(1.5mm), partly fresh orthopyroxene (1mm)	25	70	0.02	5	pyrite, galena
792.94	16	quartz(12%), orthopyroxene(4%)	quartz (0.9mm) orthopyroxene(1.0mm)	25	90	0.025	4	pyrite, galena
835	36	quartz (9%) plagioclase (15%) orthopyroxene (12%)	quartz (1.25mm) plagioclase (2.5mm) orthopyroxene (2.25mm)	20	80	0.06	6	pyrite, galena

5.3.2 WNDD006

Transmitted light:

Relict description

There were 7 slides from WNDD006. A porphyritic texture remained consistent with seriate textures common throughout. Fresh phenocryst observations showed quartz was present across all the samples in small amounts, ranging from <1 - 8%, and with the exception of 458.56 m, quartz proportions decreased with depth (Table 5.2). Quartz phenocrysts were anhedral in shape throughout WNDD006 with light to heavy fractures and embayments at 458.56 m. The remaining phenocrysts were typically euhedral to subhedral in shape with more anhedral crystals occurring at depth. Orthopyroxene, clinopyroxene, hornblende and plagioclase were present in the sample at 42.1 m, with hornblende no longer observable after 182.92 m and plagioclase and clinopyroxene no longer observable from 315.22 m. Plagioclase occurs in large quantities (25-40%) and peaks at 315.22 m with a concentration of 40%, however by 373.55 m fresh plagioclase was absent from the slide. The sample at 373.55 m had no observable fresh phenocrysts except for very space 2.5

mm quartz phenocrysts. In the remaining samples, small quantities of quartz and orthopyroxene were observable from 458.56 m onward with most orthopyroxenes slightly altered to some extent.

Alteration description of altered volcanic components

Observations of the altered mineralogy in WNDD006 displayed a relatively low percentage of relict phenocrysts (5-8%), until 373.55 m onwards where the range sits at 15 - 40%, displaying the highest concentration of relict phenocrysts at the deepest slide (530.15 m). Altered phenocrysts were primarily calcite with the exception of the sample at 228.59 m which had a notable lack of calcite; instead, the alteration of phenocrysts was in the form of sandy green-yellow-brown phenoscrysts, unknown speckled black and white phenocrysts as well as phenocrysts with a yellow-stained blotchy texture. Glomeroporphyritic clots were easily observable in shallow samples. Visual estimations of altered grains in the groundmass show low percentages of colourless transparent grains and a high percentage of murky/ dark grains; these may not all represent an alteration of the groundmass. Murky/ dark grains made up 25% (182.92 m) to 90% (228.59 m), of the altered/brown component of the groundmass. Slides with a higher proportion of alterated phenocrysts had brown/alteration groundmass percentages of 70% with the exception of the deepest slide which only had 35%. A relatively fresh groundmass was present evolving to an altered groundmass from 373.55 m onwards with blotchy textures. Plagioclase microlites were present in the

groundmass at 182.92 m (60% of groundmass), at 315.22 m (45% of groundmass) where they formed a trachytic texture in the slide. At 315.22 m a stronger trachytic texture with larger microlites was displayed (Fig. 5.4.). This trachytic texture contrasts with the sample at 228.59 m, located in between the two trachytic slides which had an almost amorphous brown groundmass. Holocrystalline patches of felsic groundmass were observed often around veins in the lower levels with the blotchy texture more pronounced as murky white grains contrasted with brown, brown-grey and yellow-stained grains.

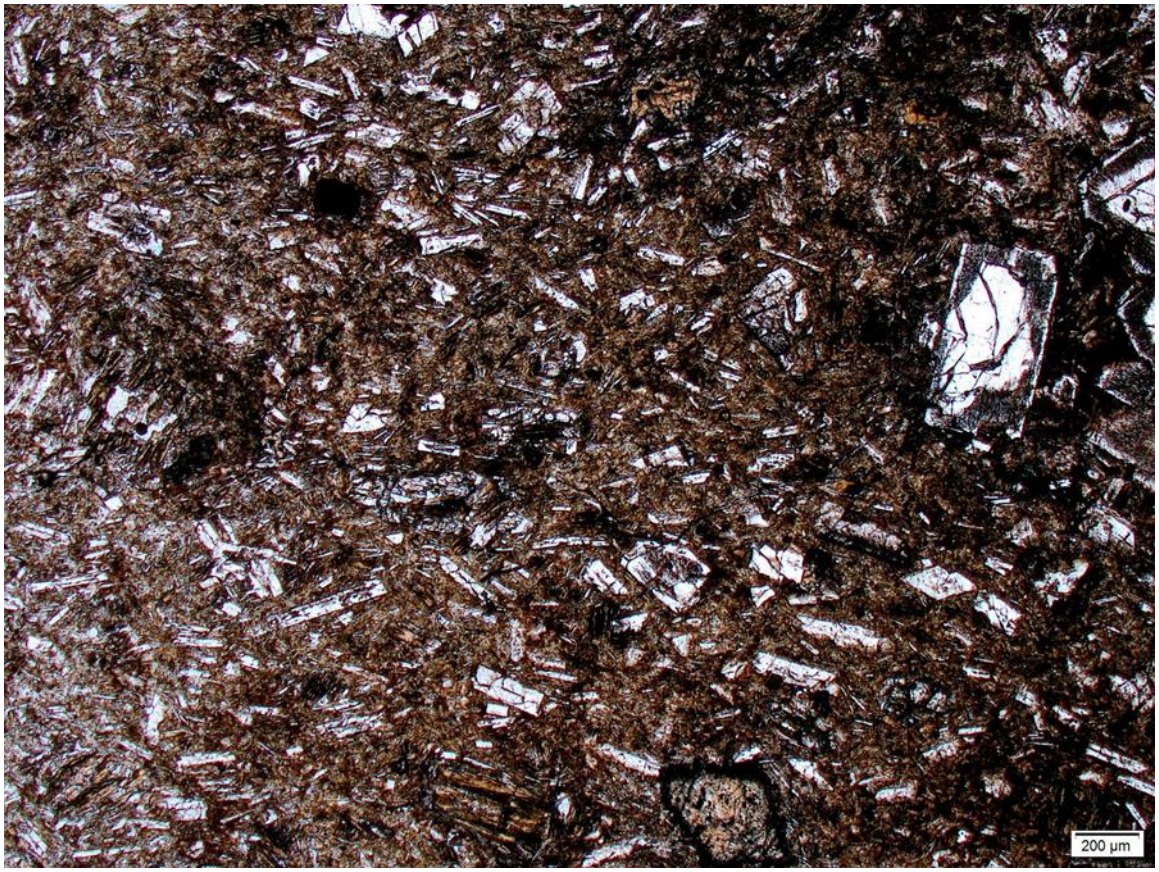

Fig. 5.4. Photomicrograph from the sample at 315.22 m in hole WNDD006 under x2.5 plane polarised light displaying trachytic plagioclase microlites some with swallow-tail features

Secondary alteration structures

WNDD006 began with an abundance of secondary features at 42.1 m including dark red to opaque stringer veins, likely oxidised or altered materials/ sulfides. Frequent anhedral breccia clasts were observed with an average a size of 4 mm and were black to dark brown in colour (slightly darker than the groundmass/matrix), bearing fresh and altered phenocrysts as well as opaque minerals. The rest of the hole was dominated by calcite veins ranging from thin stringers to 1.5 mm thick veins occurring at 530.2 m. Calcite appeared to display multiple colours, grading from an oil slick white to a sandy brown, this gradient could be observed at 182.92 m and 530.2 m.

Calcite veins displayed stockwork-like patterns at 458.56 m and in the deepest slide, there were also some holocrystalline veins, consisting of opaque minerals and crystal grains similar to those visible in the groundmass.

Reflected light:

There was a relatively low concentration of reflective minerals in WNDD006, with a notable lack of pyrite from the first three slides of the core (42.1 m - 228.59 m), instead dominated by magnetite with some smaller galena grains. Rare occurrences of chalcopyrite occurred from 182.92 m - 228.59 m and displayed an average size of 0.01 mm, with some grains noted to appear as having a similar colour, but were harder than chalcopyrite as they displayed a low level of scratching accrued from the polishing process. They predominantly occur alongside and within magnetite (or galena) crystals. These crystals continued to occur at 315.22 m with an average size of 0.02 mm occurring alongside the first pyrite of WNDD006 and small amounts of magnetite. Until 315.22 m reflective minerals had been occurring in the groundmass and in phenocrysts, with pyrite stringers being the first reflective mineral observed in veins in WNDD006. After 315.22 m, pyrite becomes the dominant reflective mineral, occurring in all remaining slides along with magnetite which doesn't phase out until 530.2 m. In the final 2 slides (458.56 m and 530.2 m) soft grey reflective grains with a brown/yellow alteration-looking halo began to occur. Pyrite was most abundant in the deepest slide of WNDD006.

Table 5.2. Petrographic summary of WNDD006

Hole 6	Phenocrysts				Groundmass		Opaques	
Depth (m)	Fresh Pheno %	present phenos	present phenos	≈Relict Pheno %	≈Brown/ altered GM%	Avg Grain size (mm)	Opaque %	Opaques minerals
42.1	36.5	quartz (5%) plagioclase(25%) orthopyroxene(2%) clinopyroxene(<1%) horneblende(1%)	quartz (0.6mm) plagioclase(0.9mm) orthopyroxene(1.2mm) clinopyroxene(0.3mm) horneblende	5	85	0.1	1	magnetite
182.92	52.5	quartz (5%) plagioclase(35%) orthopyroxene (6%) clinopyroxene (6%) horneblende (<1%)	quartz (0.5mm) plagioclase(0.75) orthopyroxene (0.5mm) clinopyroxene (0.5mm) horneblende	5	25	0.11	2	magnetite
228.59		quartz (3%) plagioclase (%) orthopyroxene (4%) clinopyroxene (4%)	quartz (0.3mm) plagioclase (%) orthopyroxene (0.43mm) clinopyroxene (0.43mm)	5	90	0.07	2	magnetite
315.22	45	quartz (1%) plagioclase (40%) orthopyroxene (1%) clinopyroxene (3%)	quartz (0.70mm) plagioclase (1.5mm) orthopyroxene (0.3mm) clinopyroxene (0.25mm)	8	55	0.18	2	magnetite
373.55	2	quartz (2%)	quartz (2.5mm)	20	70	0.12	4	pyrite, galena, magnetite
458.56	10	quartz (8%) orthopyroxene (2%)	quartz (1.7mm) orthopyroxene (0.8mm)	15	70	0.1	4	pyrite, magnetite
530.15	3.5	quartz (<1%) orthopyroxene (3%)	quartz (0.6) orthopyroxene (0.4mm)	40	35		6	pyrite, magnetite

5.3.3 WNDD007:

Transmitted light:

Relict description

There were five slides representing the 231 m long WNDD007 hole. All slides had a porphyritic seriate texture, this was less obvious in some altered slides, and have a relatively low fresh phenocryst content at depth. Anhedral quartz frequency remains relatively low throughout the whole core, occurring in its highest concentration at 8% in the 109.5 m sample with a minimum of 1% in the 159.8 m sample. Quartz displayed light to heavy fracture throughout the majority of the hole with embayments present in all slides except for the sample at 169.3 m. Fresh plagioclase, subhedral to euhedral in shape, was present until 140 m with a peak of 30% concentration in the sample at 73.5 m and a minimum abundance of 15% in the sample at 109.5 m. Plagioclase pseudomorphs were still visible in the rest of the slides below 140.9 m. Orthopyroxene was also present at a variety of depths in small quantities, (<1% - 6%). Orthopyroxene phenocrysts from 159.8 m and below have samples displaying partial alteration.

Alteration description of altered volcanic components

Altered phenocryst concentration in WNDD007 shows a linear increase with depth. Beginning at 15% in the sample at 73.5 m and reaching a maximum concentration of 35% in the sample at 169.3 m. At 73.5 m, many phenocrysts were partially altered and alteration halos around phenocrysts could be observed. Calcite frequently occurred as the dominant alteration mineral as a pseudomorph of phenocrysts. Textures in altered phenocrysts not showing the typical calcite texture often displayed a clayey, near-amorphous texture, brown in colour. The groundmass percentage of brown/altered grains follows the same pattern as the altered phenocryst abundance, increasing with depth. This begins at 30% in the sample at 73.5 m and increases to 70% in the sample at 169.3 m. The texture of the groundmass first displayed a sandy amorphous texture, this changed to the common blotchy texture at 109.5 m before returning to a sandy amorphous texture at 140.9 m (Fig. 5.5.). In deeper samples the groundmass displayed a blotchy texture. The groundmass average grain size ranges from 0.1 mm - 0.02 mm with grains typically consisting of calcite, clays, quartz ± plagioclase.

Secondary alteration structures

Veining occurred throughout the hole with the majority of the veins present being calcite with smaller quantities of felsic and opaque veins, often running within or alongside calcite veins. At 109.5 m a vein has bifurcated and the groundmass between the vein branches is brecciated.

Breccia were present in some of the slides occurring at 109.5 m 140.9 m, 159.8 m and 169.3 m. Breccia clasts increase in size with depth. At 140.9m the maximum breccia clast size was 3.25 mm and breccia clasts would bear quartz, plagioclase and calcite. By 169.3 m, the maximum recorded breccia clast size within this section was 30 mm with clasts were bearing quartz, calcite relict phenocrysts and calcite veins. Breccia clasts in this slide were also often bounded by opaque minerals. Breccia at 159.8 m appeared the most altered, bearing 55% calcite and 40% clays as well as some opaques.

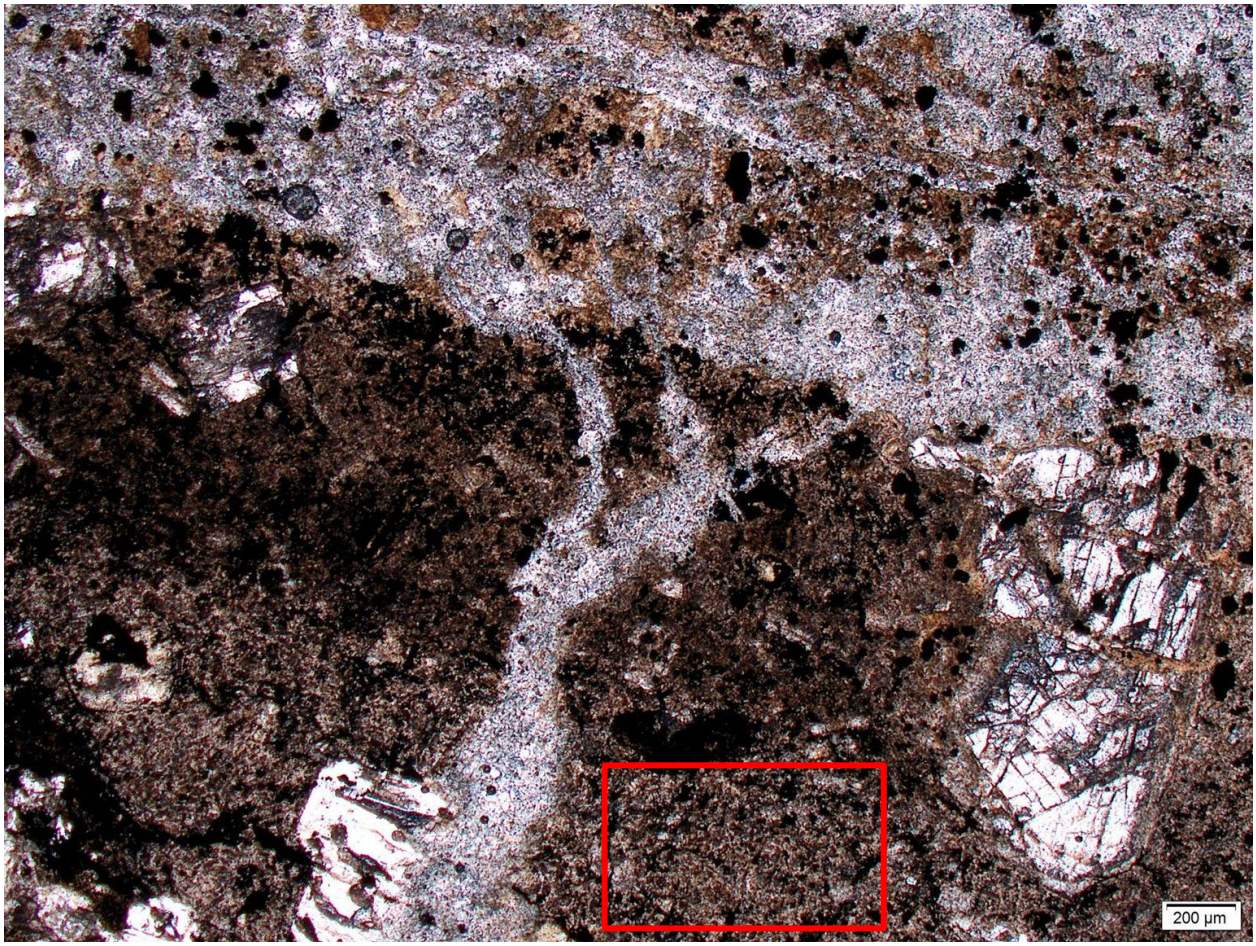

Fig. 5.5. Photomicrograph of the sample at 140.90 m in hole WNDD007 under x2.5 plane polarised light displaying the sandy textured groundmass.

Reflected light description

Reflective minerals from WNDD007 were dominated by pyrite and displayed relatively higher quantities of reflective minerals. Bimodal peaks of 12% were observed in the samples at 109.5 m and 159.8 m between lows of 5% in the sample at 73.5 m and 6% in the sample at 140.9 m (Table 5.3.). Pyrite, magnetite, galena and chalcopyrite were all observed in this hole. The hole began solely with pyrite-magnetite assemblages until 140.9 m where some possible galena began

to occur. In the next slide at 159.8 m, galena took over resulting in dominantly pyrite-galena assemblages. In this slide there was also some possible arsenopyrite, as the grain's colour was slightly whiter than pyrite, however, birefringence is hard to identify in small grains. The pyrite-galena trend continued to 169.3 m and there were sparse quantities of bright yellow grains, likely chalcopyrite. Some magnetite was also becoming present again, distinguishable as a harder mineral, displaying more scratches, unable to be buffered out from the polishing process, and commonly found alongside pyrite. It is noted that there were significantly fewer reflective minerals in the breccia clasts in this sample at 169.3 m. At shallow depths, pyrite occurred within the groundmass and phenocrysts before beginning to accumulate along the edges of veins at 109.5 m. Following 109.5 m pyrite was present in veins, groundmass and phenocrysts until 169.3 m where there was no observable vein pyrite.

Table 5.3. Petrographic summary of WNDD007

Hole 7	Phenocrysts				Groundmass		Opaques	
Depth (m)	Fresh Pheno %	present phenos	present phenos	≈Relict Pheno %	≈Brown/ altered GM%	Avg Grain size (mm)	Opaque %	Opaques minerals
73.5	40	quartz (4%) plagioclase (30%) orthopyroxene (6%)	quartz (1.0mm) plagioclase (1.6mm) orthopyroxene (0.2mm)	15	30	0.1	5	pyrite, magnetite
109.5	23	quartz (8%) plagioclase (15%)	quartz (0.5mm) plagioclase (0.8mm)	20	45	0.025	12	pyrite, magnetite
140.9	24.5	quartz (4%) plagioclase (20%) orthopyroxene (<1%)	quartz (0.7mm) plagioclase (1.2mm) orthopyroxene	20	70	0.03	6	pyrite, magnetite
159.8	1.5	quartz (1%) orthopyroxene (<1%)	quartz (0.5mm) orthopyroxene	35	85	0.023	12	pyrite, galena
169.3	3	quartz (3%)	quartz (0.65mm)	35	70	0.02	8	pyrite, galena

5.3.4 WNDD008

Transmitted light:

Relict description

Three slides from WNDD008, were described. WNDD008 had a notable lack of quartz with the shallowest slide, (55.1 m), hosting the only identifiable quartz (<1%). Other phenocrysts were abundant in all slides (55.1 m, 401.27 m and 692.33 m). Fresh plagioclase ranged from 25 - 40% and Orthopyroxene and clinopyroxene occurred at low frequencies, ranging from 2-7%.

Alteration description of altered volcanic components

Observations of secondary features showed a slight increase in altered phenocrysts with depth beginning at 15% abundance at 55.1 m and increasing to 20% abundance at 692.33 m. Altered phenocrysts in WNDD008 showed a notable lack of calcite. Instead, there was a variation of

alteration textures, making altered phenocrysts hard to identify. The sample at 55.1 m had altered phenocrysts that were colourless in plane polarised light but cross-polarised light showed the phenocrysts were heavily fractured with a blotchy groundmass-like pattern. In the remaining two slides, altered phenocrysts displayed green-yellow-brown staining or were charcoal grey. The groundmass of WNDD008 samples showed a lower percentage of brown/altered grains with depth, beginning at 70% at 55.1 m and reducing to 40% in the two deeper slides. In these slides plagioclase microlites were common. It was notable that slide 629.33 m displayed a sharp division between groundmass textures with both textures appearing relatively unaltered. One had a trachytic texture of plagioclase microlites in a vitric groundmass while the other was similar but had a pilotaxitic texture, microlites on both sides display swallow-tail features, as seen in figure 5.6.

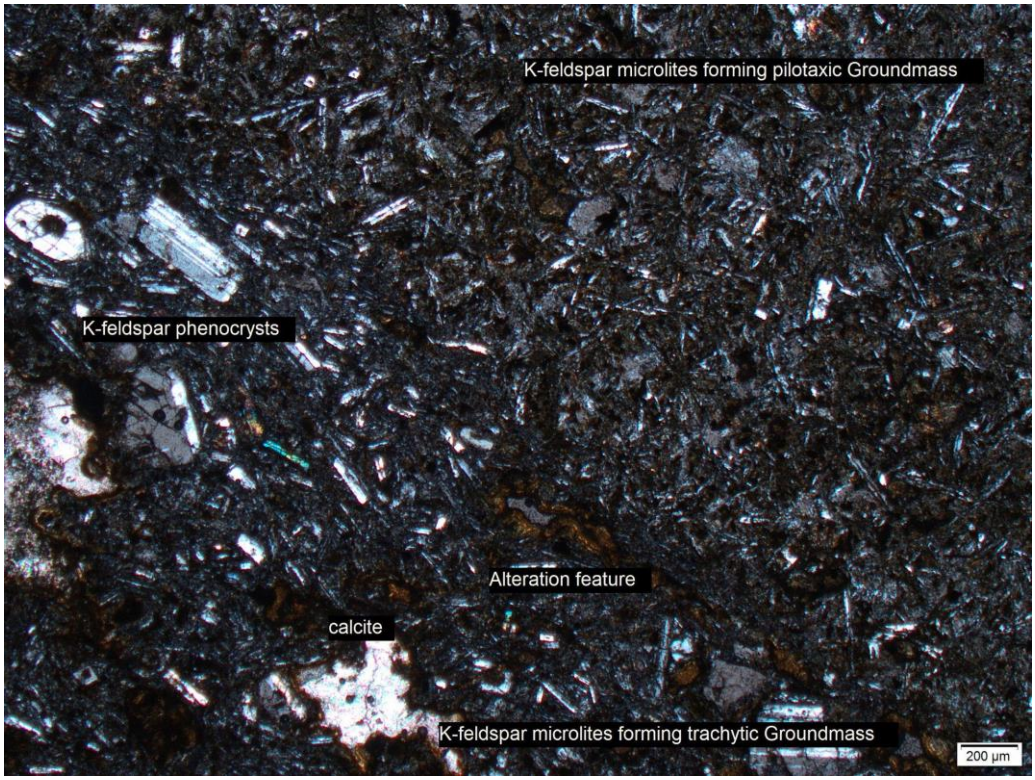

Fig. 5.6. Photomicrograph showing the sample at 692.33 m down hole WNDD008 under x2.5 cross polarised light showing sharply bordering trachytic and pilotaxitic groundmass.

Secondary structures

Veins were present in the sample at 55.1 m in the form of stringer opaque veins with red-orange staining that spread outward toward the groundmass. Also, felsic-grained, brown-green stained veins were present, with all veins penetrating phenocrysts. Veining was absent in the sample at 401.27 m before resuming at 692.33 m where calcite veins occurred near the change in groundmass reaching a maximum thickness of 3.5 mm.

Reflected light:

The reflective minerals in WNDD008 began at 55.1 m in a similar way to WNDD006 with a lack of pyrite and an abundance of magnetite. The first slide also contained small (0.0125 mm), vibrant yellow/gold grains but they appeared to have high relief and were relatively hard. The following slide (401.27 m) had a low abundance of reflective minerals with magnetite being the dominant mineral. Some magnetite at 401.27 m had an oil-slick look to it and others had laminations present. Pyrite begins to occur at 401.27 m in sparse amounts with an average size of 0.01 mm. From 692.33 m onwards pyrite became the dominant reflective mineral, occurring in the groundmass and within primary phenocrysts, with an average size of 0.02 mm. Magnetite was still common, also occurring in the groundmass and phenocrysts ranging from <0.01 mm to 0.45 mm. Some magnetite displayed a cross-hatched lamellar pattern, possibly displaying ilmenite layers. Notably, in the groundmasses displays in Fig. 5.6. the reflective mineral concentration increased from 3% in the trachytic side to 7 - 10% in the pilotaxitic side. In the final two slides, pyrite was the most common reflective mineral and occurs alongside sparse amounts of magnetite and chalcopyrite. Sphalerite was also identified at 745.43 m.

5.3.5 WNDD009

WNDD009 only had one slide in which the sample deteriorated during the sample-making process. The slide does not accurately represent the sample but some features were still evident. The slide is from 157.8m down-hole and fresh plagioclase and orthopyroxene were identified. No alteration or other secondary features were observable. Frequent pyrite was present under the reflected light microscope with sizes of 0.01 mm - 0.45 mm. Small quantities of magnetite and possible arsenopyrite were also present. Some reflective minerals displayed a slight rainbow sheen.

5.3.6 WNDD010

Transmitted light:

Relict description:

Two slides represent WNDD010, one sample located at 194.0 m and the other at 226.7 m. There was a noticeable lack in a seriate texture with a more two-dimensional porphyritic texture. Both slides showed similar fresh phenocryst characteristics with quartz, plagioclase, clinopyroxene and orthopyroxene present in both, at almost identical quantities. The quartz was anhedral and the remaining phenocrysts were subhedral to euhedral. Quartz and plagioclase phenocrysts in WNDD010 were consistently large with quartz ranging from 1.2 mm - 1.5 mm and plagioclase ranging from 1 mm -1.5 mm with a maximum observed plagioclase phenocryst up to 8.5 mm. Intense fracturing was observed in the quartz phenocrysts in both slides, as well as in some plagioclase phenocrysts from the deeper slide. Some of the pyroxene phenocrysts in slide 226.7 m showed signs of partial alteration.

Alteration description of altered volcanic components

Altered phenocrysts were also relatively similar between the two slides of WNDD010, increasing from an abundance of 15% to 18%. The average altered phenocryst size decreased from 0.75 mm to 0.6 mm however, the maximum size increased from 2.0 mm to 2.4 mm. There was a notable lack of calcite in WNDD010 with the dominant alteration phenocryst displaying an amorphous grey-brown sandy alteration texture with extremely fine grains that appear black with twinkles of white grains (0.02mm), under cross-polarised light. This same texture is also the dominant groundmass texture, making up 75% of the groundmass in slide 226.7 m (Fig 5.7.). This was a significantly different texture from the other holes. Bright yellow staining is also recorded as an alteration feature around some phenocrysts in slide 194.0 m.

Secondary alteration structures

Other secondary features include 0.05 mm stringer veins, yellow-orange in colour at 194.0 m. The veins remain the same colour under plane and cross-polarised light but, under cross-polarised light, it darkens and lightens as the stage was rotated. There were few other secondary features at 226.7 m with only a clinopyroxene vein-like structure surrounding large quartz phenocrysts.

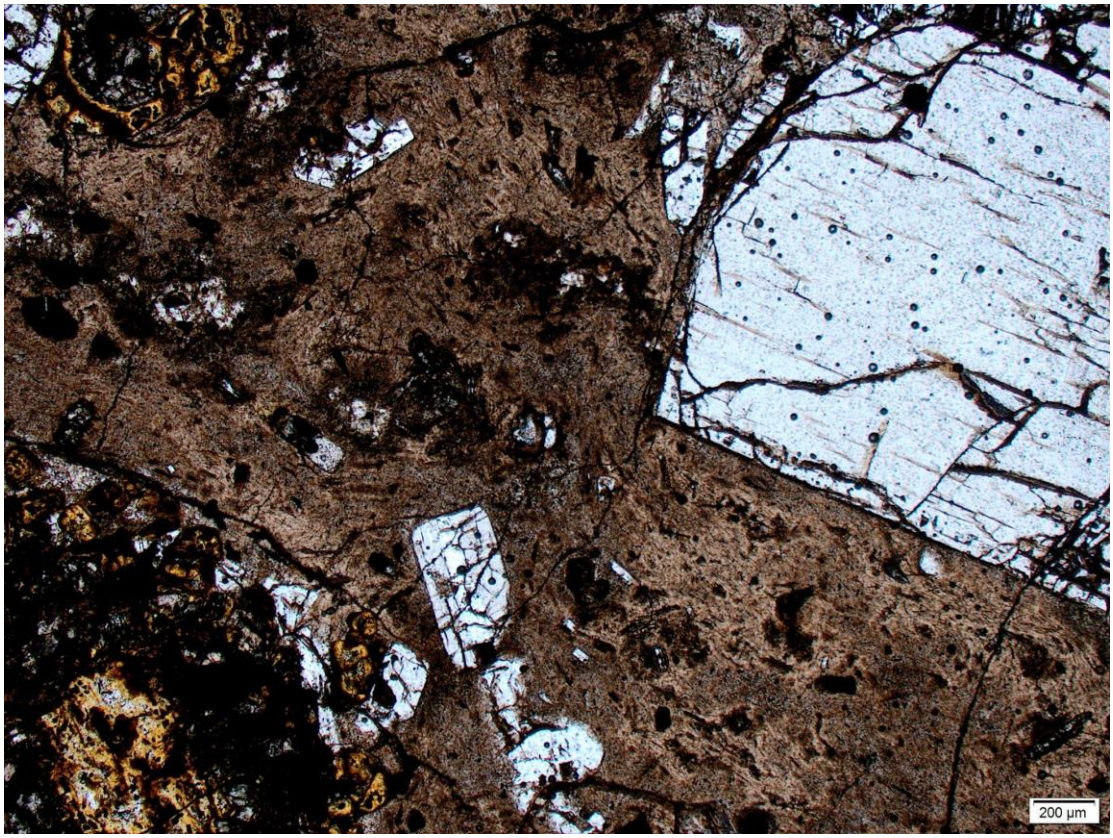

Fig. 5.7. Photomicrograph of the sample from 194.0 m down hole WNDD010 under x2.5 plane polarised light showing the dominantly sandy textured groundmass.

Reflected light:

The reflective minerals in WNDD010 had a notable lack of pyrite with the sole reflective mineral being magnetite at 194.0 m, with an average size of 0.1 mm and rarely exceeding 2.5 mm. Some grains also have a rainbow sheen to them; this may be an alteration/ oxidation feature. At 226.7 m magnetite is still the primary reflective with a similar size as 194.0 m. Almost all the magnetite in this slide displays anisotropic dark grey-black lammele/twinning.

5.4.7 WNDD011

Transmitted light:

Relict description

Six slides were made from samples taken from WNDD011. These samples most commonly displayed seriate porphyritic textures. The fresh phenocryst abundance in these slides ranged from <1 - 33%, displaying a fresh crystal abundance decrease with depth, with the exception of the last slide which had an abundance of 25.5%. The majority of these phenocrysts were plagioclase, followed by quartz and orthopyroxene. However, plagioclase became heavily altered after 98.1 m with only faint polysynthetic twinning visible and most of the phenocrysts replaced by calcite until the final slide (526.8 m). Quartz phenocrysts remained present throughout the hole, accounting for <1 - 6% of phenocrysts. Intense fracturing was present in the majority of the phenocrysts throughout the hole and quartz often displayed embayments and resorption textures. Phenocrysts were consistently large with average sizes ranging from 1.25 mm - 2.5 mm in quartz and 1.5 mm - 2.6 mm for plagioclase. A maximum size of 8.25 mm was recorded in plagioclase at 532.3 m.

Alteration description of altered volcanic components

Altered phenocryst abundance increased with depth until 440 m which displayed a 40% abundance (Table 5.4). There was an abundance decrease to the next slide (532.3 m) which showed a crystal abundance of 30%, before increasing to the maximum altered phenocryst abundance of 50% in the sample at 534.3 m. Relict phenocryst abundances then decreased to 10% in the final slide, (562.8 m). The majority of altered phenocrysts were partially and fully altered calcite pseudomorphs of plagioclase. Other textures of relict phenocrysts included an amorphous sandy brown-yellow-grey appearance with some Glomeroporphyritic clots present. The groundmass of WNDD011 was made up of felsic grains, altered grains and clays with opaques and pyroxene grains occurring in small abundances at some depths. The percentage of brown/altered grains in the groundmass displayed a nonlinear relationship to depth and ranges from 30% in the sample at 532.3 m to 90% in the sample at 534.3 m. Although spatially close, slides from 532.2 m and 534.3 m displayed contrasting textures as 534.3 m appeared to be significantly more intensely altered. At 534.3 m the main alteration feature was the brown-grey-yellow sandy alteration texture which showed extinction and weak birefringence (Fig. 5.8.), while the groundmass of the rest of the hole had a primarily blotchy texture (Fig. 5.11.).

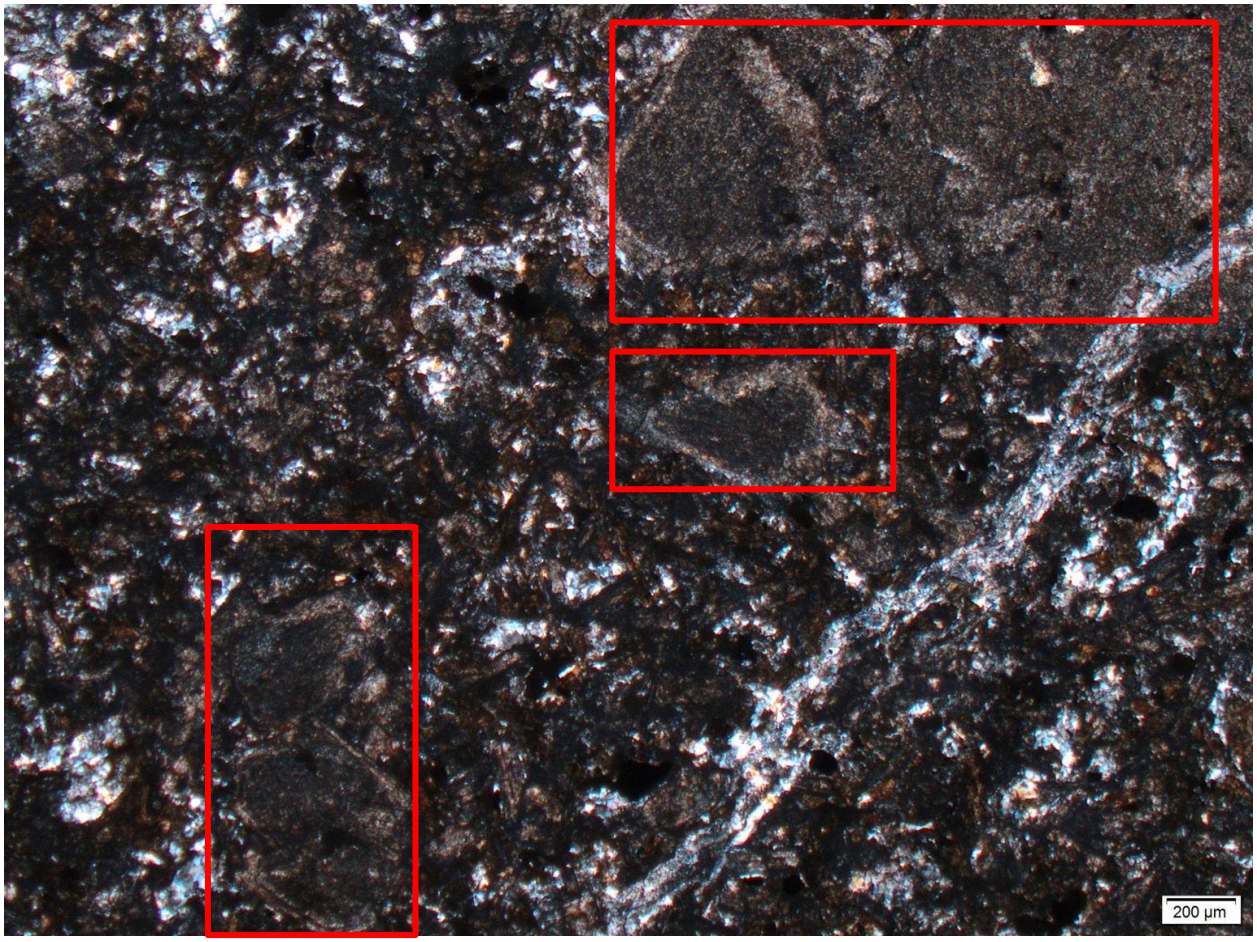

Fig. 5.8. Photomicrograph of 534.32 m down hole WNDD011 under x2.5 cross polarised light showing the sandy amorphous phenocryst alteration texture.

Secondary alteration structures

Veining began with predominantly opaque stringers alongside sparse calcite and felsic grained veins which displayed an average thickness of 0.04 mm. The sample at 98.1 m displayed multiple thick, brown, fibrous, alteration-like textured veins also bearing calcite and opaques. These veins ranged in thickness from 0.05 mm - 4.9 mm. Calcite was the main vein mineral at 440.0 m with a 0.2 mm thick vein running down the length of the slide with thinner calcite veins splitting off from it. There was also a vein structure bearing felsic crystals, calcite and opaques running through the middle of the slide. A shift to opaque vein dominance occurred at 532.3 m with a 0.2 mm thick opaque vein occurring, bordered by a 0.025 mm thick calcite vein and a few calcite stringers branching off. Veins penetrated some phenocrysts but not all. At 534.32 m calcite veins could be seen transitioning into a loosely defined mass of opaque minerals and groundmass-like grains. The deepest slide from WNDD011 showed multiple veins /trails of opaque minerals roughly 0.9 mm wide that ranged in length from less than 1 mm to over half the slide. Holocrystalline sections of core could also be seen in veins and in the groundmass from 98.1 m to 440 m.

Reflected light Description:

The reflective minerals in WNDD011 occurred fairly consistently, displaying a minimum abundance of 5% in the samples at 532.3 m and 534.3 m. Reflective mineral abundance was at its highest at 8% in the samples from 440.0 m and 562.8 m. Pyrite was the dominant reflective mineral occurring throughout the samples. At shallow levels, pyrite-magnetite assemblages were present. By 440.0 m magnetite became less common and sphalerite showed an increase in abundance. In the samples at 532.3 m and 534.3 m, chalcopyrite and grains slightly brighter than chalcopyrite were present; these could represent fine electrum/ gold specs (visible under x40 magnification). By 562.8 m, pyrite was the only reflective mineral present as well as light grey crystals, showing subtle laminations. Pyrite occurred in the groundmass and primary phenocrysts throughout the hole, but in samples from 55.52 m, 532.3 m, and 562.8 m it also occurred in veins. Reflective minerals ranged in size from <0.01 mm in the form of yellow/gold specs in samples from 532.3 m and 534.3 m to pyrite in veins over 2.5 mm in length in samples from 55.52 m and 532.3 m.

Table 5.4. Petrographic summary of WNDD011

Hole 11	Phenocrysts				Groundmass		Opaques	
Depth (m)	Fresh Pheno %	present phenos	present phenos	≈Relict Pheno %	≈Brown/ altered GM%	Avg Grain size (mm)	Opaque %	Opaques minerals
55.52	33	quartz (4%) plagioclase (25%)	quartz (1.25mm) plagioclase (2.6mm)	20	40	0.015	6	pyrite, magnetite
98.1	32.5	quartz (<1%) plagioclase (30%) orthopyroxene (2%)	quartz (1.25mm) plagioclase (2.6mm) orthopyroxene (0.75mm)	25	55	0.015	6	pyrite, magnetite
440	6.5	quartz (6%) orthopyroxene (<1%)	quartz (2.25mm) orthopyroxene	40	50	0.025	8	pyrite, sphalerite
532.3	3	quartz (3%)	quartz (2.0mm)	30	30		5	pyrite, sphalerite
534.3	<1	n/a	n/a	50	90	0.02	5	pyrite, sphalerite
562.8	23.5	quartz (3%) plagioclase (20%) orthopyroxene (<1%)	quartz (1.25mm) plagioclase (1.5mm) orthopyroxene	10	65	0.03	8	pyrite

5.4 Mineralogical distribution:

From the slides analysed, it was apparent that quartz was the most consistently occurring mineral, present in almost every slide, while plagioclase occured in the highest abundance. Calcite was the most common alteration mineral and pyrite was the most common opaque. Variation occurred in mineral assemblages with depth down-hole. Quartz occurred in almost every slide across all depths, often as the sole fresh phenocryst. It was commonly accompanied by plagioclase most commonly at shallower depths. In WNDD008 and WNDD010 traces of fresh plagioclase were found in samples at all depths. However, in the remaining holes, the only locations where fresh plagioclase was observable deeper than 350 m down-hole, was at 562.8 m in WNDD011 and 835.0 m in WNDD005. Orthopyroxene and clinopyroxene also commonly occurred alongside quartz as well as plagioclase, with orthopyroxene occurring more consistently than clinopyroxene. The first three slides of WNDD006 and WNDD008 host all four minerals, displaying a highly concentrated porphyritic texture in which plagioclase was the dominant mineral. Holes such as WNDD011, WNDD007 and WNDD006 show patterns of lessening fresh phenocryst diversity with depth, and quartz was often the only remaining primary phenocryst. In WNDD006 the minimum fresh phenocryst abundance occurred at 373.55 m, in WNDD007 it occurred at 169.3 m and in WNDD011 it occurred at 534.3 m. In holes WNDD011 and WNDD006 however, the diversity and abundance begins to increase again after the depth of minimum primary phenocryst abundance as opposed to WNDD007 which shows a continuous decrease with depth.

Altered phenocrysts and groundmass textures varied throughout each hole (Fig 5.9.; 5.10.; 5.11.) Altered phenocryst were distributed throughout all slides and vary in abundance; they typically mirrored the pattern of mineral diversity mentioned above and display the highest abundance where fresh mineral diversity was at its lowest. In WNDD005 which does not display a decrease in mineral diversity, alteration minerals have maximum abundances where fresh phenocryst abundance was at its lowest (354.79 m). Altered phenocrysts were most commonly calcite as well as altered orthopyroxenes and clinopyroxenes. Some alteration minerals were unidentifiable through petrographic techniques. Figure 5.12. shows the distribution of alteration, primarily using petrographical data as well as data from the XRD and XRF analysis, specifically altered phenocryst abundance, Sulphide abundance the percentage of obliterated groundmass and felsic to altered groundmass percentage. However, the last parameter was used carefully when inferring alteration levels due to the possible presence of hydrothermal quartz causing higher felsic grain quantities to represent altered rock. Figure 5.13. is a close up of the same angle, focused on the holes with

the most consistent data and closer proximity. In these holes the groundmass usually deteriorated with an increase in depth, with the exception of WNDD011 where the deepest sample was less altered than the previous two samples and in WNDD005 in which 614.25 m was less altered than previous slides. The groundmass deterioration with depth relationship was not always displayed; the felsic versus altered ground mass grains as WNDD006 had a low percent of altered grains in the deepest slide.

Opaque distribution was dominated by pyrite. Variations of opaque groups occurred with spatial differences. Pyrite-galena groups were dominant for the first 380 m of WNDD005 and between 629.93 m and 835.0 m in WNDD005. They also occurred from 159.8 m and deeper in WNDD007. Magnetite dominant groups occurred in the first 315.22 m of WNDD006, from 194.0 m - 226.7 m in WNDD010 as well as in the first two slides of WNDD008 (55.1 m, 401.27 m). Pyrite-magnetite groups occurred from 373.55 m in WNDD006, 692.33 m in WNDD008, in the first three slides of WNDD007 and the first 98.1 m of WNDD011. This group was observed occurring at depth and in the near-surface. A pyrite-sphalerite group was observed to occur in WNDD011 between 440.0 m and 532.3 m. Despite these descriptions, these groups often hosted other minerals in smaller quantities. Chalcopyrite and gold-like minerals occurred throughout the slides. They could occur in clusters such as the one between 380.83 m and 629.93 m in WNDD005, from 182.92 m to 228.59 m in WNDD006 and from 532.3 m to 534.3 m in WNDD011. Spot occurrences also occurred such as at 226.7 m in WNDD010, 169.3 m in WNDD007 and in the first and penultimate slides (55.1 m, 745.43 m) in WNDD008. Other possibly occurring minerals such as arsenopyrite, hematite and ilmenite occur more sporadically.

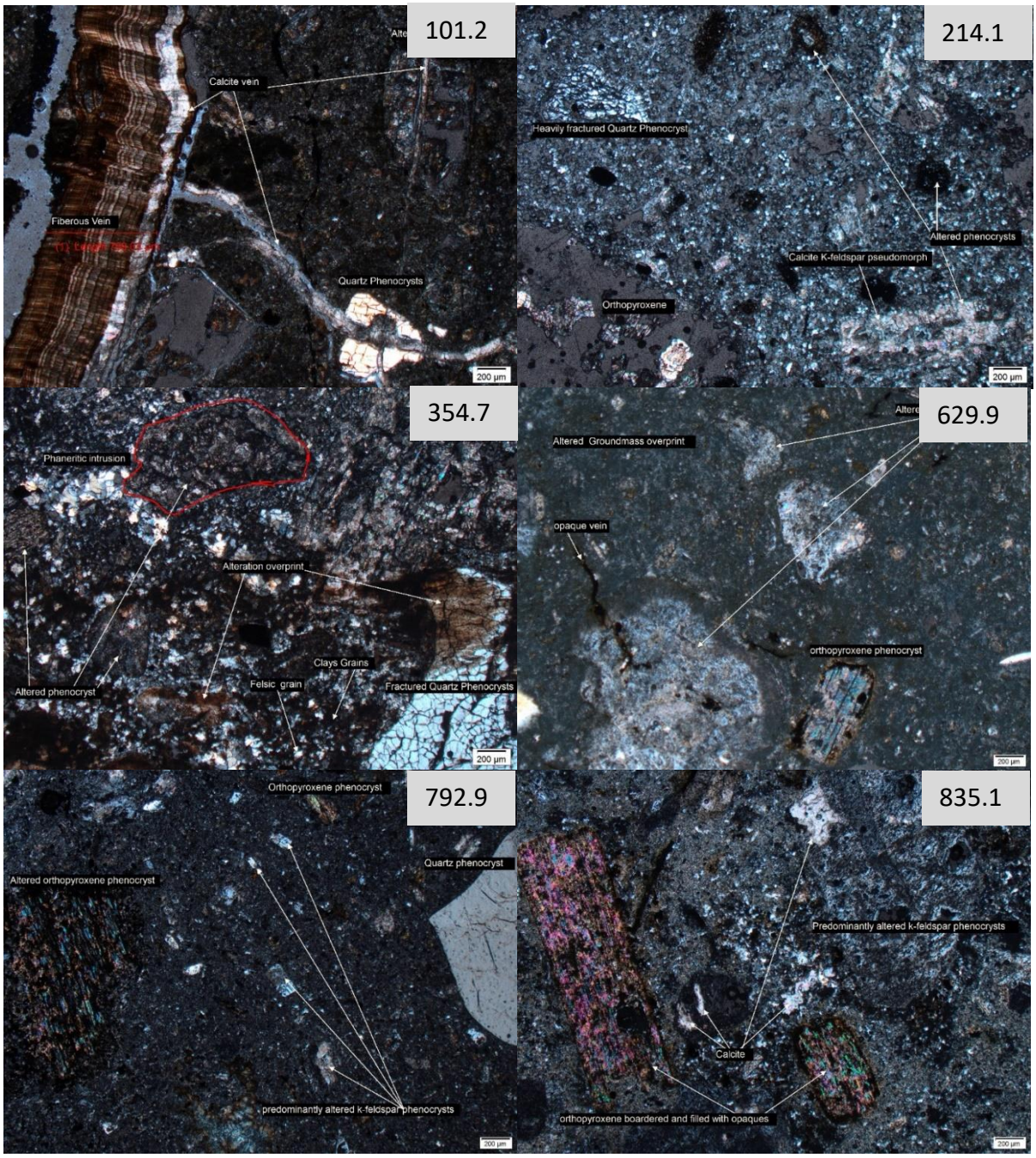

Fig. 5.9. Photomicrograph images of samples of varying depths (m) from hole WNDD005.

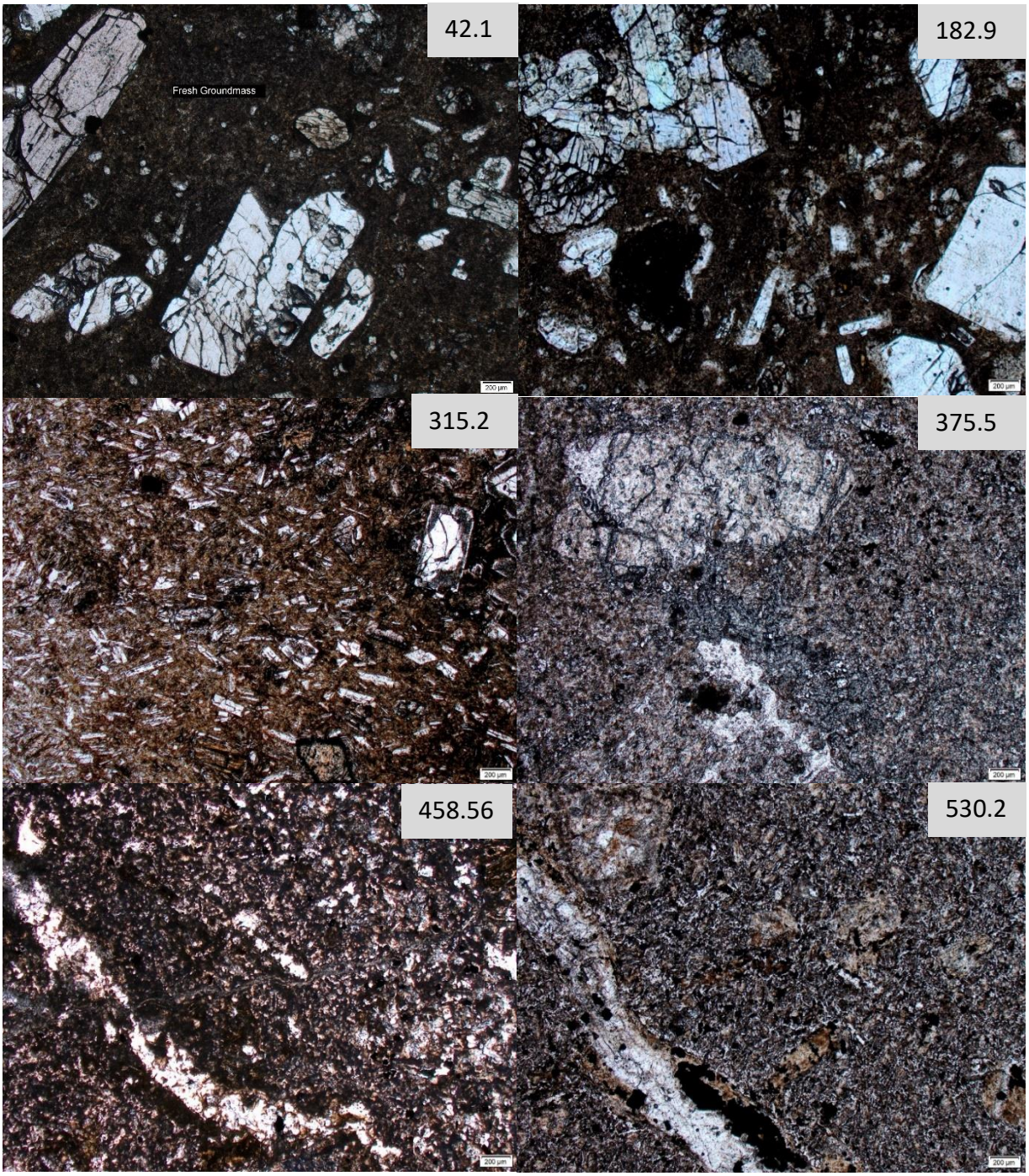

Fig. 5.10. Photomicrograph images of samples of varying depths (m) from hole WNDD006.

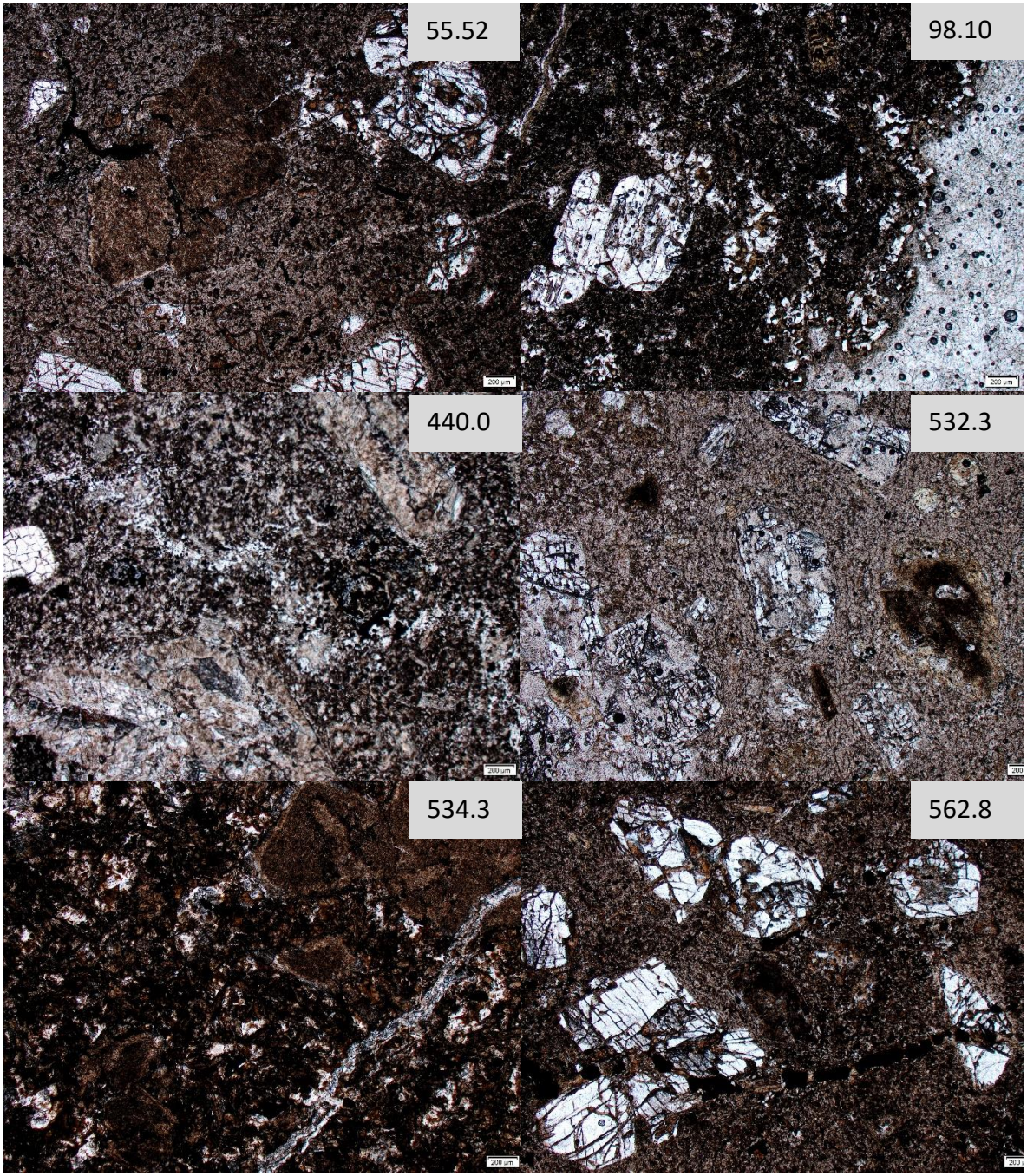

Fig. 5.11. Photomicrograph images of samples of varying depths (m) from hole WNDD0011.

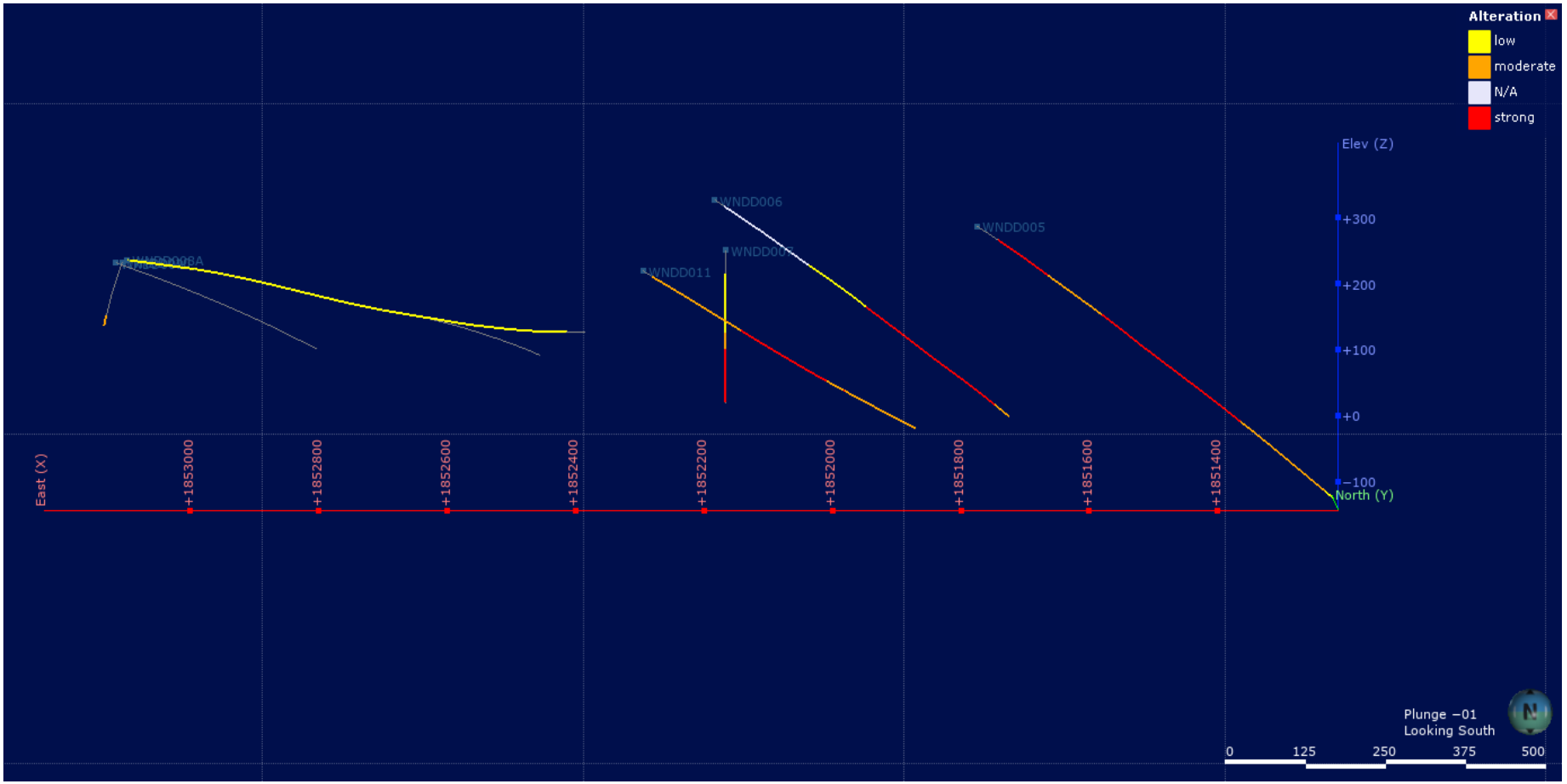

Fig. 5.12. Alteration intensity map of all holes, looking south

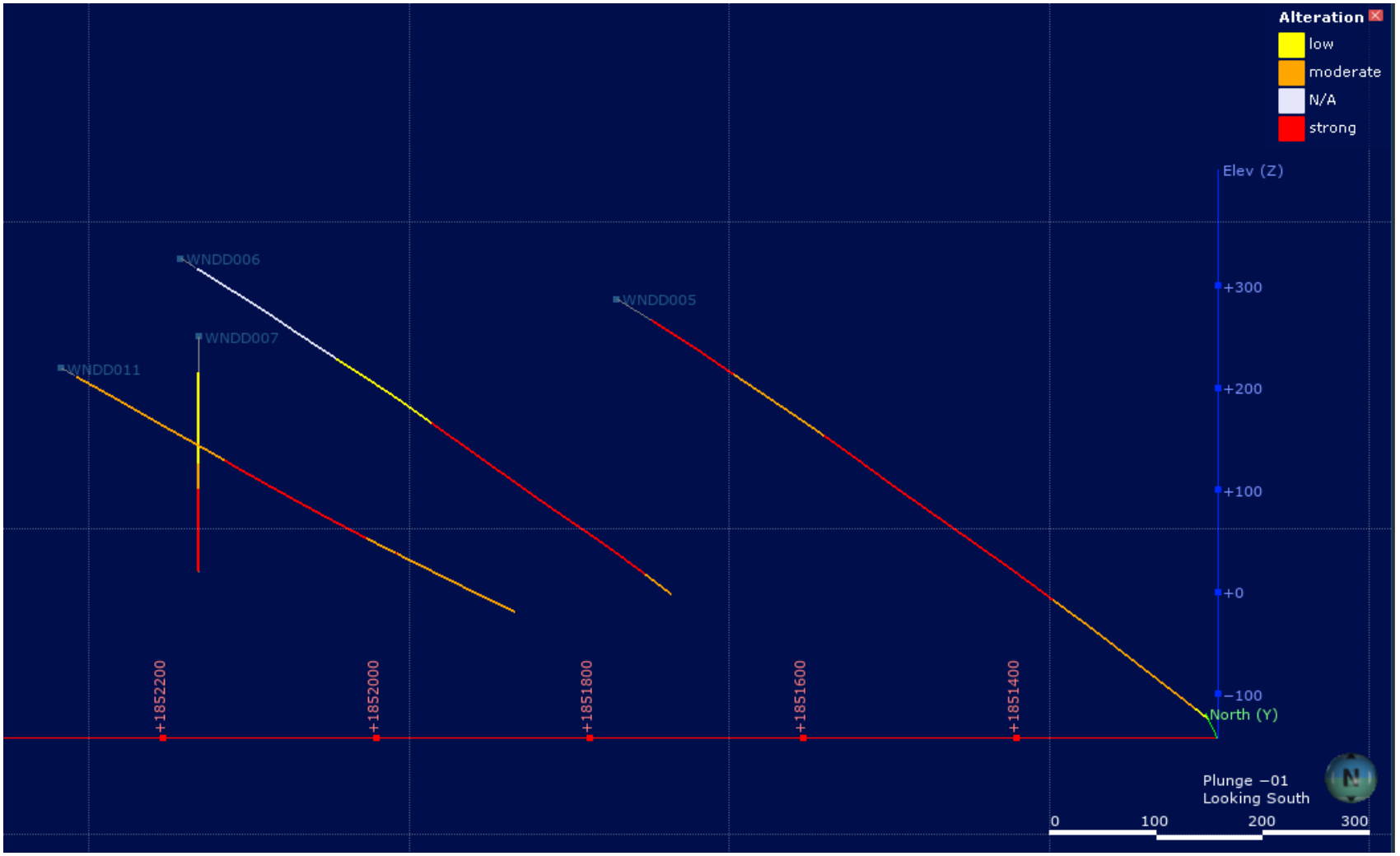

Fig. 5.13. Alteration intensity map of all WNDD005, WNDD006, WNDD007 and WNDD011 holes, looking south

5.5 XRD Analysis:

Bulk rock X-ray diffraction (XRD) analysis was conducted on six samples from WNDD006, WNDD007 and WNDD011. The purpose of this analysis was to confirm some of the results that were drawn from the microscope analysis and ensure there were no major minerals occurring in the samples that were out of the ordinary or unexpected. By running the XRD results through the Highscore software the major minerals were able to be identified. Due to instrumental delays, analysis of clay separates could not be identified

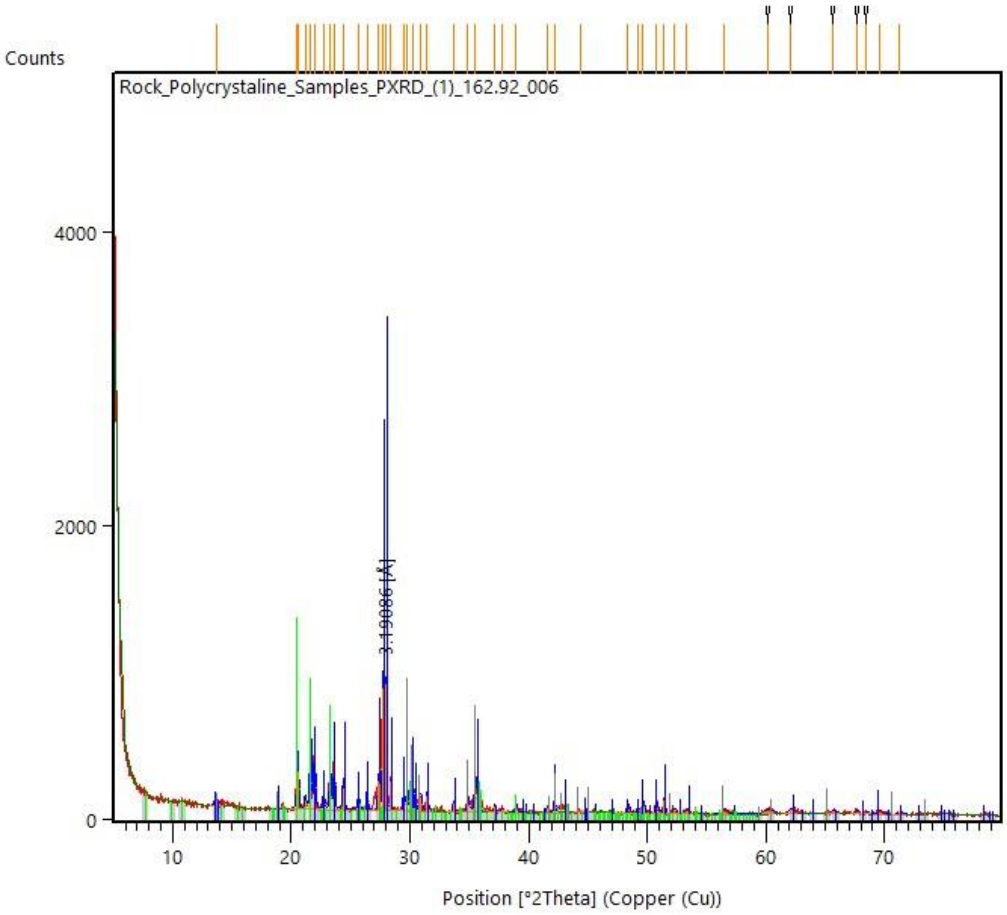

Figure 5.14. XRD Analysis results from 006- 182.92

The primary peaks on figure 5.14. were identified as plagioclase and are represented by the blue lines. This is followed by the green peaks of the next strongest match which represent quartz. The grey peaks were the final mineral group identified and are most likely to be augite. These are the expected major minerals to occur in this sample as it was a relatively unaltered andesite. The small black V shaped markers above the yellow lines on top of the chart represent the unidentified peaks.

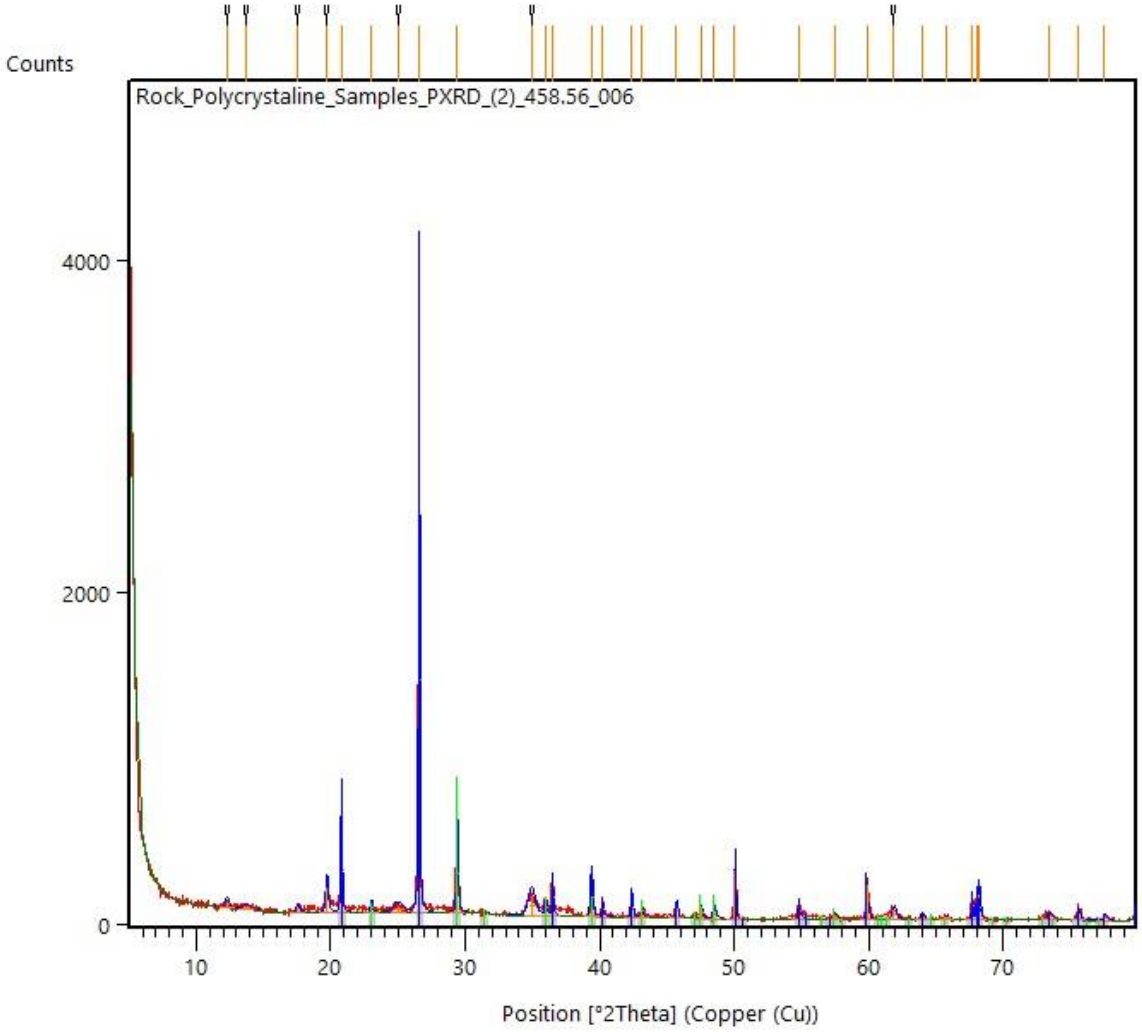

Figure 5.15. XRD Analysis results from 006- 458.56 m

Figure 5.15. shows the results from sample 458.56 m in WNDD006. This sample was composed of quartz, strongly represented by the blue peaks, and was followed by calcite which is shown from the green peaks. This was as expected with this sample appearing to be more highly altered than the sample from the chart above. There is a cluster of unidentified peaks early on in the graph from °2θ angles 12-18**.** These most likely represent clays, which were present in the majority of the altered samples, however a clay separate analysis would be required to accurately identify these.

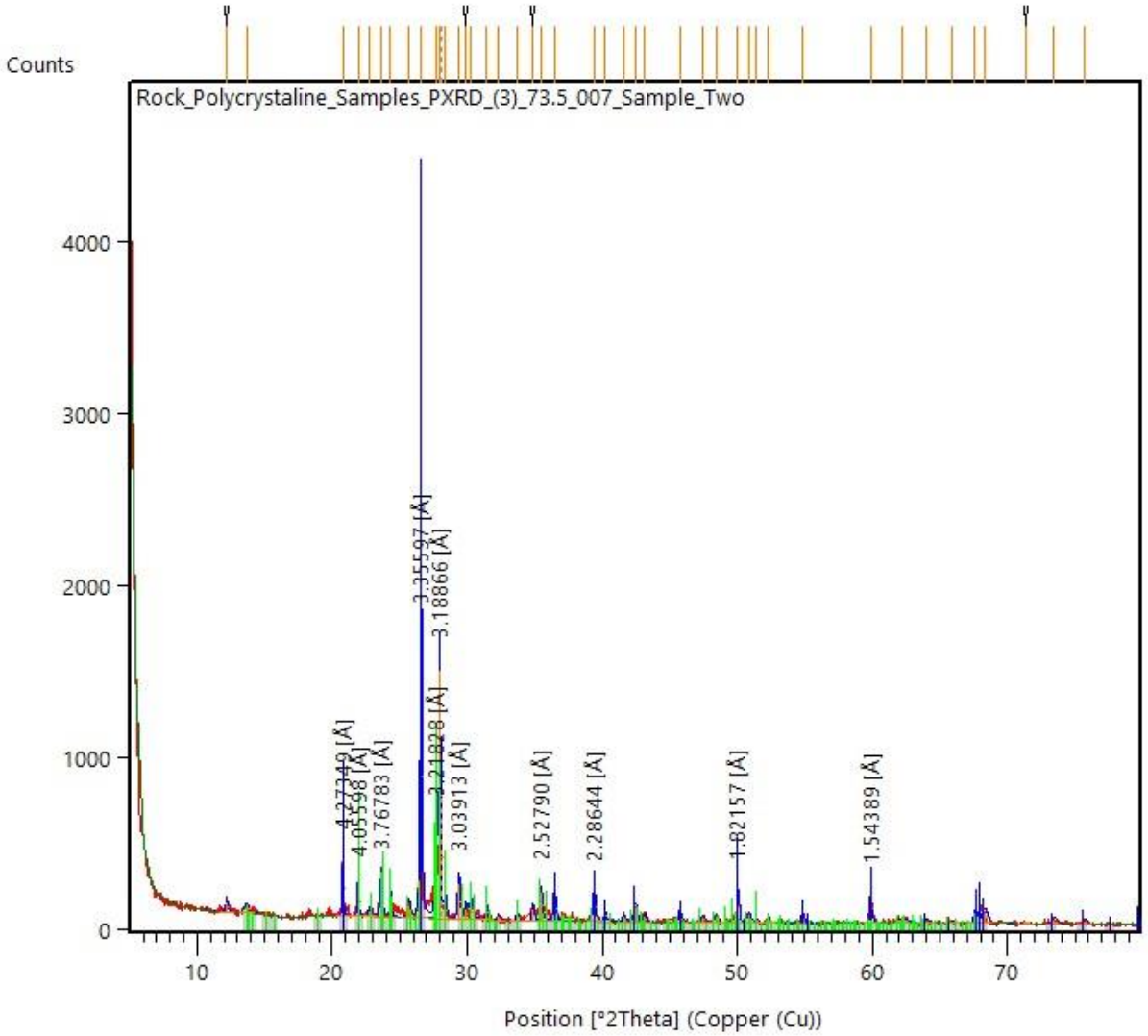

Figure 5.16. XRD Analysis results from 007- 73.50 m

Sample 73.50 m from WNDD007 shown above in figure 5.16. is composed of quartz represented by the blue line with major peaks at 3.336 Å, 4.273 Å, 3.189 Å and 1.822 Å. This is followed by plagioclase with the next strongest correlation, shown by the green peaks at 4.056 Å, 3.768 Å, 3.218 Å and 2.528 Å. As this sample was also observed to be a relatively fresh andesite, these two minerals were to be expected. The few remaining peaks scattered across the chart were too small to identify accurately but may represent augite as there were pyroxenes identified in this sample. In this sample there were also no visible clays peaks.

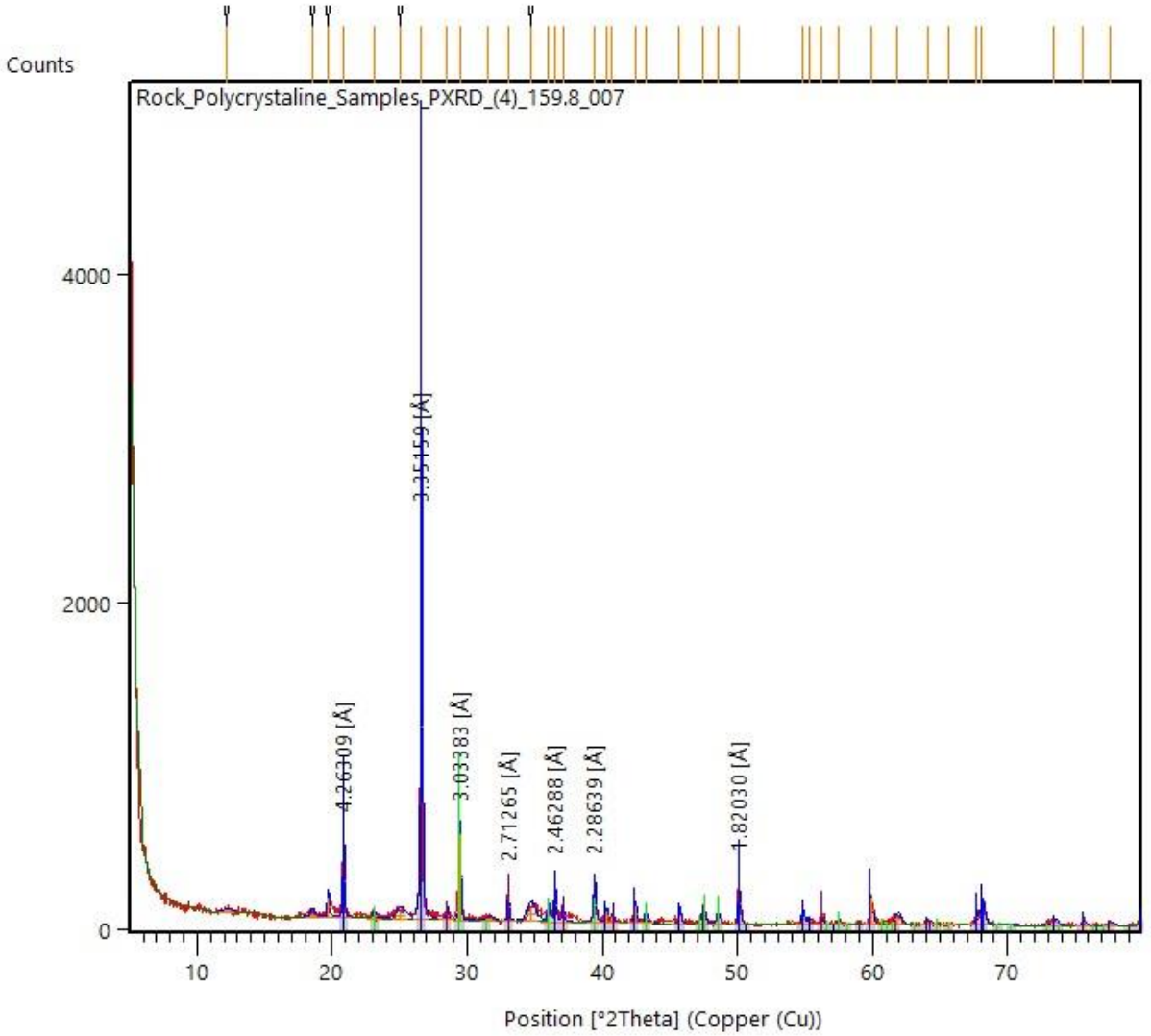

Figure 5.17. XRD Analysis results from 007- 159.80 m

Figure 5.17. shows the results from 159.80 m in WNDD007. This sample shows a strong correlation to quartz, represented by the blue peaks, with major peaks occurring at 4.263 Å, 3.352 Å, and 1.820 Å. Calcite shows the next strongest correlation which can be seen in the green peak at 3.034 Å as well as two smaller unlabeled peaks from °2θ 47-49. Finally, pyrite was identified and represented by the purple peak at 2.713 Å. As an altered sample, the results here were not surprising with the presence of alteration minerals including calcite and pyrite. However as samples with low sulfides were used, (for XRF compliance) pyrite and other sulfides will be underrepresented in the XRD samples.

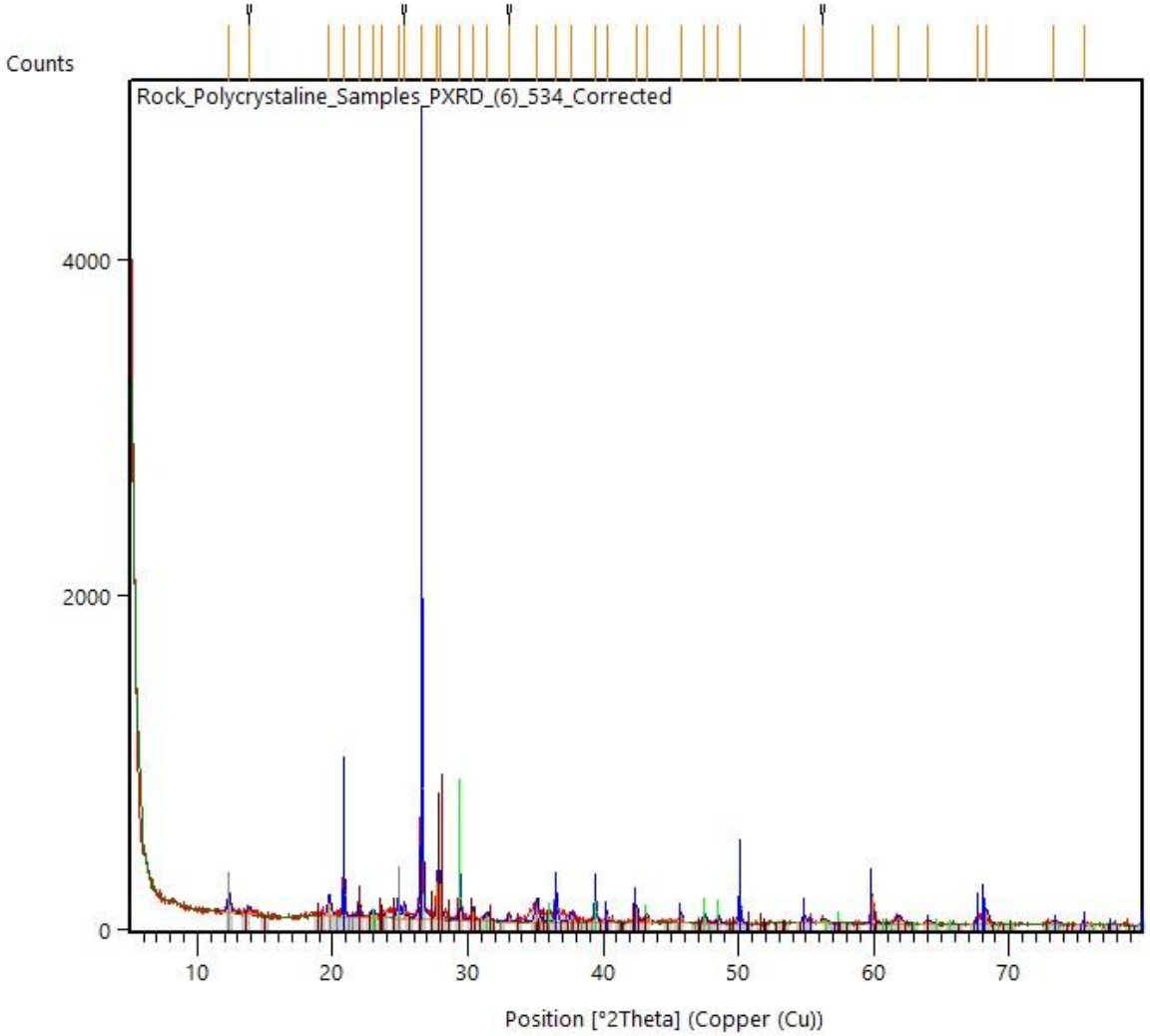

Figure 5.18. XRD Analysis results from 011- 534.30 m

The sample at 534.30 m from WNDD011 is shown in figure 5.18. This sample displayed a correlation to quartz which is shown by the blue peaks. This is followed by calcite, as is the trend with altered samples, which is represented by the green peaks. Unlike the other samples, at 534.30, there is likely to be a high quantity of clays as the grey peaks represent clays which are likely to be present in the form of kaolinite or dickite. This sample appeared to have a highly altered groundmass and appeared the most aphanitic in the photo core so these minerals could be expected in this sample with calcite and clays commonly occurring as alteration products.

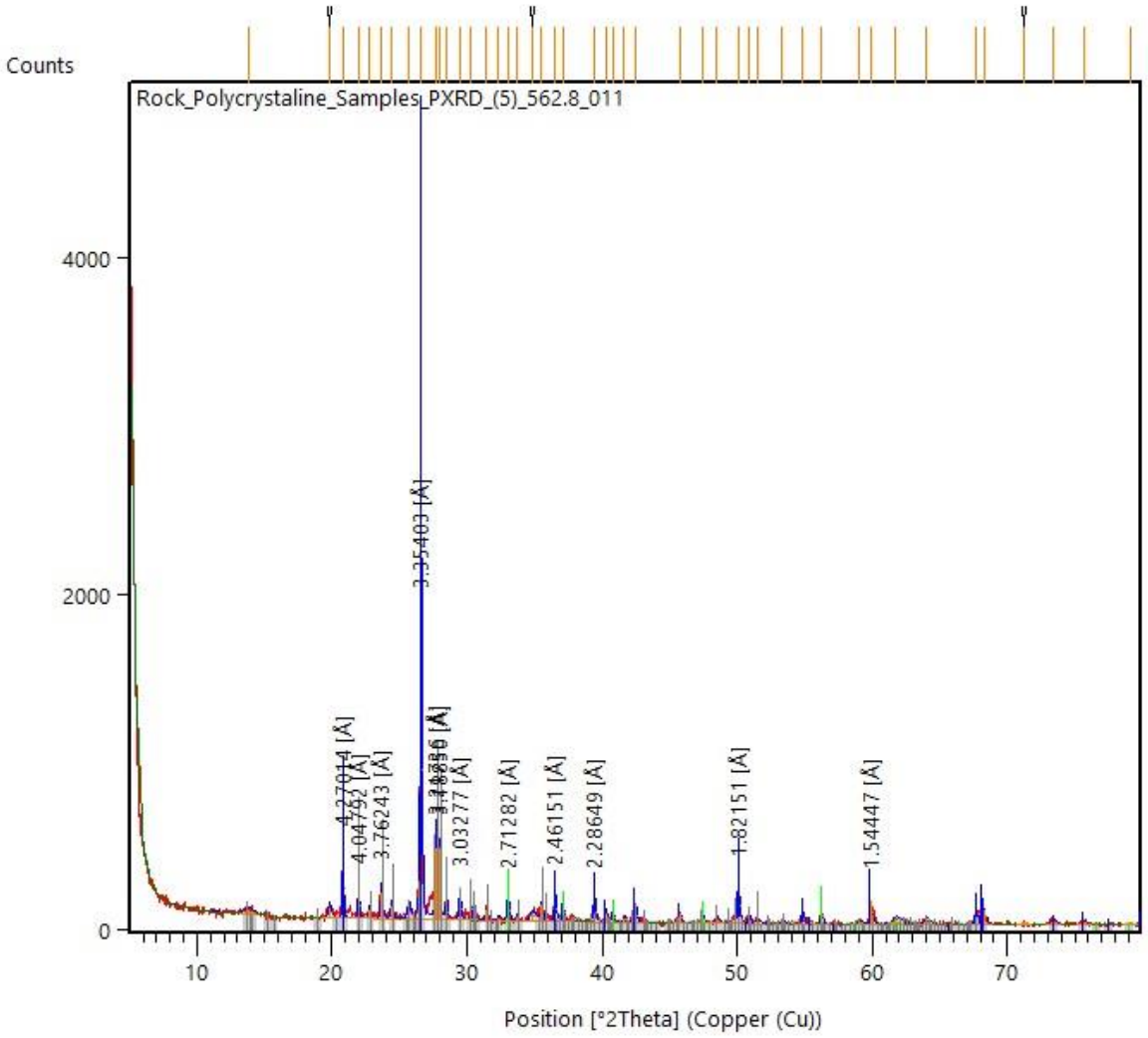

Figure 5.19. XRD Analysis results from 011- 562.80 m

Figure 5.19. shows mineral XRD results from 562.80 m in WNDD011. The strongest correlation, represented by the blue line, identifies the quartz in the sample, with the major peaks occurring at 3.354 Å, 4.270 Å, 1.822 Å and 1.544 Å. This is followed by pyrite which is shown by the green peaks, most prominent at 2.713 Å. Plagioclase was also identified as the grey peaks, present at 4.048 Å and 3.762 Å. These minerals identified almost all the peaks with an exception of three scattered across the chart. While this sample occurred at depth, it only showed minor alteration, this was evident by the presence of plagioclase and lack of calcite, however the pyrite indicated that some level of alteration has occurred. The lack of unidentified peaks at the start of the chart could represent a low quantity of clays, also indicating a fresh sample.

Chapter 6
Geochemistry

6.1 Methods

XRF (X-ray Fluorescence) analysis was used to determine specific details regarding the rock type and composition of the samples. Samples were chosen that represented the holes and the visible changes in the core while adhering with the analysis specifications of the samples and time-frame available. Samples with the least alteration were preferred as sulfides can damage the crucible used in the sample preparation process. Once the samples were chosen they were ground to a powder, using the tungsten carbide ring mill. Three 1 x 1 cm pieces for each sample were required in order to have enough sample. This was achieved by taking the off cuts from the blocks from the thin sections and cutting them with the rock saw or smashing them with a hammer to size. These pieces were then rinsed and dried in the oven overnight. Once ready they were evenly placed in the ring mill and ground for 30 - 45 seconds. The ring mill was thoroughly cleaned and dried in between each sample to avoid contamination. These powders were then stored in labelled bags.

Samples to undergo XRF analysis needed to be of a low enough sulfur content in order to be safely run in the instrument. To ensure this the samples were tested with a portable XRF (pXRF). The pXRF was attached to a lead box within which the sample was placed. Once the box was closed the pXRF could be used. The pXRF and XRF works as they emit X-rays which result in displacement of inner shell electrons, this results in a release of electromagnetic radiation with an energy equivalent to the difference in energy relative to the space between displaced electrons. Each element's energy release has a characteristic wavelength, and the intensity of the energy is proportional to the concentration of the element in the sample (Gazley and Fisher, 2014). For the pXRF, this allows for a quick summary of elements, with a focus on sulfur to ensure the sample could be run through the XRF, an instrument with similar working mechanisms but superior geochemical analysis ability. To prepare the appropriate samples for the XRF they had to be fused with a 12:22 ratio of flux and iodine. This was achieved by melting them in a furnace together before they were poured in a mould, resulting in a glass “puck” infused with the sample that could be analysed in the XRF. Finally the loss on ignition (LOI) was calculated for each sample. This was conducted by using roughly 2 grams of the powdered sample and weighing it before

heating it in the furnace at 1000 °C for an hour. After the samples were cooled they were weighed again. These two weights were compared and used to calculate the LOI. One sample was re-run through the process to ensure the quality of the sample preparation and the analysis.

6.2 XRF analysis

10 samples were prepared for XRF major element analysis which detected the levels (%) of Na_2O, MgO, Al_2O_3, SiO_2, P_2O_5, K_2O, CaO, TiO_2, MnO, Fe_2O_3, and SO_3. SrO and BaO were also analysed and presented in parts per million. The number of samples was limited due to the sulfur content of the samples, with samples exceeding 10% SO3 being unsuitable for analysis. Five of the 10 samples have less than favorable results due to the high total percentage, indicating an inaccurate analysis. As this has occurred in all the samples with a higher sulfur content, it is inferred that this is the reason for the results (Table 6.1).

Table 6.1 XRF major element analysis results

Sample	*006-182.92*	*006-315.22*	*006-373.58*	*006-458.56*	*007-73.5*	*007-109.5*	*007-140.9*	*007-159.8*	*011 534.32*	*011 562.8*
Rock type	Andesite	Andesite	Andesite	Andesite	Andesite	Andesite	Andesite	Andesite	Andesite	Andesite
Inffered level of alteration	Low level alteration	Low level alteration	Altered	Altered	Low level alteration	Altered	Altered	Altered	Altered	Altered
Major oxides										
SiO_2 (%)	61.57	54.9	58.8	60.94	60.75	57.61	54.84	56.12	55.49	62.48
$Al2O_3$ (%)	15.91	17.75	16.83	14.28	15.76	15.47	15.63	14.22	16.52	15.16
TiO_2 (%)	0.561	0.708	0.613	0.54	0.566	0.598	0.566	0.528	0.736	0.538
MnO (%)	0.108	0.068	0.12	0.12	0.067	0.088	0.131	0.113	0.129	0.081
Fe_2O_3 (%)	5.79966	6.45828	1.66931	2.91027	4.72192	5.28215	5.7103	5.4615	7.21591	4.37435
MgO (%)	4.254	4.828	2.067	3.645	3.707	4.097	3.041	4.463	5.058	2.318
CaO (%)	6.553	6.82	6.33	5.656	4.922	4.596	6.609	5.612	3.888	3.758
Na_2O (%)	2.953	2.602	0.337	0.026	2.383	1.823	2.037	0.14	1.828	2.295
K_2O (%)	1.72	0.54	1.89	1.45	1.79	1.57	1.17	1.39	1.34	1.7
P_2O_5 (%)	0.107	0.137	0.113	0.111	0.12	0.122	0.115	0.112	0.139	0.123
SO_3 (%)	0.01	3.57	0.57	0.83	0.57	3.75	5.08	6.17	2.99	6.19
SrO (Sr - PPM)	232	286	143	83	176	201	225	98	192	166
BaO (Ba -PPM)	400	278	662	405	542	460	473	310	293	450
LOI	1.34	4.96	1.65	10.58	5.84	8.36	10.11	9.85	6.03	6.88
Sum (%)	100.945	103.402	100.994	101.141	101.274	103.445	105.128	104.232	101.446	105.963

Red cells display the unsatisfactory samples, indicated by sums of more than 101.5%

6.2.1 LOI

The samples in table 6.1 with the sum highlighted in red were the samples with unfavorable results, as seen in the table these samples also host the highest sulfur content. Sulfur was not the only varying mineral in the samples with the carbon dioxide or LOI varying greatly too, often showing lower values in shallow samples notably from 182.92 m in 006 and 73.5 m in WNDD007. However in WNDD007 this value rapidly increased by 109.5 m and in WNDD006 it increased with a more gradual rate, still displaying low values at 315.22 m. The values shown for WNDD011 are also relatively low given the depth. When inferring the level of alteration the LOI can be useful, as water is held in high quantities in clays and as the presence of clays is common in altered rocks it is likely that samples with higher LOI's (from evaporated water in clays), came from more highly altered rocks. LOI can also represent the CO_2 in the sample. CO_2 occurs in the form of calcite which is another mineral representative of alteration occurring in the form of replaced plagioclase and pyroxenes.

6.2.2 Iron and magnesium oxide

Iron oxide and magnesium oxide levels fluctuate in WNDD006, increasing in the more altered samples before dropping to a relatively low level in the remaining two 006 samples. In WNDD007 the these levels consistently rose very slightly down-hole with a slight trough at 140.9 m, overall increasing iron oxide from 4.72 % to 5.71 % over 86.3 m and magnesium oxide increased from 3.70% to 4.46 % over the same distance . This trend was the opposite in WNDD011 with a significant decrease in both levels from 534.32 m to 562.8 m as iron oxide decreased from 7.21 % to 4.37 % and magnesium oxide decreased from 5.08% to 2.31 %. These measurements typically represent mafic minerals in rocks and in the fresh samples likely represent the pyroxenes and other minor mafic minerals. As alteration occurs however, it is common for the iron to be replaced in the minerals. Iron is also a common constituent of many opaque minerals such as pyrite and chalcopyrite which commonly form as alteration occurs which may explain the lack of linear patterns in these samples. It should also be noted that although normalized, altered and unaltered samples are not always ideal to make comparisons with XRF data.

6.2.3 Silica

Silica is the highest occurring element and ranges from 54.84% to 62.48%. This number remains consistent, with a minimum values at 140.9 m in 007 and peaking at 532.8 m in 011. The silica reading is most useful in determining the type of rock present as silica is the main distinguishable factor when dividing lava suites. In this case all samples fall within the range of 52-65% typical

of calc-alkaline magmas, indicating the samples represent andesite rocks. However, as many of the rocks are altered these results are not reliable especially due to the possible changes in quartz percentage from alteration such as leaching or the addition of hydrothermal quartz. XRF results of altered samples also cannot be compared with other samples due to changes from its original composition. The XRF results show that sample at 182.92m from WNDD006 was the freshest sample with a composition the most representative of fresh andesite, this was followed by sample at 73.5 from WNDD007. The remaining valid samples begin to demonstrate notable levels of alteration. While data like this would be useful in distinguishing between possible dacites and quartz-rich andesites, fresher samples from the study area, free from alteration would need to be collected and analysed. This would result in more accurate results and allow for better comparisons than using normalized data of varying alterations.

Chapter 7
Discussion

7.1 Alteration distribution

The results of the facies distribution analysis can be used alongside the observations of alteration zones and mineralogy to determine their trends in the holes. The holes WNDD005, WNDD006, WNDD007 and WNDD011 were the focus for this as they occurred in close proximity to each other and had the most consistent data in terms of core images, microscope slides, photomicrographs and XRF/XRD analysis data. Figure 7.1. shows the distribution of facies and zones of different alteration intensity against the drill holes (input depths. In appendix C). As with the previous models, white represents little to no intensity, yellow is weak intensity, orange is moderate intensity and red is high intensity of alteration. The margins of high intensity alteration zones commonly occur as breccia facies, as seen in Figure 7.1. Breccia facies occur on the margin of the high alteration zones in WNDD011, and WNDD006 and in the second high alteration zone in WNDD005. The first high intensity zone in WNDD005 ends in a breccia facies and the high alteration intensity zone in WNDD007 begins just above a breccia facies. These are most commonly variations of mosaic breccia with discrete breccia less commonly occurring on the alteration margins. Within different alteration intensity zones there are negligible trends that can be observed relating facies to each zone of alteration with a variation of facies occurring in each zone. This variation can be seen as the high intensity alteration zone in WNDD007 is composed solely of brecciated facies while the second high intensity alteration zone of WNDD005 is almost completely MCCP. It is likely that alteration is controlled by the physical porosity and permeability features of each rock rather than the facies. The IP facies only occurs in zones of moderate alteration or higher which could explain its variable and unique texture, indicating that it may have formed from alteration processes.

The petrographic method of logging is insufficient to accurately determine alteration styles, however areas of different alteration intensity can be identified based on petrographic features such as groundmass destruction, opaque and altered phenocryst content, as well as visual observation of colour from the core images and the XRF results. The model in Figure 7.2. displays lines that depict planes of different alteration intensity. As the holes are oriented in three dimensions this is hard to depict; however, the circular end of the line depicts the plane of

alteration coming into the model from the north and the arrow end of the line represents it carrying on through the image continuing to the south. The models show an increase in alteration intensity with depth, (from the yellow to the upper red line), reaching a high alteration zone (upper red line). Alteration intensity reduces to moderate levels towards the orange line, before returning to a high alteration intensity at depth, (lower red line). The model suggests there are two main paths of hydrothermal paleo-fluid at different depths, creating the two high alteration intensity zones.

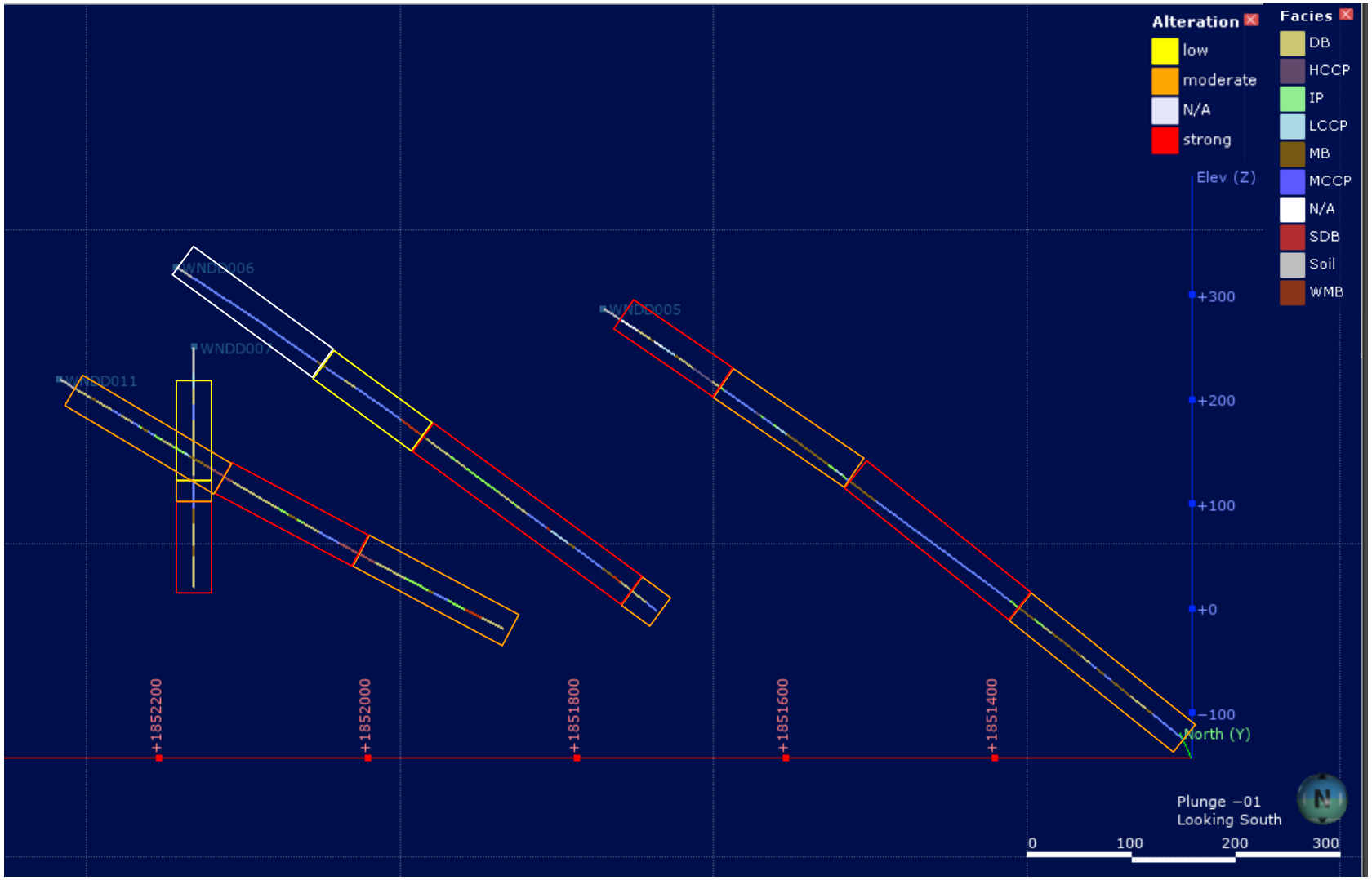

Fig. 7.1. Holes 011, 007, 006 and 005 showing facies distribution and zones of alteration. DB= discrete breccia, SDM= sparse discrete breccia, MB= mosaic breccia, WMB= weak mosaic breccia, IP= irregular pattern, HCCP= high crystal concentration, MCCP= medium crystal concentration, LCCP= low crystal concentration.

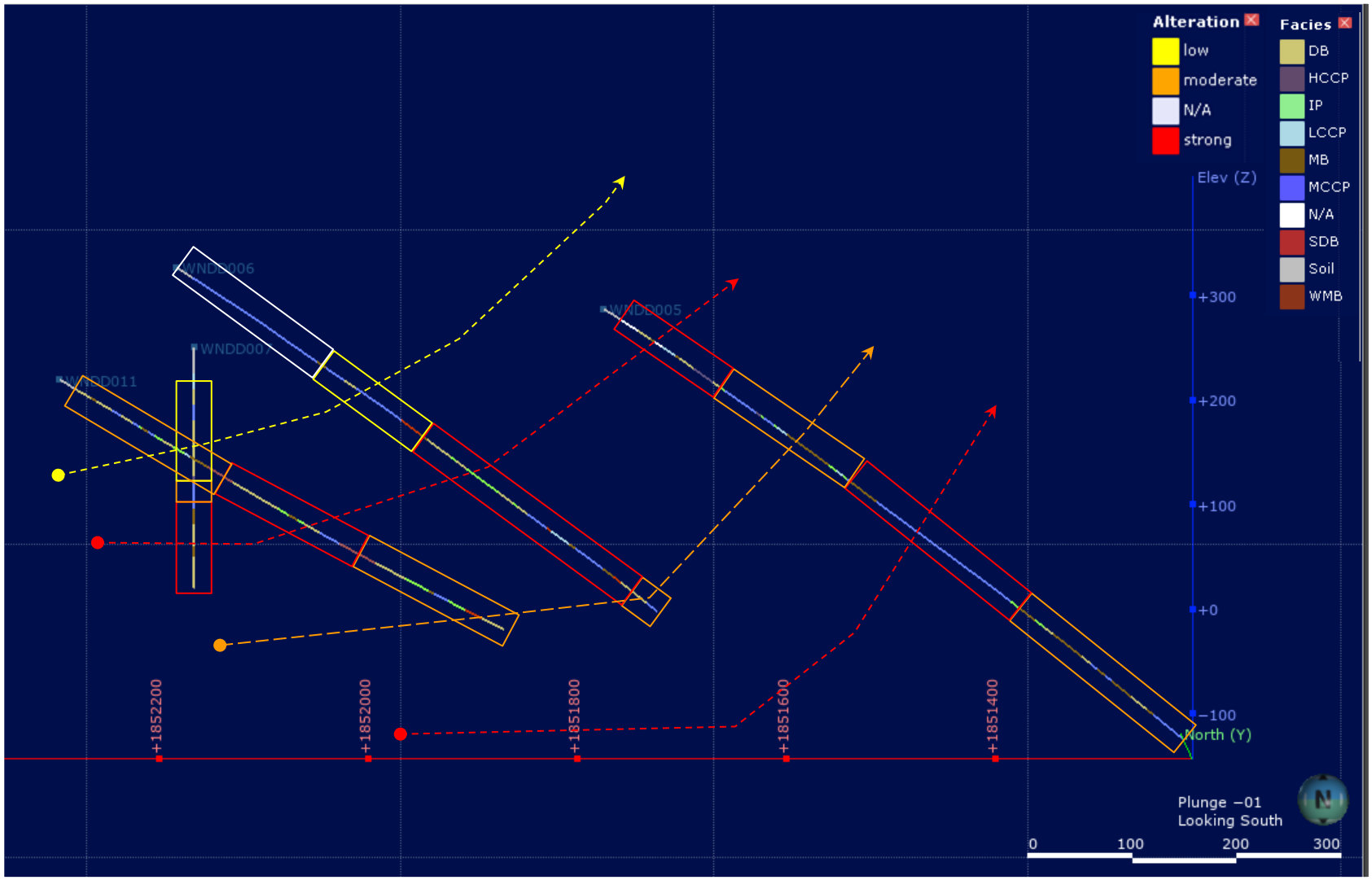

Fig.7.2. Facies against alteration model with inferred planes of alteration. Circular end of arrow representing arrow coming forward, into the view and arrow representing it plunging through it DB= discrete breccia, SDM= sparse discrete breccia, MB= mosaic breccia, WMB= weak mosaic breccia, IP= irregular pattern, HCCP= high crystal concentration, MCCP= medium crystal concentration, LCCP= low crystal concentration.

7.2 Petrography and mineralisation:

Analysis of the relict and fresh petrography of the thin section gives an insight into the processes acting on the rock before and during its emplacement. Contrarily, examination of the alteration mineralogy and secondary features allows for inferences on the processes that have influenced the rock after its genesis. These methods allow for comparisons and correlations between rocks with similar properties, and identifying properties in rocks that could be considered favourable for gold prospecting exploration. Visual thin section observations provide an idea of the level of alteration occurring, by comparing observations in this study to others.

7.2.1 Plagioclase and calcite pseudomorphs

Calcite is a common alteration mineral. Calcite forms as plagioclase is altered. Mielke et al. (2015) found that plagioclase in andesitic rocks that had undergone hydrothermal alteration in the Tauhara Geothermal field of New Zealand was commonly replaced by calcite as well as adularia and chlorite. In the thin sections calcite can often be seen as plagioclase pseudomorphs. Rocks high in calcite pseudomorph phenocrysts are likely to originally have had a high plagioclase content before they underwent alteration processes. Whilst plagioclase has a low resistance to alteration it still indicates that some level of alteration has occurred in the rock. As such, even where plagioclase is abundant, the rock is likely to have undergone low levels of alteration. However, in some cases alteration resistance can depend on the host rock, for example, the Whitianga Group Volcanics in the Waitekauri Valley, Ohinemuri, New Zealand, where plagioclase is more resistant to alteration in the dacites than the underlying andesites (Rabone, 1975). In contrast, quartz is resistant to alteration, so will often appear as the only fresh phenocryst in an altered sample. Therefore, samples with altered volcanic quartz are likely to be highly altered. However, this must be distinguished from samples that are just inherently low in quartz which is common in some andesites. It is also important to differentiate between volcanic and hydrothermal quartz. Plagioclase was often the most abundant mineral so understanding its alteration tendencies aids in explaining the high level of calcite phenocryst and helps determine the level of alteration in the rock.

7.2.3 Pyroxenes

Orthopyroxene and clinopyroxene are susceptible to alteration. Rabone (1975) identified that, in the Whitianga Group andesites, orthopyroxene was the mineral that was the most susceptible to alteration, being altered in zones of unaltered to weakly altered rock. Under weak to moderate alteration intensities, pyroxenes often alter to chlorite (Rabone, 1975). This may explain the texture of some of the yellow-green partially altered phenocrysts, observed in WNDD005 described

as being riddled with opaque minerals. If these were originally pyroxenes, then these opaque minerals are likely to be the iron oxide minerals originally in the phenocryst but excluded from the alteration process to chlorite due to their alteration resistance. As intense alteration occurs, the pyroxenes of the quartz-hypersthene andesites from the Whitianga group evolved from full chlorite alteration to replacement of chlorite by carbonates. Carbonate replacement is most likely to be in the form of calcite and possibly dolomite and siderite (Rabone, 1975). This gradient of alteration may be responsible for the various alteration phenocrysts that do not give typical calcite appearances. Pyroxenes often have a euhedral shape and can be preserved as pseudomorphs, and so some of the pseudomorphs described as plagioclase pseudomorphs may instead be altered from pyroxenes.

7.2.3 Pseudomorphs

The shape of phenocrysts is also examined and can give clues on the volcanic processes which have occurred. Pseudomorphs are comprised of alteration minerals but still retain the shape of the fresh mineral they have altered from. As plagioclase is distinctly tabular in shape they are easily identifiable when altered, especially when altered to calcite. Orthopyroxene have a variety of forms including massive, irregular and prismatic. In the samples of this study they are often seen as rectangular, so when altered it can be difficult to distinguish pyroxene and plagioclase pseudomorphs due to the similarity in shape. These pseudomorphs can be preserved even in intense alteration and can consist of calcite or clays. Pyroxene pseudomorphs that had undergone extreme alteration in Ohinemuri showed compositions of kaolinite, illite and colorless chlorites (Rabone, 1975), which may represent some near amorphous textures observed in some of the altered phenocrysts. Pseudomorphs determine that the rock has undergone alteration and preserve original phenocryst shape, aiding in relict identification.

7.2.4 Quartz

Quartz phenocrysts can suggest processes that occurred within the original magma. The frequent embayments and resorption, viewed in the quartz phenocrysts throughout the holes imply a state disequilibrium during quartz formation, possibly due to magma mingling. The average size of quartz phenocrysts varies across the thin sections ranging from 2.25 mm to 0.3 mm with the largest sizes typically occurring more than 350 m down hole. Quartz phenocryst abundance also varies, from <1% to 12% across the core, suggesting the occurrence of different lava flows. Hydrothermal quartz can also occur in the andesite groundmass, breccia matrix and veins due to hydrothermal alteration, and can obliterate the original groundmass texture, which is often

replaced by a quartz mosaic. Quartz mosaic textures can form due to the release of silica by chloritisation of pyroxenes as well as replacement of chlorite by carbonates (Rabone, 1975). Another process of hydrothermal quartz formation occurs as calcite is saturated during the first boiling event in the alteration system. As boiling propagates again after the first boiling event, the calcite is replaced with silica resulting in quartz formation (Simmons 2021). Alteration of the abundant SiO_2 in the plagioclase and glass can also contribute to the formation of hydrothermal quartz. Such hydrothermal process appears to be observable in holes WNDD005, WNDD006 and WNDD0011 and would explain the patches of coarse-grained felsic texture occurring in areas where the core appears altered. This occurrence is also observed in the Whitianga Group Volcanics in the Waitekauri Valley in quartz-hypersthene andesites (Rabone, 1975).

7.2.5 Groundmass

Genetic processes can also be inferred from the mineral distribution. A seriate texture has a continuum of crystal sizes from fine groundmass grains to coarse phenocrysts and suggests that polybaric crystallisation occurred during magma ascent. Polybaric crystallisation results from the magma pausing during accent and undergoing crystallisation at different pressures, resulting in the complex fractionation of major elements. Seriate textures are observed consistently in the majority of the holes with the exception of WNDD010 (and WNDD009 due to a lack of samples). At depths this texture becomes weaker, however this loss of seriate textures occurs in heavily altered samples, so is likely to be due to alteration. The WNDD010 thin sections also appear to have a heavily altered groundmass. It is likely that the majority of the magmas had an intermittent accent during their genesis.

7.3 Porosity

Variation in rock porosity dictates the path of subsurface fluids and is a direct catalyst to hydrothermal alteration. There are multiple controls on the flow path of fluids in rocks and this can vary between rock types/facies based on the mineral framework and secondary features present. In rocks with a tightly packed, homogenous, individual crystal framework, such as in uniform porphyritic or phaneritic textured rocks a low melt porosity will be present, forcing fluid to travel through secondary features such as joints and microfractures. Browne (1989), found that hydrothermal alteration in rocks with these tightly packed crystal structures resulted in sharp changes in alteration intensity over short distances in the Quaternary andesites from the Taupo Volcanic Z one. In contrast, rocks with a mixed population of irregular shaped crystals or clots of crystals will produce a framework with a low melt porosity allowing for fluid to penetrate through

them along interconnected pores and grain boundaries resulting in a more pervasive and homogeneous alteration style (Browne, 1989). Wyering (2014), acknowledges that andesites are likely to have a wide range of primary porosities depending on their clast arrangement and depositional history. Certain textures such as a glomeroporphyritic texture can make a rock more susceptible to alteration. This texture was observed most prominently in holes WNDD005, WNDD006 and WNDD011 and can increase porosity due to the irregular phenocryst clumps and mixed population of crystals present. The polybaric crystallization occurring as the magma cooled forms the seriate texture seen in holes WNDD005, WNDD006, and WNDD011 as well as WNDD007 and can also form glomeroporphyritic clots. This combination of textures means the rocks in this area, with these features, can facilitate the movement of hydrothermal fluids and therefore are more susceptible to alteration.

Mordensky et al. (2019), found that in andesite lavas from the Rotokawa geothermal field, thermal alteration increased the rock porosity and permeability. This was credited to a combination of quartz, calcite and clinochlore breakdown as well as stress induced microcracking from the thermal gradients and reaction driven volume changes during both heating and cooling (Mordensky et al., 2019). Such breakdown is evident in this study, observed in the obliterated groundmasses and heavily fractured phenocrysts of thin sections such as WNDD005 - 614.25 m (Fig. 5.2.) and WNDD006 530.2 m (Fig. 5.10.). This is of relevance to the rocks in this study as in epithermal environments multiple fluctuations of hydrothermal fluid propagating through permeable pathways is common (Simmons, 2021). These thin sections occur in zones of high intensity alteration, as it is likely that many of the rocks here became more permeable overtime as they were exposed to hydrothermal alteration. This alteration exposure resulted in the weakening of the rock, increasing its porosity and permeability, exposing more of the rock to alteration on the next propagation of hydrothermal fluid. Thus, creating the zones of alteration observed in this study. The style of alteration occuring can also affect the rock, demonstrated by Wyering (2015), who found in their study, that in Ngatamariki, Rotokawa and Kawerau andesites the porosity of the samples increased, and the densities decreased from high temperature alteration compared to low temperature alteration. Inferring that the alteration style is significant to the development of the porosity of host rocks. The combination of rocks in this study area forming from polybarric crytallisation, displaying glomerporphyritic clots and seriate textures resulting in rocks with higher innate porosity. High porosity rocks and evidence of continued alteration such as the various relict phenocrysts and textures, obliterated groundmass and fractured phenocrysts, also bearing the continued effects on porosity from alteration make these rocks an ideal host for epithermal

deposits. Providing an insight as to why 97% of total past gold production in the Hauraki Goldfield is from deposits hosted in andesite and dacite Coromandel Group rocks.

7.4 Facies origins

7.4.1 Coherent facies

The macroscopic analysis of the core gives an overview of the geologic setting over space allowing for the creation of facies to be inferred based on the spatial variation of the physical features in the core. Due to the nature of photo logging, the crystal concentration was one of the main distinguishing factors between facies. The low crystal concentration porphyritic (LCCP), medium crystal concentration porphyritic (MCCP) and high crystal concentration porphyritic (HCCP) facies were distinguished, and represent the coherent lavas found in the study. LCCP represents porphyritic rock with a crystal concentration of 1 - 5%, MCCP represents porphyritic rocks with crystal densities of 6 - 24% and HCCP represents rocks with a crystal density of >25%. These variations can allow for inferences to be made on magmatic origin and emplacement processes of the rock.

Phenocrysts primarily form in the magma chamber as a function of temperature and cooling time. Higher temperatures form mafic crystals in contrast to cooler temperatures which form felsic crystals. Cooling time dictates crystal size with slower cooling times resulting in larger phenocrysts in comparison to faster cooling times. The rate of magma ascent is directly related to the cooling rate of magma. As mentioned above the petrographic data shows seriate textures in the thin sections indicating variations in the ascent of the magma, resulting in possible polybaric fractional crystallization in some places. Varying rates of cooling are a possible reason for the changes in concentration of visible phenocrysts, which may have been caused by variations in rates of magma accent over time resulting in the three different facies. However, it should also be noted that in a study on andesitic flow units in Mount Ruapehu by Waight et al. (1999), with similar characteristics to the MCCP and HCCP facies, the Turoa lavas of the Mangaturuturu Formation with phenocryst abundances of 7 - 51% were geochemically analysed. It was found that the more phenocryst-rich lavas represented crystal accumulation, not only in the magma chamber (pre-eruptive) but also within individual flows (post eruptive) (Waight et al., 1999). This could indicate that post eruption cooling could also be a possible reason responsible for the variation in phenocryst abundance of the facies. Another likelihood of the change in phenocryst size could be accredited to multiple eruption events. Core has been observed on a spatial scale over hundreds

of metres. On this scale there is a high likelihood that variations in the phenocryst concentration could be accredited to the characteristics of different lavas from varying eruption events resulting in the different facies.

A more recent study by Frey and Lange (2010), described other andesite and dacite magmas with similar characteristics to those seen in these facies from the Tequila volcanic field in the western Mexican arc. Both phenocryst-poor magmas (2-5%), comparable to the LCCP facies, and phenocryst-rich magmas (10-25%) comparable to the MCCP facies are observed in the Tequila volcanic field. The low phenocryst concentration magmas erupted 685 - 225 ka with the phenocryst-rich magmas erupting less than 200 ka. Despite varying crystal concentrations both magmas have similar compositions of plagioclase + orthopyroxene + titanomagnetite + ilmenite + apatite + augite + hornblende. The phenocryst poor magmas originate from monogenetic vents while the phenocryst-rich magma originated from a stratovolcano. In these phenocryst poor magmas it was found that most of them were fluid saturated by depths greater than 6.5km, indicating that degassing was an inevitable process as the magma ascended to the surface. Degassing would also lead to an abrupt increase in liquidus temperatures, resulting in undercooling that would facilitate diffusion-limited growth textures such as the swallow tail microlites, embayments and melt inclusions presented in chapter 4. It was also deduced that magma mingling is not the only process capable of producing a diverse population of plagioclase and pyroxene compositions and textures in andesites and dacites suggesting the effects of degassing should also be considered (Frey & Lange, 2010). So despite previous evidence for magma mingling stated above, degassing of the magma to cause the phenocryst assemblage should also be considered as a process that has acted on the magmas in the study area. It may also be considered that both processes may have been active at different times, which would be possible in multiple eruption events.

The local geology of the area is composed of Waipupu and Whiritoa andesites as mentioned in 3.7 of chapter 3. The Whiritoa andesite is a pyroxene andesite of the Waiwawa subgroup. Geochemical analysis of samples from a 2012 study (Booden et al., 2012), of Whiritoa andesite from the CVZ allows for comparison with the samples analysed in this study by XRF analysis. The Whiritoa andesite had similar SiO_2, TiO_2, Al_20_3, K_20 and P_20 concentrations as WNDD006 at 373.58 m and WNDD007 at 109.5 m analysed in this study. The main difference is that the Whiritoa sample displays significantly higher Mg0 and combined iron content (7.74%). The WNDD006 sample at 182.92 m was the freshest sample in this study and displayed a silica value of 61.57% compared to the 58.37 % from the Whiritoa andesite the next freshest sample from this study,

The WNDD007 sample at 73.5 m also had a higher silica level at 60.75%. While it may be futile to compare geochemical data due to the possible variances in alteration, the higher iron and magnesium concentrations could suggest there are higher levels of mafic minerals in the Whiritoa samples than in those that were analysed from the study area. As mentioned in chapter three Brathwaite & Christie (1996), describe the Whiritoa andesite, as a phyric, plagioclase and two pyroxene andesite including dacite flows and domes with tuff breccias and lithic crystal tuff. The Waipupu formation was described as a phyric, plagioclase and two pyroxene andesite and dacite with local quartz phenocrysts, minor tuff breccia, crystal tuff, and lacustrine sediments. Quartz abundance fluctuates in the study area with some zones showing concentrations of <1% while others have 12%, the localisation of quartz in the study infers the Waipupu Formation should also be considered as the potential andesite of origin.

The Waipupu Formation andesite is a two-pyroxene andesite, originating from andesitic lava flows, often bearing lesser volcanic breccia and localized intercalations of lithic-crystal tufts with minor epiclastic sedimentary rocks (Simpson & Mauk, 2011). This andesite occurs extensively around epithermal deposits and is a significant host rock at Jubilee, Jasper Creek and Sovereign, located approximately five km WSW of the study area. Waipupu Formation andesite also occurs extensively in the world class Martha Hill deposit just four km south of the study area, with geological maps showing it extends to cover much of this area. While little work has been published on the Waipupu andesite, an extensive analysis was conducted in a study regarding the facies of the andesite peripheral to existing Waihi mine workings (Bodger, 2015). Bodger found that the crystal concentration of the Waipupu Formation andesite ranged from 10 to 60% and were dominated by feldspar and mafic minerals that were difficult to identify through the overprinting alteration. This correlates well to the abundant MCCP and HCCP facies identified. He also identified breccia facies with breccia clast size ranging from 9 to 150 mm, and these clasts are predominantly composed of feldspars with some mafic minerals. Such facies relate to the breccia in the sparse discrete breccia (SDB) and discrete breccia (DB) facies. From his six coherent facies and two breccia facies, Bodger (2015), described the Waipupu andesite as generally porphyritic with prominent but scarce quartz phenocrysts and a total crystal content of 10 - 25%, comprising 1 - 20 % feldspars, 1 -2 0% mafic minerals, and <1 -1 0% quartz. Three of the facies are designated as “quartz bearing” showing similarities to the localised quartz observed in this study. The crystal contents of Bodger’s (2015), study can also be compared to the petrography data of this study, yielding frequent similarities starting with the porphyritic texture observed. The fresh phenocryst content in the majority of the holes are within the parameters described by Bodger (2015), above, with some exception in the more heavily altered samples. The ranges of felsic phenocrysts Bodger

(2015), recorded are also a fairly similar representation of this study, however some samples reached over 30% abundance in felsic minerals. There was also a lower rate of mafic minerals in this study with many samples exhibiting no fresh mafic minerals, possibly due to variations in magma composition. However, this could also be a result of alteration as it could be inferred from the fresher samples that mafic minerals were likely present in the original rock such as in fresh phenocryst counts seen down holes WNDD006 and WNDD007. Such crystal abundances are also common in volcanic successions of modern active andesite volcanoes (Mount Ruapehu, New Zealand), as well as Late Archean andesites-dacites (Kurnalpi Terrance, Western Australia). The Waipupu andesite from Bodger's (2015) study also showed similarity in phenocryst features with polysynthetic twinning in the plagioclase and resorbed and embayed quartz being identified. Such similarities indicate similar magma chamber and/or emplacement processes acting on the rocks, presenting evidence pointing to similar origins of the rocks in the two studies and outline many similarities with the Waipupu andesite. Though the consequences of alteration have created some discrepancies, the similarities in primary mineral composition and features, phenocryst abundance and the proximity to the study area anindicate that the Waipupu Formation Andesite is a likely match to the rocks in the study area.

7.4.2 Breccia facies

The other criteria distinguishing facies was the presence of breccia. The mosaic breccia (MB), sparse mosaic breccia (WMB), discrete breccia (DB), and sparse discrete breccia (SDB) were new breccia facies identified in this study. Breccia may have occurred as a primary process in the form of autobreccia at the edges of lava flows or may be the product of hydrothermal alteration. Regardless, it is likely that all breccia present have been altered in some way by hydrothermal alteration. Some of the breccia specifically in the non-altered areas of the core resemble autobreccia, which is the product of a primary volcanic process related to the non-explosive fragmentation of flowing lava. Cooler, more viscous lava flows and lava flows subject to higher strain rates than the rest of the flow have a brittle response to stress. This results in the generation of rigid plates, blocks and spines which typically cascade down the flow front before becoming re-incorporated as the lavas flow over them. This will typically result in a carapace enclosing a coherent interior with a floor of autobrecciation being observed (McPhie et al., 1993). Sometimes parts of the brecciated surface are integrated into the interior of the flow and are preserved in the otherwise coherent lava as irregular pockets of autobrecciation. Such irregular pockets of autobrecciation are observed in the frequently varying DB and SDP facies in which often brief intervals of brecciation are observed in the otherwise coherent core. In the scope of

this study it is likely that textures and characteristics of any autobreccia have been modified by the subsequent hydrothermal alteration. This will occur as clast margins will be affected and clasts will fracture, resulting in the original clast supported or mosaic breccia transforming into an apparent matrix-supported breccia. This process is likely to be responsible for some of the brief pockets of the MB facies that appear to grade in and out of the coherent rock's groundmass. (McPhie et al., 1993).

Hydrothermal breccia develop during early vein formation, in response to the fracture propagation process catalyzed through hydrofracturing by high-pressure hydrothermal fluids which is related to temporal variations in fluid pressure (Shukla & Sharma, 2020). In this process, water-rich hydrothermal solutions common in the low sulphidation epithermal environment, interact with the rock and propagate through passages and fractures. In hydrothermal systems processes such as subcritical crack growth can allow cracks to propagate below the strength limit of the rock. Sources of stress can be defined into renewable and non-renewable stress. Renewable stress which persists through continued stress and relaxation intervals relates to tectonic activity, whilst nonrenewable stress, ceases as the initial strain subsides (Jébrak, 1997). These can account for a continuum of eight main mechanisms of hydrothermal brecciation (Fig. 7.3.), with tectonic comminution and fluid assisted being the most common. Fracture propagation and wear abrasion (the numerous interactions between micro-fragments during small scale fragmentation), make up the tectonic comminution process while hydraulic and critical fracturing are the main mechanisms of the fluid assisted process (Jébrak, 1997). Breccia associated with tectonic comminution usually display fragments of an angular morphology with a high variable range of fragment sizes. As fractures begin to propagate, usually at a slow rate, this will lead to similar sized fragments forming and as propagation speed increases fragments display a larger variation in size. Thus suggesting why the breccia vary greatly in size in certain locations of the core, and allowing for inferences on propagation speed to be made.

On the contrary, fluid assisted brecciation can occur during or before vein formation, but as this brecciation type tends to occur in low permeability rock, it is usually observed prior to extensive fragmentation at the beginning of the infilling process. This will generate in-situ fragmentation textures such as those seen in the MB and WMB facies. Lack of significant rotation is typical of hydraulic fracturing while critical fracturing can result in rotation and can occur in rather deep environments. In this type of brecciation fragments are angular with brecciation following pre-existing planes of continuity (Jébrak, 1997), sometimes seen in the MB facies. However local rounding can also occur due to hypogene exfoliation caused by pressure fluctuations (Sillitoe,

1985). It is likely that hydrothermal breccia will also be affected through margin deformation and clast fractures as further hydrothermal interactions occur.

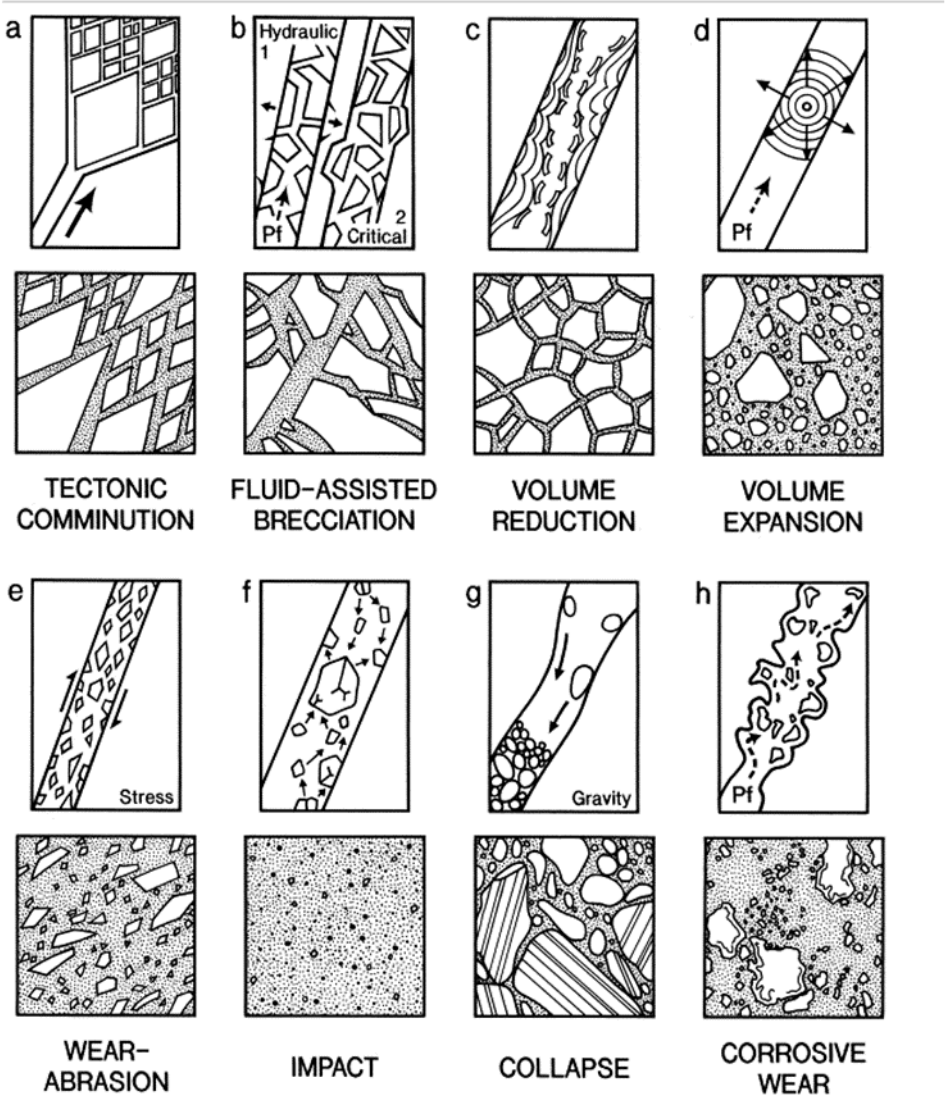

Fig 7.3. Mechanisms of hydrothermal brecciation derived from Jébrak, M. (1997).

The processes involved with hydrothermal breccia likely increase the porosity of the rock relative to non-brecciated rocks acting as a gateway to facilitate hydrothermal alteration. This could possibly explain the relation of brecciated facies to alteration zones seen in figure 7.1. Where breccia are often seen to border zones of high intensity alteration and are also commonly found in high alteration intensity zones. The fracturing occurring in breccia caused by either their formation or from secondary alteration processes (possibly all breccia facies), would increase the permeability of the rock relative to the fresh coherent facies, facilitating the flow of subsurface fluids.

The intermittent pattern (IP) facies in this study could be described as a transitional facies. This often occurs on the borders of alteration zones in areas of moderate to high alteration. The IP facieses often occurs adjacent to breccia facies (Fig 4.12.), and could be represent more permeable sections of the rock that act as paleofluid pathways facilitating alteration much like the breccia. As this facies is heavily altered it is likely to have a higher porosity as discussed above. The irregular patterns seen in these facies could be explained by interaction with hydrothermal fluids. The changes in irregular patterns may represent flow of hydrothermal fluid through more permeable sections in the rock or could represent deformed breccia due to extensive alteration. In some sections the crescents are not the same texture as the surrounding rock, instead displaying fine grained textures, it could be inferred that the crescents are the product of sediment in-filling.

7.5 Geochemistry:

Geochemistry is a useful tool when attempting to quantify hydrothermal alteration as it is possible to identify alteration vectors by analysing anomalies in the chemistry of the samples. This can be useful for exploration, as with sufficient sampling and geochemical analysis, parameters and limitations on alteration halos can be created, aiding in narrowing down the location and extent of epithermal deposits. Observations of major elements relating to the exploration of epithermal deposits are mentioned below and compared to a study carried out by Ravinder S. Singh (2015), of Waipupu andesite from the Correnso mine in the Waihi area.

7.5.1 Potassium (K)

Minerals with higher K contents were observed in close proximity to the zone of mineralisation in the Correnso mine and can be used as a vector towards orebodies in low sulfidation epithermal deposits (Singh, 2015). At Correnso this relation is emphasized in andesites below RL 950 m, inferring potassic alteration, and depleted K levels in the shallow andesite, due to prominent clay carbonate alteration (Singh, 2015). Singh (2015) found K levels of 0.13 % to 10.14 % in the Correnso samples. The samples of this study all fall into the lower end of this range, ranging from 0.54 % to 1.89 %. K levels fluctuate with depth down hole, possibly inferring multiple alteration pathways as presented in figure 7.2. The lower levels of K in the sample of this study may be due to clay carbonate alteration which can produce lower levels of K as seen in Correnso. The low levels in this study's samples could also represent “hard bars” or less permeable and less altered units in some of the shallower samples.

7.5.2 Sulphur

Sulphur is also found in higher concentrations closer to the zones of mineralisation at the Correnso deposit. The sulfur can be associated with iron, lead, Cu and zinc from which it forms pyrite, galena, chalcopyrite and sphalerite which accumulate in zones of alteration and display higher concentrations in the host rock and in veins. Singh (2015), noted these sulfides occur as pyrite in the upper part of the system while chalcopyrite, galena and sphalerite become more common closer to the main orebody. Such minerals have been frequently identified in this study (appendix B) with ranges of sulfur concentrations in the samples (0.01 % to 6.19 %) showing similar quantities to those samples from the Correnso study (0.04 % to 6.67%). However, as these are XRF results, samples with abundant sulfides were not analysed.

7.5.3 Calcium

Calcium is variable throughout the samples, ranging from 3.75 % to 6.82 % and varies throughout each hole. This may represent mobility during hydrothermal alteration. Calcite values are in the upper range of the spectrum compared to those found in Correnso which are as low as 0.03 %

7.5.4 Manganese

As with K and S concentrations, high levels of manganese have been found to occur closer to mineralisation in the Correnso deposit, especially in the andesite situated below RL 950, with few distal samples also found to have elevated levels. Values of manganese in this study (0.067 % to 0.131 %) sit in the mid-range of the Correnso samples which range from 0.004 % to 0.93 % (Singh, 2015).

7.5.5 Iron

Iron has been discussed along with magnesium in the previous chapter. It can be noted that like calcite, it occurred variably across the Correnso orebody, ranging from 0.4879 % to 9.252 % and though it occurred in high concentrations near the orebody, this was usually associated with sulfides (pyrite/chalcopyrite), and oxides (magnetite/ hematite). The andesite above RL 950 m at Correnso also demonstrated higher levels of iron (Singh, 2015). These levels are slightly higher to those in this study which ranged from 1.669 % to 7.215 %. The actual upper limit of the range will be higher in samples with higher sulfide levels. Like the Correnso study, iron occurs variably across this study area; this is likely as it will be occurring in fresh samples in the form of pyroxenes as well as altered samples in the form of sulfides and oxides.

Chapter 8
Summary and conclusions

This study was focused on an area roughly four km north of the Martha Hill Deposit in Waihi, situated in the south of the Hauraki Goldfield which consists of roughly 50 epithermal low sulphidation (adularia-sericite) Au-Ag deposits and porphyry Cu deposits. Eight new volcanic facies were identified, based on crystal abundance and breccia clast distribution. These facies included low crystal concentration porphyritic (LCCP), medium crystal concentration porphyritic (MCCP) and high crystal concentration porphyritic (HCCP), making up the coherent porphyritic facies. These facies are likely to have originated from various andesitic volcanic events, which underwent processes such as magma mingling and/or degassing resulting in the various porphyritic textures displaying ranging degrees of phenocryst concentration, from seriate textures including glomeroporphyritic clots to near aphanitic textures. The brecciated facies include the mosaic breccia (MB), weak mosaic breccia (WMB), discrete breccia (DB), and sparce discrete breccia (SDB). These facies formed primarily as secondary hydrothermal breccia but there are also some breccia originating from the auto brecciation process. It can be inferred that all the breccia have been influenced to some degree by hydrothermal alteration. The irregular pattern facies (IP), was also identified, originating from the moderate to intense alteration of other facies. These facies were used in conjunction with the Petrographic, mineralogical and geochemistry data to map alteration across the core as it changed with depth.

The facies were defined based primarily on crystal concentrations (LCCP, MCCP and HCCP), and breccia clast abundance and distribution (MB, WMB, DB and SDB). The IP facies was defined due to its unique, irregular fabric. Observed crystal concentrations ranged from 3 - 65%, displaying a range of felsic and mafic phenocrysts. The coherent facies varied in distribution with the MCCP being the most common facies overall, occurring throughout all holes while the LCCP and HCCP had more localised occurrences often with thinner intervals. Breccia facies occurred on the margins of the high alteration zones in WNDD011, WNDD007 and WNDD006 as well as the lower WNDD005 alteration zone, inferred to be a result of the increased porosity of the breccia facies. A variety of breccia facies occur across the holes, most extensively within different alteration intensity zones at varying frequencies. The distribution of the IP facies is limited to zones of moderate to high alteration, hence the connection made to its origin, occurring most extensively in WNDD006.

Thin section observations showed a dominantly porphyritic texture with many of the samples displaying a seriate porphyritic texture. These were most commonly composed of Quartz ± plagioclase ± orthopyroxene ± clinopyroxene in the fresher samples and quartz + calcite ± plagioclase in the more altered samples. Plagioclase was the most common mineral, occurring in concentrations of up to 40%. Quartz was the most consistently occurring mineral found across all the thin sections in abundances less than 12%. Othopyroxene and clinopyroxene were also present in small abundances in the fresher samples. XRF results confirmed an andesitic composition in the fresh samples. While comparable to both the Whiritoa and Waipupu Formation local andesite, the localised quartz abundances, and similarities in minerals and their concentrations to other Waipupu andesite studies as well as commonly observed features such a quartz resorption suggest the core in this study is andesite from the Waipupu Formation. The properties of these samples also relate to the successions of modern active andesite volcanoes (Mount Ruapehu, New Zealand), facies from the Tequila volcanic field in the western Mexican arc and late Archean andesites from Kurnalpi Terrance, Western Australia. The emplacement processes of the andesite can be inferred from the observed features and textures of the thin sections. Feldspar crystals most commonly displayed polysynthetic twinning with some zoning twining also observed. Quartz was commonly embayed or resorbed, suggesting the mixing of magma in the magma chamber pre-eruption. However, these embayed and resorbed quartz phenocrysts as well other observed features such as swallowtail plagioclase microlites may also suggest the process of magma degassing during magma ascention. The common seriate texture and glomeroporphyritic clots present evidence of polybaric fractionation resulting in rocks of higher porosity and permeability. The variation in features and textures infers that the Waipupu Andesite was emplaced over multiple eruption events.

A range of breccia were observed in the study area with clasts ranging in size from lapilli to blocks. While it is likely that breccia formed as autobreccia or hydrothermal breccia, due to the nature of the samples and variation in breccia facies, it is suggested that all breccia have been affected by the process of alteration. Hydraulic fracturing, and propagation of these fractures, caused during the formation of hydrothermal breccia, as well as the fracture and deformation of altered autobreccia will increase the permeability property of the rock. The permeability of the rock is relevant as it promotes the flow of hydrothermal fluids, hence supporting alteration and gold deposition. The various breccia facies indicate that multiple genisis processes took place to form the breccia across the study area. While it has been identified that hydrothermal breccia are common it is likely that continuous alteration of these facies has altered their visible morphology resulting in the variations of breccia facies. These facies also commonly grade into

one another which suggests continuous alteration formed the distinctions in the facies, explaining each breccia facies distribution relative to the zones of alteration. This could suggest that the IP facies could be a heavily altered breccia.

Pyrite was the most common opaque, occurring in pyrite + magnetite ± chalcopyrite assemblages and pyrite + sphalerite ± chalcopyrite assemblages. It occurred most extensively both disseminated in the breccia matrix and groundmass, as phenocryst and breccia clast inclusions and in veins. Magnetite and galena were also common, mostly disseminated in the groundmass or breccia matrix, while chalcopyrite and sphalerite were localized to certain areas. Arsenopyrite hematite and ilmenite occurred sporadically in smaller amounts. Observed opaques such as pyrite, sphalerite, galena, chalcopyrite and arsenopyrite are relevant as they commonly occur in epithermal zones of Au rich ore. Altered phenocrysts occurred most commonly as calcite, in concentrations of up to 50%, occurring in veins and commonly as pseudomorphs of plagioclase and pyroxenes. As found in the altered Whitianga Group Andesite, these could remain well preserved in zones of high intensity alteration. The groundmass obliteration usually occurred to greater extents in the more heavily altered samples. Altered groundmass was also determined by the presence of hydrothermal quartz. Hydrothermal quartz in these rocks likely formed through the chloritisation of pyroxenes, replacement of chlorite by carbonates as also observed in the Whitianga Group Andesite, and propagation of boiling in calcite rich zones. The findings from the mineralogical and petrographic analysis determined the intensity and relationship of alternation between holes and suggested pathways of paleoflow which could infer possible planes of alteration, displayed in figure 7.2. Graduations in alteration intensities were observed peaking at a zone from roughly RL 50 m - 300 m before the intensity lessens and peaking again at RL -100 m - 200 m.

8.1 Further work

The orientation of the drill holes made spatial correlation of data between holes difficult. Vertical drill holes would help with the reconstruction of past volcanic environments as well as correlating alteration spatially. With more time a wider sample range would benefit this study with a more intensive geochemical approach, including clay-separate XRD analysis. This would allow for the temperature sensitive clay minerals to be identified, allowing for conclusions to be drawn on the types of alteration present, providing more information about the temperatures and processes occurring in the subsurface. This along with the larger sample pool would also allow for alteration halos to be marked and potential vein zones to be identified. Sample collection related to the

specific facies identified in this study would also allow for sound relationships to be made between each facies and their specific mineralogical properties.

References

Adams, C. J., Graham, I. J., Seward, D., Skinner, D. N.B., Adams, C. J., Skinner, D. N.B., & Moore, P. R. (1994). Geochronological and geochemical evolution of late Cenozoic volcanism in the Coromandel Peninsula, New Zealand. *, New Zealand Journal of Geology and Geophysics*, *37*(3), 359-379. 10.1080/00288306.1994.9514626

Bird, D. K., & Elders, W. A. (1976). *Hydrothermal alteration and mass transfer in the discharge portion of the Dunes geothermal system, Imperial Valley of California, U.S.A* [Proc. Second United Nations Symposium on the Development and Use of Geothermal Resources]. San Francisco.

Bodger, B. (2015). *Andesite volcanic facies and hydrothermal alteration in the subsurface peripheral to existing Waihi mine workings* [Unpublished - thesis].

Booden, M. A., Smith, I. E.M., Mauk, J. L., & Black, P. M. (2012). Geochemical and isotopic development of the Coromandel Volcanic Zone, northern New Zealand, since 18 Ma. *Journal of Volcanology and Geothermal Research*, *219-220*, 15-32.

Brathwaite, R. L., & Christie, A. B. (1996). *Geology of the Waihi area, scale 1:50,000* [Institute of Geological & Nuclear Science Geological map 21] [Map]. Institute of Geological & Nuclear Science limited.

Brathwaite, R. L., & Faure, K. (2002). The Waihi Epithermal Gold-Silver-Base Metal Sulfide-Quartz Vein System, New Zealand: Temperature and Salinity Controls on Electrum and Sulfide Deposition. *Economic Geology*, *97*(2), 269-290.

Brathwaite, R. L., Torckler, L. K., & Jones, P. K. (2006). The Martha Hill epithermal Au-Ag deposit, Waihi – geology and mining history. In *Geology and Exploration of New Zealand Mineral Deposits* (25th ed., pp. 171-178). Australasian Institute of Mining and Metallurgy Monograph.

Briggs, R. M., Houghton, B. F., Mcwilliams, M., & Wilson, C. (2005). 40Ar/39Ar ages of silicic volcanic rocks in the Tauranga-Kaimai area, New Zealand: Dating the transition between volcanism in the Coromandel Arc and the Taupo Volcanic Zone. *New Zealand Journal of Geology & Geophysics*, *48*, 459-469.

Browne, P. R.L. (1978). Hydrothermal alteration in active geothermal fields. *Annual review of earth and planetary sciences*, *6*, 229-250.

Browne, P. R.L. (1989). *Contrasting alteration styles of andesitic and rhyolitic rocks in geothermal fields of the Taupo Volcanic Zone, New Zealand* [Proceedings at the 11th New Zealand Geothermal Workshop]. University of Auckland.

Christie, A. B., Rabone, S. D., Barker, R. G., & Merchant, R. J. (2006). Exploration of the Wharekirauponga epithermal Au-Ag deposit, Hauraki Goldfield. In *Geology and Exploration of New Zealand Mineral Deposits* (25th ed., pp. 137-144). Australasian Institute of Mining and Metallurgy Monograph.

Christie, A. B., Simpson, M. P., Brathwaite, R. L., Mauk, J. L., & Simmons, S. F. (2007). Epithermal Au-Ag and Related Deposits of the Hauraki Goldfield, Coromandel Volcanic Zone, New Zealand. *Society of Economic Geologists, Inc.*, *102*, 785-816.

Clarke, D. S., & Govett, G. J.S. (1990). Southwest Pacific epithermal gold: a rock geochemistry perspective. *Journal of Geochemical Exploration*, *35*, 225-240.

Cooke, D. R., & Simmons, S. F. (2000). Characteristics and Genesis of Epithermal Gold Deposits. In *Gold in 2000*. Society of Economic Geologists.

Corbett, G. J., & Leach, T. M. (1998). Southwest Pacific Rim gold-copper systems: structure, alteration, and mineralization. *Littleton, Colorado: Society of Economic Geologists*, *6*, 240.

Evans, A. M. (2009). *Ore geology and industrial minerals: an introduction*. John Wiley & Sons.

Frey, H. M., & Lange, R. A. (2010). Phenocryst complexity in andesites and dacites from the Tequila volcanic field, Mexico: resolving the effects of degassing vs. magma mixing. *Contributions to Mineralogy and Petrology*, *162*, 415-445.

Gazley, M.F., and Fisher, L.A., 2014. A review of the reliability and validity of portable X-ray fluorescence spectrometry (pXRF) data. In: Mineral Resource and Ore Reserve Estimation – The AusIMM Guide to Good Practice. Second edition. The Australasian Institute of Mining and Metallurgy, Melbourne, p. 69–82

Gifkins, C. C., Herman, W., & Large, R. R. (2005). *Altered volcanic rocks: A guide to description and interpretation*. Centre for Ore Deposit Research, University of Tasmania.

Hedenquist, J., Arribas, A., & Gonzalez-Urien, A. (2000, January 01). Exploration for Epithermal Gold Deposits. *Reviews in economic geology*, *13*, 245-277. https://doi.org/10.5382/Rev.13.07

Hedenquist, J. W., Arribas, A. R., & Gonzalez-Urien, E. (2000). Exploration for Epithermal Gold Deposits. *SEG Review*, *13*, 245-277.

Henley, R. W. (1958). The geothermal framework for epithermal deposits. *Reviews in Economic Geology*, *2*, 1-24.

Henley, R. W., & Ellis, A. J. (1983). Geothermal systems, ancient and modern. *Earth Science Reviews*, *19*, 1-50.

Henley, R. W., Truesdell, A. H., Barton, P. B., & Whitney, J. A. (1984). *Fluid-mineral equilibria in hydrothermal systems* (Vol. 1). Yale: Society of Economic Geologists.

Hochstein, M. P., & Ballance, P. F. (1993). Hauraki Rift: A young, active, intra-continental rift in a back-arc setting. In *South Pacific Sedimentary Basins, Sedimentary Basins of the World 2* (pp. 295-305). Elsevier Science Publishers.

Jébrak, M. (1997). Hydrothermal breccias in vein-type ore deposits: A review of mechanisms, morphology and size distribution. *Ore Geology Reviews*, *12*(3), 111-134.

Jones, R. S. (1968). *Gold in Meteorites and in the Earth's Crust* (603rd ed.). US Government Printing Office.

Lindgren, W. (1922). A suggestion for the terminology of certain mineral deposit. *Economic Geology*, *17*(4), 292-294. 10.2113/gsecongeo.17.4.292

Lindgren, W. (1933). *Mineral deposits. Fourth edition, revised and reset. 4th impression.* New York: McGraw-Hill.

McPhie, J., Dolye, M., Allen, R. L., & Allen, R. (1993). . *Volcanic textures: A guide to the interpretation of textures in volcanic rocks*. CODES-University of Tasmania.

Mielke, P., Prieto, A., Bignall, G., & Sass, I. (2015). *Effect of Hydrothermal Alteration on Rock Properties in the Tauhara Geothermal Field, New Zealand* [Proceedings World Geothermal Congress]. Technical University Darmstadt.

Mitchell, A. G.H., & Garson, M. S. (1982). Mineral Deposits and their Global Tectonic Settings. *Mineralogical Magazine*, *46*(340), 406-407. 10.1180/minmag.1982.046.340.24

Mordensky, S. P., Heap, M. J., Kennedy, B. M., Glig, H. A., Villeneuve, M. C., Farquharson, J. I., & Gravely, D. M. (2019). Influence of alteration on the mechanical behaviour and failure mode of

andesite: implications for shallow seismicity and volcano monitoring. *Bulletin of Volcanology*, *81*, 44.

Muffler, L. J.P., White, D. E., & Clayton, R. N. (1968). Oxygen isotope study of calcite and silicates of the River Ranch No. 1 well, Salton Sea geothermal field, California. *American Journal of Science*, *226*(10), 968-979.

Pirajno, F. (2009). *Hydrothermal Processes and Mineral Systems*. Geological Survey of Western Australia. Springer.

Pittari, A., Prentice, M. L., McLeod, O. E., Yousef Zadeh, E., Kamp, P. J.J., Danisik, M., & Vincent, K. A. (2021). Inception of the modern North Island (New Zealand) volcanic setting: spatio-temporal patterns of volcanism between 3.0 and 0.9 Ma. *New Zealand Journal of Geology and Geophysics*, *64*(2-3), 250-272.

Rabone, S. D.C. (1975). Petrography and hydrothermal alteration of Tertiary andesite-rhyolite volcanics in the Waitekauri Valley, Ohinemuri, New Zealand. *New Zealand Journal of Geology and Geophysics*, *18*(2), 239-258.

Reyes, A. G. (1990). Petrology of Philippine geothermal systems and the application of alteration mineralogy to their assessment. *Journal of Volcanology and Geothermal Research*, *43.*, 279-309.

Shukla, M. K., & Sharma, A. (2020). A brief review on breccia: it's contrasting origin and diagnostic signatures. *Solid Earth Sciences*, *5*(3), 232.

Sillitoe, R. H., & Bonham, H. F. (1984). Volcanic landforms and ore deposits. *Economic Geology*, *79*(6), 1286-1298. https://doi.org/10.2113/gsecongeo.79.6.1286

Sillitoe, R. H. (1985). Ore-related breccias in volcanoplutonic arcs. *Economic Geology*, *80*(6), 1467.

Sillitoe, R. H., & Hedenquist, J. (2003). Linkages between volcanotectonic settings, ore-fluid compositions, and epithermal precious-metal deposits. In *Volcanic, geothermal and ore-forming fluids: Rulers and witnesses of processes within the Earth* (Special Publication 10 ed., pp. 315-343). Society of Economic Geologists.

Sillitoe, R. H., & Hedenquist, J. (2003). *Volcanic, geothermal and ore-forming fluids: Rulers and witnesses of processes within the Earth* (10th ed.). Society of Economic Geologists.

Sillitoe, R. H., & Hedenquist, J. W. (2005). Linkages between Volcanotectonic Settings, Ore-Fluid Compositions, and Epithermal Precious Metal Deposits. In *Volcanic,*

Simmons, S. (2021). *Epithermal Alteration seminar* [Talk at Oceana Gold Waihi 2021 conducted by Stuart Simmons] [Verbal communication]. New Zealand.

Simmons, S. F., & Christenson, B. W. (1994). Origins of calcite in a boiling geothermal system. *American Journal of Science*, *294*, 361-400.

Simmons, S. F., White, N. C., & John, D. A. (2005). Geological Characteristics of Epithermal Precious and Base Metal Deposits. *Economic Geology 100th Anniversary Volume*, *100*, 485-522. https://doi.org/10.5382/AV100.16

Simpson, M. P., & Mauk, J. L. (2011). Hydrothermal Alteration and Veins at the Epithermal Au-Ag Deposits and Prospects of the Waitekauri Area, Hauraki Goldfield, New Zealand. *Economic Geology*, *106*(6), 945-973.

Singh, R. S. (2015). *Identifying Mineralogical and Geochemical Vectors towards the Epithermal Au-Ag Correnso Mine, Waihi* [Thesis- unpublished].

Skinner, D. N. (1986). Neogene volcanism of the Hauraki Volcanic Region. *Royal Society of New Zealand Bulletin*, *23*, 21-47.

Sørensen, B. (2013). A revised Michel-Lévy interference colour chart based on first-principles calculations. European Journal of Mineralogy. 1.

Stoffregen, R. (1987). Genesis of Acid-Sulfate Alteration and Au-Cu-Ag Mineralization at Summitville, Colorado. *Economic Geology*, *82*, 1575-1591.

Takeda, T., Shimada, N., & Ueno, H. (2001). Paleomagnetic Constraints on Mineralization Age of the Nansatsu-type Gold Deposits in Southern Kyushu, Japan. *Resource Geology*, *51*(3), 239-248.

Waight, T. E., Price, R. C., Stewart, R. B., Smith, I. E.M., & Gamble, J. (1999). Stratigraphy and geochemistry of the Turoa area, with implications for andesite petrogenesis at Mt Ruapehu, Taupo Volcanic Zone, New Zealand. *New Zealand Journal of Geology and Geophysics*, *42*(4), 513-532.

White, N. C., & Hedenquist, J. W. (1990). Epithermal environments and styles of mineralization: variations and their causes, and guidelines for exploration. *Journal of Geochemical Exploration*, *36*, 445-474.

White, N. C., & Hedenquist, J. W. (1995). Epithermal gold deposits: styles, characteristics and exploration. *SEG Newslatter*, *23*(1), 9-13.

White, N. C., Leake, M. J., McCaughey, S. N., & Parris, B. W. (1995). Epithermal gold deposits of the southwest Pacific. *Journal of Geochemical Exploration*, *54*, 87-136.

Wyering, L. D. (2014). *The influence of hydrothermal alteration and lithology on rock properties from different geothermal fields with relation to drilling* [Unpublished work] [A thesis submitted to the University of Canterbury in fulfilment of the requirements for the degree of Doctor of Philosophy in Engineering Geology]. Christchurch, New Zealand.

Zhu, Y., An, F., & Tan, J. (2011). Geochemistry of hydrothermal gold deposits: A review. *Geoscience Frontiers*, *2*(3), 367-374. https://doi.org/10.1016/j.gsf.2011.05.006

Appendices

Appendix A: Hand drawn logs

Appendix B: Microscopy notes

Appendix C: Leapfrog input Data

Appendix A - Hand drawn logs

WNDD005

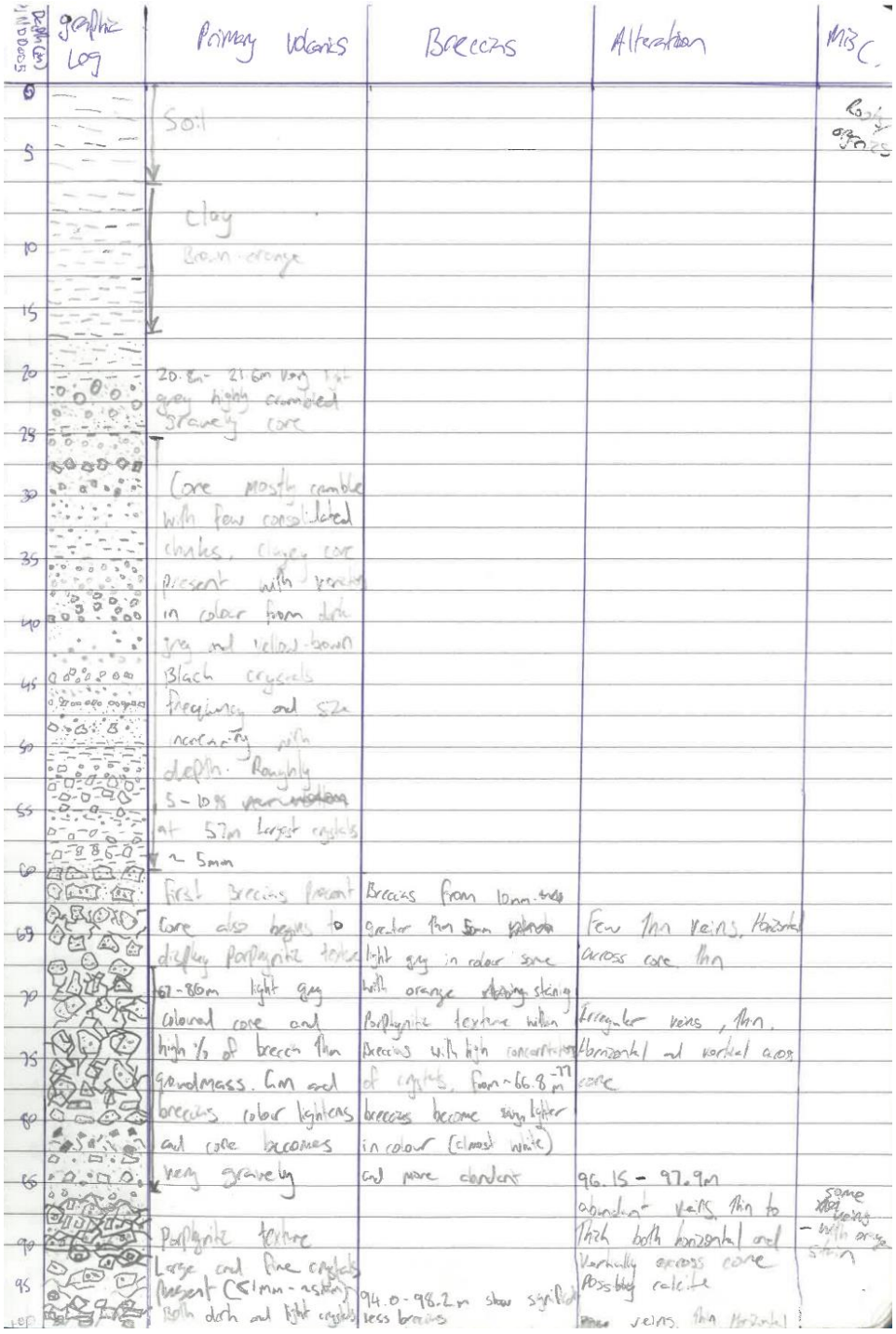

Depth (m) WINDOWS	graphic log	Primary volcanics	breccias	Alteration	Misc.
100		[sample] Porphyritic	Large mosaic	- Horizontal veins across	
105		texture, moderate	Breccias angular to	core some with orange	
		Lapilli sized black crystals	rounded, small	stain, large stockwork	
110		sparse lighter crystals	-	vein structure at 107.0m	
		- non-uniform crystal	- Breccias ranging from	~40mm at thickest,	
115		size in matrix more	20mm to >50mm	frequent thick veins (~3.5cm)	
		frequent lighter	angular to rounded	continue to 110.8m	
120		crystals	Porphyritic texture within	- Few veins	
		- irregular pattern on	- clusters of breccias	- veins increasing slightly	
125		core, white Lapilli crystals	occuring, mostly angular	with depth Section of	
		dominating	Porphyritic texture within,	discoloured core, much lighter	
130		- dramatic change (Strong Magnetic)	breccia size decreasing	between two veins at	
		in core texture at ~135m	- Breccias on average	129.6m - 129.9m	
135		as crystal size and frequency	size decreasing and		
		increase average size ~5mm	frequency drastically decrease	- Frequent small	
140		and now ~80% of core	ceasing at 136.0m	veins both vertical and	
		- Patches of core with	- Some breccia looking	horizontal in core	
145		much less crystals some	structures amongst		
		upto 20cm	strong porphyritic texture	- Thick intrusion at	
150		- some white crystals		147.9m	
		upto 10mm, more frequent	- Patches in core		
155		Patches in core with low	sometime resemble	Few Hairthin	
		density crystals, Patches	~~Breccia~~ Breccia like	veins.	
160		have similar crystal size	structures		
		- Breccia like Patches in	- more sparse crystals	- Few thick (8-10m)	
165		Porphyritic texture increasing	inside brecciation like	veins one horizontal cross	
		some areas of groundmass	structures than outside	core and one parallel	
170		lighter than others		at 164.2m and 166.1m	
		- Frequency of Large (>10mm)	- Few rounded Breccias	- Some areas of	
175		white crystals increasing some	discrete in frequency with	core much lighter	
		Patches of just groundmass	a lower concentration of	grey than others	
180		up to 30cm long	crystals within.		
		- some patches in core	- Some Breccia like patches		
185		with different texture slowing	still occuring possible white		
		flow and the pattern Large	Breccias at 182.7m		
190		white crystals present (up to 16mm)			
		- large patches of groundmass	- some massive breccia	- Few veins though	
195		(~1m) Large black and	structures 196.8 and large	thin mostly horizontal	
		white crystals present	Breccias forming below 199m	across core.	
200			angular upto 50mm		

Depth (m)	Graphic Log	Primary volcanics	Breccias	Alteration	Misc.
200–220		- Porphyritic texture with light crystals upto ~2mm. White crystals angular, Black angular to rounded. ~2m section of Aphanitic texture that appears clayey/crumbly. - Some sections of porphyritic texture appear to have interchangeable texture of Black crystals	- Breccias occuring before aphanitic section. Breccia upto ~>100mm with space crystal distribution within, mostly rounded. - Breccias after 218m Large reddish brown with denser microcrystal [illegible] than Previous Breccias	- few veins mostly white, some appear black. Both horizontal and parallel with core. - few Hair-line veins	
220–240	Crumble	- Patchy porphyritic texture until ~25m when porphyritic texture becomes very dense almost phaneritic, with much larger crystals. - crumbly clayey core, followed by irregular porphyritic texture with flow like discrepancies, then porphyritic texture appears to be split by groundmass sheets resulting in breccia like structures of porphyritic texture with smaller crystals	- Few breccias lighter than previous and smaller. - From 236m to 238.5m Large porphyritic breccia structures appear with loose mosaic pattern	- After Phaneritic like texture core become a lighter shade of grey and section 230.2m – 231.8 quite crumbly. - quite light grey section of core from 237.3 – 238.0m	
240–255		- crystals porphyritic, white crystals upto 8mm (from sample) patches absent of white crystals. Mosaic breccia like structures in groundmass and porphyritic core. - Breaks in porphyritic texture some crescent shaped curves. clayey section from 254.3–255.5m with minimal crystals.	- some diffinitive breccias other areas unsure if Breccias or seperation in porphyritic texture resulting in Breccia like structures. - similar breccia structures to last 10m but some crescent breaks at 253.8	- No veins but thick intrusion at 242.9. core mostly darker than Previous meters.	• sample Red interesting crystal at 255.9m
255–270		then porphyritic texture has larger crystals but less lower abundance until 259.8m. - Porphyritic texture varying in crystal density but consistent crystal size	- mostly made up of Large Mosaic Breccias Lapilli sized to >100mm. Some breccia have greater crystal density than others while others have a lesser density than outside	- Few horizontal veins across core. Section from 269.8m – 270.4m with lighter grey/white colour. Seems to have very Large ~90mm crystal or lithic within section	
270–283		- Low crystal density porphyritic texture with flow band like patterns of Darker groundmass. after 275.0 meters crystal density increases, and Patches of low crystal density, discoloured core possibly large breccias.	- Breccia structures but not diffinitive from 270 – 274.9m as too large. Small section with small diffinitive Breccias Before large structures		
283–292		- Patchy core alternating light and darker grey. Patches with low density/aphanitic texture and internal structures both fractured or cracked	- Breccia like structures throughout. Some very fractured. Fairly continuous crystal density inside and out and wide variety of size. ~~from~~ Mosaic texture	- Large intrusions from 284.6m onwards, thick vein structures, white across core.	
292–300		- Crystal density of porphyritic texture varying across from ~10% – 75% Both angular and rounded, Lapilli in size, light grey groundmass divided by dark [illegible]	- Mosaic texture with some smaller discrete Breccias	- Few Large white intrusions/crystals upto ~25mm across at 291.2m	

WN00005 - 300m - 400m

Depth (m)	Graphic Log	Primary volcanics	Breccias	Alteration	Mineralisation
300		- Patchy porphyritic with some dark flow band structures	- Patches where crystal density drops. Visible large Breccias, light coloured small mosaic Breccias	- Breccias very light grey - almost white	
305		- light flow band-like structures			
310		- Patchy porphyritic			
315		- alternating between dense and patchy porphyritic alternation, flow band like structures / black veins / cracks	- Zone of breccia and non-breccia alternating - small discrete breccia dominated by mosaic large	- Wavy white veins - colour of zone alternating between lighter and darker greys	
320					
325		- Patch porphyritic variety of surface texture - Low density porphyritic	- decreased breccia frequency - large discrete	- vein frequency and size increasing up to 15mm thick at 329.1	
330		- medium to high porphyritic			
335		- Black crescent lines present	- Hard to tell if large mosaic Breccias or zones of alteration, crystal density consistent in and out	- high vein frequency 15mm vein at 333.8m	
340		- Patchy colour from dark to light grey.			
345		- Medium porphyritic - Large patches of light and dark grey, fine grained porphyritic - low density - Black crescents	- few mosaic small brecciated Breccias, - large light coloured mosaic fractured breccia	- frequent hair line veins Dark vein like structure present	
350		- Medium porphyritic	- Smaller breccias discrete to mosaic	- Thin and thick veins Hair line/crescent and stockwork	
355		- dense porphyritic			
360		- medium porphyritic - dense porphyritic	- discrete Breccias less dense within their groundmass		
365		- Dense porphyritic with veins - stock work veins - slight changes in groundmass colour	- Medium Breccias discrete - Porphyritic - large dense mosaic	- Large frequent veins - stockwork like structure at 161.4m - 161.6m	
370		- medium density porphyritic	Breccia - Porphyritic		
375		- Low density porphyritic small crystals	- small discrete Breccia some black (maybe crystals) - medium discrete into fractured mosaic Breccia small to large	- white intrusive at 373.0m - altered zone 378 - 379m Large veins holding crystals ~10mm thick - crustiform texture	
380		Medium density porphyritic flow band structures at 176.6			
385		- High density porphyritic - medium density porphyritic - Lots of surface fracture	- few medium discrete Breccia, large fractured mosaic Breccia	- frequent thick veins/ intrusions up to 15mm containing minerals, altered looking	
390		- Low density - surface fracture		Section 3878. core beginning to crumble	
		crumble	- Large and small discrete Breccia - crystal density and size = outside lighter groundmass within breccia		
395		- Patchy porphyritic		- frequent veins/intrusions variety of shapes and orientations	
400					

WNDD 005 400-500m

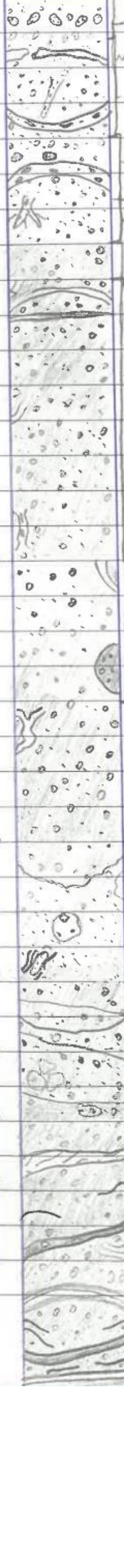

Depth (m)	Graphic Log	Primary Volcanics	Breccia	Alteration	Misc.
400		- Medium density porphyritic with smaller crystals	- Few small discrete Breccia some Dark grey some Brown-green	Very frequent veins - long parallel to core and across core with phenocrysts inside - up to 20mm	Banded [illegible] vein - [illegible]
405		medium density porphyritic Less crystals			
410		medium density porphyritic Patchy	- Few discrete breccia Dark grey	- Very Large veins with crystals within aligned with vein (33mm)	
415		Porphyritic small crystals			
420		- Porphyritic very light groundmass		- Very light groundmass almost white crumbling in some places too	
425		Porphyritic coherent medium density (40-70% crystal density) smokey coloured core, very light grey, almost white matrix		- very frequent veins in varying orientations and thickness. many intrusion like structures but hard to distinguish with groundmass with veins / intrusions	
440				- Fewer veins than previously	
445			Possible Large Breccia darker than surrounding groundmass		
450		Porphyritic coherent Medium density, some areas with low, darker clayey appearance in some places - 465m		- Large stockwork like vein 452.0m Brown looking vein also present. clayey in some areas	
465		- medium porphyritic		Section from 467.8-468.4 look like vein (vuggy) (possibly chert-pyrite clast/vein)	
		medium density porphyritic - slightly smaller crystals - [illegible] difference at 468.4m			
470		medium porphyritic with some areas low density. Black intrusions common across core	- Few [illegible] breccia small rounded, other Breccia like structures present	- Black intrusions, [illegible] common. Large white vein 474.8 possibly Boxwork vein	
480		Medium - low density Patchy porphyritic, Multiple Structures on core surface common Black streaks		- Large vein at 483.3 with internal structure, Black looking vein at 486.5 with [illegible] crystals (possible sulfide dike)	
490		medium porphyritic Dark streaks common		- veins common both Dark graphite color and White. Both curving towards top and Bottom of hole	
500					

WND0005 - 500-600m

Depth	Graphic Log	Primary Volcanics	Breccia	Alteration	MBc.
500		- Medium Porphyritic	- Few Breccia like structures	- White breccia like	
505		- Weak flow banding texture / breccia	But not definitive Breccias	intrusions - 500.7 - 500.9m	
		- high density porphyritic with patches of low density		Frequent Black veins / fractures.	
510					
515		medium porphyritic with large irregular shaped black crystals	variety of Breccias large	- weathered looking area	515 - 516.5 Drawn in more detail
		- Flow banded / Breccia mosaic and discrete pattern, fracture	and small discrete and	515 - 516.5 very densely	
		Patchy porphyritic	possible mosaic	dense texture of mosaic / fracture	
520					
		High density porphyritic	- Sparse discrete breccia rounded ~22mm grey	- frequent thick (up to ~25mm)	
525		few sections of mid to low density		Black veins / intrusions bearing	
		- White flow band like vein - 526.2m		crystals (porphyritic dense texture)	
530			- rare rounded discrete Breccia	in multiple orientations	
535		High density porphyritic	- Broken core at 535.2		
		- crystal size varies	Shows most finer	- frequent Black	
540		Between sections of smaller	crystals within core	cracks / intrusions (- Hair	
		crystals (Max crystal size ~5mm)		line) thick (~11mm) black	
545				vein at 543.2m with no	
		Medium porphyritic (40-70% crystal density) with varying crystal sizes (<1mm - >10mm)	- White Breccia like structures - Angular	visible white crystals within	
550			Rounded grey mosaic Breccias	- Dark veins frequent	
		Medium density porphyritic with	- Breccia structures more frequent	often Bearing minerals	
555		patches of high density	and appear to occur in some	sharp angled looking vein at	
		some flow band like structures	veins. Large looking breccia at 559.7m	550.9m Frequent Black Hairline	
560				Veins	
		High density porphyritic	- No definitive Breccias	- frequent hairline black	
565		with few patches of low	But possible low density	veins, dual vein at	
		density fine grained porphyritic	occurs as large Breccias	579.5m one smaller non-bearing crystals other black crystal bearing	
570					
		Medium density porphyritic	Breccia structures frequent	- Core colour changing	
575		Frequent flow band structures	clusters of mosaic Breccias	frequently from lighter	
		Patches of low density	present mostly white and	and darker shades of	
580		porphyritic	rounded	grey	
		- Low density porphyritic small average crystal size	- Mosaic breccias present	- Large (5mm) white vein	
585		medium density porphyritic	in clusters appearing to	with large (10mm) rim Black	
		- Frequent flow structures forming	form part of groundmass	intrusion	
590			in a steady gradient		
		low density porphyritic with		- Black Hairline streaks	
595		frequent flow band like	- few discrete breccia		* 590m
		- structures resulting in some	- possible large breccia in		
600		* alternating colours between white and grey	dark spot from 593.6 - 594.0m Breccia white crystals / breccia		

WNDD005 600m-700m

Depth (m)	Primary Volcanics	Breccia	Alteration	Misc.
600–619	Medium density Porphyritic (0-7?) flow banding like fabric into breccias very patterns with frequent colour variation, fabric texture appears fractured. Patchy sections with high density porphyritic texture	Small discrete breccias to large un-defining Breccias which appear altered as opposed to Cm - frequent clusters of Breccias in a gradient out of coherent Cm	- Patch alteration with sections appearing unaltered then back to altered. Breccias seem altered - Sections of altered rock like in vein like patterns	
620–631	- Alternating high and medium porphyritic texture fabric alternates between coherent and mosaic, very slight red/pink tint on high density coherent sections	- frequent clusters - few discrete large	- Patches of altered rock with marble white colour as well as what appears to be weakly altered (due to dull white)	
632–640	Mostly patchy medium-high density porphyritic with some low dense sections in Breccia showing flow band looking structures present	- Breccia like structures vary in crystal density whiteish colour, appear to be altered.		
641–650	Frequent variations from high-medium-low porphyritic density. Low density with larger crystals/Breccias. Possible compositional zoning in some crystals	- Hard to distinguish between Breccias vs large crystals, discrete vs mosaic breccia frequent		
651–662	High-med porphyritic with white patches (maybe breccias) 652.8m then into mosaic fabric with altered look - some black cracks larger than others and bearing white minerals	Mosaic section possible large Breccia complex discrete breccias on either end all possible Breccias appear altered	- frequent dark looking veins separating groundmass to show mosaic Breccia fabric - also some bearing minerals Breccias marble white	
663–668	Medium porphyritic coherent	- few discrete breccia both altered coloured and graphite grey		
669–673	Mosaic fabric, Medium density porphyritic with large irregular black crystals	- This mosaic less Breccia like than previous - more a collection of black looking veins	long fine grained vein 672.6-673.5 Possible - clay Rock-flour	
674–678	less altered section with frequent white veins and darker ground mass	- Possible some large black crystals = Breccia, few discrete	frequent white veins in section which appears less altered (675.5-676.5)	
679–681	Medium density porphyritic			
682–700	Breccia dominated. Similar texture throughout with med porphyritic compositional zoning like Breccia at 688.7m Flow Band structures also present. Medium porphyritic, high density in some Breccias compositional zoning at 698.2 also black bands bearing Breccias present	- Mostly mosaic with few large discrete color. Mostly marble white, both angular and rounded, size varies from (L2mm-76mm) - Breccia density begins to decrease and size increases	- flow structure at 694.8m. Breccias mostly appear altered. Alteration intensity increases at 575.5m	

WN0005 700m-800m

Depth (m)	Graphic Log	Primary Volcanics	Breccia	Alteration	Misc.
700		- Medium density Porphyritic	Range of Breccia sizes	Marble White colour	
705		with some flakes of LDP	most white breccias mosaic	indicates possible high	
		fabric alternating between	and some discrete Black	intensity alteration	
710		coherent and mosaic texture	Breccia all mineral bearing		
		- Flow band structures			
715		some changes colour getting	Mosaic breccia grading	- Levels of alteration	
		slightly Darker (Intervals less	in and out of coherent	possibly changing with core	
720		altered) these areas have	fabric often with	colour strong coherent	
		a higher crystal density	Black groundmass	white beginning again at	
725		(Zones such as 726.1		~ 731m, Black crystal/Breccia	
		and 727.1m) ##	Breccia in altered shows	Bearing veins/intrusions present	
730			Snow "low" relief contacts		
			- 730.8m		
735		MDP with HDP in heavily			
		Brecciated zones, large			
740		Black vein/intrusion at 738.1m			
		also fine grained intrusion at			
745		745.3 with flow band texture	* round and elongated		
		where Breccias Create	Shape and orientation of		
750		out from mosaic texture	Breccias altering*		
		ground mass is black			
755		~~alteration~~	section at 753.8 with	frequent Black veins	
			Dark grey Breccia as	and cracks stained some	
760			opposed to marble white	colour to groundmass	
				Between Breccias	
765					
		- Large irregular Black			
770		crystals			
		- MDP with patches & LDP	'low relief' Breccias	- few white veins at	
775			similar colour to 6m until	770.8m and 771.2m	
			777.0m then 'high relief'	colour indicates level	
780			Marble white Breccias -	of alteration has decreased	
		- HDP	discrete		
785				780 - 787m shows	
			'low relief' Breccias in	clays suggesting weak	
790		- Altered MDP with irregular	darker core and high relief	alteration	
		Black crystals	in lighter core with	Vein/intrusion at 789.8m	
795		- HDP in Darker core	Dark groundmass		
			large fine grained Breccia	- Possible variations	
800			discrete at 795.2	in alteration	

WNDD005 800-838.8m

Depth (m)	Graphic Log	Primary Volcanics	Breccia	Alteration	Misc.
800		MDP ~~HDP~~ with few	- Breccia like Structure		
805		Patches of HDP	Bearing gm color Breccia in black matrix	- frequent Black intrusive veins containing crystals	
810		Rich in dark crystals		- Black vein holding white vein at 802m	
815			Jigsaw breccia fading into sand mass	- Thick → 1cm Section of core black groundmass bearing Breccias	
820			- Discrete Dark Breccias		
825			- few fine grained Breccia		
830			- Angular to rounded		
835		- Black Streaks ~~of~~ in groundmass Bearing crystals		Variations in alteration	
840		~~Different~~ Black crystals			E.O.H

WNDD006

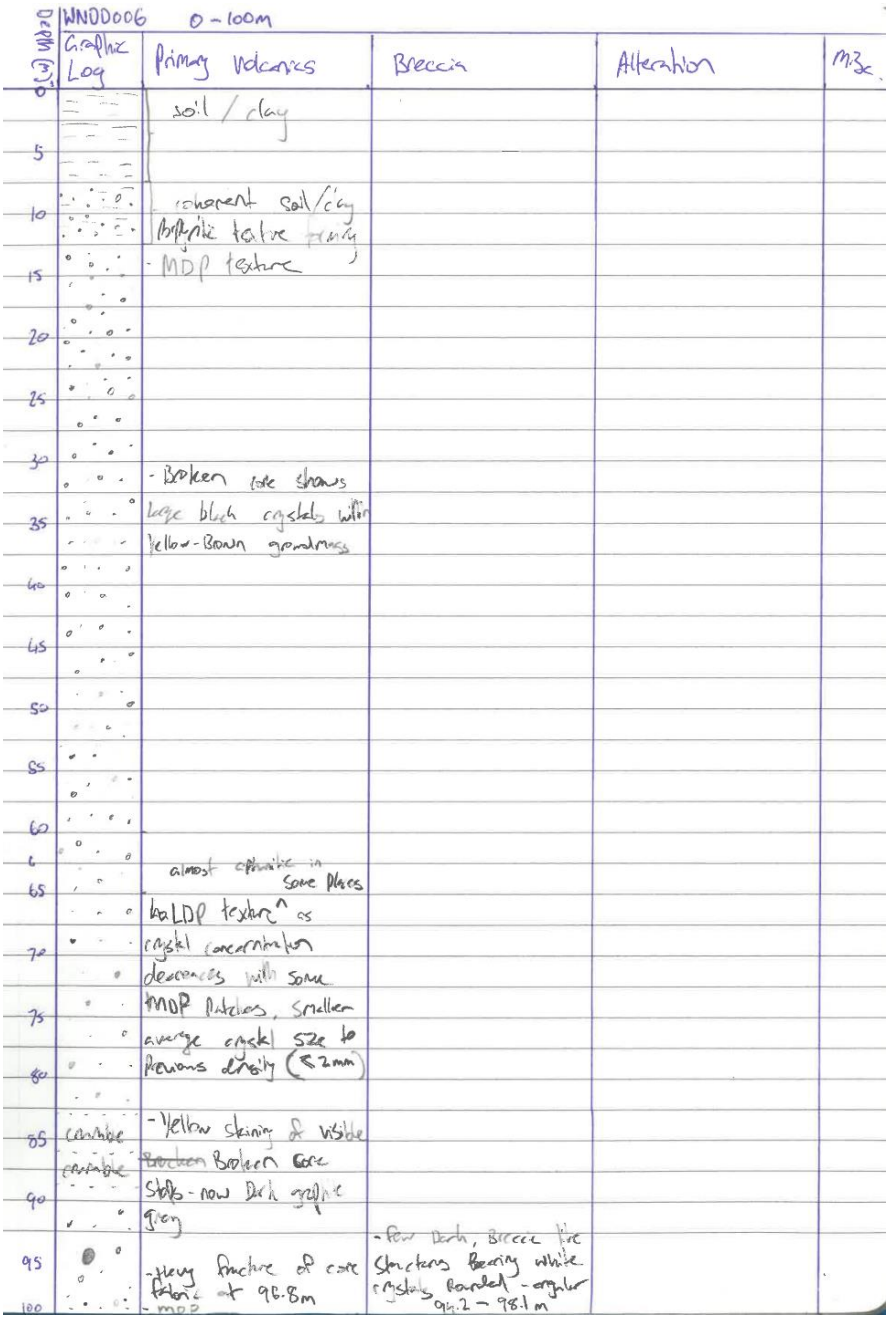
WNDD006 0 - 100m
Graphic Log
Primary Volcanics
Breccia
Alteration
Mineralisation
soil / clay
- Broken core shows
Large black crystals within
Yellow-Brown groundmass
almost aphanitic in
Some Places
- Yellow staining & visible
Broken Core
- Heavy fracture of core
- now Dark grey
- few Dark, Breccia like
Structures Bearing white
crystals Rounded - angular
94.2 - 98.1 m

WN0D006 100-200m

Depth (m)	Graphic Log	Primary Volcanics	Breccia	Alteration	Mineralisation
100		MDP with patches of LDP - small average crystal size	2 dark stains at 103.6 unsure if Breccias		
105					
110		- fracture in core shows dark grey (graphite) external grooves and white - chalky internal gravel mass	few small discrete Black breccias	White - few hair-line fractures / veins beginning to occur	
115					
120					
125					
130		HDP - some patches of MDP. Larger average crystal size ~5mm - Broken core shows Large Black crystals within - MDP with few Banding like fabric (average at 143m, 144.5m 147.5m - with lighter core	- Some Large crystals around 132.3 Possible Breccia, Black and White	Some V-shaped white veins at 132.8 - long veins parallel with core	
135					
140					
145					
150		- HDP with patches of MDP with increase of white crystal density and size ~50% ~5mm average	- Possible White breccia 150.8 small - 10mm crystals		(core loss)
155					
160					
165					
170		Patchy Porphyritic ranging from high to low over 10m (170 - 180)		- few White hairline veins / intrusions	
175					
180		- HDP - MDP with small crystal size (<2mm) average,			
185			- Black stains beginning to appear after 189m unsure if breccia, fracture or discoloration from water drying		
190		Fabric grading into mosaic non coherent then back to coherent at 200m		White intrusion at 191.3m and 192.7m	
195			- Mosaic like Breccia, large (>6mm)	- Hairline and V shaped intrusions	
200					

WND0006 200-300m

Depth (m)	Graphic Log	Primary Volcanics	Breccias	Alteration	Misc.
200		- HDP with small		- Frequent thin veins	
205		crystals, patches of MDP	- frequent dark matrix Breccias small to large (5mm - 60mm) crystal Bearing at base similar to groundmass	white, crescent vein at 201.8m	
210				Band of darker groundmass at 210.4m similar bands elsewhere but could be large Breccias	
215	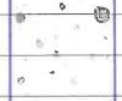				
220		- flow band like shading	-220.5m = 60mm matrix Breccia		
225		alternating MDP with LDP small crystals - patches of fine grained lighter sections of rock			
230		Possible large breccias of banding	- Large discrete and mosaic breccia, lighter grey than groundmass MDP	- few fair line white veins, frequent from 232.6m - 233.4m	
235		- frequent alternation in texture - High levels of fracture	texture within some possibly too big to distinguish in core		
240		232.3 - 241.2m has flecks with green-brown to green-yellow stained groundmass			
245				few white hairline veins	
250		- Patchy fabric mosaic/coherent (few sections almost aphanitic (240.7, 244.7)	frequent brecciation mosaic and discrete		
255	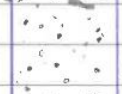	MDP ~~with 50~~ With few flecks of LDP fine grained bands	- frequent Black breccia some may be small breccia or Large crystals	- few white intrusions	
260	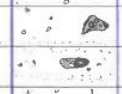	Some sections lighter giving banded appearance	both Large and small Discrete Breccia crescent		
265	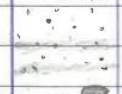				
270	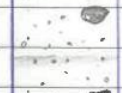	Mosaic looking fabric in some locations but core hard to see and likely result of drying water on core.			
275					
280					
285	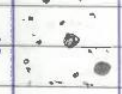				
290				- vein, white, crescent with porphyritic texture (Black crystals) - Black irregular looking veins below 290m	
295					
300					

WND0006 300-400m

Depth (m)	Graphic Log	Primary Volcanics	Alteration Breccia	Alteration	Misc.
300		HDP			
305		- MDP Broken core show white crystal intrusion in Black core	- Breccias single, dark discrete	GM colored, vein at 312.1m, few white hairline veins core	
310		core fracturing and crumbly in places after 314	- frequent loose mosaic Breccias Both light and dark small to large	beginning to brighten to lighter grey in colour and crumbling in some Places	
315		fabric frequently changing	more lighter breccias		
320		Between coherent, Breccia and loose mosaic	with depth		
325		core alternating in color from light and dark grey			
330		- MDP with some Patches of LDP	- Primarily Breccia Dark mostly discrete, light mostly loose mosaic or clusters		
335		Highly variable texture			
340		- Slightly lighter grey	Appears to have Breccias throughout crumbled section competitive zonal texture at 349.2m on Breccia	- Frequent Sections of highly crumbled core lighter colour of core - crescent white veins in opposing orientations at 344.4m	
345	crumble				
350	crumble	Core quite crumbly MDP mostly with few areas of FP LDP			
355		- frequent mosaic fabric.	- Light mosaic Breccia LDP	- core getting more crumbly - frequent white hairline veins.	
360					
365		- core colour starts to lighten at ~365m	- Breccias internal crystals mostly fine - less black Breccia fragments	crumble with light chalky colour could indicate alteration	
370		MDP fine grained with areas of HDP coarse grained crystals flow Banding like structures from 378m	- Breccia grading in and out of Cm coarser Grain internal structure - Breccias appear to be within other breccia	alternating between light and dark Cm Black crystal bearing crescent 378	
375					
380					
385		- MDP with Large irregular Black crystals >10mm	- "low relief Breccia"		
390	crumble				
395		alternating Cm color Between Dark graphite grey and lighter grey - frequent mosaic fabric	- frequent large black Breccia and crystal bearing bands MDP HDP within Breccia	white hairline veins cluster at 398.0m	
400					

WNDD006 400-500m

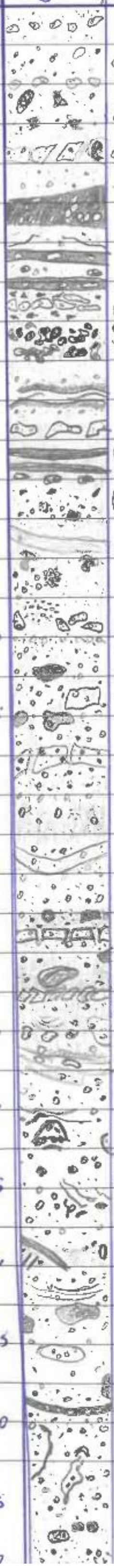

Depth (m)	Primary Volcanics	Breccia	Alteration	Misc.
400–410	MDP - LDP ash - small scale lapilli sized crystals. Alteration between mosaic and cement forms	- Discrete and mosaic breccia lapilli sized, angular and rounded. Both [illegible] and dark, crystal bearing (MDP)	Possible varying levels in alteration, flow banded pattern at 408.9m	
410–420	- Large black section in GM with white breccia within other sections of black bands present with sharp boundaries, patchy gm colours. - "colloform" like texture	Variety of breccia grading into gm at some places	Black looking veins could be groundmass between breccia	
425–435	Range from LDP - HDP frequent ~~structures~~ flow band like structures and sections of black bands through core. Porphyritic - aphanitic - phaneritic	- irregular shaped Breccia with some resulting in "colloform" looking texture		
435–445	Extreme variation in texture from LDP - HDP very patchy. Fibrous black patches could be possible lithics	variation of Breccias some appear to be very HDP texture	- Wavy band at 4328 core appears to show variations in alteration	
445–450	Mostly porphyritic - MDP-HDP few flow band patterns	Mostly LDP - MDP Breccias		
450–460	- consistent sections of coarse crystals LDP-MDP with some fine grained breccia		frequent white hairline veins in crescents pointing both up and down core	
460–470	Patchy color mostly dark. Small section of mosaic @ 463. frequent banding structures	frequent discrete breccia in black GM	few crescent white vein/intrusions mostly pointing up-hole. alteration color ~~changing~~ varying	
470–480	- More consistent coherent MDP-HDP texture with few discolorations frequent ~~of~~ banding structures	Breccias hard to distinguish but mostly mosaic	frequent veins white hair line, few thicker down core in orientation	
480–490		Mostly Dark breccias some with much finer GM than surrounding core	section of strongly altered rock at 479-480m (determined from color) - few faint High Hairline veins	
490–500	variable texture from LDP - HDP with bands of HDP in sections of LDP	variation of Breccias Some bands of HDP through LDP could be Large breccia	Long black 'vein' going down core starting at 490.1m. Large white section at 493.2m frequent white veins	

WND0006 500-600m

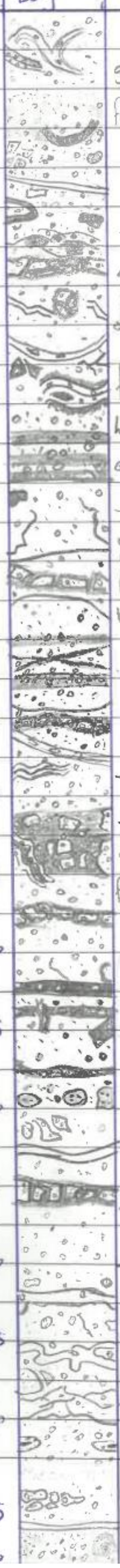

Depth (m)	Primary Volcanics	Breccia	Alteration	Misc.
500	MDP-HDP texture coarse grains in fine grained Gm few black banded structures	Breccias Darkening / black rounded Lapilli sized to 764mm Some mosaic like Breccia after 508.7	irregular white vein at 500.2m, Banded vein at 501.7m, higher level alteration colour at 505.5-507.5. Large white intrusion at ~~505.5~~ 507.5	
510	- Patchy Perlitic texture			
515	- frequent banding in color from chalky white to graphite gray, Patches of LDP	- frequent jigsaw breccia altered in colour and discrete Black breccia Some	- frequent thick (up to [illegible]mm) white vein/intrusions in various orientations	
525	frequent Gm color change White breccia like patches and black bands	Black bands could be Large breccia	~~frequent~~	
530	- Fairly consistent coarse grained MDP with few patches of HDP with finer grains			
540	- frequent black patches - Dominating coarse white crystals	Few jigsaw breccia mostly in black Gm	Thick white veins often with crystal intrusions	
550	- Banded vein structures			
	- Large sectors of black ground mass, 553-555 = frequent banding / flow banding	Jigsaw and discrete ~~white~~ beige breccia in black gm	beige	
560	- Patches of LDP	(567.4)		
	- Mostly MDL with patches of LDP and HDP	- Some Breccia looks Phaneritic - Both white and dark breccia mostly discrete	Large patches of altered colored core	
570		- Breccia with Dark outline and dark crystal dominated	irregular white intrusions 566.2 Stockwork like veins at 567.5	
	Jinish ~~together~~ on core - faint mosaic fabric			
575	] section very crumbly appears to look clayey	Mostly lighter HDP-LDP Breccia	core very crumbly	
580	mostly coarse crystals with some fine patches ~~and~~	- Frequent discrete breccia - large fine grained breccia at 586.5	- 580-581.8 altered coloured (chalky) Large white intrusions 582.4m and at 585.2m frequent white veins	
590	- Mosaic Fabric 580-581.8 and 587.3-590m - few Patches of fine grained core mostly MDP some LDP		core lightens to beige 589.6-589.8	
595	- Radial Pattern, Banded at 597.7		- core seems to be altered as colour lightens to chalky white	
600				

WNDD 006 - 600 - 700

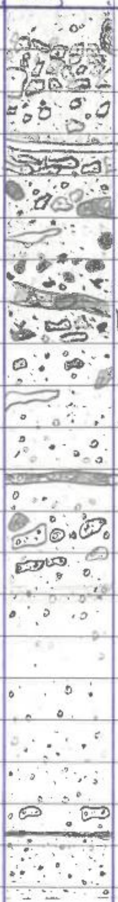

Depth (m)	Graphic Log	Primary Volcanics	Breccia	Alteration	Misc.
600		- Fine Grained dominated	frequent breccia mostly	Crumbly in spots	
605		MDP mostly mosaic	mosaic some loose mosaic	Weaker Chalky White color	
		Fabric few banded		to previous 10 m	
610		Stringers		White vein @ 607.9	
		- Slightly coarser white	- Large irregular shaped black	- Very chalky white section	
615		crystals before return	crystals of breccia 613.8 -	613.8 - 620m, Large black intrusion / vein	
		to fine crystal dominance	620m - discrete, far less	Seam bearing crystals / Breccia running down	
620		Large irregular shaped black crystals	Mosaic breccias	core ~616.3 - 616.6 (~25mm thick)	
		- White intrusion at 623.6			
625		- MDP some patches		- Weak flowing alteration	
		with finer grains	Lapilli to block sized	- Black veins bearing	
630			Breccia, white, appear	White crystals	
			altered, high grain density		
635			within		
640					
645		- Patches of MDP texture	Few altered appearing	Colours give impression	
		- large (~180mm) section of fine grained LDP core	Breccia lapilli to block	core is	
650		MDP	size	Slightly altered	
655					E.O.H 652.70m

WNDD007

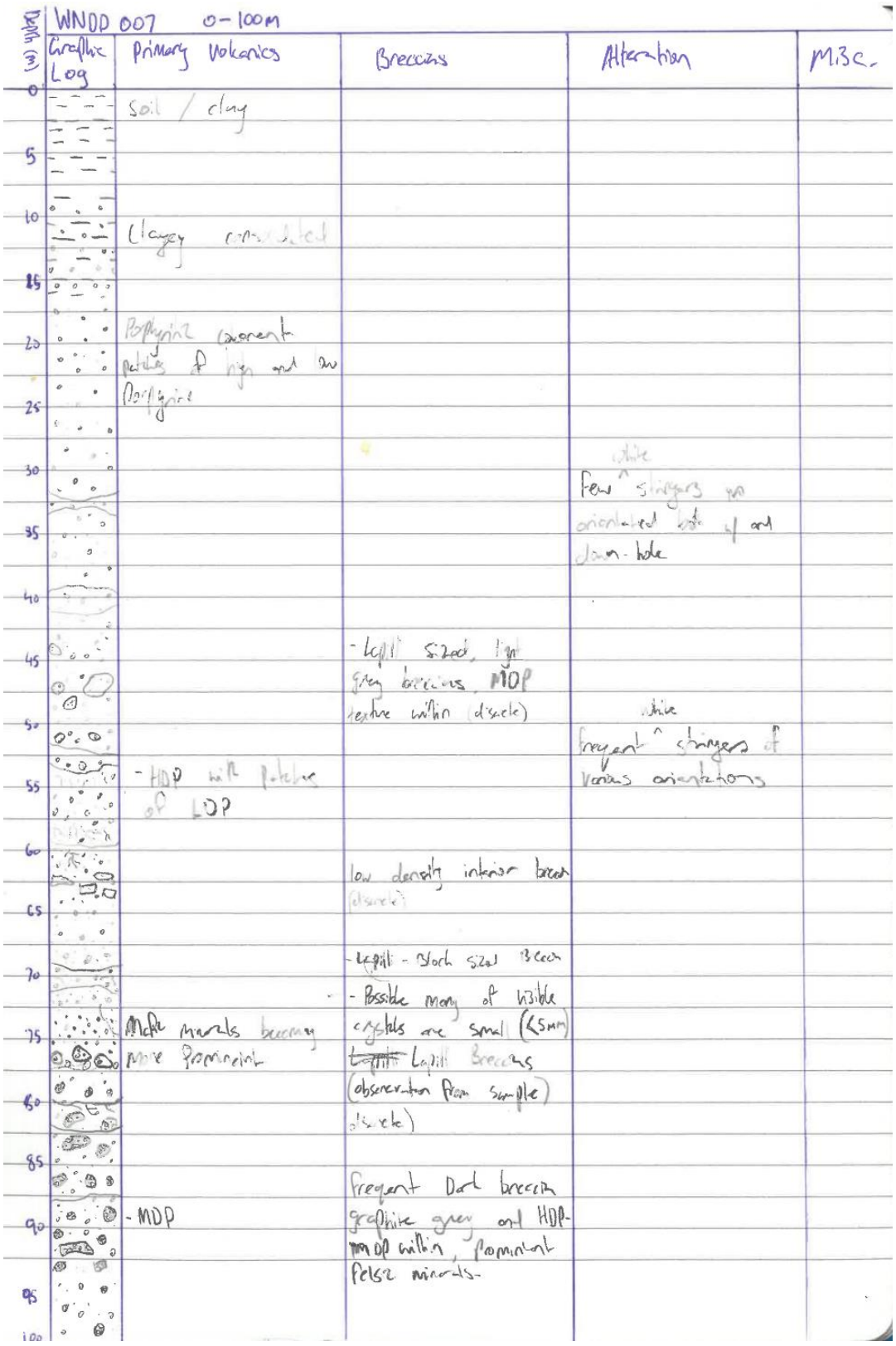
WNDD 007 0-100m
Graphic Log
Primary Volcanics
Breccias
Alteration
Misc.
soil / clay
clayey
Few white stringers not oriented
frequent white stringers of various orientations
- HDP with patches of LDP
low density intrusive breccia
- Possible many of visible crystals are small (<5mm)
Lapilli Breccias
(observation from sample)
discrete)
Frequent Dark breccia graphite grey and HDP-MDP within, prominent felsic minerals.
- MDP

WNP0007 100-200m

Depth (m)	Graphic Log	Primary Volcanics	Breccias	Alteration	Misc.
100					
105				Stringer veins wk	
110			- frequent tube lapilli to rock sized black Breccia, smaller lapilli <10mm white breccias		• Sample
115					
120		Patches of HDP		- stockwork like structure of stringer veins - wk	
125					
130		HDP		- frequent stringer veins white	
135					
140		- grades slightly finer MDP			• Sample
145				- No Mosaic Breccia in white vein like matrix	
150				- rare appears slightly layered	
155					
160					
165		- Patches of low density fine grained texture almost aphanitic	High density of breccia mosaic texture mostly smaller (<20mm)		
170			- Lapilli to Rock sized Breccia		
175		Patches of HDP			
180			- Breccia with zoning like texture at 176.9m - Breccia density decreases - some black breccias (?)		
185		- mostly HDP some bedding like structures at 181-6m	- frequent zoned Breccias ~183m	- white intrusion at 186-0 m	
190		- LDP	mosaic texture		
195		- LDP			
200					

WNDD 007 200m - 231.70m

Depth (m)	Graphic Log	Primary Volcanics	Breccia	Alteration	Misc.
200		Lapilli MDP	Mostly clast supported with		
205		-LDP - aphanitic	chalky rounded matrix	- few thin veins	
			Breccia section at 203m	- large (~20 cm) thick	
210		- MDP patches of HPP	massive breccia Patchy texture	white vein at 206.4m	
215		- Appear to have higher density of pyrite minerals	- looks like vein of breccia at 212.45m also cluster at 214m		
220		-	- ~~Breccias~~ clastous breccias		
			coarse (217m)	- frequent stringers	
225		Some irregular shaped white crystals, not	- Breccias resume (221.3m)		
230		to distinguish from breccia			
					E.O.H.
235					
240					

WNDD009

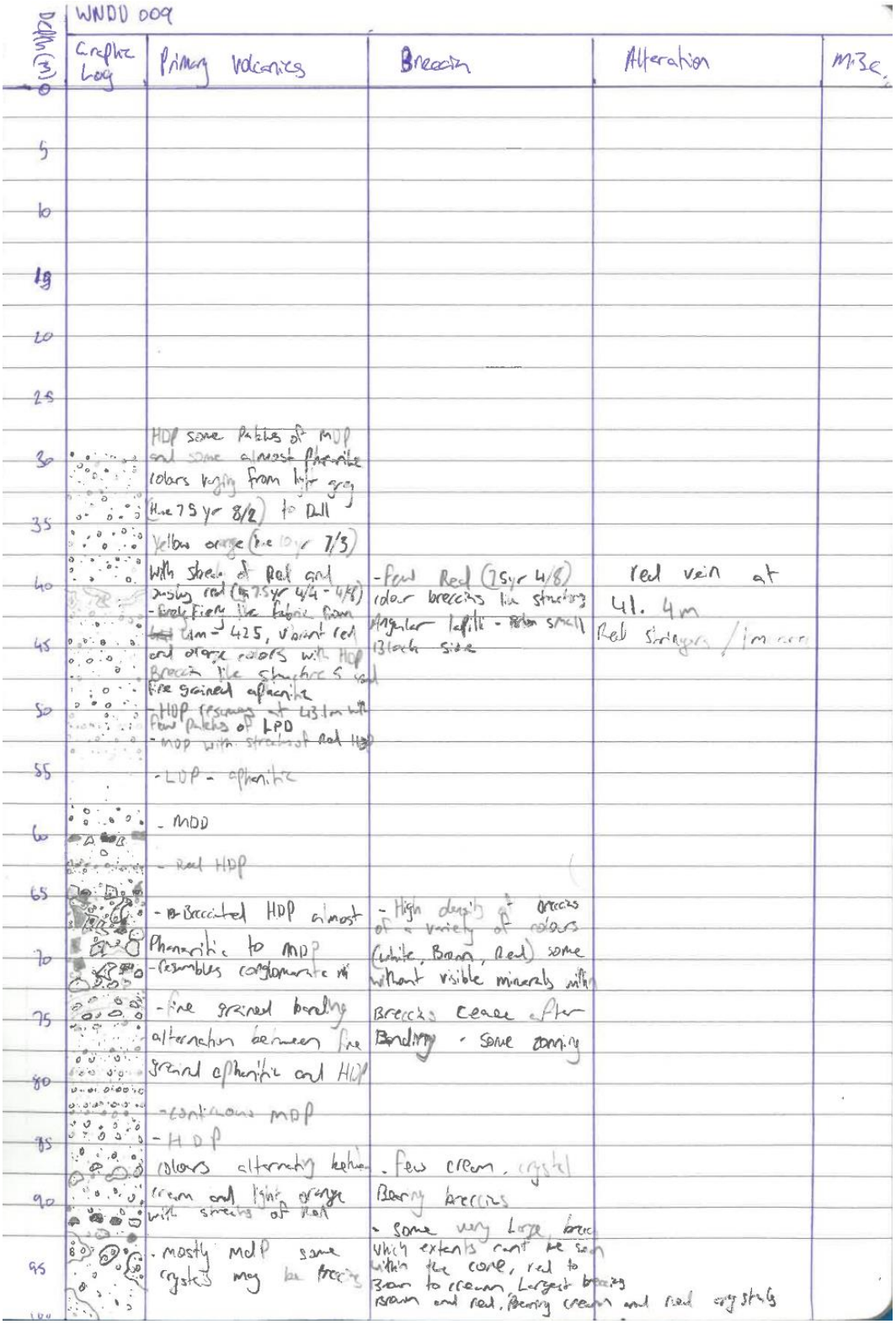

WNDD 009

Depth (m)	Graphic Log	Primary Volcanics	Breccia	Alteration	Misc.
0					
5					
10					
15					
20					
25					
30		HDP some Patches of MDP and some almost Phaneritic colors ranging from light grey (Hue 7.5 yr 8/2) to Dull			
35		Yellow orange (Hue 10yr 7/3)			
40		With sheets of Red and Purple red (7.5yr 4/4 - 4/8) - Evenly even like fabric from 41m - 42.5, vibrant red and orange colors with HDP Breccia like structure & very fine grained aphanitic - HDP resumes at 43.1m with Few Patches of LPD - MDP with streaks of Red HDP	- Few Red (7.5yr 4/8) color breccias like structure Angular lapilli - 1cm small 13cm size	Red vein at 41.4m Red Stringers / im acc	
45					
50					
55		- LDP - aphanitic			
60		- MDD			
		- Red HDP			
65		- Brecciated HDP almost	- High density of breccias of a variety of colors		
70		Phaneritic to MDP - resembles conglomerate w/	(white, Brown, Red) some without visible minerals with		
75		- fine grained banding	Breccia cease after		
		alternation between fine	Banding - some zoning		
80		grained aphanitic and HDP			
		- continuous MDP			
85		- HDP			
		colors alternating between	- few cream, crystal		
90		cream and light orange with streaks of Red	Barry breccias		
			- some very Large breccias which extents can't be seen within the core, red to Brown to cream, Largest breccia Brown and red, Barry cream and red crystals		
95		- mostly MDP some crystals may be breccia			

WNDD 009 100-200m

Depth (m)	Graphic Log	Primary Volcanics	Breccia	Alteration	Misc.
100		-MDP patches of HDP creamy brown colour (5Y 8/1)		Yellowish green to	
105		-core becomes pinkish red (7.5R 6/2)	-large red black sized breccias	Brown intrusions (hue 5Y 6/6 - hue 2.5Y 4/4)	
110		HDP almost porphyritic with breccias			
		-LDP	-Frequent breccias, varying		
115		-MDP-HDP with discrete breccias, frequent single colour ranges	in colour (Black, Brown, Pink cream) lapilli - Block sized		
120		-conglomerate like texture			
125		greenish -MDP texture, sulphur yellow hinge appearing on core			
130					
		-Red flame like texture Basalt forming breaks in ground mass forming breccia structures	-few breccia like structures in flame like texture		
135		-Blue grey (10BG 7/1) -Creamy brown (5Y 8/1) -Pink red (7.5YR 8/3) -Yellow brown (10YR 7/8)			
140					
		Flame like texture	Possible fragment breccia with irregular orientation few mosaic patterns		
145		-MDP-Blue grey			
150		-HDP-Pink red -LDP-creamy brown -MDP-yellow brown -MDP-Red brown			
155		-MDP-creamy brown	-Cluster of breccias	-Red vein like stringers frequent	
160		-Brecciated flame texture irregular black crystals Sharp boundary between yellow brown and blue grey (163.5m)	-brecciation		
165		-core colours now more consistent -greenish tint ~15cm at 168.15m	-Brecciated mosaic texture lapilli size		* Gold coloured crystals at 173.8 at 172.5m
170					
175		-LDP			
180	Crumble	-Appears to be MDP-LDP	Possible dark coloured breccias lapilli in size	Core is dark in colour and does not appear altered but significant crumbling	
185					
190		-MDP-LDP Gold coloured crystals			
195		-	-Breccias begin to occur, dark lapilli - Block white crystals		
200					

WN08 0009 200 - 300 m

Depth (m)	Graphic Log	Primary Volcanics	Breccia	Alteration	Mz
200		- Massive mosaic Breccia density decreasing in some patches but almost Pervasive texture in others	- variety of breccia Lapilli to block sized Dark and light. Some rounded but mostly angular. Zoning also apparent in some Breccia. Breccia frequent almost mosaic		
205					
210					
215					
220		- greenish tint appearing on core (7.5GY 7/1)			
225		- fine grained sedim. few breccia - Bedding fine grained and ashen very fine grained (Ephemite)			
230		- Bright Reddish green rock - some ground mass - small section of Lapilli only	Breccia		
235		- Banding - fine grained - fragmental LDP	- coarse in heavy Brecciation		
240		- fine grained beds - fine grained LDP - LDP	-	moderate crumbling core looks quite weathered / clayey	Mz
245		- MDP	- Large black breccias 248.5m - Red breccia at 249.2m		
250					
255			- Breccia hard to identify from groundmass	crumbly and clayey like surface weathering making texture / Breccia hard to identify	
260		changes in Ground mass color between olive green and light grey	- light buff yellow Breccia - 259.3 - red breccia structure - 262.8m - Zoned Breccia red and black - 263.8m - mosaic Black Breccia structure		
265			- zoned fragmental breccia Black within 267.0m	crumbled, clayey	
270					
275		- white and black banded structure - LDP			
MDP		- Ground mass lighters in color			
280					
285		- MDP throughout with changes in color from Blue grey to light grey and clayey looking texture	Color changes in core make breccias hard to distinguish. breccias frequently display zoning	- core looks clayey, lighter in color	
290					
295			- more brecciation almost mosaic		
300		- fine grained - ephemite			

WN00 009 300 - 400m

Depth (m)	Graphic Log	Primary Indexes	Breccias	Alteration	Min.
300		MDP - sap. some patches of clayey core at 301.0m	- Lapilli sized breccia Some few exceeding 64mm Dark and light grey	- Section appears clayey - Crumbly clay	
305					
310					
315			- Red tinted breccia - 314.2 - 315.1m		
320			- Breccias often LDP texture within		
325		- few flecks of MDP			
330		- LDP			
335					
340		- core begins to have olive green tint (10Y 6/2)			
345		- MDP			
350		- core begins to have red tint (10R 4/6)	- MMHDP - Phenocrysts texture breccia at 353.7m		
355		- LDP - core color change to (7.5Y 6/1)	- Red (10R 4/6) Breccia stem. tuff		
360		- MDP	- Frequent rounded Breccia		
365		- core color change to light grey (N 7/)	- Bright red Breccia at (364.5m) - Breccia become Black at core color change to light grey	- light grey color Possible alteration	
370		- Small frequent black cracks on core surface - Green tint on Broken core But surface remains light grey	- Some light grey Breccia (2.5gy 8/1) 369.2m		
375					
380					
385					
390			- Red Breccia at 391.8m 392.1m		
395	crumble	- irregular white shelled crystals	pink Breccia at 399.8m	- extremely clayey crumbled core	

WNDD 009 400-460m

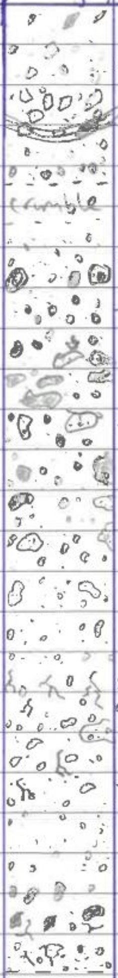

Depth (m)	Graphic Log	Primary Volcanics	Breccia	Alteration	M.S.
400		MDP	- frequent lapilli sized		
405		Some "mossy" texture & discoloration between greys - Scaly fractures at 406m - brecciated	grey and dark grey Brec..		
410				core crumbled, some	
415		- HDP	Breccias have HDP interior texture some breccias within	parts appear clayey	
420		419.1 - very rare white crystals - mosaic ~~texture~~ ~~texture~~	Breccias - frequent Breccias		
425		- MDP	- Block sized breccia, Dark and light MDP within		
430					
435					
440		Surface of core looks clayey and is fractured	- less visible large Breccia		
445		Some surface fractures - Large white crystals / Breccia at 448.5m		Patches of core clayey and crumbly	
450				But no significant other signs of alteration	
455					
460					E.O.H

WNDD011

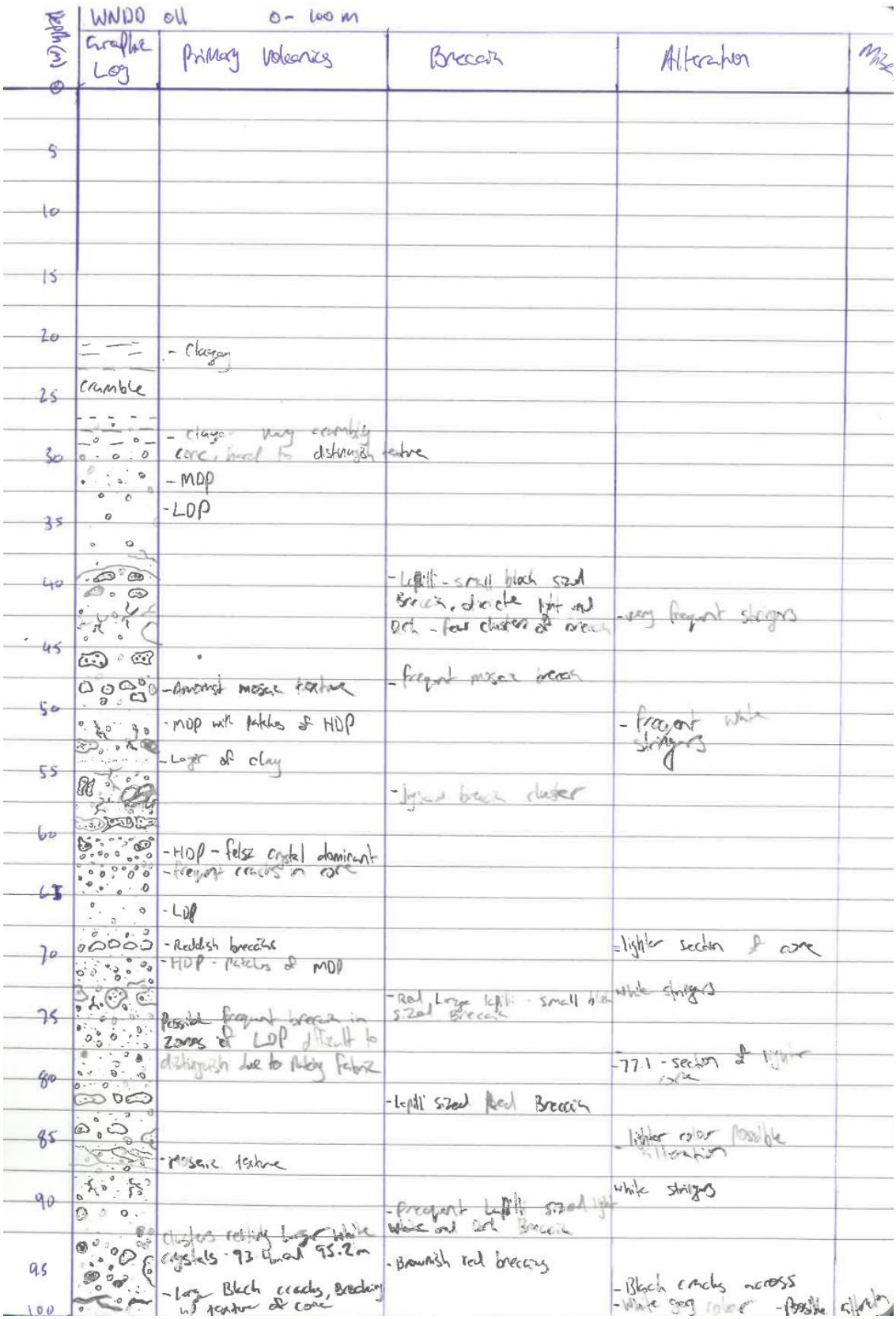
WNDD 011 0- 100 m
Depth (m)
Graphic Log
Primary Volcanics
Breccia
Alteration
- Clayey
crumble
- clayey very crumbly core, hard to distinguish texture
- MDP
- LDP
- Lapilli - small black sized Breccia, clasts light and dark - few clusters of breccia
- very frequent stringers
- frequent mosaic breccia
- Dominant mosaic texture
- MDP with patches of HDP
- frequent white stringers
- Layer of clay
- Jigsaw breccia cluster
- HDP - felsz crystal dominant
- frequent cracks in core
- LDP
- Reddish breccias
- HDP - patches of MDP
lighter section of core
white stringers
- Red Large lapilli - small sized breccia
Possible frequent breccia in zones of LDP difficult to distinguish due to fabric
-77.1 - section of lighter color
- Lapili sized Red Breccia
lighter color possible alteration
- mosaic texture
white stringers
- frequent Lapilli sized light white and dark Breccia
clusters reddish brown white crystals - 93 to 95.2m
- Brownish red breccias
- Large Black cracks, Brecciated texture of core
- Black cracks accross
- White grey color - possible silicification

WNDD 012 100 - 200m

(m) WNDD	Graphic Log	Primary Volcanics	Breccia	Alteration	Min.
100		MDP	Frequent breccias	core is frequently veiny	
105		- fractured core		- stringers present (white)	
				- White vein	
110		- mosaic texture - stringer stems present	- Mosaic breccia		
		- LDP			
115		- MDP - some large white crystals on cracks	- Brief mosaic breccia	- 113.5 - White veins slightly larger than stringer	
120		- Black Band across core followed by grey colour section of LDP (after returning to MDP)		- 115.4 - breccia / intrusion across core	
125		- 123.8m ↑ frequency in mafic minerals (until ~127.2m)	- Breccias less dense in mafic crystal - some Brown-Red breccia	- 124.8 - frequent stringers and surface fractures	
130		- Brief mosaic texture - Banding structure	- teal grey breccia - Large lapilli to block size - LDP	- core quite crumbled - 132.5 Black vein stretch	
135		- mosaic texture - Banding - some sections with MDP - Banding	- mosaic breccia		
140		- mosaic texture - MDP - Patches of HDP		- frequent stringers	
145		- Mosaic texture	some mosaic breccias light ones dark, some zoned with HDP within and MDP around outside		
150		- MDP		- White vein very sloping upward	
155		- mosaic - MDP - Deformed sloping Black banded structures		- White vein sloping downward	
160		- MDP			
		missing core			
165				165.3 - White core with Black breccia clear boundaries	
170		- Banding structure	- Elongated mosaic breccias	- frequent black stringers	
		- MDP - Half larger felsic crystal and white veins/ intrusions			
175					
180		- mosaic - MDP - Black Band downward			
		- mosaic		- long White veins/ intrusions	
185		- MDP ↑ in mafic minerals	- discrete breccias present - Black MDP - teal grey LDP	- frequent stringers	
190		- HDP ↑ in mafic minerals (until 189.3) - frequent change in core colour	- frequent breccia, some possibly too large to distinguish		
195		- mosaic some banding - MDP - Brief mosaic	- some Breccia have White outline		
200					

WNDD 011 200-300m

Depth (m)	Graphic Log	Primary Volcanics	Breccia	Alteration	MBE
200		- MDP	- Dark Breccias - almost mosaic - Light discrete breccias with fragment with relicity large felsic crystals	- Black and white veins / intrusions present	
205		- Ruptured flow foliation			
210		- mosaic	- Banding structure / zoned Breccia at 209m		
215				- White stringers	
220		- MDP - Frequent black stringers	- Frequent breccias - range of Breccia size from small lapilli to small block	- Black vein structure sloping upward - White vein and black veins / fracture running parallel with core, Large black vein at 223.7m and Large white crystal bearing vein at 224.1m sloping to 225.1m	
225					
230		Darker core (Dark blue grey) colour			
235		- Mosaic texture, some gaps between breccias Larger than others and crystal bearing		- light white-grey core - Black bands sloping upward	
240		MDP	- Breccias or Large phenocrysts within mosaic textured Breccia	- thick white veins amongst mosaic texture	
245		- Mosaic - MDP - Mosaic			
250		- MDP - Banded white intrusion structure		- frequent white stringers and white veins	
255		- light grey/white mosaic		- frequent white stringers	
260		- mosaic later vein structure		- frequent white stringers - crystal bearing white intrusion	
265		- mosaic like texture of Dark core in white matrix	- Mixture of discrete and mosaic Breccia structures	- Black intrusion surrounded by banded texture	
270		- chunky of white-grey core broken up by dark black core - Banding like texture			
275		- Mosaic - messy banding texture		- thick white crystals/intrusions white vein banded	
280		- cracked/fractured core fragments - frequent flow banding like structure		Banded white veins - frequent white intrusions	
285		- mosaic texture, flow like pattern	Breccias above fractured interior		
290		- MDP	- Banded breccia structures		
295		- various textures within small area	- clusters of mosaic Breccia as well as discrete breccia	- with Black bands though core	
300					

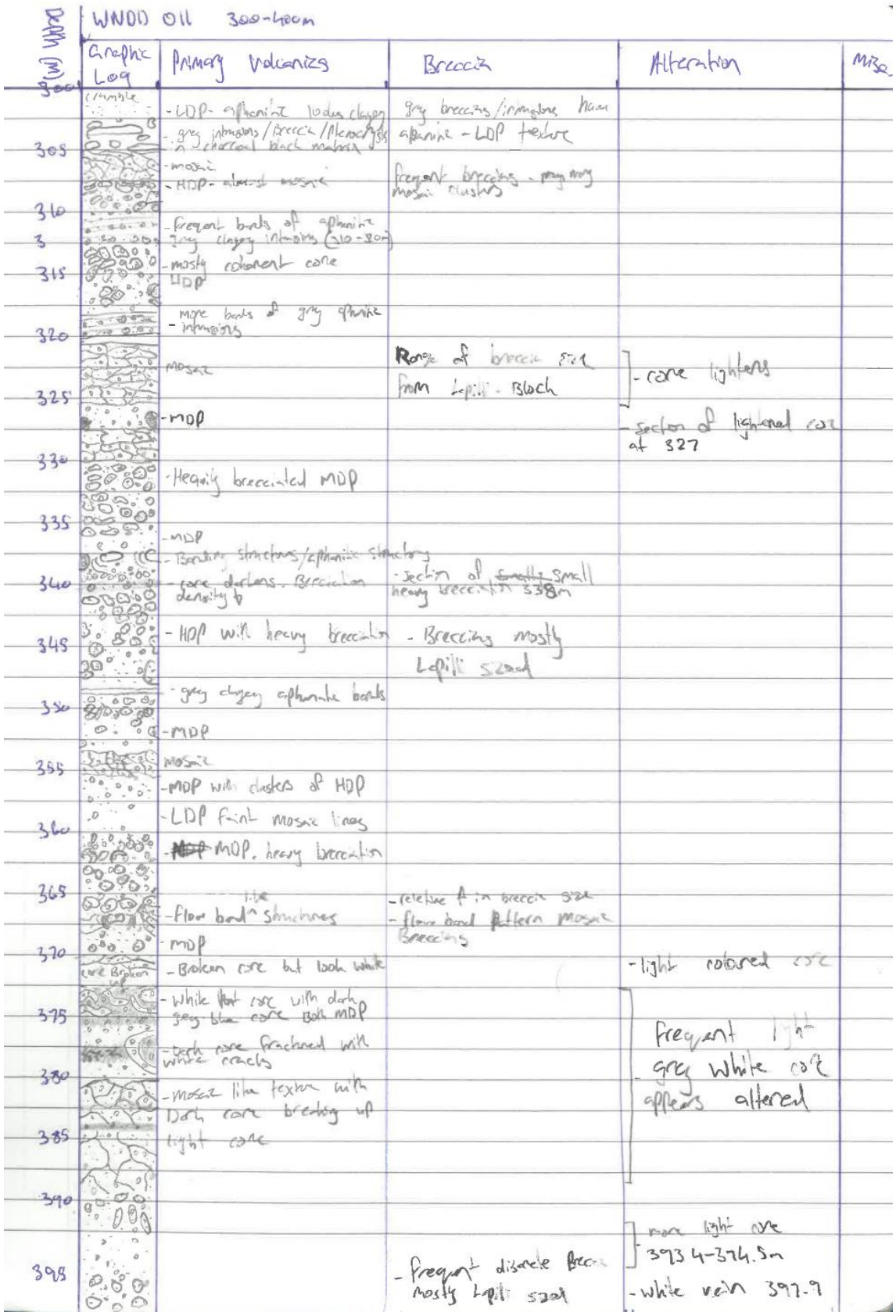
WN01 011 300-400m
Depth (m)
Graphic Log
Primary Volcanics
Breccia
Alteration
Min
- LDP- aphanitic to dense clayey
- grey intrusions / breccia / Hydrothermal in charcoal black matrix
- mosaic
- HDP- almost mosaic
- frequent bands of aphanitic grey clayey intrusions (10-80cm)
- mostly coherent core
HDP
- more bands of grey aphanitic intrusions
mosaic
- HDP
- Heavily brecciated HDP
- HDP
- Banding structures / aphanitic stretching
- core declines - Brecciation density ↓
- HDP with heavy brecciation
- grey clayey aphanitic bands
- HDP
mosaic
- HDP with clasts of HDP
- LDP faint mosaic trace
- HDP. heavy brecciation
- Flow banding structures
- HDP
- Broken core but look white
- White flat core with dark grey blue core both HDP
- Each core fractured with white cracks
- mosaic like texture with Dark core breaking up light core
- Range of breccia size from Lapilli - Block
- Section of small heavy brecciation 338m
- Breccias mostly Lapilli sized
- relative ↓ in breccia size
- flow band pattern mosaic Breccias
- frequent disacle breccia mostly Lapilli sized
- core lightens
- section of lightened core at 327
- light colored core
- frequent light grey white core appears altered
- more light core 393.4-394.5m
- white vein 397.9

WN00 011 400-500m

Depth (m)	Graphic Log	Primary Volcanics	Breccia	Alteration	Note
400		- MDP	- light grey breccia in dark grey groundmass	- white intrusion / vein	
405		- Patchy white grey / grey blue core		- multiple thick white veins - Large (stock) blue-grey intrusion	
410		- Patchy felsic large white crystals	- frequent mosaic and discrete breccia		
415		- small Lapili mosaic	- Range of discrete breccia Lapilli - block		
420		- Patchy ~~light~~ texture between breccia and LDP/aphanite core - MDP - almost phaneritic with faint mosaic lines and some irregular white crystal shapes		- frequent stringers	
425					
430		- patchy of MDP and LPDP - mosaic texture from grained aphanite			
435		- MDP - relatively large white Phenocrysts	- few large breccias MDP within, some not fully distinguishable from core	- frequent stringers	
440		- MDP (& breccias)			
445		- Aphanite - LDP		- thick white intrusion	
		- MDP Black-grey core breaking up white grey core			
450		- almost mosaic	- Dark Breccia stringers with Black veins stacked ~450.1m		
		- patchy light and dark, mosaic in some sections			
455		- blending between light and dark			
460		- Mosaic texture with MDP			
465					
470		- MDP - mosaic - MDP - mosaic		- White vein - Thick white vein, stock work like intrusion	472
475		coherent mosaic and associated mix of texture relatively large white crystals 475.5	BDH mosaic and discrete Breccias		476m
480		- mosaic			
485		LDP			
490		- MDP - frequent black bands similar to mosaic banding above, black bands in white phenocrysts			
495			- discrete and clusters of mosaic breccia similar texture as 9m		~500

WWDD all 500m600m

Depth (m)	Graphic Log	Primary Volcanics	Breccia	Alteration	Mag.
500	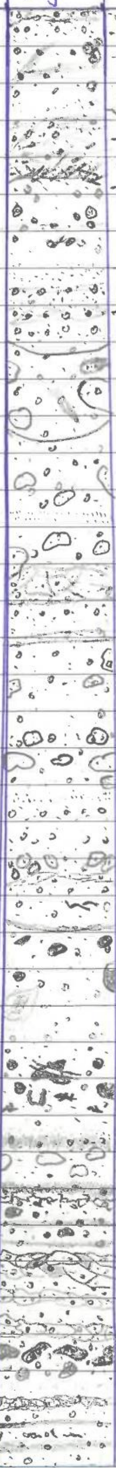	-mosaic -MDP -Patchy colors. frequent Black bands causing mosaic like texture -fine grained band	-clusters of mosaic Breccia	502m - colour wrinkles altering	502
505					
510		- mosaic MDP - Lapilli mosaic -MDP - few black bands	-few discrete breccia		
515		fine grained band with dark sections of medium grain sizes		-wavy white intrusion 520.9m	
520		- mosaic -MDP	- frequent discrete Breccia Lapilli - black some to big to distinguish, Breccia LDP within	-frequent black veins in varying orientations -Black vein bearing White crystals	
525					
530					
535			-fine grained band at 534 possibly large breccia		
540		-mosaic, mostly fine grained - MDP	discoloured band possibly Large breccia x2		
545		-LDP -MDP		549 black bands x2	
550					
555			-fine grained band maybe large Breccia		
560		-brecciated - mosaic - MDP			560 561
565		-fine grained LDP - MDP - zoning of colors - LDP in core 568.5 -MDP	Frequent discrete Black breccia -	Some ores after altered olene to 'olour	
570			-vein cutting through black section of core possibly Breccia	-white veins frequent	572 - 575
575		-irregular black shapes in white core - fine grained LDP -MDP	- Con coloured breccia mostly aphanitic		
580		- Fractured core - mosaic -MDP - frequent black bands could be large breccia	- Black breccia		580.5
585		- mosaic - MDP - mosaic - MDP - relatively finer MDP phenocrysts - mosaic			586
590		-MDP among large black breccia - fine grained			
595		-mix of texturing, mosaic, MDP frequent black banding and cracks also white crystal bearing veins at 599.9	MDP in altered Rock -P showing slightly finer Phenocrysts and more dark minerals		
600					

WNDD 011 600-700m

Depth (m)	Primary Volcanics	Breccia	Alteration	Misc.
600	- MDP - mosaic - MDP Bands of flowing texture surrounded by grey aphanitic matrix	Discrete black breccia and grey breccia when mosaic		600
605	- section of mosaic breccia MDP	- small section of mosaic breccia		-
610	- mosaic - MDP - LDP - MDP			620
615	- clusters of mosaic texture		- frequent thick white veins and intrusions	
620	- Few brown-red crystals - 619m - relative increase in grain size - HDP relatively ↑ grain size	- discrete LDP Breccias	- degree of alteration based on color appears to ↓	
625	- LDP - most various textures from 625.7 - 630.5m L Black vein bearing white intrusions and mosaic texture breccia	- mosaic sections few discrete breccia	- frequent stringers and thick white veins/intrusions	
630	- MDP - LDP	- Black breccia	- frequent black vein stretching often bearing white intrusions/veins	
635	- MDP - white intrusions - mosaic streaks of aphanitic grey - MDP - Banding structures of white intrusions, dark core and mosaic	white core		
640	- MDP with mosaic clusters - frequent black sections of core like veins - fine grained LDP - MDP			
645	- LDP - - MDP - Frequent white veins within sections of dark core	- Few discrete breccia dark - mosaic breccia in dark core		
650	- Frequent intrusion - stock work like texture - patchy core coloration white grey Graphite	Patchy color of core	- Multiple thick and stringer veins - white, varying orientations - thick white stock work intrusion being 6m - 652.3m	650
655	- slightly mosaic - MDP-LDP - core becomes grey - frequent white stringers	results in multiple breccia structures		↓
660	- MDP Frequent stringers mosaic	- Both light dark and intermediate breccia		
665	- MDP - red/brown colored Phenocrysts 664.8m - 668.4m	- Few discrete grey breccia	- Stock work like intrusion white - 669.1m	
670	- texture appears rough - texture appears smooth texture appears rough almost mosaic			
675				
680	- mosaic - HDP - MDP - almost mosaic - mossy		- frequent white intrusions	
685	- LDP patches of MDP ... - MDP	- patchy breccia structure being relatively large white Phenocrysts	- frequent white intrusions	
690		- Brown/Black ... of crystals within stock works	stockwork like intrusion 690.5m	
695	- HDP - MDP - almost mossy		- white intrusions	P.t.o

WNDD 011 700-706.8m

(3) Depth	Graphic Log	Primary Volcanics	Breccia	Alteration	Misc
700		- Brecciated massive texture	- Lapilli core rimmed Breccia		
		massive stuffed flow			
705		Breccia / lapilli in ash	- Some blocky breccia	core (grey-white)	
710			Pervasive		
715					

WNDD008

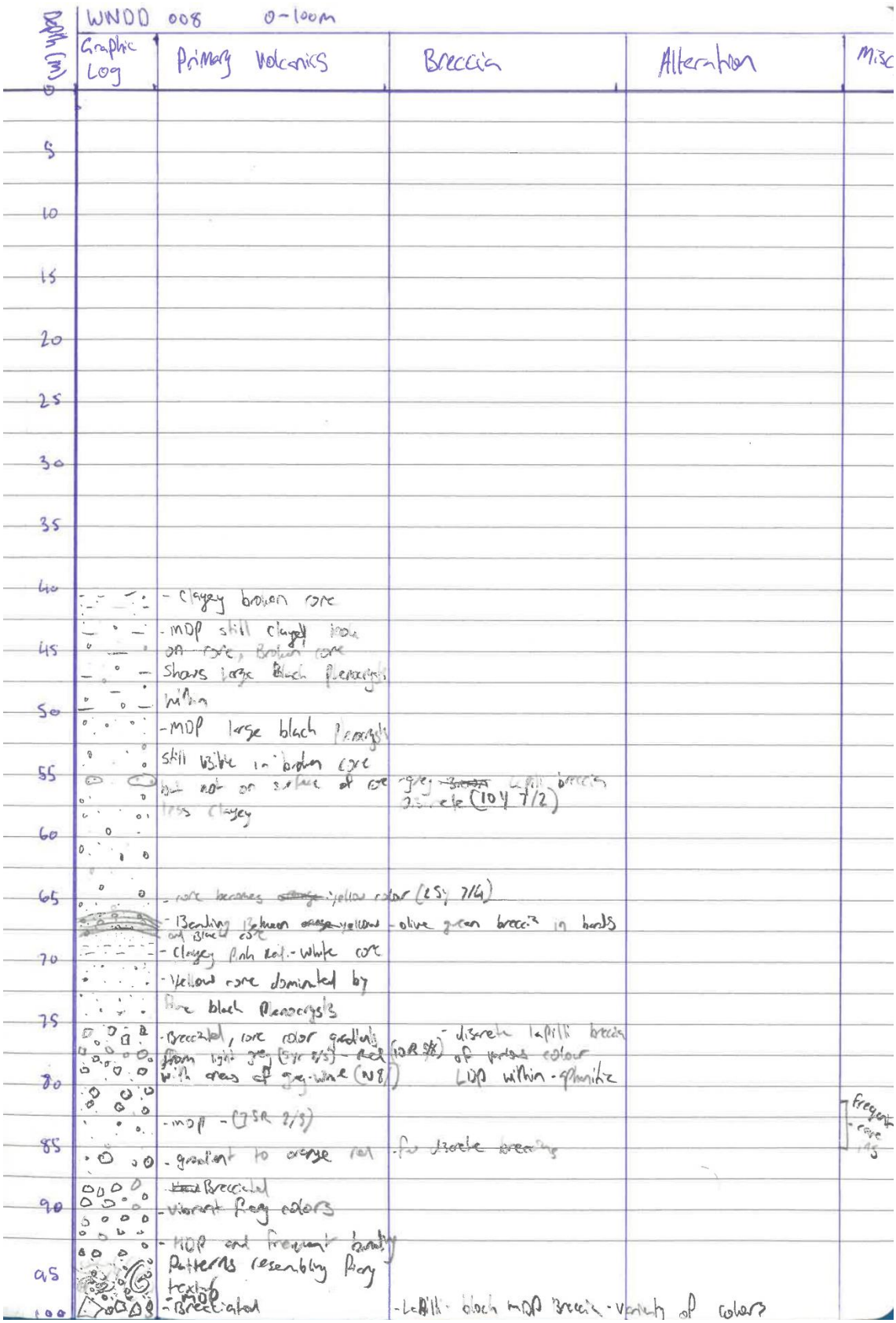
WNDD 008 0-100m
Depth (m)
Graphic Log
Primary Volcanics
Breccia
Alteration
Misc
0
5
10
15
20
25
30
35
40
45
50
55
60
65
70
75
80
85
90
95
100
- clayey broken core
- MDP still clayey broken core, Broken core
- Shows large Black Phenocrysts within
- MDP large black Phenocrysts
- still visible in broken core but not on surface of core
- less clayey
- olive green breccia in bands
- clayey Pink red - White core
- Yellow core dominated by fine black Phenocrysts
- Brecciated, core color gradual from light grey (5yr 8/1) - red with areas of grey-wine (N8/)
- discrete lapilli breccia of varied color
- LDP within - aphanitic
- MDP - (7.5R 7/3)
- gradient to orange red
- fo discrete breccia
- Brecciated
- vibrant Pink colors
- MDP and frequent banding Patterns resembling flow texture
- Brecciated
- Lapilli black MDP breccia - variety of colors
Frequent - core rig

WNDD 008 100~200m

Depth (m)	Graphic Log	Primary Volcanics	Breccia	Alteration	Misc
100		- Brecciated - MDP	- frequent breccia of		
		- MDP grey brown	various colors mostly		
105		Brecciated - LDP - orange brown	up 1/2 in size - MDP - HDP		
		- brecciated - MDP	within		
110		- MDP			
		- brecciated - LDP			
115		- MDP color grades to red	- frequent block sized breccia		
		- Brecciated - MDP - color			
120		grades back to orange brown			
		- MDP			
		- ~1m of mosaic texture			
125		- MDP			
			- cluster of mosaic breccia		
130		- Brecciated MDP			
		- 30cm of grey MDP possibly large breccia			
		- MDP - spots of discoloration			
		possible breccia			
135		- brecciated - MDP			
			mosaic breccia in vibrant		
140		- mosaic	orange - red matrix - 139.8m		
		- brecciated MDP			
		- 1m grey MDP	- discrete breccia in grey section		
		- Brecciated MDP			
145		- color grades to green/yellow	- some breccia appear to		
		- orange brown	be within other breccia		
		- grey yellow			
150		- mosaic			
		- Brecciated MDP - Red			
155		- ~1/2 meter MDP dark red/grey			
		- Brecciated MDP - red			
		- sharp change to grey - MDP ~ 0.8m			
160		- Brecciated MDP - Red			
165		- Yellow looking crystals	- some breccias with yellow		
			borders		
170		- MDP			
		- possible small lapilli breccia	- large phenocrysts appear		
			to be small breccia		
175		- MDP - frequent banding			
		olive green, grey, grey-red bands			
		- Brecciated - MDP			
180			some breccia HDP, very		
			dense with phenocrysts,		
185		- mossy texture ~ 20cm	almost aphanitic		
		- grey/red banding - MDP			
		- Brecciated - MDP			
190					
195		sharp change, grey HDP with			
		- few breccias ~1m			
200		- Breccia MDP			

WN00 008 200-300

Depth (m) WN00	Graphic Log	Primary Volcanics	Breccia	Alteration	Min.
200		Brecciated mdp	Lapilli - Block sized breccia		
205		~70cm MDP Brecciated MDP	various clasts mdp - HPd texture, various colors		
210		- Brecciated MDP - LDP	white streak across red core - possibly breccia		
215			HDP Breccia texture		
220		- Brecciated HDP - Brecciated MDP - MDP - grey and yellow grey clasts - pink - white - MDP - Yellow orange - Brecciated MDP			
225		- fine grain LDP ~10cm - Brecciated MDP			
230		- grey MDP - red MDP - Yellow brown brecciated MDP			
235			- mostly lapilli sized fan Blocks		
240		frequent color gradients	Brecciation Monocrys		
245		- yellow grey color			
250		- HDP ~1m Brecciated - MDP Brecciated grey red color - HDP ~2m Brecciated - Brecciated MDP grey with sections of grey-red color			
255		grey yellow			
260		- Brecciated HDP			
265		- Brecciated aphanitic - Sand yellow - Brecciated - HDP			
270		- pockets of white - yellow			
275		- MDP - LDP			
280		- sharp change to dark grey MDP Brecciated - mostly lapilli almost mosaic texture	- Few breccias, possible Brecciation texture as many large Phenocrysts may be breccias to small to see in core image		
285					
290					
295		- MDP - core becomes very fractured and crumbly			
300		- consolidated, Rock - Brecciated LDP	A relative breccia size in grey core		

WNDD 008 300-400

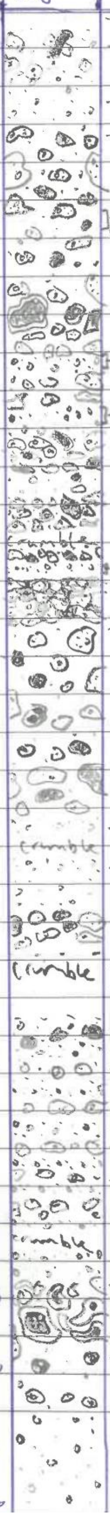

Depth (m)	Graphic Log	Primary Volcanics	Breccia	Alteration	m.3c.
300		- fine grained LDP	- frequent Lapilli - black		
		- Brecciated MDP	Breccia light grey,		
305		- MDP - fractured / Rubbly sten	black and dull red		
		- Brecciated MDP	some overlapping others		
310			usually MDP texture		
		brecciation increasingly slightly decreasing			
315					
320			- Zoned breccia		
		- MDP section			
325		- MDP section			
330					
335		- MDP section			
		- loosely mosaic			
340		- Brecciated - MDP	- Small block sized Red breccia		
345			- lithics / Breccia within Breccia 347.4m		
350					
		- MDP			
355		- MDP - Appears mafic mineral dominated			
360		- Brecciated MDP	- red large Lapilli sized Breccia		
365		- mostly crumble, small pieces of mosaic and MDP texture			
		- Brecciated MDP	- apparent red Breccia		Frequent Lapilli
		- MDP - red tinge in core			
370		- B MDP			
		- MDP			capping
		- B - MDP			
375		- MDP - red tinge			
		- B - MDP			
		- MDP - Brighter red tinge	Some fractured Breccia		
		- B - MDP			
		- MDP			
380		- B - MDP			
		- MDP			
385		- very loose Large mosaic	- frequently large block zoned Breccia and breccia within Breccia - 385.3 - 387.1		
390		- MDP - LDP with patches of small Red core / Breccia	- Red Breccia - 387.2		
			- few red Lapilli breccias		
395					
400					

Appendix B

Relict and altered thin section descriptions

Slide no.	Hole no.	Depth (m)	Texture:	Transmitted light- Relict description:	Transmitted light- Altered description:
1	**5**	101.2	Porphyritic	Well-formed **Quartz** phenocrysts, anhedral in shape, heavily fractured with an average size of ≈0.36mm at a frequency of ≈8%. No other clear fresh phenocrysts. Frequent quartz indicating possible relict **plagioclase.** Roughly 2% opaques.	Relict Phenocrysts anhedral to subhedral in shape with an average size of 0.8mm with a frequency of **20%.** Gm (groundmass) is very fine grained with an average grain size of ≈0.025mm and mainly consists of two grain types; a low birefringence white grain, (≈15%) and a brown grain which appears to be fairly altered, (≈85%).
2	**5**	241.14	Porphyritic	**Quartz** phenocrysts, anhedral in shape with heavy fracture, few holes and embayment's and an average size of ≈0.7mm at a frequency of 8%. Limited **orthopyroxene** phenocrysts at a frequency of <1%. No fresh plagioclase but frequent calcite indicating relict plagioclase. few pseudomorphs also present. Roughly 3% opaques.	Relict phenocrysts, often fractured anhedral to subhedral in shape with an average size of ≈1.0mm and a frequency of **≈25%.** Frequent calcite alterations as well as frequent black-yellow, opaque riddled alteration textures. Also many altered phenocrysts are bordered by opaques. Gm made up of irregular brown-yellow (≈50%) and white grains, (≈50%), with an average grain size of ≈0.05mm. Few very fine, (≈0.01mm) grained opaques in gm also.
3	**5**	354.79	Porphyritic	**Quartz** phenocrysts, anhedral in shape with heavy fracture, few holes and embayment's. With an average size of ≈2mm and a maximum size of 4.5mm at a frequency of ≈7% Fresh quartz grains also appearing frequently in the gm. Some areas of gm appear to have a phaneritic texture but it is more likely that this is a highly fractured and fragmented quartz phenocryst. No other fresh phenocrysts. low frequency of **plagioclase** and **orthopyroxene** pseudomorphs. High frequency of grains with triangular shape. Roughly 3% **opaques.**	Relict phenocrysts with anhedral shape, and indistinct boundaries, making many difficult to identify. High levels of calcite alterations as well as yellow-brown, opaque riddled alteration and brown-grey sandy alteration textures. Some brown staining also present on some grain. The Gm displays multiple textures made up of white quartz grains (≈0.1mm) and brown-grey grains, likely altered grains and clays, (≈0.1-0.5mm).

4	**5**	380.83	Porphyritic	**Quartz** phenocrysts, anhedral in shape with light fracture and some embayment's. Average size of ≈1.0mm at a frequency of ≈10%. Some quartz phenocryst beginning to alter from the outside inwards resulting in altered halo zones around the quartz phenocrysts. Likely reliced **plagioclase** but no clear pseudomorphs but calcite present. Also, likely reliced **orthopyroxene** present but no clear evidence due to heavy alteration. Roughly ≈3% opaques.	Relict phenocrysts have a subhedral to euhedral shape, and many are fragmented. The average size is ≈1.25mm with a frequency of **≈30%.** Frequent calcite alterations with some grey-brown sandy alteration textures also. Many altered phenocrysts also have a higher frequency of opaques in them. The gm appears to be altered with a blotchy texture with sharper boundaries on grains. This texture consists of a ≈65% irregularly shaped white grains of low birefringence, likely quartz +- plagioclase, and ≈ 35% light grey-brown to brown grains, possibly altered grains and/or clays. some areas of the gm have a higher density of calcite . Average gm grain size is 0.01mm.
5	**5**	540.07	Porphyritic	**Quartz** phenocrysts with light to moderate fracture, anhedral shape, embayment's and holes. Average size of ≈1.15mm at a frequency of ≈10%. Some partly altered plagioclase with twinning still faintly visible but most phenocrysts fully altered. Possible reliced **orthopyroxene** present also but no fresh phenocrysts except for one small one hidden in large quartz embayment. Roughly 8% **opaques.**	Relict phenocrysts, subhedral to anhedral in shape with an average size of ≈1.5mm at a frequency of **≈27%.** Many calcite alterations with a yellow brown alteration texture also occurring sometimes with phenocrysts filled with opaques. Gm consists of amorphous sandy light brown texture (≈45%) amongst a blotchy white (≈20%, likely quartz +- plagioclase) and dark brown texture, (≈35%, likely clays). Average grain size in gm ≈ 0.015mm.
6	**5**	614.25	Porphyritic	**Quartz** phenocrysts, anhedral in shape with light to heavy fracture, frequent embayment's and holes and an average size of ≈0.9mm with a frequency of ≈8%. Some quartz appears to be beginning to alter. There also appears to be reliced **plagioclase** inferred from the calcite presence and pseudomorphs as well as reliced **orthopyroxene,** evident from the alteration texture and colour of some phenocrysts as well as reliced phenocryst riddled with opaques. Roughly 12% **opaques.**	Relict phenocrysts with subhedral to anhedral shape and often fragmented. Calcite alterations common as well as dark yellow to charcoal grey, opaque riddled and bordered phenocrysts. Some phenocrysts with sandy yellow brown to calcite alteration show irregular coral-like alteration texture. Gm has blotchy brown and white texture with ≈55% brown grains, likely clay and altered grains, ≈40% white grains, likely quartz +- plagioclase and ≈5% opaques. Average Gm grain size ≈0.035mm.
7	**5**	629.93	Porphyritic	**Quartz** phenocrysts with embayment's, fracture, holes, anhedral shape with an average size of ≈1mm at a frequency of ≈12%. **Orthopyroxene** phenocrysts heavily altered, yellow in colour,	Relict phenocrysts, subhedral to anhedral with an average size of ≈1.25mm at a frequency of **≈20%.** Frequent calcite alterations from reliced feldspars, as well as yellow stained alteration phenocrysts

				anhedral in shape and often riddled with opaques. Reliced **plagioclase,** no fresh phenocrysts, evident from calcite and pseudomorphs. Roughly 5% opaques.	riddled with and boarded by opaques, likely a pyroxene alteration feature. Blotchy gm texture with ≈75% brown, likely clayey alteration material, ≈10% altered grains, ≈12% white grains and ≈3% opaques. Gm has an average grain size of ≈0.014mm.
8	**5**	791.12	Porphyritic	**Quartz** with, minor fracture, embayment's, anhedral shape and an average size of ≈1.5mm with a maximum size of 5mm at a frequency of ≈12%. **Orthopyroxene** phenocrysts, euhedral to anhedral in shape with an average size of ≈1mm with a frequency of ≈ 2%. Orthoclase partly altered. Reliced **plagioclase** present but all fully altered, identifiable by pseudomorphs and presence of calcite. Roughly 5% **opaques.**	Relict phenocrysts, euhedral to anhedral in shape, with an average size of ≈1.75mm and a frequency of **≈25%.** Frequent calcite alterations, also common yellow stained sandy alteration features, with phenocrysts often riddled with opaques. Areas of fresh gm, evident from the presence of original plagioclase microlites, overprinted by blotchy brown and white alteration texture. Also ≈3% opaques in gm. Average gm grain size ≈ 0.02mm.
9	**5**	792.94	Porphyritic	**Quartz** phenocrysts with no to moderate fracture, embayment's, anhedral shape and an average size of ≈0.9mm at a frequency of ≈12%. **Orthopyroxene** with euhedral to subhedral shape and an average size of ≈1.0mm at a frequency of 4%. all orthopyroxene partly altered. No fresh **plagioclase** but many pseudomorphs altered to calcite. roughly 4% **opaques.**	Relict Phenocrysts, fractured, subhedral to anhedral in shape with an average size of 1.75mm at a frequency of **25%.** High quantities of calcite as well as altered orthopyroxene. Also, brown-yellow sandy alteration texture and black-grey speckled alteration texture. Gm has blotchy brown-green and white texture with ≈10% white grains, likely quartz +- plagioclase and ≈90% green to brown grain which is likely altered grains +- orthopyroxene grains +- clays. also opaques present in gm.
10	**5**	835.19	Porphyritic	**Quartz** phenocrysts with anhedral shape, light to moderate fracture, few embayment's, with an average size of ≈1.25mm at a frequency of ≈9%. **Plagioclase** phenocrysts with euhedral to anhedral shape. Plagioclase phenocrysts partly altered but polysynthetic twinning still visible on many phenos. Average size of ≈2.5mm with a frequency of ≈15%. Subhedral to euhedral **orthopyroxene** phenocrysts, all altered to some degree. with an average size of ≈2.25mm and a frequency of ≈12%. Roughly 6% **opaques.**	relict phenocrysts with anhedral to subhedral shape and often fractured. Average size of ≈1.75mm at a frequency of **≈20%.** Many phenocrysts altered to calcite as well as altered orthopyroxenes with very faint birefringence visible. Dark brown/yellow clayey alteration texture on some phenos, surrounded by yellow stained gm. Opaques frequent throughout phenocrysts. gm has weak blotchy texture consisting of white grains, (≈20%), likely quartz +- plagioclase, yellow stained grains, (≈50%), likely alteration feature on some grains. Also dark brown grains are present, (≈30%) which are likely clays. the white grains are the largest with an

					average size of ≈0.1mm while the yellow are the smallest with an average grain size of ≈0.02mm.
11	**6**	42.1	Porphyritic	Fresh **quartz** with anhedral shape and an average size of ≈0.6mm at a frequency of ≈5%. Subhedral to anhedral **plagioclase** with an average size of ≈0.9mm and an average frequency of ≈25%. **Orthopyroxene** with anhedral to subhedral shape and an average size of ≈1.2mm at a frequency of ≈2%. some orthopyroxene showing alteration. **Clinopyroxene** with anhedral shape and an average size of 0.3mm at a frequency of 4%. <1% **hornblende** and roughly 1% **opaques.**	Few relict phenocrysts with a subhedral to anhedral shape and an average size of ≈1.0mm at a frequency of ≈**5%**. Relict phenocrysts mostly unidentifiable and have speckled black and white texture. Weak blotchy textured gm with few white grains, (≈15%), likely plagioclase +- quartz, and an abundance of green-yellow-brown grains, (≈85%), likely to be altered grains and some clays. Not a high abundance of dark brown patches in gm relative to other blotchy gms.
12	**6**	182.92	Porphyritic	Fresh **quartz** anhedral in shape with an average size of ≈0.5mm at a frequency of ≈5%. **Plagioclase** with euhedral to subhedral shape, with an average size of 0.75mm and maximum size of 6.5mm and a frequency of ≈35%. Some plagioclase showing alteration. **Orthopyroxene** and **Clinopyroxene** with subhedral to anhedral, with an average size of ≈0.5mm and a combined frequency of ≈12%. Some pyroxenes showing slight alteration. **Hornblende** in small quantities, (<1%). Roughly 2% **opaques.**	Relict phenocrysts with a subhedral to anhedral shape and an average size of ≈0.9mm at a frequency of **≈5%.** Some calcite alterations as well as a yellow brown sandy alteration texture which appear heavily altered. The gm is appears relatively fresh with an abundance of ≈0.1mm plagioclase microlites, (≈60%) often displaying a trachytic texture. The remainder if the gm consists of opaques, (≈8%) and a grey brown matrix, (≈25%) and oxp +- quartz grains, (≈12%).
13	**6**	228.59	Porphyritic	Fresh **quartz** with anhedral shape and an average size of ≈0.3mm at a frequency of ≈3%. Subhedral to euhedral **plagioclase** with both zoning and twinning present. Anhedral to subhedral **clinopyroxene** and **orthopyroxene** with an average size of ≈0.43mm and a maximum of 2.5mm (clinopyroxene) and 1.5mm (orthopyroxene) with a combined frequency of ≈8%. Possible hornblende phenocrysts but not able to fully identify. Roughly 2% **opaques.**	Few altered phenocrysts, anhedral in shape, with an average size of ≈0.8mm and a frequency of **5%.** Lack of calcite but frequent green-yellow-brown sandy alteration texture and many altered phenocrysts often filled with opaques. Gm has a weak blotchy texture with various shades of brown making up almost amorphous gm. Few murky white grains (≈10%) with mostly various brown patches, (≈90%). gm average grain size ≈0.07mm.

14	**6**	315.22	Porphyritic	Anhedral **quartz**, with an average size of ≈0.7mm at a frequency of ≈1%. Anhedral to subhedral **plagioclase** with an average size of ≈1.5mm at a frequency of ≈40%. Some plagioclase phenocrysts undergone minor to major alteration. **Clinopyroxene** with anhedral shape and some with slight alteration and an average size of 0.25mm. at a frequency of ≈3%. **Orthopyroxene** with euhedral to anhedral shape, and frequently partly altered. Average size ≈0.3mm at a frequency of ≈1%. Likely some **hornblende** also evident from pseudomorphs but too altered to be sure, (<1%). Roughly 2% **opaques.**	Higher % of Relict phenocrysts than slide 13 with mostly feldspar alterations, some calcite present. Average Relict phenocryst size ≈1.3mm at a frequency of **≈8%** with minor to heavy alteration occurring on phenocrysts. Gm shows mixed texture with fresh, ≈0.2mm microlites, (≈45%) overprinted by alteration line yellow/ brown stained grains, (≈55%) likely clay alterations.
15	**6**	373.55	Porphyritic	No fresh phenocrysts except for one larger (>2.5mm) heavily fractured and possible partially altered, embayed quartz phenocrysts. There are also many small (<0.1mm) unaltered quartz grains. Shape of some Relict phenocrysts indicates possible historic feldspar phenocrysts. Roughly 4% opaques.	Relict phenocrysts, anhedral in shape, frequently fragmented with an average size of ≈1.25mm, at a frequency of **≈20%.** Frequent calcite as well as blotchy fragmented grain texture. The gm seems altered with a larger blotchy texture of larger patches of white (≈30%) grains, likely quartz, +- plagioclase grains and sandy light and dark brown grains, (≈70%) , likely clays as grains twinkle in xpl. Average gm grain size ≈0.12mm.
16	**6**	458.56	Porphyritic	Fresh **quartz,** anhedral in shape with light to heavy fracture, few embayment's and an average size of ≈1.7mm and a frequency of ≈8%. Altered **Orthopyroxene** barely identifiable with few phenocrysts only partly altered, with an average size of 0.8mm and a frequency of ≈2%. No distinguishable plagioclase, likely all altered due to abundance of quartz.	Relict phenocrysts, anhedral in shape, frequently fragmented and primarily unidentifiable, but hight calcite indicates plagioclase. Other alteration textures include a blotchy fragmented white and brown grains. An average size of ≈2.0mm at a frequency of **≈15%,** however some phenocrysts are hard to distinguish from the gm. Gm appears altered with a blotchy texture with 3 main grains, white grains, (≈30%), likely quartz +- plagioclase, light brown grains, (≈30%) likely altered grains and dark brown grains, (≈40%), likely clays. Gm grain size average ≈0.1mm

17	**6**	530.2	Porphyritic	Few fresh **quartz** phenocrysts, with anhedral shape, an average size of ≈0.6mm and a frequency of <1%. **Orthopyroxene** phenocrysts present, most phenocrysts altered to some extent. Subhedral to anhedral in shape win an average size of ≈0.4mm and at a frequency of ≈3%. Altered **plagioclase** phenocrysts, some distinguishable as pseudomorphs as well as the abundance of calcite. Roughly 6% **opaques.**	Relict phenocrysts with anhedral to euhedral shape, many of which are unidentifiable. Average size ranging from ≈0.1 to ≈3.0mm at a frequency of **40%.** Calcite a common alteration feature as well as a yellow stained blotchy texture and the amorphous sandy brown-grey-yellow texture. The gm has a blotch texture of murky white grains, (≈55%) likely quartz +- plagioclase +- orthopyroxene and dark brown grains (≈35%) likely clays as well as a yellow stained grain, (≈5%) possibly an alteration feature. there were also some opaques.
18	**7**	73.5	Porphyritic	Fresh **quartz**, anhedral shape with some embayment's present, light to heavy fracture. Average size of ≈1.0mm with a maximum size of 3.5mm at a frequency of ≈4%. Fresh **plagioclase** mostly subhedral with few anhedral and euhedral. Average size of ≈1.6mm with a maximum size of 6.5mm at a frequency of 30%. some plagioclase phenocrysts displaying altering. **Orthopyroxene** at an average size of ≈0.2mm and a frequency of ≈6%. Roughly 5% **opaques.**	Relict phenocrysts, anhedral to subhedral in shape with an average size of ≈0.75 and a frequency of **≈15%.** Frequent plagioclase relics with calcite common as well as pseudomorphs. Some phenocrysts display a halo zone of alteration with fresh phenos remaining in centre and outer phenos is altered. The gm consists of dull white sandy amorphous texture (≈65%) bearing brown-grey clays and altered grains (≈30%) as well as white grains, opx grains and opaques. Average gm grain size ≈0.1mm.
19	**7**	109.5	Porphyritic	Fresh **quartz** with anhedral shape, heavy fracture, embayment's and an average size of ≈0.50mm at a frequency of ≈8%. Some quartz appears to be beginning to alter. **Plagioclase** phenocrysts mostly all display minor to major alteration with subhedral to euhedral shape. Average phenocryst size of ≈0.8mm with a frequency of ≈15%. Roughly 12% **opaques.**	Relict phenocrysts, Anhedral to euhedral in shape, with an average size of ≈0.50mm and a frequency of **≈20%.** Mostly altered plagioclase to calcite with some plagioclase pseudomorphs present. Blotchy clayey brown and white grained gm like texture seen in some Relict phenocrysts. Gm exhibits blotchy dull white grains, likely quartz +- plagioclase (≈50%) and brown clayey grains, likely clay, (≈45%) texture with few opaques and calcite. average gm grain size is ≈0.025mm.
20	**7**	140.9	Porphyritic	Fresh **quartz** anhedral in shape with light to heavy fracture and some embayment's. Average size of ≈0.70mm at a frequency of ≈4%. **Plagioclase,** euhedral to anhedral shaped. Some phenocrysts with light to heavy alteration with an average size of	Relict phenocrysts, anhedral to euhedral in shape, average size of ≈0.50mm with a frequency of **≈20%.** Most alteration to calcite with some sandy brown-grey-yellow alteration textures. Gm consists of amorphous sandy brown-white grains (≈70%), brown clayey grains, (≈20%) and

				≈1.2mm and frequency of ≈20%. <1% **orthopyroxenes** and roughly 6% **opaques.**	opaques , (≈10%) with an average grain size of ≈0.03mm
21	**7**	159.8	Porphyritic	Few fresh **quartz** phenocrysts, anhedral in shape, embayment's present and fractured, with an average size of ≈0.50mm at a frequency of ≈1%. **Plagioclase** pseudomorphs present but no fresh plagioclase phenocrysts as are all now calcite. Some partly altered **orthopyroxenes** (<1%).Roughly 12% opaques.	Heavily altered Relict phenocrysts. Majority of which are subhedral to anhedral in shape and many have been broken apart. Average size is ≈1.1mm at a frequency of **≈35%** and are mostly all calcite. Some Relict phenols show green-brown staining or gm like blotchy alteration textures. The gm has a blotchy texture and is made up of fine grained murky white grains, ≈40% and brown clay grains, ≈55% with an average size of ≈0.023mm. There are also breccia present all sizes exceeding 5.0mm and going up to 19.5mm. Breccia Gm consisted of calcite, ≈55% and brown clayey grains, ≈ 40% with a few opaques and white grains.
22	**7**	169.3	Porphyritic	Fresh **quartz,** anhedral shape with light to heavy fracture, an average size of ≈0.65mm at a frequency of ≈3%. No other fresh **phenocrysts** but some plagioclase pseudomorphs, fully altered. Roughly 8% **opaques.**	Mostly altered slide with many Relict phenocrysts, euhedral to anhedral in shape with an average size of ≈1.5mm at a frequency of **≈35%.** Many phenocrysts altered to calcite, implying primary plagioclase phenocrysts. Other alteration textures include a dark grey-brown clayey texture. Multiple breccias present, charcoal grey to murky white in colour with an average size of ≈3mm and a maximum size of 30mm. Breccias bearing calcite, quartz, opaques, Relict phenocrysts and calcite veins. Breccias often boarded by opaques. The gm appears heavily altered with a botchy texture of brown clays (≈70%) around fine grained white crystals (≈25%) with an average grain size of ≈0.02mm. fine grained calcite (≈0.025mm) and opaques also present in gm.

23	**8**	55.1	Porphyritic	Fresh **quartz** with anhedral shape, heavy fracture an average size of ≈0.3mm at a frequency of <1%. Fresh **plagioclase** with anhedral to euhedral shape, an average size of ≈0.25mm at a frequency of ≈25%. O**rthopyroxene** and **clinopyroxene** (≈4% combined) some orthopyroxene beginning to alter with some grains turning to a deep orange/ brown colour in both ppl and xpl. roughly 3% opaques.	Relict phenocrysts with frequent heavy fracture, an average size of ≈1.2mm at a frequency of **≈15%.** Many altered phenocrysts unidentifiable and still white in ppl but under xpl show alteration texture of heavy fracture with blotch gm like pattern and a variation of extinctions. The gm is blotchy with white plagioclase microlites +- quartz (≈30%) amongst clayey dark brown/ grey spots (≈70%) Gm grains have an average size of ≈0.03mm.
24	**8**	401.27	Porphyritic	Fresh **plagioclase** euhedral to anhedral in shape with an average size of ≈1.0mm and maximum size of 5.0mm at a frequency of ≈30%. **Clinopyroxene** with subhedral shape, an average size of ≈0.3mm and a maximum size of 1.1mm at a frequency of ≈3%. **Orthopyroxene,** subhedral to euhedral in shape and with an average size of ≈0.35mm and maximum size of 1.2mm at a frequency of ≈4%. Quartz also possible similar in size to plagioclase with euhedral shape but difficult to distinguish from plagioclase. roughly 3% opaques.	Relict phenocrysts, primarily with a subhedral to euhedral shape but some with a anhedral shape. An average size of ≈0.45mm and maximum size of 4.5mm at a frequency of **≈18%.** Little to no calcite with primary alteration feature being green-yellow-brown staining. Gm is ≈60% white grains (plagioclase microlites and other white grains) as well as ≈35% brown stained grains, likely clay or altered grains. as well as opaques.
25	**8**	692.33	Porphyritic	Fresh **plagioclase** euhedral to anhedral in shape with average size of ≈0.45mm and a maximum size of 3.6mm at a frequency of ≈40%. **Orthopyroxene** phenocrysts with euhedral to anhedral shape and an average size of ≈0.25mm at a ≈2% frequency. **Clinopyroxene** with anhedral to subhedral shape, an average size of ≈0.25mm at a frequency of ≈4%. Some quartz possibly present but hard to distinguish from plagioclase. Roughly 5% opaques.	Relict phenocrysts, euhedral to anhedral in shape with an average size of ≈0.5mm and a maximum size of 3.5mm at a frequency of **≈20%.** Most Relict phenocrysts are unidentifiable with a green to yellow staining or a charcoal grey colour. Two main gm textures, both appear quite fresh. Majority of slide has trachytic texture of gm and is composed of plagioclase microlites (≈ 0.1mm, ≈60%) in a vitric matrix with some brown staining occurring and visible under xpl with roughly 10% brown altered/clayey grains. The other gm is similar but with a pilotaxitic texture and a higher % of alteration. Gm is composed of ≈40% white grains, ≈35% brown alteration grains in a partly altered matrix.
26	**8**	745.43	Porphyritic	Poor Slide plagioclase, clinopyroxene and orthopyroxene identifiable	Poor slide altered phenocrysts and calcite identifiably but gm not suitable for analysis

27	**8**	832.95	Porphyritic	Poor slide- Plagioclase and clinopyroxene identifiable	poor slide- Altered phenocrysts and calcite identifiable but gm not suitable for analysis (appears more altered than slide 26)
28	**9**	157.8	Porphyritic	Poor slide- only distinguishable mineral is **plagioclase** and possibly **orthopyroxene**	N/A
29	**10**	194	Porphyritic	Fresh **Quartz** anhedral in shape, heavily fractured with an average phenocryst size of ≈1.2mm and a frequency of ≈4%. Fresh **plagioclase** with a subhedral to euhedral shape with an average size of ≈1.0mm with a maximum size of 8.5mm at a frequency of ≈35%. Both **orthopyroxene** and **clinopyroxene** present with an average size of ≈0.15mm and a combined frequency of ≈4% with more clinopyroxene present than orthopyroxene. ≈5% opaques.	Relict phenocrysts, subhedral to anhedral shape with an average size of ≈0.75 with a maximum of 2mm at a frequency of **≈15%.** Majority of gm is amorphous grey brown sandy alteration texture, extremely fine grained, that appears black with twinkles of white grains (0.02mm)under xpl and goes up an order when the birefringence slider is used. Other alteration textures include bright yellow staining present around some altered phenocrysts.
30	**10**	226.7	Porphyritic	Fresh **Quartz,** with an anhedral shape and heavy fracture. Average phenocryst size of ≈1.5mm and a maximum size of 3.5mm with a frequency of ≈5%. **Plagioclase** phenocrysts with subhedral to euhedral shape and some with heavy fracture. Average phenocryst size of ≈1.5mm at a frequency of ≈35%. **Clinopyroxene** phenocrysts with anhedral to subhedral shape with an average size of ≈0.4mm at a frequency of ≈3%. <1% **orthopyroxenes.** some pyroxene phenocrysts beginning to alter. ≈3% **opaques.**	Relict phenocrysts of subhedral to anhedral shape with an average size of ≈0.6mm and a maximum size of 2.4mm at a frequency of **≈18%.** lack of calcite but Frequent amorphous grey brown sandy alteration texture, extremely fine grained, that appears black with twinkles of white under xpl and goes up an order when the birefringence slider is used. This texture appears to be the majority of the gm (≈75%) of the slide with the rest being a variation of the blotchy texture with a combination of white yellow, brown and grey grains as well as a few opaques.
31	**11**	55.52	Porphyritic	**Quartz** with heavy fracture, euhedral shape and some holes/impregnations. Average phenocryst size of ≈1.25mm with a maximum size of 4mm and a frequency of ≈4%. **Plagioclase** phenocrysts with a subhedral to anhedral shape, frequent fracture and an average size of ≈1.5mm with a maximum of 5mm. Plagioclase frequency of ≈25% with frequent alteration of plagioclase phenocrysts. Roughly 6% **opaques.**	Relict phenocrysts of subhedral to anhedral shape with an average size of ≈1.0mm at a frequency of **≈20%.** Frequent calcite alterations, likely from plagioclase. The Gm consists of a blotch texture of dull white grains (≈60%) and brown grey clay-like grains (≈40%) as well as some opaques. The average gm grain size is ≈0.015mm

32	**11**	98.1	Porphyritic	Fresh **quartz** with heavy fracture and anhedral in shape. Average size phenocrysts of ≈1.25mm with a frequency of <1%. Some quartz phenocrysts had halo feature around grain, possible alteration feature. **Plagioclase** phenocrysts, anhedral to euhedral in shape with an average size of ≈2.6mm with a frequency of ≈30%. many plagioclase phenocrysts partly altered. **Orthopyroxenes** with a relatively green colour in ppl and low birefringence green in xpl, anhedral to subhedral in shape with an average size of ≈ 0.75mm with a maximum size of 1.75mm and mostly altered to some degree. Roughly 6% **opaques.**	Relict Phenocrysts, displaying a anhedral to subhedral shape with an average size of ≈1.5mmand a frequency of **≈25%.** Many crystals have altered to calcite. The gm appears altered with murky white grains, possibly quartz ± feldspar (≈45%) as well as brown clay and altered grains (≈55%). the average size of gm crystals are ≈0.015mm with a few opaques and orthopyroxenes grains also in the gm.
33	**11**	440	Porphyritic	Fresh **Quartz** with heavy fracture and holes/ embayment's. **Phenocrysts** are l with an average size of ≈2.25mm and frequency of ≈6%. Plagioclase pseudomorphs visible that have been heavily altered to calcite. There are no fresh plagioclase phenocrysts. Some **orthopyroxene** (<1%) phenocrysts that have been partly altered in slide and roughly ≈8% **opaques.**	Relict Phenocrysts with an anhedral to subhedral shape and an average size of ≈1.75mm with a frequency of **≈40%.** Many calcite alterations in slide. The gm appears reasonably altered with ≈50% blotch brown, likely clay grains and ≈50% blotchy white grains, likely quartz ± plagioclase. Average grain size in gm is ≈ 0.025mm with some opaques and calcite also in gm.
34	**11**	532.3	Porphyritic	**Quartz,** anhedral, fractured, embayment's/holes in phenocrysts. Average pheno size ≈2.0mm with a frequency of ≈3%. **Plagioclase** present but primarily fully altered with some larger phenocrysts partly altered. Plagioclase is subhedral to anhedral with an average size of ≈1.75mm and a maximum size of 8.25mm with a frequency of ≈35%. Most phenocrysts now calcite with a few pseudomorphs. ≈5% **opaques.**	Relict Phenocrysts, subhedral to anhedral with an average size of ≈ 2.30mm and a frequency of ≈40%. Primarily calcite, likely from plagioclase as well as unidentifiable altered phenocrysts with a sandy brown-grey-yellow alteration texture. The gm is **≈30%** blotchy brown grain, likely clay, and ≈70% murky white grains, some slightly elongated and some circular. this is likely plagioclase ± quartz.
35	**11**	534.32	Porphyritic	Very limited fresh rock, majority altered beyond recognition with exception of one white anhedral crystal with high second order birefringence colours. This was possibly a **clinopyroxene** or very thick **quartz**. There were also a few fine grains of unaltered **quartz**. Few **plagioclase** pseudomorphs	Extremely altered slide. Relict Phenocrysts, anhedral - subhedral. Average size of ≈ 1.25mm but up to 3.25mm and a frequency of ≈ **50%.** Some calcite present in slide but primarily brown-grey-yellow sandy alteration texture showing extinction and weak birefringence. very altered gm with ≈10% white murky

				distinguishable in altered phenocrysts. ≈5% **opaques**	grains, ≈70% yellow-brown clayey grains and ≈20% sandy alteration textured grains. Average gm grain size of ≈0.02mm with few opaques.
36	**11**	562.8	Porphyritic	Fresh **Quartz**, anhedral, fractured, embayment's and holes in phenocrysts. Average pheno size≈ 1.25mm with a frequency of ≈ 3%. Fresh **plagioclase**, subhedral to anhedral, frequent fracture. Average pheno size ≈1.5mm with a frequency of ≈20%. Some phenocrysts beginning to altered to calcite with some fully altered. ≈8% **opaques** and <1% **orthopyroxene**	Relict Phenocrysts, subhedral to anhedral with an average size of ≈ 0.75mm but up to 2.5mm and a frequency of **≈10%.** Primarily calcite as well as a sandy brown-grey-yellow alteration texture. The gm appears moderately altered with blotchy murky white grains (≈35%)and dark brown/yellow grains, likely clays and altered grains, (≈65%). Few opaques also present.

Secondary structures and reflected light thin section descriptions.

Slide no.	Hole no.	Depth (m)	Transmitted light - Veins:	Reflected light:
1	**5**	101.2	Frequent calcite stringers as well as a few red-brown fibrous veins ≈0.8mm thick and transition to calcite in the centre from an unknown mineralogy.	Pyrite occurring mostly in very thin veins, anhedral and average size of ≈0.025mm rarely in gm and phenocrysts, Galena phenocrysts, up to 0.2mm subhedral to anhedral in shape. Possible magnetite also present as light grey, hard anisotropic grains. clusters of soft light grey grains alongside large fibrous vein, possibly galena or chalcocite, some laminations present but may be alteration feature
2	**5**	241.14	≈0.15mm thick vein running through the middle of the slide horizontally for the length of the slide. Consisting primarily of calcite with smaller quantities if white grains as well as opaques.	frequent pyrite occurring in veins, phenocrysts, gm and bordering phenocrysts. Anhedral in shape and up to 0.25mm in size. Galena scarce <1% anhedral shape.
3	**5**	354.79	Appears to have some phaneritic textured white grain veins but just as likely that these are fractured and fragmented quartz phenocrysts.	Pyrite, subhedral to anhedral in shape with an average size of 0.25mm. ≈5mm arsenopyrite intrusion/ vein?
4	**5**	380.83	There are a few stringer veins which are composed of calcite and are roughly 2mm long on average. There are also thicker and longer veins which appear to consist of white low birefringence grains as well as opaques and are ≈0.75mm thick.	Pyrite present in vein, gm and phenocrysts with clusters of large crystals, ≈0.12mm. Galena common as phenocrysts and as grains in gm, ≈0.07mm anhedral shape. Chalcopyrite in phenocrysts? Not isotropic in some cases- Anhedral shape ≈0.05mm.
5	**5**	540.07	N/A	Pyrite, occurring in veins, gm and phenocrysts. Large crystals >1mm occurring in phenocrysts. Galena, mostly as grains in gm ≈0.05mm. Arsenopyrite, anhedral in shape, ≈0.05mm, chalcopyrite, ≈0.0125mm anhedral.
6	**5**	614.25	Very thin (≈0.035mm) vein running across roughly half of the thin section and is composed of small phaneritic white grains and calcite as well as some opaques. Other possible poorly defined veins but hard to decipher between calcite of vein and phenocryst.	Pyrite frequently occurring in phenocrysts as small ≈0.01 mm grains dotted throughout reliced phenocrysts as opposed to a larger coherent crystal. Pyrite also common as small grains throughout the gm. Arsenopyrite, subhedral to euhedral, occurring in phenocrysts, ≈0.075. Galena common as grain in gm with anhedral shape and ≈0.05mm. Some possible hematite or magnetite, similar to galena but appears to heave greater relief and slightly bluer tinge, however bireflectance and anisotropy not clear.

7	**5**	629.93	Two main veins, with one travelling diagonally across slide at a thickness of ≈0.25mm and composed of low birefringence and stained brown grains. The other vein travels parallel with thin section at a thickness of ≈0.3mm and consists of a calcite and opaques.	Pyrite common as small grains ≈0.01 in gm and in phenocrysts. Larger crystals (up to 0.7mm in vein at top of vein of slide travelling horizontally along slide, commonly occurring alongside large chalcopyrite (up to 0.3mm) and galena≈ 0.3mm. Chalcopyrite Anisotropy difficult to detect but crystals seem too dull to be gold. galena also occurring and as phenocrysts ≈0.2mm and grains in gm
8	**5**	791.12	Two main veins running across the slide, one at a width of ≈0.2mm and the other at ≈0.35. Both veins are opaque and penetrate phenocrysts. Aome areas of vein are boarded by yellow brown staining, likely an alteration feature.	Pyrite occurring in veins that run across the slide, in sections over 6mm long, smaller amounts in phenocrysts at an average size of roughly 0.15mm with little in the gm. Galena also common, mostly in phenocrysts at an average size of roughly 0.093mm.
9	**5**	792.94	Two main veins running across slide, both are opaque veins, one is ≈0.2mm and the other is ≈0.35mm, both penetrate through phenocrysts.	Pyrite occurring most frequently in the gm at around 2% with an average size of ≈0.03mm. Larger crystals up to 0.45mm occurring in phenocrysts and pyrite veins also present. Galena occurring in the gm at a much lesser frequency than pyrite with an average size of ≈0.1mm as well as in phenocrysts up to 0.2mm in size
10	**5**	835.19	N/A	Pyrite occurring mostly as small grains in both gm and in phenocrysts with an average size of ≈ 0.1mm and rarely with grains larger than 0.2mm. Galena also common in both gm and phenocrysts with a higher ratio relative to pyrite compared to slide 9. galena has an average size of ≈0.05 mm. possible arsenopyrite.
11	**6**	42.1	frequent dark red/opaque veins mostly stringer sized, possibly alteration material. And frequent breccial, anhedral in shape black to slightly darker brown than the gm and bearing phenocrysts, opaques and reliced phenocryst. Average breccia size ≈4mm. intrusion of gm, ≈2.75mm thick down edge of slide with finer grained more altered looking rock , seemingly with a higher % of clays.	notable lack of pyrite, and abundance of galena and/or magnetite. Soft look of some crystals indicate galena but harder looking crystals some with bluish grey lamellae (possibly hematite) indicate magnetite. Both have same grey isotropic colour. Some slightly blue anisotropic minerals occurring in some phenocrysts could also indicate hematite. (unsure in mineral is anisotropic or if colour change is an alteration feature. single 0.025mm grain of bright yellow/ gold colour, however grain appears to be similar hardness as galena (possibly gold or pyrite) Also possible ilmenite present as seen in anisotropic grain which displays a dull pink tinge. grains mostly occurring in phenocrysts.
12	**6**	182.92	Calcite vein running parallel with slide and has ox-bow like bend in it. Roughly 1.0mm thick. Calcite changes shade from white to a sandy brown texture and back to white throughout vein. The gm around the vein is denser/ more closely phaneritic than rest of the slide.	notable lack of pyrite. Magnetite (or galena, but looks too high relief) common in gm and in phenocrysts. Smaller galena grains common also mostly in gm. Light yellow/gold coloured grain occurring alongside magnetite(or galena) grains, especially along boarder of long white vein visible to naked eye. possibly chalcopyrite- or gold/ electrum. Average size of grey

				crystals is roughly 0.15mm and rarely exceeds 0.25mm. (larger crystals likely all magnetite) Gold/yellow crystsals have an average size of roughly 0.01mm.
13	**6**	228.59	Few stringer veins with a width of ≈0.06mm. Primarily calcite veins of various orientations, penetrating phenocrysts. Some stringers of unknown deep red brown colour also penetrating phenocrysts.	notable lack of pyrite. Magnetite (or galena, but looks too high relief) common in gm <0.01mm and in phenocrysts, average size of ≈0.04mm and rarely exceeding 0.3mm. Smaller galena-looking grains common also mostly in gm. Light yellow/gold coloured grains (gold/ chalcopyrite) occurring as intrusions within magnetite(or galena) crystals. Same coloured light gold crystals also occur within non-reflective phenocrysts as intrusions as rarely occur in the gm, usually around the edge pf phenocryst. They have an average size of ≈0.01mm and a maximum of 0.04mm
14	**6**	315.22	Few stringer veins, too thin to distinguish with a larger calcite vein running diagonally across slide at a width of ≈0.6mm, penetrating phenocrysts. An opaque vein also runs alongside this calcite vein.	Pyrite occurring in stringer veins, phenocrysts often with irregular shape and gm. Sizes range from <0.01mm grains to >0.4mm crystals Light gold crystals similar to slide 13 and 14 rarely occurring with an average size of ≈0.02mm. Magnetite occurring in gm, average size of ≈0.1mm sometimes conjoining with pyrite crystals.
15	**6**	373.55	One large main vein in slide with a few stringers. All veins bearing calcite. Main vein measured at 0.75mm thick but crack in rock prevents accurate measurements. Some veins also bear a mixture of phaneritic grains.	relatively low reflectives, mostly pyrite occurring in the gm and in phenocrysts, average size of ≈0.08mm. Few magnetite grains as well as some galena also present.
16	**6**	458.56	Frequent stringer veins , with an average width of ≈0.05mm and maximum thickness of 0.5mm, penetrating phenocrysts. Stockworks of thin calcite stringer veins in various orientations with some sandy brown alteration texture veins also present. ≈0.2mm veins of phaneritic white grains also present, sometimes merging into a calcite vein.	relatively low reflectives, pyrite occurring in gm and phenocrysts with an average size of ≈0.03mm. Magnetite also occurring, Possible galena? Soft Grey crystals common surrounded by brown/yellow alteration like texture. Also brown/yellow in XPL. Small grains within phenocrysts <0.01mm bright yellowish colour, likely pyrite.
17	**6**	530.2	Veins range from stringer veins up to 1.5mm thick veins. Majority of veins calcite in composition often merging in and out of amorphous sandy brown-grey-yellow alteration looking material. This material also occurs in vein alongside calcite. Some opaque veins and some gm like grain veins. opaques also occur alongside calcite and sandy textured	Abundant pyrite (≈5-7%) occurring in gm, veins and phenocrysts, small (≈0.01) grains to >0.8mm crystals. Anhedral with various shapes. Same soft grey crystal with brown yellow alteration halos present also.

			material. Veins occurring in various orientations. Larger veins penetrating phenocrysts.	
18	**7**	73.5	Calcite stringer veins and calcite +- quartz, plagioclase, opaques and altered grains in gm like mix present, with some veins wedged between cracks of larger plagioclase phenocrysts.	Pyrite present in gm and phenocrysts with an average size of ≈0.08mm. Magnetite more common than pyrite, occurring in gm and phenocrysts with an average size of ≈0.2mm. Some looking to have a brownish tinge, likely an oxidation effect.
19	**7**	109.5	One main calcite vein, (≈0.3) which splits into two, creating intrusion, bearing breccia and a slightly different gm with a higher % of white grains. The breccia are dark brown and subhedral to anhedral in shape, ranging in size from 0.25mm to 3.25mm. Breccia bear opaques, quartz, plagioclase and calcite. Calcite is also more frequent in the intrusion. opaques also common along side calcite vein.	Primarily pyrite occurring in gm, phenocrysts and accumulating along the edges of veins, taking up ≈3% of the slide, with an average size of ≈0.01mm and showing euhedral to anhedral shape. Magnetite present with an average size of ≈0.1mm and often occurring in conjunction with pyrite. Some grey crystals as described above with yellow/brow colour in Reflected XPL.
20	**7**	140.9	Frequent calcite veins from 0.10mm to 0.60mm, cutting through phenocrysts and in various orientations. Smaller veins stem from the larger veins. Veins of opaques running along side calcite vein/ within calcite vein. Larger veins also bearing quartz and what appears to be breccia which are brown with small white grains and opaques within. Some veins consist of sandy brown-grey-yellow material which appears to be alteration texture. this sandy texture is seen merging in and out of calcite in vein.	abundant pyrite, occurring in gm, phenocrysts and veins, at a frequency of ≈5% sizes range from <0.01mm grains to >2.5mm crystals in veins. With various shapes from euhedral to anhedral. Magnetite present with an average size of ≈0.2mm also possible galena from soft look but same colour as magnetite, often smaller in size.
21	**7**	159.8	Few calcite veins (≈0.20mm) and loosely opaque veins (≈0.13mm) in various orientations with some opaque veins bordering breccia boundaries.	Primarily pyrite, occurring in gm, veins and phenocrysts, at a frequency of ≈4%. Sizes range from <0.01mm to greater then 0.5mm with an average of ≈0.8mm. Galena present with some appearing to have the brown/yellow appearance. Possible small quantities of arsenopyrite as some grains are bright like pyrite but slightly whiter, however no bireflectance.

22	**7**	169.3	Multiple veins in various orientations, mostly stringer veins, but thickest is 0.4mm. All veins calcite veins with some also bearing quartz and opaques. Few veins penetrating phenocrysts.	Primarily pyrite, occurring in gm and phenocrysts, significantly lower concentration of reflective within breccias. Pyrite frequency ≈3%, anhedral to euhedral in shape. With an average size of ≈0.03mm and rarely exceeding 0.15mm. Brighter yellow grains sparsely present, likely chalcopyrite. Galena likely the grey grains present, soft with the brown tint in reflective XPL. Also possibility of magnetite presence due to harder grey isotopic crystal, commonly occurring alongside pyrite.
23	**8**	55.1	Few stringer veins, of various compositions, opaque veins with frequent deep red/orange staining surrounding vein and spreading to gm. some veins deep red/ orange and show no change in colour from ppl to xpl. White grain veins, possibly quartz +- plagioclase occurring as well as veins of brown green stained altered material. all penetrating phenocrysts.	Notable lack of pyrite. Magnetite common in gm, vein and phenocrysts. Average size of ≈0.015mm and rarely exceeding 0.23mm. Small (≈0.0125) grains gold colour, looks more gold than chalcopyrite but also appears to have relief/ looks hard. Possibly electrum/ gold though apparent hardness would not match.
24	**8**	401.27	N/A	Low frequency of reflectives, mostly magnetite with an average size of 0.12mm with frequent grains <0.01mm and few exceeding 0.23mm. Some with rainbow sheen like pattern on top, possibly alteration/oxidation. Some magnetite seem to have laminations within them. Sparse pyrite grains with an average size of ≈0.01mm
25	**8**	692.33	Calcite intrusions near boarder of the two gm's traveling horizontally across slide. 3.5mm at thickest point and roughly 15mm in length from edge of the slide.	Pyrite abundant ≈3% occurring in gm and phenocrysts. Sizes vary from <0.01mm to >0.4mm with an average size of ≈0.02mm. Magnetite is also common, occurring gin the gm and in phenocrysts with sizes ranging from <0.01mm to 0.45mm. Some magnetite has cross-hatched pattern. possible ilmenite grain. section in slide with pilotaxitic texture has a higher abundance of reflective at ≈7-10%.
26	**8**	745.43	Poor slide- stringer calcite vein and stringer quartz/plagioclase vein present	poor slide- Primarily pyrite occurring in apparent gm as phenocryst, at an average size of ≈0.1mm rarely exceeding 0.25mm. Possible sphalerite and chalcopyrite crystals in sparce numbers.
27	**8**	832.95	N/A	Poor slide- Primarily pyrite in apparent gm as well as phenocrysts and possibly in veins. Average size of ≈0.04mm rarely exceeding 0.28mm. Small quantities of magnetite and chalcopyrite. Rainbow sheen like reflective vein (possibly effect of alteration/oxidation/slide genesis. possibly pyrite. same colour rainbow sheen reflective bordering some phenocryst.

28	**9**	157.8	N/A	Poor slide- Primarily pyrite, occurring in gm and phenocrysts. ≈90% of reflectives <0.02mm with few pyrite crystals exceeding this in phenocrysts up to 0.45mm. Sparse quantities of magnetite and possible arsenopyrite. Some rainbow sheen texture phenocrysts also present
29	**10**	194	very thin (≈0.05mm) stringer veins yellow orange colour, same colour under ppl and xpl but darkens and lightens under xpl. Penetrating phenocrysts.	Magnetite the sole identifiable reflective. Average size of ≈0.1mm, rarely exceeding 0.25mm. Some rainbow sheen like grains present. Likely oxidised magnetite.
30	**10**	226.7	Minimal veins but clinopyroxene vein like structure surrounding large quartz phenocryst.	Primarily magnetite, ≈2% occurring in both gm and phenocrysts. With an average size of ≈0.12mm, rarely exceeding 0.2mm. Almost all magnetite crystals have anisotropic dark grey- black lamellae/ twinning. One possible chalcopyrite and pyrite grain.
31	**11**	55.52	Frequent stringer veins running mostly parallel with the slide, consisting mainly of opaques with some calcite and white grains. Average vein width of ≈0.04mm.	Pyrite rich sample, >99% of reflectives are pyrite, occurring in phenocrysts, gm and veins. Average crystal size ≈0.1mm with some pyrite in vein extending over 2.5mm. Sparse magnetite with an average size of 0.15mm
32	**11**	98.1	Multiple thick veins/intrusions mostly parallel with the slide, with one being horizontally orientated. Veins consist of brown fibrous, alteration-like texture, calcite and opaques. Some red staining also present near vein. Veins /intrusions range from 0.05mm to 4.9mm at thickest part of calcite intrusion. Brown material has various shades and mostly occurs alongside calcite but also is seen merging into/from calcite veins.	Range of reflectives including pyrite, magnetite, sphalerite, possibly hematite in the form of lamellae within magnetite and possibly galena. Pyrite occurring in gm and phenocrysts with an average size of ≈0.05mm. Magnetite common and often contains lamellae of anisotropic mineral and some have black twinning feature. Average size ≈0.1mm. Grey mineral occurring in red stained vein but too small to identify- possibly magnetite.
33	**11**	440	Calcite vein present, ≈0.2mm thick, running parallel down length of the slide and cutting through phenocrysts. There are secondary, thinner calcite veins split off from the main vein like tributaries. A loosely defined meandering vein structure consisting of white crystals, likely quartz ± plagioclase, calcite and opaques runs through the middle of the slide.	Primarily pyrite, occurring in gm and phenocrysts. Average size of ≈0.02mm while rarely exceeding 0.3mm. Euhedral to anhedral irregular shaped crystals. Sphalerite also common, occurring in masses of grains that typically cover ≈0.3mm on average. Sparse magnetite grains.

34	**11**	532.3	Opaque vein, likely sufides ≈0.2mm thick running diagonally across slide. Vein bordered by 0.025mm thick calcite like layer and a few calcite stringers which are branching off. The vein penetrates some phenocrysts but not all. There is also a small vein-like structure that is short with a thickness of 0.1mm with an altered gm texture.	Pyrite common with an average size of ≈0.12mm occurring in gm, phenocrysts and vein. Lengths of pyrite in vein exceed 2.5mm. Shape irregular subhedral to anhedral. Sphalerite common, occurring on gm and phenocryst, with an average size of ≈0.1mm, subhedral to anhedral shape. likely chalcopyrite present in from of soft, dull, strong yellow coloured crystal. Bright yellow/gold crystals, different colour from pyrite, possibly gold/ electrum or bright chalcopyrite, grains >0.01mm so hard to determine if isotropic.
35	**11**	534.32	A 0.15mm vein travels parallel to the slide for most of the length of the thin section, bearing calcite with a few wite and opaque grains. This vein intersects a thicker vein (0.4mm) bearing calcite and plagioclase ± quartz which is running diagonally across bottom of slide. This vein transitions into a loosely defined mass of opaques and gm like grains and white grains as the vein progresses.	Pyrite and sphalerite common. Pyrite have an average size of ≈0.05mm and occurs in gm and phenocrysts. Sphalerite occurs also in gm and phenocrysts, often occurring in masses of grains averaging a size of ≈0.25mm. Possible chalcopyrite grains sparsely occurring <0.01mm. slightly more golden grains similar to pyrite, possible gold/electrum but may also be chalcopyrite.
36	**11**	562.8	Multiple veins/trails of opaques running through slide ≈0.9mm wide. Penetrating through phenocrysts. Vein lengths from less than 1mm to over half of the slide.	Frequent pyrite in veins, phenocryst and gm, anhedral in shape, light grey phenocryst appeared to be mostly altered and was slightly yellow under XPL and looked to show subtle laminations. Other grey mineral appears anisotropic but could be a phenocryst that's not fully altered.

Appendix C

Facies input data:

HoleID	from	to	Facies
WNDD005	0	25	Soil
WNDD005	25	50	N/A
WNDD005	50	70	DB
FWNDD005	70	75	MB
WNDD005	75	87	N/A
WNDD005	87	106	LDP
WNDD005	106	112	MB
WNDD005	112	134	DB
WNDD005	134	162	HDP
WNDD005	162	175	DB
WNDD005	175	180	IP
WNDD005	180	225	MDP
WNDD005	225	232	HDP
WNDD005	232	235	IP
WNDD005	235	250	MDP
WNDD005	250	255	IP
WNDD005	255	270	LDP
WNDD005	270	330	MB
WNDD005	330	340	IP
WNDD005	340	350	LDP
WNDD005	350	355	IP
WNDD005	355	360	MDP
WNDD005	360	400	MB
WNDD005	400	590	MDP
WNDD005	590	600	IP
WNDD005	600	625	MB
WNDD005	625	637	IP
WNDD005	637	650	DB
WNDD005	650	690	MB
WNDD005	690	705	DB
WNDD005	705	713	MDP
WNDD005	713	725	MB
WNDD005	725	735	MDP
WNDD005	735	762	MB
WNDD005	762	785	DB
WNDD005	785	795	MB
WNDD005	795	838.8	MDP

HoleID	from	to	Facies
WNDD006	0	20	Soil
WNDD006	20	188	MDP
WNDD006	188	200	MB
WNDD006	200	223	MDP
WNDD006	223	240	DB
WNDD006	240	300	MDP
WNDD006	300	326	SDB
WNDD006	326	337	MB
WNDD006	337	370	DB
WNDD006	370	376	IP
WNDD006	376	390	DB
WNDD006	390	435	IP
WNDD006	435	455	DB
WNDD006	455	460	IP
WNDD006	460	475	DB
WNDD006	475	500	MDP
WNDD006	500	506	SDB
WNDD006	506	529	LDP
WNDD006	529	538	MB
WNDD006	538	575	MDP
WNDD006	575	590	MB
WNDD006	590	600	SDB
WNDD006	600	637	DB
WNDD006	637	652.7	MDP
WNDD007	0	25	Soil
WNDD007	25	40	LDP
WNDD007	40	55	DB
WNDD007	55	70	MDP
WNDD007	70	75	DB
WNDD007	75	124	DB
WNDD007	124	130	HDP
WNDD007	130	155	MDP
WNDD007	155	170	MB
WNDD007	170	190	DB
WNDD007	190	200	MB
WNDD007	200	230.5	DB
WNDD009	0	27	N/A
WNDD009	27	62	HDP
WNDD009	62	75	DB
WNDD009	75	94	HDP
WNDD009	94	125	DB
WNDD009	125	161	MDP

HoleID	from	to	Facies
WNDD009	161	175	DB
WNDD009	175	188	N/A
WNDD009	188	288	DB
WNDD009	288	294	MB
WNDD009	294	305	DB
WNDD009	305	368	MDP
WNDD009	368	430	DB
WNDD009	430	460	MDP
WNDD011	0	30	Soil
WNDD011	30	55	DB
WNDD011	55	62	MB
WNDD011	62	88	DB
WNDD011	88	105	MDP
WNDD011	105	125	DB
WNDD011	125	135	MDP
WNDD011	135	140	IP
WNDD011	140	150	MB
WNDD011	150	162	MDP
WNDD011	162	175	IP
WNDD011	175	192	DB
WNDD011	192	212	IP
WNDD011	212	220	LDP
WNDD011	220	250	MB
WNDD011	250	290	WMB
WNDD011	290	365	DB
WNDD011	365	380	IP
WNDD011	380	395	MB
WNDD011	395	406	IP
WNDD011	406	430	DB
WNDD011	430	459	MDP
WNDD011	459	515	WMB
WNDD011	515	560	DB
WNDD011	560	595	IP
WNDD011	595	603	MB
WNDD011	603	625	MDP
WNDD011	625	650	IP
WNDD011	650	675	SDB
WNDD011	675	706.8	DB

Alteration input data

HoleID	from	to	Alteration level
WNDD005	50.1	171	10
WNDD005	171	297.5	5
WNDD005	297.5	620	10
WNDD005	620	710	5
WNDD005	710	820	5
WNDD005	820	838.8	1
WNDD006	20	203	-3
WNDD006	203	330	1
WNDD006	330	616	10
WNDD006	616	652.7	5
WNDD007	35	125	1
WNDD007	125	150	5
WNDD007	150	230	10
WNDD008	0	1000	1
WNDD010	190	226	5
WNDD011	25	270	5
WNDD011	270	490	10
WNDD011	490	533	5
WNDD011	533	535	10
WNDD011	535	706	5